

NACA-TM 1407

6567

014479



TECH LIBRARY KAFB, NM

# NATIONAL ADVISORY COMMITTEE FOR AERONAUTICS

TECHNICAL MEMORANDUM 1407

FREE CONVECTION UNDER THE CONDITIONS OF  
THE INTERNAL PROBLEM

By G. A. Ostroumov

Translation of "Svobodnaya convectzia v ousloviakh  
vnoutrennei zadachi."

Published by State Publishing House, Technico-Theoretical  
Literature, Moscow - Leningrad, 1952.



Washington

April 1958

AFMDC  
TECHNICAL LIBRARY  
AFL 2811



FREE CONVECTION UNDER THE CONDITIONS OF THE INTERNAL PROBLEM

By G. A. Ostroumov

Translation of "Svobodnaya convectzia v ousloviakh  
vnoutrennei zadachi."

Published by State Publishing House, Technico-Theoretical  
Literature, Moscow - Leningrad, 1952.

## CONTENTS

	Page
CHAPTER 1. GENERAL CHARACTER OF INVESTIGATION . . . . .	1
1. Definition of Gravitational Convection . . . . .	1
2. M. V. Lomonosov - Initiator of Scientific Problem of Thermal Gravitational Convection . . . . .	2
3. External and Internal Problems . . . . .	7
4. Practical Value of Chosen Case . . . . .	8
CHAPTER 2. FUNDAMENTAL EQUATIONS OF GRAVITATIONAL CONVECTION. . . .	10
1. Physical Sense of Different Terms of Each Equation . . . . .	10
2. Mathematical Character of Equations. . . . .	12
CHAPTER 3. "FUNDAMENTAL" (LINEARIZED) EQUATIONS OF GRAVITATIONAL CONVECTION . . . . .	16
1. Form of "Fundamental" Equations. . . . .	16
2. Remarks on Experimental and Mathematical Significance of "Fundamental" Equations. . . . .	17
3. Case of Vertical Channel . . . . .	17
4. Formation of Components of Harmonic Equations. . . . .	19
5. General Properties of Solutions of "Fundamental" Equations of Gravitational Convection. . . . .	20
6. Form of Solution of Biharmonic Equation in Cylindrical Functions. . . . .	22
CHAPTER 4. SOLUTION OF PROBLEMS OF THERMAL GRAVITATIONAL CONVECTION	24
1. General Boundary Conditions. . . . .	24
2. Special Boundary Conditions. . . . .	25
3. Basis of Solution Scheme . . . . .	26
4. Method of Solution . . . . .	28
CHAPTER 5. STEADY CONVECTION IN VERTICAL CHANNEL OF ROUND SECTION .	29
1. Diametral Antisymmetry of Free Convective Flow . . . . .	29
2. Criterional Significance of Convection Parameter . . . . .	33
3. Thermal Role of Pipe Walls . . . . .	35
4. Superposition of Forced and Free Thermal Convection. . . . .	37
5. Application of Cylindrical Functions of Complex Variable Where Temperature in Upper Part of Vertical Channel is Higher Than in Lower Part . . . . .	41
CHAPTER 6. UNSTEADY REGIME OF GRAVITATIONAL THERMAL CONVECTION IN VERTICAL CHANNEL OF ROUND CROSS SECTION . . . . .	43
1. General Observations . . . . .	43
2. Periodic Process of Cooling Nonsolidified Casting. . . . .	43
3. First Stage - Pouring Strongly Turbulent Hot Fluid . . . . .	44
4. Second Stage - Developing Free Convective Motion . . . . .	48
5. Third Stage - Cooling Fluid in Presence of Convection. . . . .	50
Rapid Variant. . . . .	50
Slow Variant . . . . .	52

	Page
CHAPTER 7. CONVECTION IN INCLINED SLIT AS EXAMPLE OF CONVECTION IN CHANNEL OF NONROUND CROSS SECTION . . . . .	55
1. Simplification of "Fundamental" Biharmonic Equation . . . . .	55
2. Higher Temperature in Lower Part . . . . .	57
3. Higher Temperature in Upper Part . . . . .	58
4. Concluding Remarks. . . . .	59
CHAPTER 8. EXPERIMENTAL INVESTIGATIONS OF WATER. . . . .	61
1. Thermal and Convective Parameters of Water. . . . .	61
2. Interpolational Formula for 0°-40° C Interval . . . . .	61
3. Standard Convective Curve and Interpolated Formula for 0°-40° C Interval . . . . .	62
CHAPTER 9. EXPERIMENTAL MODELS . . . . .	64
1. Glass Model . . . . .	64
2. Metal Model . . . . .	66
3. Temperature Recording . . . . .	67
4. Investigating Thermal Parameters of Model . . . . .	70
CHAPTER 10. EXPERIMENTAL INVESTIGATION OF FREE THERMAL CONVECTION IN VERTICAL MODELS OF ROUND CROSS SECTION FOR STEADY REGIME. .	80
1. The Two Regimes of Thermal Convection and Their Dividing Critical Point. . . . .	80
2. Constancy of Value of Convection Parameter in Laminar Regime. . . . .	83
3. Quantitative Characteristic of Above-Critical Regime of Thermal Convection. . . . .	83
4. Presence of Transverse Temperature Gradients and Results of Their Measurements. . . . .	84
5. Fluctuation of Azimuth of Transverse Temperature Gradient .	87
CHAPTER 11. EXPERIMENTAL INVESTIGATION OF UNSTEADY REGIMES OF THERMAL CONVECTION IN MODELS OF ROUND CROSS SECTION. . . . .	88
1. Theoretical Considerations for Steady Process . . . . .	88
2. Fundamental Differences in Unsteady Regimes in Presence and in Absence of Convection. . . . .	90
3. Unsteady Processes Described by Transverse Thermocouples. .	91
4. Forced Thermal Fluctuations Produced by Modulation of Heater Power. . . . .	92
5. Natural Thermal Damping Fluctuations in Convection for Models of Finite Length . . . . .	93
CHAPTER 12. END PHENOMENA OF THERMAL CONVECTION IN MODELS OF ROUND SECTION (INVESTIGATED BY TEMPERATURE RECORDING METHOD) . . . .	94
1. General Distribution of Temperatures Averaged Over Cross Section Along Entire Vertical Model . . . . .	94
2. Variable-Length-Column Method . . . . .	95
3. Moving-Plunger Method . . . . .	98
4. Displacement Method . . . . .	99
5. Conclusion. . . . .	100

	Page
CHAPTER 13. OPTICAL METHODS OF INVESTIGATING CONVECTION IN MODELS OF SPECIAL FORM . . . . .	101
1. Introductory Remarks . . . . .	101
2. Prismatic-Vessel Method. . . . .	102
3. Vertical-Deflection Method . . . . .	108
4. Lattice Method . . . . .	109
5. Application of Lattice Method to Experimental Investigation of Laminar Convection in Cavity of Convenient Shape. . . . .	113
CHAPTER 14. CONCLUDING SUMMARY OF EXPERIMENTAL INVESTIGATIONS OF LINEAR AND QUASI-LINEAR CASES . . . . .	116
CHAPTER 15. CASES REQUIRING SOLUTION OF NONLINEAR EQUATIONS OF GRAVITATIONAL CONVECTION. . . . .	118
1. Practical Significance of Nonlinear Cases and Restriction of Scope of Problem. . . . .	118
2. Observations on General Method of Solution of Nonlinear Equations. . . . .	119
3. Heat Losses Through Imperfect Heat Insulation. . . . .	121
4. Axial Symmetry . . . . .	128
5. Diametral Antisymmetry . . . . .	135
6. Convection in Horizontal Channel of Round Cross Section. . . . .	142
7. Convection in Spherical Cavity . . . . .	153
CHAPTER 16. EXPERIMENTAL INVESTIGATION OF THERMAL CONVECTION IN CAVITIES OF SPECIAL FORM. . . . .	161
1. Statement of Problem . . . . .	161
2. Convection in Spherical Cavity . . . . .	162
3. Convection in Cylindrical Cavity with Horizontal Axis. . . . .	163
4. Concluding Remarks . . . . .	164
CHAPTER 17. THERMAL CONVECTION IN INCLINED MODEL OF CIRCULAR CROSS SECTION . . . . .	166
1. Description of Experimental Setup. . . . .	166
2. Laminar Regime . . . . .	166
3. Generalization of Experimental Results . . . . .	168
4. Above-Critical Regime. . . . .	169
CHAPTER 18. CONCLUSION. . . . .	171
CHAPTER 19. SUPPLEMENTARY TOPICS. . . . .	174
1. Electrolytical Method of Measuring Temperatures. . . . .	174
2. Problem of Geothermal Gradient . . . . .	176
3. Problem of Natural Ventilation . . . . .	178
4. Problem of Velocity of Evaporation . . . . .	180
REFERENCES . . . . .	186

## MOST IMPORTANT SYMBOLS

$\nabla$		"nabla" spatial differentiation, dimensions 1/cm
$\nabla\theta$	=	grad $\theta$ ; $(\nabla\mathbf{v}) = \text{div } \mathbf{v}$
$[\nabla\mathbf{v}]$	=	rot $\mathbf{v}$ , $(\mathbf{v}\nabla)\mathbf{v} = (\mathbf{v} \text{ grad})\mathbf{v}$
$\Delta = \nabla^2 = \frac{\partial^2}{\partial x^2} + \frac{\partial^2}{\partial y^2} + \frac{\partial^2}{\partial z^2}$		sign of Laplacian, dimensions 1/cm <sup>2</sup>
$\mathbf{v} = \mathbf{v}(x,y,z,t)$		velocity vector of fluid particle, cm/sec
$p = p(x,y,z,t)$		pressure determined by convective phenomena, bar = dyn/cm <sup>2</sup>
$g$		gravity acceleration vector, $g = 981 \text{ cm/sec}^2$
$\beta \equiv \partial \ln \rho / \partial \theta$		coefficient of change of density with temper- ature of fluid, 1/deg
$\beta_1 \equiv \partial \ln \rho / \partial C$		coefficient of change of density with concen- tration, cm <sup>3</sup> /g
$\theta = \theta(x,y,z,t)$		temperature, °C
$\nu \equiv \mu / \rho$		coefficient of kinematic viscosity of fluid, cm <sup>2</sup> /sec
$\kappa \equiv \lambda / \rho c$		coefficient of temperature conductivity of fluid, cm <sup>2</sup> /sec
$D$		coefficient of diffusion in fluid, cm <sup>2</sup> /sec
$\rho$		density of fluid, g/cm <sup>3</sup>
$C$		concentration of admixture, g/cm <sup>3</sup>
$dr \equiv dx dy dz$		element of volume, cm <sup>3</sup>

## CHAPTER 1

## GENERAL CHARACTER OF THE INVESTIGATION

## 1. Definition of Gravitational Convection

Gravitational convection is the term used in hydrodynamics to denote the phenomenon that occurs in the field of universal gravitation in connection with the fact that the different particles of a fluid possess different densities.<sup>1</sup> The denser particles sink and the less dense particles float in the surrounding fluid. We understand "fluid" to be a liquid that possesses surface tension as well as gases. The hydrodynamical side of the problem lies in the fact that the particles of the fluid do not move in empty space but move among other similar particles so that each particle in its motion occupies only the place of some other particles it pushes aside. A "particle of fluid" contains within itself a huge number of molecules.

The reason for the differences in density usually lies in the differences in temperature or composition, particularly in the concentration of the admixtures dissolved in the fluid. In addition to these most common reasons for the differences in density, other causes may be present (e.g., electrostriction, thermomagnetic (ref. 3), and thermoelectrostatic effects). The most widely studied form of gravitational convection is the temperature (or heat) convection and for this reason it is desirable to investigate this phenomenon in more detail. It is not difficult to relate it with the diffusion (or concentration) form of convection since the corresponding quantitative expressions reveal great similarity.

The convection is called free if the stresses (including the normal pressure) to which the fluid is subjected at its boundaries do not perform mechanical work, that is, if all the boundaries of the fluid are stationary. The case where this is not true is termed forced convection. It corresponds to the action on the fluid of some mechanical suction pumping the fluid.

---

<sup>1</sup>Besides gravitational convection there are the phenomena of electrostatic convection (ref. 1) and magnetic convection (ref. 2) that arise in the electrostatic and magnetic fields.

There may also be encountered an intermediate case where free convection is imposed on the forced motion of the pumped fluid (ch. 5, sec. 4).

The present report concerns itself almost exclusively with free convection.

## 2. M. V. Lomonosov - Initiator of Scientific Problem

### of Thermal Gravitational Convection

4281

The first investigator to approach scientifically the phenomena of heat convection in nature was the academician M. V. Lomonosov, who first correctly explained the fundamental mechanism of meteorological phenomena. In his work "On Atmospheric Phenomena Arising from Electrical Forces" (1753), he discussed the meteorological phenomena in detail, adduced proofs of the correctness of his explanations, and urgently advocated the scientific views he had worked out.

After first pointing out the importance of the prediction of the weather for human activities, and the difficulties and unpopularity of such predictions, Lomonosov continues, "I have often wondered when I observed that in the winter time after the thawing of the air in which snow had melted terrible frosts suddenly set in, which, after a few hours, made the mercury in a thermometer drop from 3° or 5° above freezing<sup>2</sup> to 30° below freezing and at the same time occupy a space of more than 100 miles. Comparing these with the winters of 1709 and 1740 which were fierce almost over the entire European continent, I wondered even more and very greatly desired to seek the cause of such a sharp change. Most remarkable of all was the fact that thaws almost always occur with air motion and a strong tendency of the weather to cloudiness, while on the contrary, a frost begins to show its rigor after the sky has cleared" (pp. 13-14).

Lomonosov also noted that fluids are more heat conductive than solid bodies when heat is conducted upwards: "In agreement with sound considerations is the fact that the fluidity of sea water and the degree of temperature above or near the freezing point is maintained for a large extent of the sea and also for the subterranean heat which passes through the sea bottom. Thus, the open seas that are free from ice impart more heat to the winter air than mother earth locked in a frozen shell and covered with deep snows which bar the underground heat" (p. 15).

---

<sup>2</sup>The author refers to a 150° temperature scale (instead of the 100° Celsius scale).

4281

Lomonosov asked further, "What is the reason that sea winds stop blowing?" And he answered: "In giving this question my attention I observed a difference of heat and density between the lower air and that which moves upward. That the heat is greater below than above, or speaking generally, in the winter a stronger cold exists above the clouds than below is a judgment obtained by an investigation artificially performed and confirmed by agreement with the atmospheric phenomenon. The upper part of the atmosphere itself is much less heated by the sun than the lower part. Moreover, the winter surface heated by the sun and the rays reflected by it have a greater effect in the lower atmosphere than in the middle or upper atmosphere. The summer hail and the frozen summits of high mountains reveal the truth of this to the eyes and impress on us the fact that in the midst of summer there is always a rigorous winter not very high above our heads."

CA-1 back

Referring to geodetists, who, in the Peruvian mountains "measured the earth's sphere and suffered from frosts and exuded perspiration," Lomonosov continues, "By a prolonged and painstaking skill and an accurate computation, it has been shown that at a known and definite height of the entire atmosphere there reigns a rigorous and continual frost that covers the summits of high mountains with a perpetual snow. If this extends continuously under the very equator, it is easy to conclude how great the force of the frost is in our climate near the same summit."

Having remarked on the phenomenon of hail, Lomonosov continues, "However, this in truth occurs and clearly shows the terrible frost produced at altitude in the snow nucleus of the falling hail." Remarking that in Yeniseisk frosts of  $131^{\circ}$  below freezing were observed ( $-87.5^{\circ}$  C), assuming that the same temperature prevails at the height of 1 verst (1.0668 km), and computing the corresponding densities of the air, Lomonosov arrived at the following conclusion: "Therefore, it is clear that the lower atmosphere is often less dense and proportionately lighter than the upper. This state of the air, which could be studied further, is sufficiently evident from Aerometric rules and is also confirmed by examples. I have explained first that of all the motion of the air in mine pits arises from a different density, where at 50 or less sajenes (1 sajene = 2.134 meters) its flow arises from these causes. Moreover, even in houses in winter, the warm air near the stove rises and, the cool air near the windows descends, a phenomenon which can easily be seen by observing the motion of smoke. Therefore, to a height, which extends over 100 or 200 sajenes, the air of the lower weight opposes the natural laws. It descends and gradually mixes with the lower air casting a severe frost over us. It descends without appreciable motion since in one second it hardly moves several inches, and in two hours it drops 100 or 200 sajenes contending with the currents that rise to meet it." As an experimental proof of this hypothesis, Lomonosov refers to the observation of fumes issuing from pipes; but still more profound is the following remark: "A second effect of these motions is

the clearness of the sky, for although here the density of the air is largely a casual factor, by their rising and sinking, the clouds spread over a large area, then thin out and disappear. Thus, the sudden winter frosts arise by the lowering of the middle atmosphere. Therefore, the fact that it begins without any motion of the wind ceases to be remarkable. Such a drop of the middle atmosphere into the lower must occur in the summer, a circumstance which the disposition of the air tending toward this drop confirms sufficiently. Let us assume that the air, in a state to produce hail in summer, is at a height of 300 sajenes and contains within it a temperature of  $50^{\circ}$  below freezing (which in all probability may be affirmed); at which time the air in the lower atmosphere near the ground is heated to  $40^{\circ}$  or  $50^{\circ}$  above the previously mentioned freezing point: Then, in accordance with my experiments and computations, the density of the upper air as compared with the lower air is of the ratio 6:5; but by the pressure of the upper air, the lower air is compressed and becomes more dense by about one-tenth part. In this state, by the immovable laws of nature, the upper part of the atmosphere should descend deep enough into the lower part so when mixed with the warm air, it will come to equilibrium. This flow of rising and descending air must occur as often as the weight of the upper atmosphere exceeds the weight of the lower; in addition, the lower air must meet the upper and contend with the upper at a different height and different tendency in proportion to the height and difference in heat and density. Finally, this will occur more easily when, by the strong summer heat, the surface of the earth is heated, and the air lying above the earth warms and expands at the same time that an exceeding great cold above the clouds condenses the middle part of the atmosphere."

4281

A little further on Lomonosov continues, "But as soon as the lower air expands by the force of the heat and becomes more rare, the cold and dense part of the atmosphere must descend downward and the lower air rise upward in its place. I shall try to present the phenomena of these interchanges as briefly as possible to your mental eyes, as far as may be understood from my words and as you yourselves have seen and can remember. When the upper atmosphere of a large weight descends to the bottom, it does not spread everywhere at the same horizontal plane, but for different circumstances of the solar rays, according to the position of the clouds and the unevenness of the ground surface, it produces a different rarefaction in the air. And so it descends in places such as the shade of a mountain, or a high building, or a thick cloud where the air is thicker and heavier. It rises upwards where the slope of a mountain is turned to the motion of the sun, or through cloud openings, and is heated by the impinging rays. For this reason, when the thunder clouds ascend before the rain, a large part of the lower clouds move upward and downward like hills; fleecy vapors spread toward the earth and eddying whirls howl; dark abysses open; and above these phenomena the clear sky is covered with a dark blue color. All these circumstances then show, that when a part of the middle atmosphere filled with hot

vapors descends and covers the clearness of the sky with a blue darkness, penetrates the lower clouds with its uneven descent, passes through these, and contends with the encountering air" (p. 22).

4281

After several lines Lomonosov again points out, "The more the lower part of the atmosphere is heated, the more readily the upper part lowers itself into it. Whichever part feels less heat rarifies to a lesser degree. This can conveniently be ascertained from the rise of the mercury in a thermometer and the lowering of the atmospheric pressure. When the solar rays intersect through the clouds, the air cools in the shade of the clouds and must warm up. For this reason, it would be necessary for the air to move from the edges of the shade to its center. A similar action should follow from the growth of falling rain drops because the humid vapors and the water particles unite and heat the large quantities of air in them. However, such motion of the air toward the center of the shade hardly ever occurs, but I do not doubt that the contrary has been the case as observed by all of you. For the advancing clouds charged with lightening not only are preceded by rushing motions but also, passing by, give forth strong winds to the side, leaving behind a stillness over a large area. Where does this stream of air arise? It arises from the pressure of the upper atmosphere, which in compressing the lower is broken up on all sides and strives particularly toward that side where it encounters the least resistance" (p. 24).

Turning to the effect of the local topography Lomonosov states further, "The air in mountainous localities seldom is in equilibrium, because it must rise in places facing the sun, descend in the shade, and thereby more easily draw to itself a part of the cold and heavy upper atmosphere which accelerates its motion and moves it nearer to the ground. By the agreement of so large a number of changes and phenomena, I hope to have shown that my theory does not rest on a weak foundation."

After several pages, Lomonosov returns to the subject of convection. "After the setting of the sun, the lower atmosphere cools more rapidly than the earth's surface, which is saturated with the moisture of vegetation. Through this, the cold air, on coming in contact with the still warm earth, is heated, expands, becomes lighter, and rises until, on being cooled, it comes to equilibrium" (pp. 39-40).

When he came forward with this exhaustive explanation of convective meteorological phenomena, it was naturally impossible for Lomonosov not to encounter oppositions and objections. For this reason, he found it necessary to give in addition "proper explanations on the matter of electrical atmospheric phenomena" (p. 65). The most important and colorful of these explanations is the first: "The subject of the descent and ascent of the atmosphere has been briefly touched upon by Mr. Franklin in his letters. However, that I owe nothing to him in my theory as to the cause of an electrical force in the air is clear from the following

paragraphs: (1) concerning the descent of the upper air, I had already given it thought and discussed it several years ago. I saw the Franklin papers for the first time when my discourse was almost completed, in which matter I refer to my colleagues; (2) the descent of the upper atmosphere was proposed by Franklin in a report of only a few words. I deduced my theory from the sudden setting in of great frosts, that is, on the basis of circumstances that are unknown in Philadelphia, where Franklin lives; (3) I proved in a memorandum that the upper air is not only able, but at times must descend into the lower air; and (4) on this basis I have explained many phenomena connected with the thundering force, of which no trace is mentioned by Franklin. All this is added here not because I want to put myself above him, but is added in order to follow the wish of my colleagues, who demanded that I subjoin my justification" (p. 65).

4281

The theory of M. V. Lomonosov is based on carefully worked tests: IV. "On Multiple Causes," page 17, line 31. The tests for determining the different densities of the air at different degrees of heat, for all otherwise equal conditions, were studied by me in manometric tubes of equal width without bulbs and without using other vessels. Although the different quantity of vapors changed the proportion of the expansion, the average was found to be correct. That is, air  $50^{\circ}$  below freezing as compared with air which is warm at the aforementioned freezing point is in volume ratio 10:11, but as compared with air at  $50^{\circ}$  above the freezing, the warm air is in the ratio of 10:12 or 5:6. Hence, to  $4^{\circ}$  above the freezing there corresponds a volume of air of 554, and to  $131^{\circ}$  below freezing, there corresponds a volume of air of 419. For this reason, the volume of the former to that of the latter will be 554:419, or almost 4:3. That is, the air of the lower atmosphere will be lighter than the other by a one-fourth part. V. "My Explanation," page 18, line 8. "In addition to the motion of the air which occurs in mines, explained in the new Commentaries in the first volume, there are natural proofs of the ascending and descending of air in the free atmosphere" (p. 66). Further on, Lomonosov presents, explains, and illustrates the case of diurnal winds on the Waldstatt Sea in the Alps. He completed this example with the words: "Moreover, in sultry summer days the ground surface apparently swells because the rising warm air mixes with the descending cold air" (p. 67). (See also ch. 13.)

After a new computation of the coefficient of expansion of the air in "Explanation VI," Lomonosov in "Explanation VII" gives a figure which leaves no doubt that he discovered, understood, and quite correctly explained the idea of convection.

In another of his works, Lomonosov again returns to the convective phenomena: "On the Free Motion of Air Observed in Mines from the First Volume of New Commentaries," 1763, (ref. 4). Here he describes and explains two cases of convection that take place in mines if the following

conditions are observed: (1) the mine must have two openings on the bottom surface situated at different heights above the sea level, and (2) the temperature of the free air must differ from the temperature of the ground layers cut through by the mine (ch. 5, sec. 4).

The excerpts quoted previously show that M. V. Lomonosov was the first person to study carefully the phenomenon of heat convection as a result of many years of observation, to explain correctly this phenomenon, to lay the foundations of meteorological phenomena, and to put forth much effort in popularizing the laws revealed by him.

These facts imposed upon Soviet physicists their duty to continue unceasingly the investigations of Lomonosov and, with modern means, to study the phenomenon of gravitational convection, and to extend the scope of the problems that it embraces.

### 3. External and Internal Problems

Among all the possible cases of thermal gravitational convection the cases that have been subjected to the greatest engineering and technical investigation are those where the heater used for this purpose had much smaller dimensions than those of the vessel used to contain the fluid. The study of these cases was primarily conditioned by the practical demands of steam boiler plants. The combination of these conditions is included under the general concept of the "external problem of heat convection."

The contrary cases, where the dimensions of the heater or the cooler are comparable with the dimensions of the vessel containing the fluid, are combined under the general concept of the "internal problem." Of these cases, the one subjected to the most detailed engineering and technical investigation is the case of the transfer of heat from one solid body to another through a thin layer of fluid (ref. 5, p. 86), and from the wall of a pipe to the fluid moving within it (ref. 5, p. 87 and ff.)

The technical character of these investigations is conditioned by the aim that they pursue, namely, to give an over-all estimate of the quantity of heat transferred by the whole convective process rather than going into the details of the motion of the fluid particles and the distribution of their temperatures. The source for these investigations is frequent and diversified tests, and the results are generalized by the methods of the theory of similarity or theory of models.

With this engineering approach to the phenomena of gravitational convection, the physico-mathematical approach is of great significance. In the latter approach, the hydrodynamic side of the process and the

temperature distribution are studied in detail. The investigation is conducted both by experimental methods and by the mathematical devices of classical hydrodynamics.

The two most important experimental methods are the hydrodynamical methods of recording the motion of light-scattering particles introduced into the transparent fluid, and the optical methods based on the dependence of the index of refraction of a transparent fluid on its density (temperature, concentration). The value of these methods depends on the fact that with a correct test set-up neither the introduced particles nor the light rays appreciably distort the phenomenon under investigation. Of lesser value are the thermal methods whose application is attended with the flow distorting behavior of the fixed thermometers in the fluid (thermocouples or resistance thermometers).

The mathematical devices of classical hydrodynamics consist of skillful methods for solving the complicated hydrodynamic equations of heat convection. Of these, the first method used was that of Raleigh which reduces to the finding of solutions that are periodic in space (ref. 6). This method was applied by numerous investigators (ref. 7) who were primarily guided by their aim to solve certain problems of meteorology. There are also a few known successful attempts to investigate mathematically problems of the external type (e.g., ref. 8). The difficulties, arising in the mathematical treatment for solving the problem, have attracted great mathematicians to whom special technical problems were foreign. For this reason, the analysis was usually limited to the mechanical phase of the phenomenon and only in rare cases did it touch its thermal phase.

Thus, there arises the urgent need of investigating whether there are any cases of an accurate solution of the equations of thermal convection and the associated question of the methods of solving these equations approximately. The investigation itself should not be limited to the mechanical side of the problem but must also give a clear account of its thermal (or concentrational) aspect.

#### 4. Practical Value of Chosen Case

An exact solution of the equations of thermal convection may be obtained for a case that has great practical value. This is the case of the thermal convection in a cylindrical vertical cavity heated from below or on a side. The practical value of this case is determined by the following circumstances:

(1) The heat which is propagated in the earth's core from the pyrosphere to the surface passes at some places through cavities containing liquids or gases. In these, a convective motion may arise so

4281

that a certain amount of heat is transferred upwards and is added to the heat transferred by the molecular thermal conductivity. The distribution of the temperatures both within the cavity and in the surrounding mines depends on the form and intensity of the convective motion. Practically the most important case of such a cavity is a vertically drilled well. Geologists often judge the distribution of the temperatures within the layers of the earth's core by the distribution of the temperature in the fluids filling such wells. However, the temperature of the fluid in the well may actually be determined not only by the temperature of the neighboring layers but also by the convective motion in the fluid. A consciously critical approach to the results of the measurements sharpens the most important geothermal concepts (ref. 9).

(2) Many plants make use of chemical processes in liquids and gases accompanied by changes of temperature or concentration. Reservoirs having the form of tanks or columns are often used. Under certain conditions convective phenomena may be excited in these containers either spontaneously or by artificial means. Sometimes these phenomena are desirable; at other times they are injurious. In any case, their conscious control improves or accelerates the production.

CA-2

(3) In the casting of large articles the process of cooling the casting does not occur instantly. The cooling of a casting through the wall of the casting mold may bring about convection phenomena in the casting. The convection complicates the process of cooling and solidification and may serve as a cause of desirable or harmful forms of shrinkage phenomena. A conscious control of the convective processes opens up a way to reduce the spoilage in casting. The characteristic feature of convective processes here is their steady regime. Here also belong the cases of the seasonal freezing of water tanks (of certain forms).

(4) Production installations often have the form of heated and ventilated pits. The conditioning of the air in these chambers, introduced for the purposes of professional hygiene, cannot be correctly designed if the phenomena of thermal convection and diffusion are not considered. In this book the case of convection in a cylindrical channel is investigated by physico-mathematical methods and contains brief conclusions regarding engineering and technical applications.

## CHAPTER 2

## FUNDAMENTAL EQUATIONS OF GRAVITATIONAL CONVECTION

4281

## 1. Physical Sense of Different Terms of Each Equation

The process of gravitational convection is described by the following equations (ref. 1):

$$\dot{\underline{v}} + (\underline{v}\nabla)\underline{v} = -\frac{\nabla P}{\rho} + g(\beta\theta + \beta_1 C) + \nu \Delta \underline{v} \quad (2.1)$$

$$\dot{\theta} + \underline{v} \times \nabla \theta = \Delta \theta \quad (2.2)$$

$$\dot{C} + \underline{v} \times \nabla C = \Delta C \quad (2.3)$$

$$\dot{\rho} + \nabla(\rho \underline{v}) = 0 \quad (2.4)$$

The first of these equations was obtained from the Navier-Stokes equation. The physical meaning of each term of this equation may be ascertained if the equation is multiplied by the mass of an element of volume ("particle") of the fluid  $\rho d\tau$ ; where it is useful to bear in mind that in hydrodynamics, two methods of describing the motion of a fluid are applied. The so-called Lagrange method studies the paths of the different individual particles of the fluid during the entire process. The Euler method considers the distribution of the velocities in the entire volume of the fluid at a given instant.

The term  $\dot{\underline{v}}$  represents the acceleration of a particle of volume  $d\tau$  at a given point of space at a given instant. It may be called the Euler acceleration. In connection with the fact that the expression  $\rho \underline{v} d\tau$  enters in the equation of the second law of Newton, this term of the Navier-Stokes equation may be called the Newtonian term.

The expression  $[\underline{v}\nabla]\underline{v} = \frac{1}{2} \nabla v^2 - [\underline{v}[\nabla \underline{v}]]$  in steady flow represents the acceleration of a material particle of mass  $\rho d\tau$  moving along a given trajectory. It may be called the Lagrange acceleration. The components  $\frac{1}{2} \nabla v^2$  and  $-\underline{v}[\nabla \underline{v}]$  are analogous to the tangential and normal

accelerations of the particle. The tangential component arises in the nonuniform motion of the material particle along its path. The normal component arises in the motion of the point along a curvilinear path. The term  $[\nabla v]_v$ , in particular, drops out in the case where all the particles of the fluid move rectilinearly, uniformly, and along parallel paths. The parallel requirement is added because, for example, in a radial spreading of an incompressible fluid from a single source the motion of all the particles, although rectilinear, is not uniform: the farther away from the source the less the velocity.

In connection with the fact that the expression  $\frac{1}{2} v^2 \rho d\tau$  enters in the Bernoulli hydrodynamic equation, the expression  $\frac{1}{2} \nabla v^2$  may be called the Bernoulli force.

The entire left side of equation (2.1) may be called the inertia part.

The expression  $-\nabla p d\tau$  represents the force of the hydrostatic pressure and may be called the Pascal force.

If the fluid does not everywhere have the same temperature  $\theta$  and concentration  $C$  of the additive mixed with it, its density will be different at various points and will be given by  $\rho = \rho_0(1 + \beta\theta + \beta_1 C)$  where  $\rho_0$  denotes the density of the solvent for  $\theta = 0^\circ$  and  $C = 0$ ,  $\beta$  denotes the temperature coefficient of the density and  $\beta_1$  denotes the concentration coefficient of the density. Thus the expression

$$g\rho_0(\beta\theta + \beta_1 C) \quad (2.5)$$

represents the relative weight of a fluid particle  $d\tau$ . We do not consider here the phenomena of thermodiffusion. This expression may be called the Archimedes force. It determines the gravitational character of the phenomenon under consideration.

The expression  $\nu \rho d\tau \Delta v$  represents the force of viscous friction acting on the particle  $d\tau$ . This expression may be called the Poiseuille force.

From this analysis it is seen that equation (2.1) represents a summary expression of a number of elementary generally known physical laws referring to one gram of fluid and holds true for any particle of fluid.

This equation is not entirely accurate in the following respects. Actually, the density of the fluid in the Archimedes force is given by the more complicated expression as follows:

$$\rho = \rho_0 + \frac{\partial \rho}{\partial \theta} \theta + \frac{1}{2} \frac{\partial^2 \rho}{\partial \theta^2} \theta^2 + \dots + \frac{\partial \rho}{\partial C} C + \frac{1}{2} \frac{\partial^2 \rho}{\partial C^2} C^2 + \dots + \frac{\partial^2 \rho}{\partial \theta \partial \rho} \theta C + \dots + \frac{\partial \rho}{\partial p} p + \dots \quad (2.6)$$

Of this expression, equation (2.1) uses only the first approximation

$$\left. \begin{aligned} \frac{1}{\rho} \times \frac{\partial \rho}{\partial \theta} &= \beta \\ \frac{1}{\rho} \times \frac{\partial \rho}{\partial C} &= \beta_1 \end{aligned} \right\} \quad (2.7)$$

Moreover, bearing in mind that  $\beta\theta$ ,  $\beta_1 C$  are usually not large in comparison with unity,  $\rho$  may be set equal to  $\rho_0$ .

The equation of heat conduction (2.2) is called the Fourier-Kirchhoff equation. If this equation is multiplied by  $\rho c d\tau$ , the first term represents the quantity of heat expended per second for heating an element of volume, and the second term represents the quantity of heat carried away by convection from this element of volume. On the right side the expression  $\alpha \Delta \theta \rho d\tau \equiv \lambda \Delta \theta d\tau$  represents the quantity of heat flowing up to an element of volume by heat conduction of the surrounding particles of fluid. Thus, equation (2.2) expresses the law of conservation of energy. The coefficient  $\alpha$  is called the coefficient of temperature conductivity (thermal diffusivity).

The equation of diffusion (2.3) is sometimes called the Fick equation and formally agrees with equation (2.2). The meaning of the different terms is analogous to the meanings of the corresponding terms of equation (2.2). As a whole, equation (2.3) expresses the physical law of the conservation of matter (admixture). The coefficient  $D$  is called the diffusion coefficient.

The equation (2.4) is called the continuity equation, and likewise expresses the law of the conservation of matter (that of the basic fluid or solvent instead of the admixtures).

Equations (2.2), (2.3), and (2.4) accurately express the elementary physical laws they represent. Equations (2.1) to (2.4) are true both for laminar and turbulent motions of the fluid.

## 2. Mathematical Character of Equations

In equations (2.1) to (2.4), it is assumed that we are dealing with a fluid whose physical properties, (i.e., the parameters) are known.

The unknowns in these equations are as follows: the velocity  $\underline{v}$ , the pressure  $p$ , the temperature  $\theta$ , and the concentration  $C$ , altogether four functions, one of which is vectorial. For their determination, we have a precisely sufficient number of simultaneous equations, one of which is vectorial. The arguments of these functions are the coordinates and time. Equations (2.1), (2.2), and (2.3) are partial differential equations of the second order (through the Laplacian  $\Delta$ ); equation (2.4) is of the first order. Equations (2.1) to (2.4) are homogeneous; they do not contain free terms.

All of these equations are nonlinear. The nonlinearity is recognized both in the structure of the equations themselves and in the nonlinear properties of the physical parameters of the fluid.

Actually, all the parameters of the fluid are functions of the temperature. Generally, the viscosity  $\nu$  is most strongly dependent on the temperature and also on the concentration of certain admixtures. To a lesser degree, the parameters of the fluid generally depend on the pressure  $p$ .

The nonlinear structure of the equations is reflected by the following terms: the Lagrange term (eq. (2.1)), and the convective terms (eq. (2.2)) and (2.3), and the entire eq. (2.4)). All nonlinear properties of equations (2.1) to (2.4) are connected with their coordinate terms; the terms depending on the time ( $\dot{\underline{v}}$  and  $\dot{\theta}$ ) are linear.

Methods for solving nonlinear differential equations giving an accurate solution in a finite number of operations are unknown. It is this difficulty which explains why the physico-mathematical side of the phenomenon has been relatively and moderately investigated.

One of the properties of a nonlinear homogeneous equation is that if we have found two solutions of such equation by some method, the sum of these solutions will not solve this equation. The fundamental property of linear homogeneous equations is the converse of this property which reflects the physical principle of superposition. Hence, it is still necessary to defer attempts at an accurate solution of equations (2.1) to (2.4) in their general and rigid form.

It is necessary, in the first place, to limit oneself to those cases where it is possible to assume that the parameters of the fluid either do not depend on the temperature and pressure or depend on them to such a slight degree that the general character of the phenomenon is undisturbed by this dependence. This is called parametric linearization of the equations. In this case, the problem may be approximately solved for the entire setup with improvements in the accuracy at different places of the setup in correspondence with the temperature and pressure there obtained. In general, this restriction is not too troublesome (except ref 2).

In the second place, it is necessary to investigate carefully those cases where it is possible to remove the nonlinearity from the structure of the equations, that is, to bring about their structural linearization.

The previously mentioned difficulties of solution of the nonlinear equations led to the parametrical linearization of equation (2.4) as early as 1903 (ref. 3). It was established that, within the range of the fundamental properties of convective phenomena, it is possible to assume  $\nabla p = 0$  in the systems of (2.1) to (2.4) everywhere except for the Archimedean term in equation (2.1). As a result, equation (2.4) becomes

$$\dot{\rho} + \nabla(\rho \underline{v}) = \dot{\rho} + \nabla p \times \underline{v} + \rho \nabla \underline{v} = 0$$

and assumes the form

$$\nabla \underline{v} = 0 \quad (2.8)$$

As mentioned previously, the structural linearization of equation (2.1) is brought about when the Lagrange acceleration is equal to zero and the paths of the fluid particles (the "lines of flow") form a parallel bundle. If we take the z-axis of a Cartesian system of coordinates parallel to this bundle, we have

$$\left. \begin{aligned} v &\equiv v_z \equiv v(x,y) \\ v_x &\equiv 0 \\ v_y &\equiv 0 \\ \frac{\partial v}{\partial z} &= 0 \end{aligned} \right\} \quad (2.9)$$

Under the condition of the structural linearization of equation (2.1), equations (2.2) and (2.3) may be "structurally linearized" if the z-component of the temperature and concentration gradients are constant, that is,

$$\left. \begin{aligned} \frac{\partial^2 \theta}{\partial z^2} &= 0 \\ \frac{\partial^2 C}{\partial z^2} &= 0 \end{aligned} \right\} \quad (2.10)$$

Experience shows (ch. 10), that this is the typical case.

In view of the fact that the majority of the tests have been conducted with heat convection, and by assuming that in industry also heat problems are more important than those of diffusion, and also by taking into account the symmetry of the temperature and diffusion in the equations, further study will consider only temperature. Wherever necessary, the diffusion problems may be investigated along the same pattern. The phenomena of thermodiffusive convection require independent investigation.

TR27

## CHAPTER 3

"FUNDAMENTAL" (LINEARIZED) EQUATIONS OF  
GRAVITATIONAL CONVECTION

4281

## 1. Form of "Fundamental" Equations

Bearing in mind the parametric and structural linearization of the initial equations carried out in the preceding paragraphs and confining ourselves to thermal convection we obtain, for the steady state, the following system of linear homogeneous equations

$$0 = -\frac{1}{\rho} \times \frac{\partial p}{\partial z} + g \cos \alpha \beta \theta + \nu \Delta v \quad (3.1)$$

$$0 = -\frac{1}{\rho} \times \frac{\partial p}{\partial y} + g \sin \alpha \beta \theta \quad (3.2)$$

$$Av = \kappa \Delta \theta \quad (3.3)$$

$$\frac{\partial v}{\partial z} = 0 \quad (3.4)$$

Account was taken of relation (2.9) in virtue of which all these equations are scalar and there has been put

$$\frac{\partial \theta}{\partial z} = A \quad (3.5)$$

The YZ plane has been taken through the gravitational acceleration vector  $g$  which forms the angle  $\alpha$  (fig. 1) with the Z-axis. It is understood that equations (3.1) to (3.4) describe only the laminar motion of the fluid.

## 2. Remarks on the Experimental and Mathematical Significance of "Fundamental" Equations

Much effort has been expended in proving experimentally the admissibility of the basic assumptions which underlie the setting up of a system of equations (3.1) to (3.4) (chs. 10 and 13). As a result, it has been found that these assumptions are actually typical for a wide range of experimentally produced thermal convection phenomena. At the same time, the linearity (and homogeneity) of these equations makes possible their elementary solution in closed form. We thus find, in this system of equations, the key to the detailed physico-mathematical investigation of a certain class of experimentally producible phenomena. For this reason, the system (3.1) to (3.4), its solutions, and those conditions which determine the occurrence of this case will be termed "fundamental" in the following paragraphs.

This term is further justified by the following considerations. The degree of accuracy of an experimental check of any theoretical assumptions can never be considered perfect. In any experiment small deviations will always exist from the ideal case that is described by the equations. It is possible to distinguish a wide group of experimentally produced phenomena in which the ideal situation will form the principal and essential nucleus while the previously mentioned small phenomena will play a negligibly small part. It is this group which serves as the proof of the correctness of the basic assumptions. But, in addition, a second still wider group of phenomena can be distinguished in which these small deviations will no longer be negligible owing to their insufficient smallness. These, however, can be mathematically taken into account as nonlinear corrections to the solution of the linearized system (3.1) to (3.4).

Thus, equations (3.1) to (3.4) not only play an independent part in giving an exact solution of the problems of experimentally produced phenomena but also play the very important auxiliary part of providing a basis for the mathematical solution of not strictly linear problems by the method of successive approximations (ch. 15).

## 3. Case of Vertical Channel

Bearing in mind that the experimental verification of those cases for which  $\sin \alpha$  is not small encounters great difficulties (ch. 17), we assume that the channel is vertical, the Z-axis collinear with the acceleration of gravity vector  $g$ , and the angle  $\alpha = \pi$ . Then

$$\left. \begin{aligned} [\underline{g}\underline{v}] &= 0 \\ \cos \alpha &= -1 \end{aligned} \right\} \quad (3.6)$$

We likewise assume, for the present, that  $\partial p / \partial z = 0$  (ch. 5, sec. 4). The scalar equations (3.1) to (3.4) then become

$$-g\beta\theta + v\Delta v = 0 \quad (3.7)$$

$$Av - \kappa\Delta\theta = 0 \quad (3.8)$$

Eliminating from these equations either  $\theta$  or  $v$  by applying the Laplace operator to one equation, we obtain quite identical equations in  $v$  or  $\theta$ , for example:

$$g\beta Av - \kappa v \Delta \Delta v = 0$$

or

$$\Delta \Delta v - k^4 v = 0 \quad (3.9)$$

where

$$k^4 = \frac{g\beta A}{v\kappa} \quad (3.10)$$

The process of elimination was possible because of the commutativity of the operations of multiplication and of forming the Laplacian. For example, in eliminating  $\theta$ , it was assumed that

$$g\beta\Delta\theta = \Delta(g\beta\theta) \quad (3.11)$$

The result does not depend on whether the function of the coordinates  $\theta$  is multiplied by the constant number  $g\beta$ , and then from the product a new function, the Laplacian  $\Delta$ , is formed, or conversely, whether the Laplacian of  $\theta$  is formed first and the result is then multiplied by the constant number  $g\beta$ . Equation (3.9) is a linear homogeneous incomplete biharmonic equation (refs. 1 and 2) with constant coefficients (within the assumed limits). By definition, the symbols  $\Delta\Delta$  has the following meaning:

$$\begin{aligned} \Delta\Delta v &\equiv \Delta(\Delta v) \equiv \text{div grad div grad } v \\ &\equiv \nabla(\nabla\{(\nabla v)\}) \equiv \nabla^4 v \equiv \frac{\partial^4 v}{\partial x^4} + 2 \frac{\partial^4 v}{\partial x^2 \partial y^2} + \frac{\partial^4 v}{\partial y^4} \end{aligned} \quad (3.12)$$

From the system (3.7) we obtain

$$\theta = \frac{v}{g\beta} \Delta v \quad (3.13)$$

If the system (3.7) to (3.8) is solved for  $\theta$ , we obtain, from (3.8),

$$v = \frac{\kappa}{A} \Delta\theta \quad (3.14)$$

## 4. Formation of Components of Harmonic Equations

Equation (3.9) is customarily solved by the following symbol method (ref. 3, p. 197). We assume

$$0 = (\Delta - k^2)(\Delta + k^2)v = \Delta\Delta v - k^2(\Delta v) + \Delta(k^2v) - k^4v = \Delta\Delta v - k^4v \quad (3.15)$$

Because of the commutative property

$$k^2(\Delta v) = \Delta(k^2v) \quad (3.16)$$

Hence, the repeated equation (3.15) is true. But expressions (3.15) can be equal to zero only if at least one of the following equations is true:

$$\left. \begin{aligned} (\Delta - k^2)v_1 &= \Delta v_1 - k^2v_1 = 0 \\ \Delta v_1 &= k^2v_1 \end{aligned} \right\} \quad (3.17)$$

$$\left. \begin{aligned} (\Delta + k^2)v_2 &= \Delta v_2 + k^2v_2 = 0 \\ \Delta v_2 &= -k^2v_2 \end{aligned} \right\} \quad (3.18)$$

Since equation (3.9) is linear (and homogeneous), its most general solution will be any linear combination of solutions of equations (3.17) and (3.18) (satisfying the boundary conditions discussed in the following example):

$$v = v_1 + v_2 = v(x, y) \quad (3.19)$$

There is then obtained from equations (3.5) and (3.13)  $\theta = \theta(x, y) + Az$ , namely,

$$\theta - Az = \theta_1 + \theta_2 = \frac{v}{g\beta} (\Delta v_1 + \Delta v_2) = \frac{v}{g\beta} (k^2v_1 - k^2v_2) = \frac{vk^2}{g\beta} (v_1 - v_2) \quad (3.20)$$

Since equations (3.17) and (3.18) are each of the second order, there enter altogether, in the final solution, four arbitrary constants determined from the boundary conditions.

4281

6A-3 back

## 5. General Properties of Solutions of "Fundamental"

## Equations of Gravitational Convection

Even before discussing the question of the boundary conditions, a number of important general conclusions can be drawn from the form of the solutions (3.19) and (3.20).

(1) The total volume of the fluid flowing upward in the plane  $z = 0$  through the area  $S$  bounded by the contour  $L$  in time  $t$  is equal to (fig. 2)

$$\left. \begin{aligned} V &= \iint_S vt \, dx \, dy = t \iint_S (v_1 + v_2) \, dx \, dy \\ &= \frac{t}{k^2} \iint_S (\Delta v_1 - \Delta v_2) \, dx \, dy = \frac{t}{k^2} \oint_L \left( \frac{\partial v_1}{\partial n} - \frac{\partial v_2}{\partial n} \right) dl \end{aligned} \right\} \quad (3.21)$$

where the Ostrogradsky-Green theorem was used. The sign  $\partial/\partial n$  denotes differentiation along the normal to the contour  $L$ ,  $dl$  denotes the differential arc of the contour, and  $\oint$  denotes integration over the closed contour.

(2) The total flow of heat due to molecular thermal conductivity (there is no other convective-heat conduction in the direction perpendicular to the  $z$ -axis) through the lateral surface of a cylinder of height  $h$  with base  $S$ , bounded by the contour  $L$ , over a time  $t$  is equal to

$$\left. \begin{aligned} Q_1 t &= t \oint_L \lambda \frac{\partial \theta}{\partial n} h \, dl = t \lambda h \oint_L \frac{\partial}{\partial n} (\theta_1 + \theta_2) \, dl \\ &= \frac{t \lambda h v k^2}{g \beta} \oint_L \left( \frac{\partial v_1}{\partial n} - \frac{\partial v_2}{\partial n} \right) \, dl \\ &= \frac{t \lambda h v k^4}{g \beta} V = h \rho c A V \end{aligned} \right\} \quad (3.22)$$

4281

If we assume that the motion of the fluid is directed by the walls of the vertical cylindrical channel having the cross section  $S$ , then it is seen from equation (3.22) that the flow of heat passing from the channel walls into the fluid, under the assumptions made, is proportional to the total quantity of fluid flowing through the section of the channel. If at certain points of the cross section the fluid flows upward and at other points downward, then it may be found that the total quantity of fluid passing through will be equal to zero ("closed" channel, pure natural convection). In this case, at certain points of the perimeter of the channel walls the heat may pass from the walls to the fluid and at other points from the fluid to the walls, but the total general flow of heat will likewise be equal to zero. With such a natural convective flow having a constant gradient and constant velocity over the height (but variable over the cross section), the fluid does not heat or cool all the channel walls.

If a certain distance along the channel an over-all transfer of heat occurs from the fluid to the walls or conversely, then one of the assumptions made drops out. For example, it is possible that an artificial pumping of the fluid occurs through the channel, and the actual motion of the fluid then represents the superposition of forced and free convection (ch. 5, sec. 4). In this case, equations (3.1) to (3.4) cease to be linear. Or, it may be that an axial gradient exists so that  $\partial v/\partial z \neq 0$  (i.e., the transverse components of the velocity are not zero (eq. (2.9))). In this case, the linear description of the process is an inaccurate approximation, in some cases, admissible (ch. 10), and in other cases requiring essential corrections (ch. 15).

(3) The total flow of heat carried upward by convection in time  $t$  through the area  $S$  in the plane  $z = 0$  is given by

$$\left. \begin{aligned}
 Q_t &= \iint_S v t \rho c \theta \, dx \, dy \\
 &= \rho c t \iint_S (v_1 + v_2)(\theta_1 + \theta_2) \, dx \, dy \\
 &= \frac{\rho c t v k^2}{g\beta} \iint_S (v_1 + v_2)(v_1 - v_2) \, dx \, dy \\
 &= \rho c t \sqrt{\frac{A v}{g\beta x}} \iint_S (v_1^2 - v_2^2) \, dx \, dy
 \end{aligned} \right\} (3.23)$$

To this convective heat flow it is necessary to add the molecular heat flow

$$Q_2 t = - \lambda \Delta s t \quad (3.24)$$

### 6. Form of Solution of Biharmonic Equation in Cylindrical Functions

The general solution of the biharmonic equations (3.9), (3.15), (3.17), and (3.18) has been worked out in great detail in terms of cylindrical functions. If we set

$$\left. \begin{aligned} x &= r \cos \varphi \\ y &= r \sin \varphi \\ r^2 &= x^2 + y^2 \\ \operatorname{tg} \varphi &= \frac{y}{x} \end{aligned} \right\} \quad (3.25)$$

then (ref. 3, p. 200 and following)

$$\Delta v_1 = \frac{\partial^2 v_1}{\partial x^2} + \frac{\partial^2 v_1}{\partial y^2} = \frac{\partial^2 v_1}{\partial r^2} + \frac{1}{r} \times \frac{\partial v_1}{\partial r} + \frac{1}{r^2} \times \frac{\partial^2 v_1}{\partial \rho^2} = k^2 v_1 \quad (3.26)$$

Setting

$$v_1 = v_0(r) \times \cos(n\varphi + \gamma_1) \quad (3.27)$$

we obtain from equation (3.26):

$$\frac{\partial^2 v_0}{\partial r^2} + \frac{1}{r} \times \frac{\partial v_0}{\partial r} = \left( \frac{n^2}{r^2} + k^2 \right) v_0 \quad (3.28)$$

A solution of the last (linear) equation is given by any cylindrical function  $F_n$  (or a linear combination of them) of order  $n$  of the argument  $(ikr)$  satisfying the boundary conditions, which will be considered later in this report. The solution of equation (3.26) will then be

$$v_1 = \sum_{n=0}^{\infty} F_n(ikr) \cos(n\varphi + \gamma_1) \quad (3.29)$$

In the light of the last transformation it is useful for what follows to give the following simplified characterization of cylindrical functions. A cylindrical function is a function of the coordinates  $r$  and  $\phi$ , for which the operation  $\Delta$ , by equation (3.26), is equivalent to multiplication by  $k^2$ . Cylindrical functions have been well tabulated (refs. 4 to 6).

The choice of the cylindrical functions themselves and their coefficients in linear combinations must be made by considering the boundary conditions.

In contrast to many other cases of the application of cylindrical functions for the solution of physical problems, in this case all functions entering equation (3.29) are characterized by the same value of the parameter  $k$ . It is determined in accordance with equation (3.10) by certain unitary parameters of the same fluid in which there exists a single vertical temperature gradient  $A$ .

By analogy with equations (3.26), (3.28), and (3.29) for equation (3.18), we find in place of equation (3.29)

$$v_2 = \sum_{n=0}^{\infty} [F_n(-kr) \times \cos(n\phi + \gamma_2)] \quad (3.30)$$

Considering equation (3.20), we obtain for the temperature

$$0 - Az = \frac{vk^2}{g\beta} \sum_{n=0}^{\infty} [F_n(ikr)\cos(n\phi + \gamma_1) - F_n(-kr)\cos(n\phi + \gamma_2)] \quad (3.31)$$

It is useful to have in view the following formula which permits the transition from the higher to the lower orders of the cylindrical functions, which are particularly well tabulated, so that

$$F_n(x) = \frac{2(n-1)}{x} F_{n-1}(x) - F_{n-2}(x) \quad (3.32)$$

Of these particularly well tabulated functions, it is convenient to use the Bessel functions  $J_n$  and the Neumann functions  $N_n$ .

## CHAPTER 4

SOLUTION OF PROBLEMS OF THERMAL GRAVITATIONAL  
CONVECTION

4281

## 1. General Boundary Conditions

For all thermal problems investigated, referring to the convection of a fluid within a cylindrical channel, the following general boundary conditions are characteristic:

(1) Within the channel of cross section  $S$ , bounded by the contour  $L$  and near the surface  $z = 0$ , the velocities and temperatures are finite, continuous and single-valued with the required number of derivatives.

(2) The total quantity is given of fluid  $V$  passing through the channel. For example, in the case of free convection alone, it is equal to zero ("closed" channel).

(3) At the channel wall, the velocity of the adhering boundary layer of fluid is equal to zero:

$$v_L \equiv 0 \quad (4.1)$$

(4) The temperature is continuous within the adhering boundary layer (does not have any jump)

$$\theta_L = (\theta_e)_L \quad (4.2)$$

(5) The flow of heat is continuous within the adhering boundary layer (does not originate from any chemical exothermal or endothermal reaction nor other accumulation or generation of heat):

$$\lambda \left( \frac{\partial \theta}{\partial n} \right)_L = \lambda_e \left( \frac{\partial \theta_e}{\partial n} \right)_L \quad (4.3)$$

## 2. Special Boundary Conditions

To the general boundary conditions there must be added, in each case, special boundary conditions of the heat distribution in the mass surrounding the channel or in the channel wall, that is, some information must be given relative to  $\theta_e$ .

These boundary conditions are generally divided into two classes: namely, nonhomogeneous and homogeneous (ref. 1). Two forms of the typical nonhomogeneous conditions in the heat transfer are given as follows:

(1) The temperature  $\theta_L$  is given at any point of the contour  $L$ . This is the simplest boundary condition that may be directly substituted in the solution (eq. (4.7)), and that gives the required result. These conditions, in their turn, must satisfy the following initial conditions: along each generatrix (parallel to the  $Z$ -axis) the temperature must vary according to the linear law (eq. (3.5)). Hence, the contour of the  $L$  section is involved and not the entire surface of the channel wall. If in particular cases this requirement of the boundary condition is not observed, it is impossible to use the "fundamental" linearized equations for the solution of these cases due to inequalities, (eq. (2.9)),

$$v_x \neq 0$$

$$v_y \neq 0$$

(2) The heat flow  $\lambda(\partial\theta/\partial n)_L$  is given entering the fluid from the surrounding mass. This condition can likewise be substituted in the solution and will give the required answer after more or less complicated computations. This boundary condition must satisfy the consequence from the initial conditions, namely formula (3.22), otherwise equation (2.9) will again be violated and the phenomenon will be unsteady.

The most typical homogeneous boundary condition is the proportionality between the heat flow and the temperature at each point of the contour  $L$ ; the coefficient of proportionality varying from point to point in correspondence with the special thermal properties of the surrounding mass and the geometrical configuration of the contour  $L$ :

$$\left( \frac{\lambda \frac{\partial\theta_e}{\partial n}}{\theta_e} \right)_L = f(l) = f_1(r, \varphi) \quad (4.4)$$

In order to be able to use the "fundamental" equations, it is necessary that equation (2.9) be observed, that is, that the functions  $f$  and  $f_1$  are independent of the coordinate  $z$ .

The case considered most is the one for which the thermal properties of the surrounding mass are characterized by the following extremely general assumption: at finite distances from the channel there are neither heat sources nor sinks in the surrounding mass:

$$\Delta\theta_e \equiv 0 \quad (4.5)$$

This assumption does not exclude the presence of any kind of thermal phenomena in the surrounding mass. For example, the channel fluid serves as a source of the local thermal phenomena in the channel region in correspondence with formula (3.22). Moreover, the surrounding region permits the existence of heat flows caused by the presence of "infinitely" removed sources and sinks. The latter must be at such a distance from the channel that the gradients they produce in the surrounding mass (in the absence of the channel) do not appreciably depend on the coordinates in the immediate vicinity of the channel. In particular, formula (3.5) represents a reflection of one of these distributions of the thermal field in the surrounding mass.

The application of homogeneous boundary conditions reduces the problem of the solution of equations (3.9), (3.20), and the ones to follow to the problem of characteristic values, examples of which will be given later.

In certain cases boundary conditions of the different classes may be combined with each other. The solution of a linear differential equation simultaneously satisfying certain boundary conditions is equal to the sum of solutions each of which individually satisfies each class and form of boundary conditions. However, a physical sense will be possessed only by those solutions which correspond to the same values of the parameters  $A$  and  $k$ . This characteristic of the problem investigated differs from numerous popular problems connected with the investigation of the biharmonic equation, and the phenomena of heat transfer.

### 3. Basis of Solution Scheme

With account taken of the boundary conditions, the process of solution of the concrete problem can be indicated in the following manner. In the surrounding mass in the plane  $z = 0$ , the contour  $L(r, \varphi)$  is given of the section of the channel (fig. 3). We divide the contour into elements  $dl$ , the center of each element having the coordinates  $r$  and  $\varphi$ . Using expressions (3.29) and (3.31) and the general and special boundary conditions and having some value of  $A$  corresponding to  $k$ , we write the following equations for each of the elements:

$$\begin{aligned}
v_L = 0 = & \sum_{n=0}^{\infty} [a_{n1} J_n(ikr) \cos(n\varphi + \gamma_{n11}) + \\
& a_{n2} N_n(ikr) \cos(n\varphi + \gamma_{n12}) + \\
& b_{n1} J_n(-kr) \cos(n\varphi + \gamma_{n21}) + \\
& b_{n2} N_n(-kr) \cos(n\varphi + \gamma_{n22})] \quad (4.6)
\end{aligned}$$

$$\begin{aligned}
\theta_L = \frac{vk^2}{g\beta} & \sum_{n=0}^{\infty} [a_{n1} J_n(ikr) \cos(n\varphi + \gamma_{n11}) + \\
& a_{n2} N_n(ikr) \cos(n\varphi + \gamma_{n12}) - \\
& b_{n1} J_n(-kr) \cos(n\varphi + \gamma_{n21}) - \\
& b_{n2} N_n(-kr) \cos(n\varphi + \gamma_{n22})] \quad (4.7)
\end{aligned}$$

$$\left( \frac{d\theta}{dn} \right)_L = \left( \frac{\partial \theta}{\partial r} \times \frac{dr}{dn} + \frac{\partial \theta}{\partial \varphi} \times \frac{d\varphi}{dn} \right)_L \quad (4.8)$$

If the boundary conditions are not homogeneous, the left sides of equations (4.7) and (4.8) are given. If, however, the boundary conditions are homogeneous; in particular, if equation (4.5) holds, then instead of equations (4.7) and (4.8) (or in addition to them if the boundary conditions are mixed) the external problem equation (4.5) must be solved. The solution of this external problem will be in the cylindrical coordinates (eq. (3.25)) expressions of the form

$$\theta_e = Az + E \ln \frac{r}{R} + \sum_{n=1}^{\infty} [c_{n1} r^n \cos(n\varphi + \gamma_{n1}) + c_{n2} r^{-n} \cos(n\varphi + \gamma_{n2})] \quad (4.9)$$

The significance of the expression  $E \ln r/R$  will be discussed later (ch. 5, sec. 4); for the present, we assume that  $E = 0$ .

In this way, there is obtained a system of sets of equations (4.6) to (4.9), in the unknown constants

$$a_{n1}, a_{n2}, \dots, b_{n1}, b_{n2}, \dots, c_{n1}, c_{n2}, \dots,$$

and

$$\gamma_{n1}, \gamma_{n2}, \dots, \gamma_{n11}, \gamma_{n12}, \dots$$

The number of sets of these equations is equal to the number of elements  $d_l$  divided by the contour  $L$  of the cross section.

If it is found that these equations are simultaneous, the chosen value of  $k$  is suitable. In the contrary case, it is necessary to choose a new value of  $k$ , that is, of the temperature gradient  $A$ , and to repeat the operation of solving the equations.

In principle, even an infinitely large number of elements of the contour  $L$  can be treated with a finite degree of accuracy for each value of the parameter  $k$  by a finite number of mathematical operations (ref. 2). Hence, in any case the existence of a solution need not occasion any doubts.

#### 4. Method of Solution

In general, however, the solution according to the preceding scheme is very laborious. Hence, only those general considerations have significance which permit: (1) the separation of the typical cases for which the number of equations is essentially reduced and, (2) those cases which may serve as guides rendering the investigation of associated variants superfluous or essentially facilitating this investigation. The most important of these general considerations is the consideration of symmetry. In general, these considerations lead to a rational locating of the origin of coordinates and, also, to assigning a direction to the zero azimuth in order to eliminate, as far as possible, the azimuthal corrections  $\gamma_{n11}, \gamma_{n12}, \dots$

Later on in this report, examples of the application of these considerations will be given.

## CHAPTER 5

## STEADY CONVECTION IN VERTICAL CHANNEL OF ROUND SECTION

## 1. Diametral Antisymmetry of Free Convective Flow

For a channel of round cross section, on the basis of equations (3.19), (3.29), (3.30), and the general boundary condition 1, it is convenient to write:

$$v = v_0 \left[ \frac{J_0(ikr)}{J_0(ikR)} - \frac{J_0(kr)}{J_0(kR)} \right] + \left. \begin{aligned} &v_1 \left[ \frac{J_1(ikr)}{J_1(ikR)} - \frac{J_1(kr)}{J_1(kR)} \right] \cos \varphi + \\ &v_2 \left[ \frac{J_2(ikr)}{J_2(ikR)} - \frac{J_2(kr)}{J_2(kR)} \right] \cos 2\varphi + \dots \end{aligned} \right\} \quad (5.1)$$

The convenience of this expression lies in the circumstance that the boundary condition 3 (eq. (4.1)) is automatically satisfied for  $r = R$  at the channel wall. In this expression the Neumann functions are absent because of boundary condition 1, since these functions go to infinity at the origin when  $r \rightarrow 0$ . The direction of the XZ-plane from which the azimuthal angle  $\varphi$  is calculated is chosen from considerations of symmetry parallel to the external gradient. As special boundary conditions we assume, as in equation (4.5),

$$\frac{\partial \theta_e}{\partial z} = A; \quad \left( \frac{\partial \theta_e}{\partial x} \right)_{\infty} = -B \quad (5.2)$$

By equation (4.9), these conditions are rewritten as follows:

$$\theta_e = Az + \left( -Br + \frac{D}{r} \right) \cos \varphi \quad (5.3)$$

where  $D$  denotes an unknown coefficient. By equations (4.7) and (5.1) for the temperature within the channel, we obtain:

$$\theta = Az + \frac{\nu k^2}{g\beta} \left\{ v_0 \left[ \frac{J_0(ikr)}{J_0(ikR)} + \frac{J_0(kr)}{J_0(kR)} \right] + v_1 \left[ \frac{J_1(ikr)}{J_1(ikR)} + \frac{J_1(kr)}{J_1(kR)} \right] \cos \varphi + v_2 \left[ \frac{J_2(ikr)}{J_2(ikR)} + \frac{J_2(kr)}{J_2(kR)} \right] \cos 2\varphi + \dots \right\} \quad (5.4)$$

While in equation (5.1) it is still possible to substitute Neumann functions so that, by mutual compensation, they do not give infinity when  $r \rightarrow 0$ , they will necessarily, because of the sign change in the last equation, give infinity when  $r \rightarrow 0$ . For this reason, the coefficient of these functions in solution (5.1) must be identically equal to zero (i.e., these functions must be excluded from the solution).

In correspondence with the general boundary conditions equations (4.2) and (4.3) and substituting equations (5.3) and (5.4), we obtain for  $r = R$

$$\theta_+ - \theta_0 = 2 \frac{\nu k^2}{g\beta} v_1 = -BR + \frac{D}{R}; \quad (5.5)$$

$$\theta_+ \cos \varphi = (\theta)_{r=R}; \quad \theta_0 = (\theta)_{r=0}$$

$$-\frac{\lambda \nu k^2 v_1}{g\beta} \left\{ \frac{ik \left[ \frac{J_0(ikR)}{J_1(ikR)} - \frac{J_1(ikR)}{ikR} \right]}{J_1(ikR)} + \frac{k \left[ \frac{J_0(kR)}{J_1(kR)} - \frac{J_1(kR)}{kR} \right]}{J_1(kR)} \right\} = \lambda_e \left( -B - \frac{D}{R^2} \right) \quad (5.6)$$

$$v_0 = v_2 = \dots = 0 \quad (5.7)$$

Eliminating the coefficient  $D$  from equations (5.5) and (5.6), we obtain

$$\frac{\lambda \nu k^2 v_1}{\lambda_e g\beta} \left[ \frac{ikR J_0(ikR)}{J_1(ikR)} + \frac{kR J_0(kR)}{J_1(kR)} - 2 \right] = BR + \frac{D}{R} = 2BR - 2 \frac{\nu k^2 v_1}{g\beta} \quad (5.8)$$

or

$$BR^3 = \frac{\nu(kR)^2 v_1}{g\beta} \left\{ \frac{\lambda}{\lambda_e} \left[ \frac{ikR J_0(ikR)}{2J_1(ikR)} + \frac{kR J_0(kR)}{2J_1(kR)} - 1 \right] + 1 \right\} \quad (5.9)$$

From this equation it is seen that in the case under consideration, the laminar motion of the fluid (expressed by its "amplitude"  $v_1$ ) is uniquely determined by the following conditions: by the parameters of the fluid and thermal conductivity of the surrounding mass  $\lambda_e$ , by the diameter of the channel  $2R$ , and by the regime of its operation- the transverse gradient  $B$  and the longitudinal gradient  $A$  (through the parameter  $k$ ).

Because of this motion of the fluid, it will transfer upward by convection a quantity of heat determined by equation (3.23). If the equation is rewritten to apply to the given concrete case, the following equation is obtained:

$$\begin{aligned}
 Q &= \frac{\rho c v k^2 v_1^2}{g\beta} \int_S \int \left\{ \left[ \frac{J_1(ikr)}{J_1(ikR)} \right]^2 - \left[ \frac{J_1(kr)}{J_1(kR)} \right]^2 \right\} \cos^2 \varphi r dr d\varphi \\
 &= -\frac{\pi \rho c v v_1^2}{2g\beta} \left\{ \left[ \frac{kR J_0(ikR)}{iJ_1(ikR)} \right]^2 + \left[ \frac{kR J_0(kR)}{J_1(kR)} \right]^2 + 2 \left[ \frac{kR J_0(ikR)}{iJ_1(ikR)} - \frac{kR J_0(kR)}{J_1(kR)} \right] \right\}
 \end{aligned} \tag{5.10}$$

Eliminating  $v_1$  from equations (5.9) and (5.10) gives equations that permit expressing this heat directly in terms of the fluid parameters and the thermal conductivity of the surrounding mass, the channel diameter, and the channel operating regime. This elimination gives:

$$R^3 \sqrt{\frac{2\pi \rho c g \beta}{-v}} \times \frac{B}{\sqrt{Q}} = F_1(\xi) + \frac{\lambda}{\lambda_e} F_2(\xi) = G\left(\xi, \frac{\lambda}{\lambda_e}\right) \tag{5.11}$$

$$R^3 \sqrt{\frac{2\pi \rho c g \beta}{-v \lambda^2}} \times \frac{B \lambda_e}{\sqrt{Q}} = \frac{\lambda_e}{\lambda} F_1(\xi) + F_2(\xi) = H\left(\xi, \frac{\lambda}{\lambda_e}\right) \tag{5.12}$$

where the first factor on the left side is determined by the channel radius, the second by the fluid parameters, while the third connects the transverse temperature gradient  $B$  with the heat quantity  $Q$  transported by convection. On the right side we have a linear function of the ratio of the heat conductivity of the fluid  $\lambda$  to the heat conductivity of the surrounding mass  $\lambda_e$ ;  $F_1(\xi)$  and  $F_2(\xi)$  are coefficients of the function  $(\lambda_e)$  and were determined by the axial gradient of the temperature in terms of a nondimensional parameter such as equation (3.10):

$$\xi^4 = (kR)^4 = \frac{g\beta}{v\lambda} \times A \times R^4 \tag{5.13}$$

Table I gives the values of the functions

$$\left. \begin{aligned}
 F_1(\xi) &= \frac{2\xi^2}{\left[ \frac{\xi J_0(i\xi)}{-iJ_1(i\xi)} \right]^2 + \left[ \frac{\xi J_0(\xi)}{J_1(\xi)} \right]^2 - 2 \left[ \frac{\xi J_0(i\xi)}{-iJ_1(i\xi)} + \frac{\xi J_0(\xi)}{J_1(\xi)} \right]}^{1/2} \\
 F_2(\xi) &= \frac{1}{2} F_1(\xi) \times \left[ \frac{\xi J_0(i\xi)}{iJ_1(i\xi)} + \frac{\xi J_0(\xi)}{J_1(\xi)} - 2 \right] \\
 G \left( \xi, \frac{\lambda}{\lambda_e} \right) &= F_1(\xi) + \frac{\lambda}{\lambda_e} F_2(\xi) \\
 H \left( \xi, \frac{\lambda}{\lambda_e} \right) &= \frac{\lambda_e}{\lambda} F_1(\xi) + F_2(\xi)
 \end{aligned} \right\} (5.14)$$

4281

It is to be noted that for a considerable distance about the point  $\xi = 0$ , the dependence of  $F_1$ ,  $F_2$ ,  $G$ , and  $H$  on  $\xi^4$  is very nearly linear.

By analyzing the preceding computations, it may be established that the case discussed corresponded to the mixed special boundary conditions. In expression (5.5), the term  $BR$  represents the nonhomogeneous part of these conditions, and the term  $D/R$  represents their homogeneous part. For this reason, the coefficient  $D$  was excluded from further expressions and the coefficient  $B$  determined the final result of the computations.

Therefore, the purely homogeneous case, when  $B = 0$ , is of special interest. From equation (5.9) it is then seen that the expression in braces acquires the meaning of a fundamental equation for determining the "characteristic values" of the argument  $kR = \xi$ .

$$\xi \left[ \frac{J_0(i\xi)}{-iJ_1(i\xi)} + \frac{J_0(\xi)}{J_1(\xi)} \right] = 2 \left( 1 - \frac{\lambda_e}{\lambda} \right) \quad (5.15)$$

The value  $kR = 0$ , that is,  $A = 0$  for the condition  $B = 0$ , corresponds to the condition of complete isothermy and in steady state processes does not represent convective flow of the fluid.

The characteristic values of  $\xi$  of the transcendental equation (5.15) depend on the relation of the thermal conductivity of the fluid and of the surrounding mass as shown in table II and figure 4.

The azimuth  $\phi$  in this case drops out entirely from the computations. It is, mathematically speaking, arbitrary. The experiment is described in chapter 10, section 5.

It is important to note that the amplitude of the velocity  $v_1$  in this case is determined by the quantity of heat transferred by convection, that is, by equation (5.10) and not by equation (5.9) from which it drops out because of equation (5.15). Thus, within the range of the linearized treatment, it may be shown that the investigated form of convective flow can transfer arbitrarily large quantities of heat upward. As a matter of fact, for large velocities of fluid motion, we should expect some phenomena similar to turbulence. Due to this fact, the linear treatment becomes insufficient. Actually, both the velocities of the laminar flow and the quantity of heat transferred by convection are limited (ch. 10, sec. 3).

## 2. Criterional Significance of Convection Parameter

The structure of the parameter  $\xi^4$  follows from its criterional significance in the sense of the theory of similarity:

$$\xi^4 = (kR)^4 = \frac{g\beta AR^4}{\nu^2} \times \frac{\nu}{\alpha} = Gr \times Pr \quad (5.16)$$

The Grashof number  $Gr$  and the Prandtl number  $Pr$  in this combination (product) are the usual criteria of the theory of similarity when it is a question of the transfer of heat from solid bodies to fluids or conversely. In such cases this product plays the role as an argument and the Nusselt number as a function (ref. 1).

In this case, the Nusselt number is zero because there is no overall transfer of heat from the channel wall, the heat being transmitted upward by convection from one part of the fluid to another. In this heat transfer some significance may be ascribed to the Nusselt number, in particular, by denoting this number as the ratio of the heat transferred from the lower to the upper part of the liquid by convection plus molecular thermal conductivity, to the heat transfer only by molecular conductivity according to equations (3.23), (3.24), and (5.10)

$$Nu^{**} = 1 + \frac{Q}{Q_2} \quad (5.17)$$

However, since in the linear treatment the "amplitude" of the velocity  $v_1$  is obtained as arbitrary, and the value of  $Q$  is likewise arbitrary,  $Nu^{**}$  according to equation (5.17) becomes indeterminate.

4281

CA-5

On the other hand, the criterion  $\xi^4$  also acquires a special, double significance. In the first place, it is the criterion of stability of the fluid; and secondly, it is simultaneously the criterion of stability of the fluid motion. This subject will be discussed in more detail in chapter 10, sections 1 and 3. Few other examples are known of such coincidence in one numerical value of different meaning contents of this criterion.

In the absence of an axial gradient, for  $A = 0$  (i.e., for  $\xi = 0$ ), the transverse temperature gradient  $B$  uniquely determines the quantity of heat transferred upward by convection. Letting  $\xi \rightarrow 0$  in expressions (5.1) and (5.4), we obtain

$$\left. \begin{aligned} v &\rightarrow v_{11} \frac{r}{R} \left[ 1 - \left( \frac{r}{R} \right)^2 \right] \cos \varphi \\ \theta &\rightarrow -8v_{11} \frac{v}{g\beta R^2} \times \frac{r}{R} \cos \varphi \\ BR^3 &\rightarrow 4 \frac{v v_{11}}{g\beta} \left[ 1 + \frac{\lambda}{\lambda_e} \right] \end{aligned} \right\} \quad (5.18)$$

where  $v_{11}$  represents a new limiting "amplitude" of the process. The quantity of heat transferred is determined by expression (3.23)

$$Q = \rho c \int_0^R \int_0^{2\pi} v \theta r \, dr \, d\varphi = \frac{1}{48} \times \frac{g\beta}{v\lambda} \times \frac{B^2}{\frac{1}{\lambda} + \frac{1}{\lambda_e}} \times R^6 \quad (5.19)$$

Note that the fluid motion in this case recalls the Poiseuille case in many respects, and the temperature distribution is the same as it would be in a solid body.

The case discussed here is diametrically antisymmetrical about the Y-axis, both with respect to the velocities and the temperatures, as seen from equations (5.1), (5.4), and (5.7). Hence, the total-volume flow  $V$  of the fluid and the over-all heat interchange of the fluid with the channel walls, according to equation (3.22), is equal to zero, the duct is "closed"; we are dealing exclusively with free convection.

As an example, figure 5 shows the distribution of velocities, temperatures, and heat flows in a circular channel for the case where  $\lambda = \lambda_e$  as a function of the distance from the channel axis (i.e., in a meridional section). The line of temperatures is prolonged into the

surrounding mass outside the channel boundary. Figure 6 shows the distribution of the same magnitudes in the form of isolines in the plane where  $z = 0$ ; the isotherms again being prolonged into the surrounding mass. Figure 7 shows the same curves as figure 5 to a larger arbitrary scale.

### 3. Thermal Role of Pipe Walls<sup>3</sup>

If the phenomenon under investigation is observed in a channel which is not drilled in a dense block but in a pipe inserted in a block, the value of  $\lambda$  entering formula (5.6) and the others will depend on the thermal conductivity of the material of the pipe  $\lambda_1$ , of the block  $\lambda_2$ , as well as on the pipe radii, the internal radius  $R$ , the external radius  $R_1$ , and on the temperature gradient  $B_2$  in the surrounding mass. Let us find to what equivalent value of the thermal conductivity  $\lambda_e$  the thermal conductivity of the pipe and also the equivalent value of the gradient  $B$  correspond.

By considering the fact that for the case of a pipe no heat sources are assumed to be either in the pipe or in the surrounding mass, then

$$\Delta\theta_1 = \Delta\theta_2 = \Delta\theta_e = 0 \quad (5.20)$$

we find, with similarity to equation (5.3)

$$\left. \begin{aligned} \theta_1 &= \left(-B_1 r + \frac{D_1}{r}\right) \cos \varphi + Az \\ \theta_2 &= \left(-B_2 r + \frac{D}{r}\right) \cos \varphi + Az \end{aligned} \right\} \quad (5.21)$$

The temperatures inside the pipe  $\theta_1$  and outside the pipe  $\theta_2$  join each other at the outer boundary of the pipe at the radius  $R_1$  without fluctuations in the temperature and thermal flow

$$\left. \begin{aligned} \theta_e &= -B_1 R_1 + \frac{D_1}{R_1} = -B_2 R_1 + \frac{D_2}{R_1} \\ \lambda_1 \left(-B_1 - \frac{D_1}{R_1^2}\right) &= \lambda_2 \left(-B_2 - \frac{D_2}{R_1^2}\right) \end{aligned} \right\} \quad (5.22)$$

<sup>3</sup>This section utilizes data from the work of V. V. Slavnov.

At the inner surface of the pipe the temperature of its material unites with the fluid temperature in such a manner as though a channel were drilled in a dense mass with the temperature conductivity  $\lambda_e$  and the channel temperature  $\theta_e$ :

$$\left. \begin{aligned} \theta_e &= -B_1 R + \frac{D_1}{R} = -BR + \frac{D}{R} \\ \lambda_1 \left( -B_1 - \frac{D_1}{R^2} \right) &= \lambda_e \left( -B - \frac{D}{R^2} \right) \end{aligned} \right\} \quad (5.23)$$

There is thus obtained a system of four simultaneous equations connecting the following 11 magnitudes:

$$\begin{array}{ccc} B & B_1 & B_2 \\ D & D_1 & D_2 \\ \lambda_e & \lambda_1 & \lambda_2 \\ R & R_1 & \end{array}$$

Of these,  $R$ ,  $R_1$ ,  $\lambda_1$ ,  $\lambda_2$ , and  $B_2$  are given; the unknowns are  $B$  and  $\lambda_e$ . It may thus appear that the four equations are not sufficient for eliminating the excess unknowns  $B_1$ ,  $D$ ,  $D_1$ , and  $D_2$ . The structure of equations (5.22) and (5.23) is such, however, that it is possible to proceed without these eliminations.

In fact, eliminating the expressions  $D_2 \lambda_2 / R_1^2$  and  $D \lambda_e / R^2$  from equations (5.22) and (5.23), respectively, we obtain

$$\left. \begin{aligned} B_1(\lambda_1 + \lambda_2) - \frac{D_1}{R_1} (\lambda_2 - \lambda_1) - 2\lambda_2 B_2 &= 0 \\ B_1(\lambda_1 + \lambda_e) - \frac{D_1}{R^2} (\lambda_e - \lambda_1) - 2\lambda_e B &= 0 \end{aligned} \right\} \quad (5.24)$$

Now through elimination of the expression  $\frac{D_1}{R_1 R^2} \times (\lambda_2 - \lambda_1)(\lambda_e - \lambda_1)$  from the latter equations, we obtain

$$B_1 \left[ \frac{(\lambda_1 + \lambda_2)(\lambda_e - \lambda_1)}{R^2} - \frac{(\lambda_1 + \lambda_e)(\lambda_2 - \lambda_1)}{R_1^2} \right] = 2 \left[ \frac{B\lambda_e(\lambda_2 - \lambda_1)}{R_1^2} - \frac{B_2\lambda_2(\lambda_e - \lambda_1)}{R^2} \right] \quad (5.25)$$

Whatever the values ascribed to the magnitude  $B_1$ , equation (5.25) remains valid if we assume

$$\frac{(\lambda_1 + \lambda_2)(\lambda_e - \lambda_1)}{R^2} - \frac{(\lambda_1 + \lambda_e)(\lambda_2 - \lambda_1)}{R_1^2} = \frac{B\lambda_e(\lambda_2 - \lambda_1)}{R_1^2} - \frac{B_2\lambda_2(\lambda_e - \lambda_1)}{R^2} = 0 \quad (5.26)$$

then, the final expressions are obtained

$$\left. \begin{aligned} \frac{\lambda_e}{\lambda_1} &= \frac{\frac{\lambda_2}{\lambda_1} \left[ 1 + \left( \frac{R}{R_1} \right)^2 \right] + \left[ 1 - \left( \frac{R}{R_1} \right)^2 \right]}{\frac{\lambda_2}{\lambda_1} \left[ 1 - \left( \frac{R}{R_1} \right)^2 \right] + \left[ 1 + \left( \frac{R}{R_1} \right)^2 \right]} \\ \frac{B}{B_2} &= \left( \frac{R_1}{R} \right)^2 \times \frac{\frac{\lambda_2}{\lambda_1} \left[ 1 + \left( \frac{R}{R_1} \right)^2 \right]}{\frac{\lambda_2}{\lambda_1} \left[ 1 + \left( \frac{R}{R_1} \right)^2 \right] + \left[ 1 - \left( \frac{R}{R_1} \right)^2 \right]} \end{aligned} \right\} \quad (5.27)$$

By using these equations, tests conducted in pipes may be compared with the theory worked out for a channel in a dense homogeneous block. We remark again that the case considered here is that of diametrically antisymmetrical convection.

#### 4. Superposition of Forced and Free Thermal Convection

In contrast to the previously discussed case, we shall now consider the case where the fluid in an open channel is drawn by an outside pump. In this case we are justified in expecting the superposition of forced and free convection. In equation (3.1) an essential part is then played by the pressure produced by the pump; and for the vertical channel, we must write in place of equation (3.7)

$$-\frac{1}{\rho} \times \frac{\partial p}{\partial z} - g\beta\theta + \nu\Delta v = 0 \quad (5.28)$$

Equation (3.8) remains valid

$$Av = \kappa \Delta \theta; \quad v = \frac{\kappa}{A} \Delta \theta \quad (5.29)$$

Eliminating  $v$  from these equations, we get

$$\Delta \Delta \theta - \frac{g\beta A}{\nu \kappa} \theta = \frac{A}{\rho \nu \kappa} \times \frac{\partial p}{\partial z} \quad (5.30)$$

The preceding incomplete biharmonic equation is linear, but nonhomogeneous by the assumptions made; the right side of the equation is not zero. Guided by the usual rules we first seek a solution of the homogeneous equation coinciding in form with equation (3.9):

$$\Delta \Delta \theta_0 - k^4 \theta_0 = 0 \quad (5.31)$$

By bearing in mind that for a vertical channel the condition  $\partial p / \partial x = \partial p / \partial y = 0$ ,<sup>4</sup> is observed, then, by analogy with equation (3.19) and in correspondence with equation (3.20), and by making use of the general rules of solving nonhomogeneous equations, we obtain the following conditions:

$$\theta_0 = \theta_1 + \theta_2; \quad \theta = \theta_0 + Az = \theta_0 - \frac{1}{\rho g \beta} \times \frac{\partial p}{\partial z} \quad (5.32)$$

whence

$$\frac{\partial p}{\partial z} = -\rho g \beta Az; \quad p = -\frac{1}{2} \rho g \beta Az^2 \quad (5.33)$$

Integration of equation (5.33) provides the assumption that the pressure produced by the action of the pump drops to zero precisely in the plane  $z = 0$ , or in other words, that the  $XY$  plane passes through that section of the channel which is considered the origin of the pressure computation.

In comparing this result with the case discussed previously we note that this case does not introduce any new terms in the solution of the equations.

The forced pumping of the fluid does not show up in the pressure or in new terms in the solutions, but only in the added quantity of heat which the pumped fluid transmits to the walls, and only in the flow rate of the pumped fluid (according to equation (3.22)). In particular, the

<sup>4</sup>Due to the fact that all the vectors in equation (3.1) are collinear.

Poiseuille case corresponds to  $A \rightarrow 0$  and  $k \rightarrow 0$ , and it is obtained if the following formulas employ a series expansion of Bessel functions, which consider only the first two terms.

$$J_0(u) \underset{u \rightarrow 0}{\rightarrow} 1 - \frac{1}{4} u^2 \quad (5.34)$$

Using equations (5.32) and (3.14) as well as equation (3.10), we obtain the same form of solution, namely,

$$v = v_0 \left[ \frac{J_0(ikr)}{J_0(ikR)} - \frac{J_0(kr)}{J_0(kR)} \right] + v_1 \left[ \frac{J_1(ikr)}{J_1(ikR)} - \frac{J_1(kr)}{J_1(kR)} \right] \cos \varphi + v_2 \left[ \frac{J_2(ikr)}{J_2(ikR)} - \frac{J_2(kr)}{J_2(kR)} \right] \cos 2\varphi + \dots \quad (5.35)$$

$$\theta = Az - \frac{vk^2}{g\beta} \left\{ v_0 \left[ \frac{J_0(ikr)}{J_0(ikR)} + \frac{J_0(kr)}{J_0(kR)} \right] + v_1 \left[ \frac{J_1(ikr)}{J_1(ikR)} + \frac{J_1(kr)}{J_1(kR)} \right] \cos \varphi + v_2 \left[ \frac{J_2(ikr)}{J_2(ikR)} + \frac{J_2(kr)}{J_2(kR)} \right] \cos 2\varphi + \dots \right\} \quad (5.36)$$

As special boundary conditions, which now are more exactly specified, equation (4.9) is used

$$\theta_e = Az + \left( -Br + \frac{D}{r} \right) \cos \varphi + E \ln \frac{r}{R} + \theta_{e0} \quad (5.37)$$

On the basis of the general boundary conditions (eqs. (4.2) and (4.3)), we write

$$\begin{aligned} \theta_R &= Az + 2 \frac{vk^2}{g\beta} (v_0 + v_1 \cos \varphi + v_2 \cos 2\varphi + \dots) \\ &= Az + \left( -BR + \frac{D}{R} \right) \cos \varphi + \theta_{e0} \end{aligned} \quad (5.38)$$

$$\begin{aligned} \frac{\lambda vk^3}{g\beta} v_0 \left[ \frac{iJ_1(ikR)}{J_0(ikR)} + \frac{J_1(kR)}{J_0(kR)} \right] + v_1 \left[ -\frac{J_0(ikR)}{iJ_1(ikR)} + \frac{J_0(kR)}{J_1(kR)} - 2 \right] \cos \varphi &= \lambda_e \left[ \left( -B - \frac{D}{R^2} \right) \cos \varphi + \frac{E}{R} \right] \end{aligned} \quad (5.39)$$

Eliminating  $D$  from the preceding equation, we again obtain equation (5.8); instead of equation (5.7), only  $v_2 = 0$  remains. Moreover, there is found

$$2 \frac{vk^2 v_0}{g\beta} = \theta_{e0} \quad (5.40)$$

$$\frac{\lambda}{\lambda_e} \times \frac{\theta_{0e}}{2} \left[ \frac{iJ_1(ikR)}{J_0(ikR)} + \frac{J_1(kR)}{J_0(kR)} \right] = \frac{E}{R} \quad (5.41)$$

The total volume of fluid pumped upward through the channel, according to equations (3.21) and (5.41), is computed to be

$$\begin{aligned} \frac{V}{t} &= \int_0^R \int_0^{2\pi} v r dr d\phi = 2\pi v_0 \int_0^R \left[ \frac{J_0(ikr)}{J_0(ikR)} - \frac{J_0(kr)}{J_0(kR)} \right] r dr \\ &= - \frac{2\pi v_0 R^2}{kR} \left[ \frac{iJ_1(ikR)}{J_0(ikR)} + \frac{J_1(kR)}{J_0(kR)} \right] = \frac{2\pi \lambda_e E}{\rho c A} \end{aligned} \quad (5.42)$$

On the basis of equation (3.22), the physical sense of the magnitude  $E$  is determined from equation (4.9).

$$-2\pi \lambda_e h E = Q_1 \quad (5.43)$$

namely, this magnitude in a certain scale is equal to the heat flow passing through from the channel walls into the fluid over a distance of 1 centimeter of the channel height. There is thus established a relation between  $Q_1$ ,  $E$ , and  $A$ , (i.e.,  $k$ ). The term containing  $v_0$  describes both the free and forced part of the convective flow, but it is equal to zero in the absence of forced convection. The phenomenon described by this term possesses a strict axial symmetry.

In the absence of a transverse gradient,  $B = 0$ , either  $v_1 = 0$  or the considerations leading to equation (5.15) are valid. The term containing  $v_1$  describes only the free part of the convective process.

It is again necessary to emphasize that the magnitude  $kR$  in all terms of equations (5.35), (5.36) and so forth has the same value.

As an example, figure 8 shows the results of a computation of several cases for the condition of absence of a horizontal gradient  $v_1 = 0$  and  $B = 0$ . On the axis of abscissa is laid off the value of  $v_m$  to an

arbitrary scale and on the axis of ordinates the parameter  $(kR)^4$ , proportional to the vertical gradient  $A$ , is laid off. The figure shows several points in these coordinates and together with these shows the corresponding velocity distributions (solid curves) and temperatures (dotted curves) along the channel diameter. The equivalent Poiseuille parabola is drawn on each sketch. The coordinates of the selected points and some numerical data for this figure are given in tables III, IV, and V.

### 5. Application of Cylindrical Functions of Complex Variable

Where Temperature in the Upper Part of Vertical

Channel is Higher Than in the Lower Part

In the computations, the case must be encountered where  $A$  is greater or less than zero so that  $(kR)^4$  receives a positive or negative sign. The computations are carried out with the aid of the same Bessel function tables (ref. 2), bearing in mind the following circumstances. In equation (5.1) and further on, the magnitudes  $\pm ikR$  and  $\pm kR$  are roots of the characteristic equation (3.10)

$$(kR)^4 = \frac{g\beta AR^4}{\nu\kappa} \quad (5.44)$$

for the differential equation (3.9). If we denote

$$|kR|^4 = |\xi|^4 = \frac{g\beta(-A)R^4}{\nu\kappa} \quad (5.45)$$

its corresponding roots will be

$$\xi_{12} = \pm \sqrt{i}\xi; \quad \xi_{34} = \pm \sqrt{-i}\xi$$

$$\sqrt{i} = \frac{1+i}{\sqrt{2}}; \quad \sqrt{-i} = \frac{1-i}{\sqrt{2}} = -i\sqrt{i} \quad (5.46)$$

Hence, in equation (5.1) and so forth, it is now necessary to write  $J_0(\sqrt{i}kr)$  in place of  $J_0(ikr)$ , and  $J_0(\sqrt{-i}kr)$  in place of  $J_0(kr)$  and so forth, where it is useful to remember that

$$J_0^*(\sqrt{-i}kr) = J_0(\sqrt{i}kr); \quad J_1^*(\sqrt{-i}kr) = J_1(\sqrt{i}kr) \quad (5.47)$$

with the asterisk denoting the conjugate value of the complex magnitude. In the expressions similar to equation (5.1) and so forth, terms of the following form will enter:

$$\begin{aligned} \frac{J_n(\sqrt{ikr})}{J_n(\sqrt{ikR})} - \frac{J_n(\sqrt{-ikr})}{J_n(\sqrt{-ikR})} &= \frac{J_n^*(i\sqrt{ikr})}{J_n^*(i\sqrt{ikR})} - \frac{J_n(i\sqrt{ikr})}{J_n(i\sqrt{ikR})} \\ &= \left[ \frac{J_n(i\sqrt{ikr})}{J_n(i\sqrt{ikR})} \right]^* - \frac{J_n(i\sqrt{ikr})}{J_n(i\sqrt{ikR})} \end{aligned} \quad (5.48)$$

4281

In particular, for  $n = 0$

$$\left[ \frac{J_0(i\sqrt{ikr})}{J_0(i\sqrt{ikR})} \right]^* - \frac{J_0(i\sqrt{ikr})}{J_0(i\sqrt{ikR})} = 2i \frac{\text{ber}(kr) \times \text{bei}(kR) - \text{bei}(kr) \times \text{ber}(kR)}{\text{ber}(kR)^2 + \text{bei}(kR)^2} \quad (5.49)$$

Correspondingly, in expressions similar to equation (5.4) and so forth, there enter the terms

$$ik^2 \left\{ \left[ \frac{J_0(i\sqrt{ikr})}{J(i\sqrt{ikR})} \right]^* + \frac{J_0(i\sqrt{ikr})}{J(i\sqrt{ikR})} \right\} = 2ik^2 \frac{\text{ber}(kr) \times \text{ber}(kR) + \text{bei}(kr) \times \text{bei}(kR)}{\text{ber}(kR)^2 + \text{bei}(kR)^2} \quad (5.50)$$

Thus, the expressions for the velocities and temperatures are obtained as real only in the case where the "amplitudes" of the velocity  $v_0$  are assigned purely imaginary values.

The symbols  $\text{ber}$  and  $\text{bei}$  denote the cylindrical functions of Thomson.

These formulas were used in drawing the figures and in some of the tables.

## CHAPTER 6

UNSTEADY REGIME OF GRAVITATIONAL THERMAL CONVECTION IN  
VERTICAL CHANNEL OF ROUND CROSS SECTION

## 1. General Observations

Let us consider a block in which a vertical cylindrical duct or channel has been drilled, and consider also a certain temperature gradient characterized at infinity and produced by both the vertical component A and the horizontal component B according to equation (5.2). Into this channel a heated (or cooled) fluid is suddenly introduced. Since the channel walls are colder (or warmer) relative to the fluid, thermal convection in the fluid may be set up under known conditions. This convection will transfer heat upward and, thus, distribute the temperature further. If we are dealing with a casting poured into a cold form or mold, this redistribution may influence the development of the process of solidification of the melt. We shall not consider the process of solidification associated with the heat of fusion. We shall restrict ourselves to the case where  $B = 0$ .

## 2. Periodic Process of Cooling Nonsolidified Casting

For simplifying the computations the following periodic process is assumed, which is probably typical. However, other typical processes with their own periods are possible.

The first stage of the process will be that of filling the channel with a strongly turbulent fluid which, on coming in contact with the channel walls, is simultaneously cooled. Because of the strong turbulence of a nonthermal origin, effective thermal conductivity and diffusivity of the fluid will be much higher than those tabulated (molecular). Such a fluid will, therefore, in the thermal relation, represent the analog of a strong heat-conducting-solid body which had been cooled after a sudden heat impulse was imparted on the axis of a cylindrical system of coordinates. Such a thermal process has been investigated well and is discussed in the following paragraphs. The deciding factor in the process is the increase in the turbulence coefficient of the thermal

4281

CA-6 back

diffusivity of the fluid. Particularly, simple relations are obtained in the case where the form into which the fluid is poured does not constitute an infinitely extended homogeneous body but may be considered as a thin-walled vessel more or less thermally insulated from an infinite reservoir of constant temperature.

As a whole, the first stage is characterized by the fact that its violent mechanical nonthermal processes have excluded the possibility of the occurrence of a more or less definite convective thermal motion. The duration of the first stage is determined by the lessening in the fluid of turbulent motion and by the decrease of the thermal diffusivity of the fluid.

The second stage sets in when the turbulent motion is essentially ended, and the thermal convective motion is initiated and develops within the frame of the thermal pattern produced during the first stage. The transfer of this heat by convection is not, however, large at this time, and no essential distribution of the temperature has been produced during this time. The duration of the second stage is determined by the magnitude of the kinematic viscosity of the fluid, that is, by the ratio between the forces of inertia and friction.

Finally, the forces of inertia in the convective motion practically dwindle to nothing. A more or less stable convective motion is established which gradually dies down as the temperature differences produced diminish. As a result, the convective orderly transfer of heat distributes the temperature; the upper part becoming warmer than the lower. The distribution proceeds slowly as compared with the rate of cooling of the fluid in a cross section. This distribution constitutes the third, and last, stage of the process. The character of the third stage depends on the cross-sectional mean temperature distribution produced at the start of this stage. It is possible that, in the course of the third stage, the character of the process will slowly change as a result of the process of the upward heat transfer. Moreover, the character of the third stage depends on the absolute rate of cooling, that is, on the intensity of the heat removed from the fluid by the channel walls. In this connection it is desirable to investigate two variants, one of which is rapid and the other slow.

### 3. First Stage - Pouring Strongly Turbulent Hot Fluid

In the case of infinite extension of the surrounding mass, the process in it is described at small distances from the channel and at the initial instants by the following function of the distance and the time (refs. 1 to 3).

$$\left. \begin{aligned} \theta_{e1} &= \frac{Q}{4\pi\kappa_e t} e^{-\frac{r^2}{4\kappa_e t}} \\ r &< h \\ t &< \frac{h^2}{4\kappa_e} \end{aligned} \right\} \quad (6.1)$$

If the channel were infinite, that is, if the distances of interest  $r$  were always much less than the channel height  $h$ , this formula would be very accurate. If, however, the channel height is not large as compared with the distance at which the temperature still plays an essential role, then at distances greater than  $h$ , the channel in the infinite surrounding mass resembles a point. This relation then holds

$$\left. \begin{aligned} \theta_{e2} &= \frac{Q}{pc} \frac{e^{-\frac{r^2}{4\kappa_e t}}}{(4\pi\kappa_e t)^{3/2}} \\ r &> h \\ t &> \frac{h^2}{4\kappa_e} \end{aligned} \right\} \quad (6.2)$$

Because of the cylindrical field of the temperature distribution, equation (6.1) goes over into the spherical distribution equation (6.2), approximately at that instant, then

$$t_1 \approx \frac{h^2}{4\kappa_e} \quad (6.3)$$

the temperature path equation (6.1) near the instant  $t_1$  in the channel neighborhood will change gradually and in the limit go over into equation (6.2).

In these formulas  $Q$  represents the heat content of the fluid poured into the channel,

$$Q = \pi R^2 h p c (\theta_H - \theta_{e\infty}) \quad (6.4)$$

where  $\theta_H$  is the initial fluid temperature, and  $\theta_{e\infty}$  the mean temperature of the fluid walls and the surrounding mass. The process of

cooling at each distance  $r$  is characterized by its specific time, formulas (6.1) and (6.2),

$$t = \frac{r^2}{4\kappa_e} \quad (6.5)$$

The thermal behavior of the channel fluid can hardly be described by mathematical formulas in the first stage of the process. It may be assumed that it is approximately described by formula (6.1). This description will be sufficiently accurate for those instants of time  $t$  where

$$\frac{R^2}{4\kappa_e} = t_3 < t > t_2 = \frac{R^2}{4\kappa} \quad (6.6)$$

that is, after the passage of the characteristic cooling time at the channel walls ( $r = R$ ). The symbol  $\kappa$  denotes the heat conductivity of the fluid increased by the turbulence. Expanding the exponential function in equation (6.1) into a series, we may write

$$\theta \approx \frac{Q}{\rho ch} \frac{1}{4\pi\kappa_e t} \left[ 1 - \frac{t_2}{t} \left( \frac{r}{R} \right)^2 \right] \quad (6.7)$$

The distribution of the fluid temperature thus tends to the parabolic law. The height of the corresponding paraboloid gradually decreases with time according to the hyperbolic law

$$\theta \approx \theta_H \frac{t_3}{t} \left[ 1 - \frac{t_2}{t} \left( \frac{r}{R} \right)^2 \right] \quad (6.8)$$

Hence, the total temperature decreases with time according to the  $-3/2$  power, analogous to equation (6.2).

If the fluid is poured into a channel of a heat insulated pipe, the equation describing its cooling process will be (2.2) for  $v = 0$ . The boundary conditions are homogeneous

$$\left( \frac{\partial \theta}{\partial r} \right)_{r=R} = - \frac{\theta_{r=R}}{H} \quad (6.9)$$

where  $H$  denotes the "reduced" thickness of the heat insulation. Because equation (2.2) has now become linear and homogeneous and because of the homogeneity of the boundary conditions, we assume the exponential dependence of the temperature on the time. For this purpose, we rewrite equation (2.2) thus

$$\Delta \theta = \frac{1}{\kappa} \dot{\theta} \quad (6.10)$$

4281

The solution, similar to equation (3.26), is

$$\theta = \sum_{m=1}^{\infty} \theta_{Hm} e^{q_m t} J_0 \left( \sqrt{\frac{q_m}{\kappa}} r \right) \quad (6.11)$$

It is rendered exact by the boundary conditions equation, (6.9) which assume the following concrete form:

$$\left. \begin{aligned} \sum_m \sqrt{\frac{-q_m}{\kappa}} J_1 \left( \sqrt{\frac{-q_m}{\kappa}} R \right) &= \frac{1}{H} \sum_m J_0 \left( \sqrt{\frac{-q_m}{\kappa}} R \right) \\ \frac{\sum_m \sqrt{\frac{-q_m}{\kappa}} R \times J_1 \left( \sqrt{\frac{-q_m}{\kappa}} R \right)}{\sum_m J_0 \left( \sqrt{\frac{-q_m}{\kappa}} R \right)} &= \frac{R}{H} \end{aligned} \right\} \quad (6.12)$$

The extreme values of the nondimensional parameter that enters here will be:

when  $H \rightarrow \infty$ ;

$$\sqrt{\frac{-q_m}{\kappa}} \times R \rightarrow 0$$

$$q_m \rightarrow 0$$

when  $H \rightarrow 0$ ;

$$J_0 \left( \sqrt{\frac{-q_m}{\kappa}} R \right) \rightarrow 0$$

$$\sqrt{\frac{-q_m}{\kappa}} R \rightarrow \alpha_m = 2.405, 5.520, \dots$$

(6.13)

In the last and least favorable case, the exponent rapidly increases with the number of the term of the summation equation (6.11). For example,

$$q_2 = \left( \frac{5.520}{2.405} \right)^2 q_1 = 5.25q_1 \quad (6.14)$$

4281

Therefore, in expression (6.11) the second term will decrease much more rapidly than the first. In particular, when the first term decreases to  $1/e$  times the initial value, the second term decreases to  $e^{-5.25} \approx 1/300$  of its initial value. The smaller will then be the values of the following terms of equation (6.11). We shall, therefore, use only the first term of the sum of equation (6.11), and write

$$\theta \approx \theta_H e^{q_1 t} J_0 \left( \sqrt{\frac{-q_1}{\kappa}} \times r \right) \approx \theta_H e^{q_1 t} \left[ 1 - \frac{(-q_1)R^2}{4\kappa} \times \left( \frac{r}{R} \right)^2 \right] \quad (6.15)$$

Comparing this expression with equation (6.8), we recognize the quadratic term in the brackets and the dependence on the time given by the factor before the brackets. In contrast to equation (6.8), however, the form of the paraboloid now no longer changes with time, but the time dependence is greater than in the exponential formula (6.8).

The duration of the first stage in the case of the heat insulated pipe may be roughly estimated by the characteristic, that at the instant of its completion all terms of equation (6.11) starting with the second term are less than  $1/e$  times their initial value. This characteristic determines the duration of the first stage in the least favorable case thus

$$t_4 = \frac{1}{-q_1} \approx \frac{R^2}{\kappa(5.25)^2} \approx \frac{R^2}{27.5\kappa} \quad (6.16)$$

Generally, however, the duration of the first stage will be shorter. The similarity of the expressions in equations (6.7), (6.8), and (6.15) permits assuming an approximation for the computations

$$e^{-t_2/t} \approx J_0(kR) \quad (6.17)$$

In this case, the duration of the first stage is evaluated by formula (6.6).

All the preceding considerations show that the corresponding formulas exclusively describe the dying down of the process  $q_1 < 0$ . Thus, at the end of the first stage the distribution of the temperatures over the channel radius is always found to approximate the parabolical.

#### 4. Second Stage - Developing Free Convective Motion

The second stage under conditions of fluid laminar motion is described by the equations in which the fluid parameters correspond to their steady, molecular (tabulated) values. Because at the end of the first

stage the temperature distribution over the channel cross section is the same in all cases (namely, approximately parabolical), to determine the maximum duration of the second stage it is necessary to treat only the single equation, so that

$$\dot{v} = -\frac{1}{\rho} \times \frac{dp}{dz} - g\beta\theta + v\Delta v \quad (6.18)$$

The second stage includes the steady state of motion described by equation (6.18). The duration of this stage, speaking generally, is not determined by the forces ( $g\beta\theta$ ) which give rise to it, but is determined by the fluid properties ( $v$ ) and the form of the fluid flow. Hence, we assume

$$\left. \begin{aligned} v &= (u + u_0)e^{qt} \\ qu_0 &= v\Delta u_0 \end{aligned} \right\} \quad (6.19)$$

where  $u$  represents the effect of the pressure gradient and  $u_0$  represents the solution of a homogeneous equation similar to equation (6.10)

$$u_0 = u_1 J_0 \left( \sqrt{\frac{-g}{\nu}} r \right) \quad (6.20)$$

The solution is made exact by the following two boundary conditions; namely, the presence of an adhering layer and the closeness of the channel cavity. The first condition gives

$$(v)_{r=R} = \left[ u + u_1 J_0 \left( \sqrt{\frac{-g}{\nu}} R \right) \right] e^{qt} = 0 \quad (6.21)$$

The second condition gives

$$\int_0^R \int_0^{2\pi} vr \, dr \, d\varphi = \left[ 2\pi \frac{R^2 u}{2} + u_1 \frac{J_1 \left( \sqrt{\frac{-g}{\nu}} \times R \right)}{\sqrt{\frac{-g}{\nu}} \times R} 2\pi R^2 \right] e^{qt} = 0 \quad (6.22)$$

Whence, eliminating the ratio  $u/u_1$ , we obtain

$$2 \sqrt{\frac{-g}{\nu}} R J_0 \left( \sqrt{\frac{-g}{\nu}} R \right) = J_1 \left( \sqrt{\frac{-g}{\nu}} R \right) \quad (6.23)$$

By considerations analogous to those adduced in connection with equation (6.15) and the adjoining equations, the smallest root (besides

4281

CA-7

$q = 0$ ) of this transcendental equation is of interest. Computations give as its value

$$\left. \begin{aligned} \sqrt{\frac{-q}{\nu}} R &= 5.127 \\ q &= -\frac{26.49\nu}{R^2} \\ t &\approx \frac{1}{-q} = \frac{R^2}{26.49\nu} \end{aligned} \right\} \quad (6.24)$$

4281

Because for the majority of fluids  $\nu/\kappa = Pr$  is greater than unity, the duration of the second stage is less than that of the first stage (eq. (6.16)).

### 5. Third Stage - Cooling Fluid in the Presence of Convection

#### Rapid Variant

The third stage is characterized by the parallel dying down of both the thermal and the hydrodynamic phenomena. Denoting the general damping exponent by  $q$ , we write in place of equations (2.1) and (2.2)

$$\left. \begin{aligned} qv &= -g\beta\theta + \nu\Delta v \\ q\theta + Av &= \kappa\Delta\theta \end{aligned} \right\} \quad (6.25)$$

the motion of the fluid being assumed laminar.

In these expressions the considerations connected with the derivation of formulas (5.33), (3.7), and (3.8) are taken into account and, therefore, the pressure term is omitted. Eliminating  $\theta$  from these equations, we obtain successively

$$\theta = \frac{1}{g\beta} (\nu\Delta v - qv) \quad (6.26)$$

$$q(\nu\Delta v - qv) + g\beta Av = \kappa(\nu\Delta\Delta v - q\Delta v) \quad (6.27)$$

$$\Delta\Delta v - q\left(\frac{1}{\nu} + \frac{1}{\kappa}\right)\Delta v + \frac{q^2 - g\beta A}{\nu\kappa} v = 0 \quad (6.28)$$

This is a complete biharmonic homogeneous equation. We shall solve it by a widely used symbolic device explained in deriving equation (3.19). We set

$$\left. \begin{aligned} (\Delta + k_1^2)(\Delta + k_2^2)v &= \Delta\Delta v + (k_1^2 + k_2^2)\Delta v + k_1^2 k_2^2 v = 0 \\ \Delta v_1 + k_1^2 v_1 &= 0 \\ \Delta v_2 + k_2^2 v_2 &= 0 \end{aligned} \right\} v = v_1 + v_2 \quad (6.29)$$

Comparing equations (6.28) with equation (6.29) and multiplying  $k_1$  and  $k_2$  by  $R$ , we obtain

$$\begin{aligned} x + y &= (k_1 R)^2 + (k_2 R)^2 = -qR^2 \left( \frac{1}{v} + \frac{1}{\kappa} \right) \\ xy &= (k_1 R)^2 \times (k_2 R)^2 = \frac{q^2 R^4 - g\beta AR^4}{v\kappa} \end{aligned} \quad (6.30)$$

In these equations  $x$  and  $y$  denote nondimensional auxiliary variables (not space coordinates). Putting in turn  $q = \text{constant}$  and  $A = \text{constant}$ , we obtain a system of isolines on the  $xy$  plane. It may be shown<sup>4</sup> that the isoline  $q = \text{constant}$  represents parallel equidistant straight lines, and  $A = \text{constant}$  represents a family of hyperbolas referred to the asymptotes

$$\left. \begin{aligned} \frac{x}{y} &= \frac{v}{\kappa} = \text{Pr} \\ \frac{x}{y} &= \frac{\kappa}{v} = \frac{1}{\text{Pr}} \end{aligned} \right\} \quad (6.31)$$

These isolines are sketched in figures 9 and 10. In these coordinates the isoline  $q = 0$  passing through the even quadrants, corresponds to the previously discussed case of steady processes. For further treatment of the equations, we assume all general boundary conditions, and as special conditions we make use of the homogeneous conditions (eq. (6.9)) and requirement (eq. (6.22)) on the "closeness" of the channel cavity.

<sup>4</sup>This work was carried out in 1947 by Y. Korchemkin by applying the rules of analytic geometry. He likewise proved with complete rigor that the transformations given are a necessary and unique consequence of the basic assumption that the velocities are parallel to the surface generators of the channel.

4281

CA-7 back

The solution of equations (6.29) and (6.26) analogous to equations (5.1) and (5.4) is then written as follows:

$$v = v_0 \left[ \frac{J_0(k_1 r)}{J_0(k_1 R)} - \frac{J_0(k_2 r)}{J_0(k_2 R)} \right] \quad (6.32)$$

$$\theta = \frac{1}{g\beta R^2} \left\{ \left[ v(k_1 R)^2 + qR^2 \right] \frac{J_0(k_1 r)}{J_0(k_1 R)} - \left[ v(k_2 R)^2 + qR^2 \right] \frac{J_0(k_2 r)}{J_0(k_2 R)} \right\} \quad (6.33)$$

4281

The requirement of "closeness" of the cavity is expressed as follows:

$$\begin{aligned} 0 &= \int_0^R vr \, dr = v_0 \frac{1}{J_0(k_1 R)} \int_0^R J_0(k_1 r)r \, dr - \frac{1}{J_0(k_2 R)} \int_0^R J_0(k_2 r)r \, dr \\ &= v_0 R^2 \left\{ \frac{J_1(k_1 R)}{k_1 R J_0(k_1 R)} - \frac{J_1(k_2 R)}{k_2 R J_0(k_2 R)} \right\} \end{aligned} \quad (6.34)$$

This equation establishes a definite relation between the auxiliary coordinates  $xy$  represented in figure 11. From the meaning of the laminar processes under consideration, it is advantageous to consider only those forms of convection flows of the cooled fluid where the cross section of the pipe is divided into no more than two zones, namely, the central circular zone where the fluid moves upward, the peripheral annular zone where the fluid moves downward. This consideration restricts the curve to the point with coordinates

$$\begin{aligned} y &= (2.405)^2 \approx 5.8 \\ x &= (5.520)^2 \approx 30 \end{aligned} \quad (6.35)$$

From its quantitative expression this variant corresponds to large values of the difference  $x-y$  or to an unsteady temperature gradient (warmer in the lower part) and may be realized only at catastrophically rapid cooling of the model. The analogous case for the diametrically antisymmetric fluid motions is discussed in reference 4.

#### Slow Variant

Together with the rapid variant a slow variant may also be encountered in practice where because of sluggish cooling the rate of cooling  $\theta$  may, over a large time interval, be considered small and, moreover, constant. The corresponding equations will have the form

$$\left. \begin{aligned} 0 &= -\frac{1}{\rho} \frac{dp}{dz} - g\beta\theta + v\Delta v \\ \dot{\theta} + Av &= \kappa\Delta\theta \end{aligned} \right\} \quad (6.36)$$

Determining  $\theta$  from the first equation and substituting in the second equation, we obtain

$$\dot{\theta} + Av = \kappa\Delta\theta \quad (6.37)$$

Setting

$$v = v_0 - \frac{\dot{\theta}}{A} \quad (6.38)$$

we observe here that  $v_0$  represents the known solution of the homogeneous equation (3.9). The solution must be made exact by using the boundary conditions that express the presence of a boundary layer and the closeness of the channel. We finally obtain,

$$v = \frac{\dot{\theta}}{A} \left\{ \frac{\left[ J_1(kR) - \frac{kR}{2} J_0(kR) \right] J_0(ikr)}{J_0(ikR) \times J_1(kR) + iJ_1(ikR)J_0(kR)} + \frac{\left[ iJ_1(ikR) + \frac{kR}{2} J_0(ikR) \right] J_0(kr)}{J_0(ikR) \times J_1(kR) + iJ_1(ikR)J_0(kR)} - 1 \right\} \quad (6.39)$$

The temperature  $\theta$  may likewise be determined from the preceding paragraphs and from equation (6.36). To these expressions are entirely applicable the considerations on the complex values of the parameter  $k$  obtained if it is warmer upward than downward (ch. 5, sec. 5). Because of the transfer of heat by upward convection, this is almost required to be the case.

We restrict ourselves to the case where the temperature is still practically constant ( $A = 0$ ) along the model height. From equation (6.36) we then find

$$\left. \begin{aligned} \Delta\theta &= \frac{\dot{\theta}}{\kappa} \\ \theta &= \theta_0 - \theta_1 \left( \frac{r}{R} \right)^2 \\ \theta_1 &= -\frac{R^2 \dot{\theta}}{4\kappa} \end{aligned} \right\} \quad (6.40)$$

The Navier-Stokes equation takes the following form:

$$0 = -\frac{1}{\rho} \times \frac{dp}{dz} - g\beta\theta_0 + g\beta\theta_1 \left(\frac{r}{R}\right)^2 + \nu\Delta v \quad (6.41)$$

By considering the boundary layer and the closeness of the channel, its solution is found to be

$$v = \frac{g\beta R^4 \dot{\theta}}{192\nu\kappa} \left[ 1 - 4\left(\frac{r}{R}\right)^2 + 3\left(\frac{r}{R}\right)^4 \right] \quad (6.42)$$

4281

This convective process transfers upward just that quantity of heat which covers the heat losses of the upper layers. The thickness of this layer  $h$  of which the heat losses are made up by convection, is obtained as

$$h = \frac{g\beta\dot{\theta}R^6}{\nu\kappa^2} \times \frac{1}{2304} \quad (6.43)$$

If this thickness is of the order of the channel radius or larger, the convection may appreciably retard the cooling of the upper part of the casting in comparison with the lower part. By taking this fact into account, the setting phenomena may be consciously controlled (ref. 5), and the casting spoilage reduced.

In a cavity containing fluid periodically heated and cooled there, or course, arises the phenomenon of the gravitational-thermal "detector effect," that is, a vertical temperature gradient arises in which the temperature in the upper part is higher than in the lower part. For each half-cycle of cooling or heating, a convection occurs which carries a definite portion of the heat upward. The accumulation of such portions produces the detector effect.

## CHAPTER 7

CONVECTION IN INCLINED SLIT AS EXAMPLE OF CONVECTION  
IN CHANNEL OF A NONROUND CROSS SECTION<sup>5</sup>

## 1. Simplification of "Fundamental" Biharmonic Equation

As an example of the theoretical investigation of laminar convective phenomena in a channel of a nonround cross section, we consider the thermal convection in an infinite inclined slit filled with fluid and bounded by semi-infinite solid masses with plane parallel boundaries. In the surrounding masses a constant temperature gradient with the following components is produced by an infinitely distant heat source; (1) parallel to and (2) normal to the slit. The system is illustrated in figure 12. The gravity acceleration vector lies in the yz-plane.

$$\left. \begin{aligned} \frac{\partial \theta_e}{\partial z} &= A \\ \frac{\partial \theta_e}{\partial y} &= -B \\ \Delta \theta_e &= 0 \end{aligned} \right\} \quad (7.1)$$

$$\frac{\partial A}{\partial x} = \frac{\partial A}{\partial y} = \frac{\partial A}{\partial z} = \frac{\partial B}{\partial x} = \frac{\partial B}{\partial y} = \frac{\partial B}{\partial z} = 0$$

It is assumed that there is no temperature gradient component in the external mass along the x-axis. From considerations of symmetry, it must be assumed that there will likewise be no temperature gradient component within the fluid. Hence, there will be no velocity component along this axis

<sup>5</sup>This chapter is compiled from data obtained by G. N. Guk.

$$\left. \begin{aligned} \frac{\partial \theta_e}{\partial x} &= 0 \\ \frac{\partial \theta}{\partial x} &= 0 \\ v_x &= 0 \end{aligned} \right\} \quad (7.2)$$

Under these conditions in the laminar regime a convective flow with only one velocity component along the z-axis<sup>6</sup> is evidently possible

$$\left. \begin{aligned} v &= v_z \\ \frac{\partial v}{\partial x} &= 0 \\ \frac{\partial v}{\partial z} &= 0 \end{aligned} \right\} \quad (7.3)$$

The equation of gravitational thermal convection for the steady state then assumes the form of the linear equations

$$\left. \begin{aligned} 0 &= -\frac{1}{\rho} \times \frac{dp}{dz} + g\beta\theta \cos \alpha + \nu \frac{d^2 v}{dy^2} \\ \nu A &= \kappa \frac{d^2 \theta}{dy^2} \end{aligned} \right\} \quad (7.4)$$

By analogy with the foregoing paragraphs we shall consider the parameters of the fluid as constant, that is, we shall assume the parametrical linearization of these structurally linearized equations.

Using the results of chapter 5, section 4, where the case of the superposition of free and forced convection was discussed, we choose the origin for z in the section where  $dp/dz = 0$ . We restrict ourselves to the case where there is no external pump to draw the fluid across the slit so that only free convection occurs, and the cavity is "closed." By analogy with the more complicated cylindrical case discussed in chapter 5, section 1, we obtain

<sup>6</sup>It is clear, however, that this is not the only solution and for certain, not as yet formulated conditions, it may pass over into others (e.g., into a cellular Bénard solution (see ch. 13, plate XX)).

$$vA = - \frac{\kappa v}{g\beta \cos \alpha} \cdot \frac{d^4 v}{dy^4} \quad (7.5)$$

or

$$\left. \begin{aligned} \frac{d^4 v}{dy^4} &= k^4 v \\ k^4 &= - \frac{g\beta A \cos \alpha}{\nu \kappa} \end{aligned} \right\} \quad (7.6)$$

This ordinary linear homogeneous differential equation of the fourth order is easily solved by an elementary exponential substitution. After very simple, although rather laborious computations in terms of trigonometric and hyperbolic functions of a real or complex argument, the solution reduces, with account taken of the boundary conditions, to two qualitatively different solutions depending on the sign of the parameter  $k^4$ .

## 2. Higher Temperature in Lower Part

In this case the following conditions hold:

$$\left. \begin{aligned} h^4 &> 0 \\ v &= v_1 \left[ \frac{\text{sh } ky}{\text{sh } kR} - \frac{\sin ky}{\sin kR} \right] \\ \theta - Az &= - \frac{\nu k^2}{g\beta \cos \alpha} v_1 \left[ \frac{\text{sh } ky}{\text{sh } kR} - \frac{\sin ky}{\sin kR} \right] \end{aligned} \right\} \quad (7.7)$$

On the boundary at the wall of the slit, the absence of a heat-flow jump (see, General Boundary Conditions, ch. 4, sec. 1) gives

$$\lambda \left( \frac{d\theta}{dy} \right)_{y=\pm R} = - \lambda_e B \quad (7.8)$$

whence

$$\frac{\nu k^3 v_1}{g\beta \cos \alpha} \left[ \frac{\text{ch } kR}{\text{sh } kR} + \frac{\cos kR}{\sin kR} \right] = \frac{\lambda_e}{\lambda} B \quad (7.9)$$

The difference in temperature on both boundaries of the slit (the "temperature drop") is obtained equal to

$$\theta_+ - \theta_- = -4 \frac{vk^2}{g\beta \cos \alpha} v_1 \quad (7.10)$$

The total heat flow upward along the slit on a segment of width  $X$  is

$$Q = -2Xv_1^2 \frac{\rho cvk}{g\beta \cos \alpha} \left[ \frac{\text{sh } 2kR}{(\text{sh } kR)^2} + \frac{\sin 2kR}{(\sin kR)^2} \right] \quad (7.11)$$

4281

### 3. Higher Temperature in Upper Part

In this case  $k^4 < 0$ . We set

$$|k| \equiv \sqrt{2m} \quad (7.12)$$

The preceding computations give

$$v = v_1 \left[ \frac{\cos my \times \text{sh } my}{\cos mR \times \text{sh } mR} - \frac{\sin my \times \text{ch } my}{\sin mR \times \text{ch } mR} \right] \quad (7.13)$$

$$\theta - Az = -\frac{vk^2}{g\beta \cos \alpha} v_1 \left[ \frac{\cos my \times \text{sh } my}{\cos mR \times \text{sh } mR} + \frac{\sin my \times \text{ch } my}{\sin mR \times \text{ch } mR} \right]$$

The temperature drop over the width of the slit gives

$$\theta_+ - \theta_- = -4 \frac{vk^2}{g\beta \cos \alpha} v_1 \quad (7.14)$$

The transverse heat flow through a square centimeter is

$$\frac{2\lambda vm^3}{g\beta \cos \alpha} v_1 \left[ \frac{\cos mR \text{ ch } mR - \sin mR \text{ sh } mR}{\sin mR \times \text{sh } mR} + \frac{\sin mR \times \text{sh } mR + \cos mR \times \text{ch } mR}{\sin mR \times \text{ch } mR} \right]$$

$$= \frac{4\lambda vm^3}{g\beta \cos \alpha} v_1 [\text{cth } 2mR + \text{ctg } 2mR] = \lambda_e B \quad (7.15)$$

The longitudinal heat flow along the slit upward is expressed by more complicated functions.

The intermediate case, when  $A = 0$ , is solved in an elementary way. From the second equation of equation (7.4), we obtain

$$\left. \begin{aligned} \frac{d^2\theta}{dy^2} &= 0 \\ \lambda \frac{d\theta}{dy} &= -\lambda_e B \\ \theta &= -\frac{\lambda_e}{\lambda} B y \\ \theta_+ - \theta_- &= -2 \frac{\lambda_e}{\lambda} B R \end{aligned} \right\} \quad (7.16)$$

From the first equation of equation (7.4), we obtain

$$\left. \begin{aligned} \frac{d^2v}{dy^2} &= -\frac{\lambda_e B g \beta \cos \alpha}{\lambda v} y \\ \frac{dv}{dy} &= -\frac{\lambda_e B g \beta \cos \alpha}{\lambda v} \times \frac{1}{2} (y^2 + b) \\ v &= -\frac{\lambda_e B g \beta \cos \alpha}{6\lambda v} (y^3 + 3by + c) \end{aligned} \right\} \quad (7.17)$$

Taking into account the presence of the boundary layer  $(v)_{\pm R} = 0$  and restricting ourselves to the antisymmetrical case, we eliminate the arbitrary constants of integration  $b$  and  $c$  and obtain

$$\left. \begin{aligned} v &= \frac{g \beta \cos \alpha R^3 \lambda_e B}{6v\lambda} \left\{ \frac{y}{R} \left[ 1 - \left( \frac{y}{R} \right)^2 \right] \right\} \\ Q &= \frac{2}{45} \times (\lambda_e B)^2 \frac{g \beta \cos \alpha}{\lambda v \kappa} \times R^5 \end{aligned} \right\} \quad (7.18)$$

#### 4. Concluding Remarks

In all of the three variants discussed, making use of the results obtained with circular cross sections, we considered only the antisymmetrical conditions.

4281

CA-8 back

In the first two cases we have groups of three simultaneous transcendental equations that connect with each other the following five parameters of the convective process: the "amplitude" of the velocity  $v_1$ , the transverse gradient of the temperature in the surrounding mass  $B$  or the transverse heat flow  $\lambda_e B$ , the temperature drop over the width of the slit  $\theta_+ - \theta_-$ , and the longitudinal temperature gradient  $A$  (in terms of  $k$  and  $m$ ). Thus, for the definition of the problem two of these parameters must be given. In addition, the parameters of the fluid must be known, the heat conductivity of the surrounding mass  $\lambda_e$ , and the width of the slit  $2R$ . As previously stated, it must be assumed that the only solution reflecting the actual physical process can be that which corresponds to the smallest root  $kR$  of these equations, which (because of their transcendental character) have an infinitely large number of roots.

For the intermediate case, much more simple relations are obtained.

## CHAPTER 8

## EXPERIMENTAL INVESTIGATIONS OF WATER

## 1. Thermal and Convective Parameters of Water

Among all possible fluids, water ( $H_2O$ ) in its widespread existence occupies an exclusive position. For this reason it may serve as an object of actual production processes as well as a substance for experimental model investigation. The latter application is favored because water contains a number of singular properties. We may here remark on the large heat capacity of water and the anomalous thermal expansion in the interval from  $0^\circ$  to  $4^\circ$  C. For this reason, water occupies first place in the list of fluids capable of serving as objects of investigation.

Table VI gives a selection of tabulated data for water in the interval from  $0^\circ$  to  $100^\circ$  C and for certain other fluids. Column 8 gives the "convection parameter"  $g\beta/v\alpha$ , computed from these data, which enters into many of the preceding formulas. Figure 13 shows the temperature dependence of several water parameters in the interval from  $0^\circ$  to  $100^\circ$  C. Preliminary tests have shown that piped water does not differ much from distilled water in the magnitude of the parameter  $g\beta/v\alpha$ .

2. Interpolational Formula for  $0^\circ$  to  $40^\circ$  C Interval

To facilitate the computations connected with the application of the convection parameter at intermediate points not listed in the table, an interpolated formula has been computed (work done by N. M. Lurye) for the interval from  $0^\circ$  to  $40^\circ$  C. The formula represents the equation of a curve very accurately passing through the points given in table VI in the  $0^\circ$  to  $40^\circ$  C interval (the interpolated Lagrange formula):

$$\frac{g\beta}{v\alpha} = 100(-20.5 + 5.022\theta - 0.0070\theta^2 + 0.00765\theta^3 - 0.000059\theta^4 - 0.0000013\theta^5) \frac{1}{\text{cm}^3 \text{deg}} \quad (8.1)$$

## 3. Standard Convective Curve and Interpolated

Formula for 0° to 40° Interval

As shown previously (fig. 4), the conditions for the existence of a steady laminar convective motion in a vertical duct are equations of the type of equation (5.15) (in the absence of a horizontal gradient) or equation (7.9), so that,

$$\xi^4 = (kR)^4 = \frac{g\beta}{\nu\alpha} \times R^4 \frac{d\theta}{dz} = f\left(\frac{\lambda}{\lambda_e}\right) \quad (8.2)$$

4281

whence follows:

$$\frac{g\beta}{\nu\alpha} d\theta = \xi^4 \frac{dz}{R^4} \quad (8.3)$$

Hence

$$\int_0^\theta \frac{g\beta d\theta}{\nu\alpha} = \left(\frac{\xi}{R}\right)^4 z \quad (8.4)$$

This formula gives the distribution of the average temperature over the cross section along the cavity length within the presence of a steady laminar convective process. The origin from which the vertical distances are computed is taken in the section where the temperature is equal to 0° C. Integration corresponding to the interpolated formula (8.1) gives

$$\left(\frac{\xi}{R}\right)^4 z = 100 \left\{ -20.5\theta + 2.511\theta^2 - 0.0023\theta^3 + 0.00191\theta^4 - 0.000012\theta^5 - 0.0000002\theta^6 \right\} \text{cm}^{-3} \quad (8.5)$$

This formula is valid from 0° to 40° C. It gives the standard law of distribution of the mean temperature over the cross section in a channel for laminar convection. It is found that the details of the system, the channel radius  $R$ , and the relative thermal conductivity of the surrounding mass (in terms of the function  $\xi^4$ ) affect only the scale of the vertical distances  $z$ , but does not affect the shape of the curve.

Table VII gives the coordinates of certain points of this standard curve.

The standard convective curve is a more accurate form of the approximate basic assumption that the vertical temperature gradient is constant, as follows from formula (2.10). Actually, this constancy is valid for the presence of laminar convection only over a short distance of the

duct in which both the temperature and the fluid parameters remain constant. The standard convective curve represents the actual law of temperature distribution simplified to the linear by parametric linearization in the fundamental equations (3.1) to (3.4) and those following.

It is useful to remark that the wider the duct, the larger the scale of the vertical distances proportional to the fourth power in the formula of the standard convective curve. The narrower the duct, the larger the vertical temperature gradient and with it, the greater the possibility of a considerable disruption of the linearity of the equations. For appreciable flow velocities, it is found that the temperatures and fluid parameters in one part of the horizontal cross section differ considerably from the temperatures and parameters in another part of the section. Because viscosity strongly decreases with temperature, it is found that the cross section of the rising hot stream is appreciably less than the cross section of the descending cold stream (for a "closed" duct).

TCH

## CHAPTER 9

## EXPERIMENTAL MODELS

4281

## 1. Glass Model

In the course of verifying the preceding theory, a number of models having a similar construction were investigated. The majority of the tests were conducted with glass models filled with distilled water. This kind of model is represented by a glass burette provided with a series of thermocouples. The burette was chosen because the opening of such a tube was calibrated with the same accuracy with which the burette was prepared, and also because it is well known. As shown by certain measurements, the manufactured burettes are sufficiently round (i.e., have almost the same diameters for any azimuth). However, the degree of cylindricality and circularity (not ellipticity) must be verified in preparing a convective model from the burette. The need for an accurate knowledge of the model diameter follows from the circumstance that this diameter (or radius) enters to the fourth power in the formulas. Hence, an error of 1 percent in the diameter will give an error of 4 percent in the temperature gradient.

In typical experimental investigations, a fundamental problem is usually the determination of the mean characteristic temperature gradient over the cross section (and over the perimeter of the section in diametrical antisymmetry) of the model. For measuring this mean gradient, the burette is provided with averaging (over the perimeter) thermocouples arranged as follows:

Attached to the burette are tightly soldered strips of thin wire or foils, preferably of brass. The conducting lead from the strip is further extended up to the switch of a galvanometer. Along several (four) equidistant generators of the cylinder are stretched thin constantan wires, each one soldered to each strip. In this way, each strip forms a multiple (quadruple) thermocouple.

The difference of the average temperatures at the points where two strips are located is accompanied by the appearance of a proportional electromotive force between the copper wires extending from the model to the switch. The magnitude of this EMF is about 42 microvolts per degree temperature difference.

The number of these multiple thermocouples on the burette, their arrangement, and the distances between them are determined by considerations with regard to the object of the experimental investigation conducted. These considerations are discussed in describing the experiments.

For measuring the mean temperature at each zone of the model, these thermocouples, giving the average over the perimeter, have proven themselves entirely satisfactory because with thin wires, the part played by their thermal conductivity is small, and the errors caused by the thickness of the wall (if this thickness is uniform) are mutually compensated for on the cold and warm sides of the model.

A heater coil is situated at the lower part of the model for heating purposes. This heater consists of a high resistance insulated (preferably enameled) wire wound directly on the glass of the burette. The wire of the coil is extended by copper (preferably flexible) leads to the current source, where the leads are joined lying on the glass as far as possible. The length of the heating coil is from one to two outer diameters of the model. The turns of high-resistance wire are wound as close together as possible. The resistance of the heater is chosen to suit the voltage of the current source so that it is often necessary to make the heater of several wires connected in parallel. The wire is then wound on the burette in "multiple threads" (a term taken from screw-cutting technology).

Both wire systems, the measuring and the heating systems, are tightly attached to the glass of the burette by fiber bandages (preferably of down threads).

For stabilizing the outside temperature and the radiation fields, the model is placed in a jacket of a thick-walled copper or aluminum tube from 5 to 10 times the length of the model diameter. The gap between the model and the jacket is equalized by means of centering disks put on the model and accurately entering the inside of the jacket. This gap is filled with pure magnesium oxide (pharmaceutical name *magnesia usta*) used as a heat insulation.

Figure 14 shows a diagram of part of the model done in sections. The fiber bandages are not shown.

For measuring the "cross temperatures" (the temperature differences between the hot and cold side of the model in a cross section) and for determining the azimuth of this cross temperature, corresponding "cross thermocouples" must be used.

Figure 15 shows a diagram of a pair of cross thermocouples designed for these measurements. Four equidistant generators of the cylinder are placed along four elongated strips of copper foil. The weaker the

4281

CA-9

convective phenomenon investigated, the shorter these strips should be. At the center of each strip are soldered the ends of thin constantan wires extending to the diametrically opposite strip and the ends of copper wires going to the switch of a galvanometer (thermocouples I and II). The entire system is tightly attached to the glass of the burette by fiber bandages, not shown on figure 15.

For investigating the distribution of the cross-temperature gradients along the model at an azimuth fixed by the intentional inclination of the model from the vertical, several cross thermocouples must be arranged along the model. While the construction of the previously described models requires a certain experience and suitable care in operation, the construction of multiple cross thermocouples requires very much more preliminary and adjustment work. However, even with this method, the providing of a satisfactory model is extremely laborious, and it is still difficult to recommend some good method (ref. 1, p. 997; ch. 11, sec. 3).

The glass models, prepared by the methods described previously, generally had an internal diameter of about 1 centimeter and sometimes 0.526 centimeter (for an outer diameter of 0.835 cm).

It is necessary to take care that the model (notwithstanding the presence of the heat insulating jacket) should be located in a place where the temperature is constant without air vents or heating installations. In an extreme case it may be located in a closet having closely fitting doors. If these conditions are not observed, the results of measurements are difficult to interpret.

## 2. Metal Model

For investigating convection the model used was constructed by V. V. Slavnov and follows the fundamental features of the glass model. Figure 16 shows the constructional and electrical scheme of the apparatus. The letters a, b, c, and d denote the dimensions of the metal tube connected with the funnel e by means of the connecting piece B. The numbers 1 and 2 denote two stages of quadruple thermocouples. The thermocouples are located on equidistant generators of the pipe. Using copper and constantan conductors of the same length, the quadruple thermocouples are joined at special junctions to common conductors connected to the change-over switch of the galvanometer. Because the material of the tube is electrically conductive (and not identical with the copper or the constantan of the thermocouple), it is necessary to join separately the copper and constantan conductors with the galvanometer through a two-pole switch, including a junction of fixed temperature  $t_1$  in the circuit of each constantan wire. These junctions are attached to the bulb of thermometer T and are individually insulated. As a control one of the thermocouples is connected with a thermocouple attached to

the bulb of a second thermometer  $t_2$  in the same manner. The bulbs of both thermometers with the attached thermocouple are dipped in paraffin and placed in Dewar flasks.

A heater consisting of high-resistance enameled wire wound directly on the metal of the tube is situated in the lower part of the model.

The model is provided with thermal insulation which fills the metal jacket.

### 3. Temperature Recording

The investigated thermal processes are comparatively slow processes. At the thermal diffusivity of water (for room temperature), about  $2 \times 10^{-3}$  square centimeters per second, and diameters of the model of the order of 1 centimeter, the duration of steady thermal processes will be of the order of 500 seconds. At the same time, the period of vibration of the prevalent mirror galvanometers, which must be used because of the smallness of the thermal emf, of the order of 42 microvolts per  $^{\circ}\text{C}$ , is of the order of 5 seconds. Thus, the recording of the readings of one thermocouple by one galvanometer is excessive. Roughly speaking, this is equivalent to obtaining over a hundred readings during one process.

However, the specification of the thermoelectric recordings requires constant checking of the zero position, and the specification of convective processes requires the recording of temperatures at certain points of the model (close analogy with synoptics). Hence, it is entirely natural to determine somewhat the amount of accuracy in order to gain considerably in reliability and clarity.

The widely applied method of recording the readings of several thermocouples consists in the successive recording of the readings of different thermocouples by means of a single galvanometer. The galvanometer is switched from one thermocouple to another in a time interval during which the galvanometer pointer succeeds in reaching a new position and recording this position on the photographic plate.

Naturally, the requirements on the aperiodicity of the galvanometer must here, be raised and the choice of the critical resistance requires careful attention. A change in sensitivity cannot be attained by shunting the galvanometer alone, or by merely increasing the added resistance in the thermocouple circuit. Both these magnitudes must be varied in such a manner that the resistance of the external circuit of the thermometer does not change and become equal to the critical resistance.

If the resistance of the galvanometer is denoted by  $\rho$ , the critical resistance by  $R_0$ , the resistance of the galvanometer shunt by  $r$ , the

4281

CA-9 back

added resistance in the thermocouple circuit by  $R$ , and the relative lowering of the sensitivity (through the voltage) by  $n$ , we obtain the following two equations with the unknowns  $r$  and  $R$ :

$$\left. \begin{aligned} \frac{1}{r} + \frac{1}{R} &= \frac{1}{R_0} \\ \frac{\frac{1}{\rho} + \frac{1}{r}}{\frac{1}{\rho}} \left( R + \frac{\rho r}{\rho + r} \right) &= n(R_0 + \rho) \end{aligned} \right\} \quad (9.1)$$

The first equation of these equations expresses the requirement that the external circuit of the galvanometer must always have a critical resistance. The second equation of these equations connects the required magnitudes with the relative lowering of the sensitivity  $n$ . If the second equation is multiplied by the current giving unit deflection of the galvanometer, it expresses the requirement that this unit current should occur for the shunted galvanometer (left side) for  $n$  times the voltage (right side), as against the nonshunted galvanometer.

Solving these equations, we obtain the following convenient formulas:

$$\left. \begin{aligned} R &= nR_0 \\ r &= \frac{n}{n-1} R_0 \end{aligned} \right\} \quad (9.2)$$

The formulas show that by carefully determining  $R_0$  it is possible to choose the shunt  $r$  and the added resistance  $R$  for any lowering of the sensitivity of the galvanometer  $n$ .

As a switch for the galvanometer the step selectors used in the automatic telephone station are recommended. These selectors have several stages containing from 10 to 30 contact segments and also give a wide combination possibility. Near the model the selectors require a secure arrangement in removable jackets which help to protect them from dust. The contact surfaces of the segments and the springs must be wiped occasionally with a cotton cloth, wet with alcohol. Glazed paper or emery cloth must be entirely avoided.

The leads from the thermocouples should be soldered to the segments. Since there are a large number of these leads, it is necessary to arrange the model close to the switch. It is recommended that the leads be made of multiple-strand wire resulting in a flexible braid of enameled copper conductor of approximately 0.4-millimeter diameter contained in a fiber braid. This braid may initially be drawn together with a piece of lighting cord.

It is recommended that the thermocouples be connected to the segments in such a manner that the successive switching of the segments would be accompanied by the successive recording of the fluctuating temperatures (i.e., in the course of a cycle the recordings of the cases of temperature rises should be grouped together, and the cases of temperature drops should also be grouped together, so that the transition from the rising to the lowering temperatures will occur as infrequently as possible, no more than once per cycle). This requires great care in marking the ends of the multistrand wire before soldering the ends of the wire to the thermocouples and segments. The observance of this rule greatly increases the meaning of the photorecordings.

The step selector is subjected to the action of an electromagnet. The connection of the electromagnet is effected from the contactor of the control cam disk, located on the shaft of a Warren motor. In preparing the contactor, it is advantageous to make use of semifinished material such as that used for the telephone apparatus.

The breaking spark of the electromagnet circuit produces rapid wear of the contacts. The safe wear of the electromagnet of the step selector requires power of the order of 20 watts, maintained for a short time. Hence, depending on the source of the current brought to act on the electromagnet, various schemes are recommended for retarding the wear of the contacts.

For low voltage sources of current (a battery of 4 to 4.5 volts) the electromagnet must be wound with enameled wire of an approximate diameter of 0.6 millimeter, altogether, about 400 turns and about 1 ohm resistance. Here, it is recommended to use the contact device with which the armature is usually provided, as is shown in figure 17. At the instant the current circuit is closed by the cam disk of the Warren motor (working contact 1), the armature of the electromagnet of the step selector has not yet opened the block contact 2, shunting the added resistance of about 10 ohms. A total current of the order of 4 to 5 amperes, sufficient for the instantaneous operating of the step selector (switching of the galvanometer to the following thermocouple), passes through the winding electromagnet. Contact 2 opens practically without a spark, and through winding electromagnet a current of about 0.5 ampere, sufficient only to hold the electromagnet armature in the attracted position, starts to flow. The armature drops when contact 1 opens, and like contact 2, occurs practically without a spark. The very slight residual spark may be eliminated by shunting the electromagnet with a resistance of approximately 100 ohms.

In this low-voltage scheme it is necessary to pay great attention to the condition of the contacts. It is particularly harmful to use oil which may find its way from the motor to contact 1. It is recommended to wind high-resistance wire (a resistance of 10 to 100 ohms) on the

bobbin of the electromagnet and, thereby, avoid excessive construction detail.

With a high-voltage current source (e.g., a hard rectifier of 300 volts), it is recommended to bring the electromagnet into action with a condenser, according to the scheme of figure 18. The center of the figure shows a typical (selenium) rectifier. The center of the rectifier is connected with the phase wire of the city current through a block condenser. The capacity of this condenser is conveniently chosen because, in the case of a faulty circuit, it should serve to limit the current, and thus protect the rectifier from overheating. For example, for a limiting current of the rectifier of 40 milliamperes, its capacity should be chosen of the order of 1 microfarad.

The rectifier charges the main condenser of large capacity (electrolytic). The size of this condenser is chosen experimentally as a function of the parameters of the electromagnet. This scheme is not exacting regarding the parameters of the electromagnet but functions well with electromagnets containing a greatly differing number of windings and, therefore, having different resistances. The higher the number of windings, the smaller the capacity of the condenser sufficient for good operation of the scheme, but the more destructive is the breaking spark in working contact 1. The closing contact spark does not strongly affect the working contact.

In the regulation of the step selector it is necessary to note carefully that the operation of the electromagnet should occur instantly and rapidly, and it should also be accompanied by the jumping of the contact springs as far as possible from the center of one segment to the center of the neighboring segment, and so on along the entire selector.

The wires to the photo recording galvanometer may be sufficiently long, and the galvanometer itself can be situated in the photo laboratory.

Further on, examples of photo recordings will be given. On the latter, the recordings of the same object serve as indicators of the time. The distance between the recordings corresponds to the lag of the switch multiplied by the number of segments or objects recorded. On many of the recordings flaws, ejections, gaps, and scallops will be found. These imperfections served as reasons and material for the previously discussed guiding remarks.

#### 4. Investigating Thermal Parameters of Model

The early theory of the thermal convection of a round channel connects the parameter of thermal convection (the critical vertical temperature gradient  $A$ ) with the thermal conductivity of the surrounding mass

$\lambda_e$  (see fig. 4). Hence, where the experimental investigation verifies this theory it is necessary to compare the results obtained with this value of the thermal conductivity of the surrounding mass, equivalent to the corresponding parameter of the given model.

Although the thermal properties of the materials of which the model is made may be known, the construction of the model is, nevertheless, sufficiently complicated. Hence, the computation of the equivalent thermal conductivity may not be theoretically reliable. Thus, there arises the constant requirement of a method for directly determining the over-all thermal parameters on the model, one of which is the equivalent thermal conductivity of the surrounding mass.

The preceding method is based on the photorecording of a special thermal process occurring in the air-filled model. This special process is produced by a small heater coil, heated by a constant current and drawn inside the model from end to end with a constant velocity with the aid of a special pile-driver arrangement.

The heater (fig. 19), is constructed in the following manner. On a glass tube 120 millimeters long and 1.0/3.0 millimeter in diameter a red copper pulley (2) is securely mounted. The groove of the pulley is filled up to the edges with coil 3 of constantan wire, which constitutes the heater itself. The diameter of the pulley is such that it fits inside the model, almost without friction. A double copper wire from the heater of the make PShDL with a 0.21-millimeter diameter serves, at the same time, as a lifting cable. The heater entered into the vertically arranged model under the action of its own weight, increased by a lead weight, not shown in the figure. The cable is attached to the drum of the photorecording apparatus thus serving simultaneously as a pile-driver mechanism. Hence, the velocity of motion in the duct of the model is equal to the rate of the photo recording.

Figure 20 shows schematically the model investigated and the junctions of the thermocouples to the switch segments where T denotes the tube of the model, A the aluminum jacket, M the charge of magnesium powder, insulating the model from the jacket, and P the moving heater. The dotted lines denote the constantan wires of the thermocouples.

The equation of heat balance applicable to an element of the tube length  $dz$  (fig. 21), may be written

$$\rho c S dz \frac{\partial \theta}{\partial t} + 2\pi R_1 \alpha dz \theta = \lambda_1 S \frac{\partial^2 \theta}{\partial z^2} dz + \frac{\partial P}{\partial z} dz \quad (9.3)$$

where  $\rho$  is the density of the material of the pipe;  $c$ , the heat capacity;  $\lambda_1$  the heat conductivity;  $S$ , the cross section of the tube wall;  $2R_1$ , the outer diameter;  $\theta$ , the temperature of the tube element  $dz$  averaged over the volume;  $P$ , the power input of the heater; and  $\alpha$ , a coefficient characterizing the heat transfer from the tube to the heat insulation.

Collected on the left side of the equation are the terms characterizing the heat loss in the heat capacity of the element and in the heat losses; collected on the right side of the equation are the terms characterizing the heat gain through the thermal conductivity of the wall and the heater. Dividing by  $dz$ , bearing in mind that the power  $P$  of the heater moving with velocity  $v$  is a function of the argument  $(t - z/v)$ , and regrouping the terms, we obtain

$$\left. \begin{aligned} \lambda_1 S \frac{\partial^2 \theta}{\partial z^2} - \rho c S \frac{\partial \theta}{\partial t} - 2\pi R_1 \alpha \theta &= - \frac{\partial P}{\partial z} \\ P &= P\left(t - \frac{z}{v}\right) \end{aligned} \right\} \quad (9.4)$$

We set

$$\left. \begin{aligned} x &= t - \frac{z}{v} \\ dz &= -v dx \\ P &= P(x) \end{aligned} \right\} \quad (9.5)$$

and seek to obtain the solution of this nonhomogeneous, linear-partial and differential equation with constant coefficients in the form

$$\left. \begin{aligned} \theta &= \theta(x) = \theta\left(t - \frac{z}{v}\right) \\ \frac{\partial \theta}{\partial t} &= \theta' \\ \frac{\partial^2 \theta}{\partial z^2} &= \frac{1}{v^2} \theta'' \end{aligned} \right\} \quad (9.6)$$

This substitution gives the following ordinary differential equation:

$$\theta'' - \frac{\rho c v^2}{\lambda_1} \theta' - \frac{2\pi R_1 \alpha v^2}{\lambda_1 S} \theta = - \frac{v^2}{\lambda S} \frac{dP}{dx} \quad (9.7)$$

This linear but nonhomogeneous equation with constant coefficients may, in our case, be reduced to a homogeneous equation. Because the axial dimensions of the heater are so small that it may be considered as a point source of heat. The function  $P(x)$  will, therefore, be zero everywhere except at the point where the heater is situated at the given moment ("delta function"). At this point, the entire power  $P$  of the heater is produced. Thus

when  $x \neq 0$

$$\frac{\partial P}{\partial x} = 0$$

when  $x = 0$

$$\int_{-\infty}^{+\infty} \frac{\partial P}{\partial x} dx = P_0$$

(9.8)

Equation (9.7) for all values of  $x$ , except  $x = 0$ , assumes the form

$$\theta'' - \frac{\rho c v^2}{\lambda_1} \theta' - \frac{2\pi R_1 \alpha v^2}{\lambda_1 S} \theta = 0 \quad (9.9)$$

We shall seek a solution in the following form:

$$\theta = \theta_0 e^{qx} \quad (9.10)$$

whence, after substituting in equation (9.9), we obtain

$$q^2 - \frac{\rho c v^2}{\lambda_1} q - \frac{2\pi R_1 \alpha v^2}{\lambda_1 S} = 0$$

$$q = \frac{\rho c v^2}{2\lambda_1} \left[ 1 \pm \sqrt{1 + \frac{2\pi R_1 \alpha \lambda_1}{(\rho c v)^2 S}} \right] \quad (9.11)$$

$$0 < q_1 = \frac{\rho c v^2}{2\lambda_1} \left[ 1 + \sqrt{1 + \frac{2\pi R_1 \alpha \lambda_1}{(\rho c v)^2 S}} \right]$$

$$0 > q_2 = \frac{\rho c v^2}{2\lambda_1} \left[ 1 - \sqrt{1 + \frac{2\pi R_1 \alpha \lambda_1}{(\rho c v)^2 S}} \right] \quad (9.12)$$

$$|q_1| > |q_2|$$

4281

CA-10

when  $x < 0$

$$\left. \begin{aligned} \theta &= \theta_0 e^{q_1 x} \\ \lg \theta &= \lg \theta_0 + q_1 x \lg e \\ \frac{d \lg \theta}{dx} &= \frac{d \lg \theta}{dt} = q_1 \lg e = 0.4343 q_1 \end{aligned} \right\} \quad (9.13)$$

when  $x = 0$

$$\theta = \theta_0 \quad (9.14)$$

when  $x > 0$

$$\left. \begin{aligned} \theta &= \theta_0 e^{q_2 x} \\ \frac{d \lg \theta}{dx} &= 0.4343 q_2 \end{aligned} \right\} \quad (9.15)$$

when  $x = \pm \infty$

$$\left. \begin{aligned} \theta &= 0 \\ \theta' &= 0 \\ \theta'' &= 0 \end{aligned} \right\} \quad (9.16)$$

The trend of the curve  $\theta = \theta(x)$  is shown in figure 22, or in semi-logarithmic scale, in figure 23.

The entire heat, obtained by the tube from the heater, is, in the final analysis, expended only in the heat transfer characterized by the parameter  $\alpha$ . Mathematically, this corresponds to the following: integrating each term of equation (9.3) between the limits  $-\infty$  to  $+\infty$ , we obtain

$$\int_{-\infty}^{+\infty} \rho c S \frac{\partial \theta}{\partial z} dz + 2\pi R_1 \alpha \int_{-\infty}^{+\infty} \theta dz = \lambda_1 S \int_{-\infty}^{+\infty} \frac{\partial^2 \theta}{\partial z^2} dz + P_0 \quad (9.17)$$

$$-v \rho c S \int_{-\infty}^{+\infty} \theta' dx + 2\pi R_1 \alpha \int_{-\infty}^{+\infty} \theta dz = -\frac{\lambda_1 S}{v} \int_{-\infty}^{+\infty} \theta'' dx + P_0 \quad (9.18)$$

$$-v\rho c S \theta \Big|_{-\infty}^{+\infty} + 2\pi R_1 \alpha \int_{-\infty}^{+\infty} \theta \, dz = -\frac{\lambda_1 S}{v} \theta' \Big|_{-\infty}^{+\infty} + P_0 \quad (9.19)$$

Because of the relations (9.16), the substitutions give zero. Hence,

$$\alpha = \frac{P_0}{2\pi R_1 \int_{-\infty}^{+\infty} \theta \, dz} \quad (9.20)$$

Moreover, from equations (9.13), (9.14) and (9.15) there is obtained

$$\begin{aligned} \int_{-\infty}^{+\infty} \theta \, dz &= -v \int_{-\infty}^0 \theta_0 e^{q_2 x} \, dx - v \int_0^{+\infty} \theta_0 e^{q_1 x} \, dx \\ &= \theta_0 v \left[ \frac{1}{q_1} + \frac{1}{-q_2} \right] \end{aligned} \quad (9.21)$$

Having experimentally determined the form of the function  $\theta = \theta(t)$  for  $z = \text{constant}$  by photorecording and having measured the photorecord of figures 22 and 23, the integral may be obtained by the direct summation method of  $\theta = \theta(z)$  as well as by the (check) computation method in terms of the slopes of the curves  $q_1$  and  $q_2$ . Thus, the expression (9.20) permits determining the first thermal parameter of the model  $\alpha$  characterizing the heat losses.

We recall that it is connected with the thermal conductivity of the insulation  $\lambda_2$  by the relation (ref. 2, p. 27), so that

$$\left. \begin{aligned} 2\pi R_1 \alpha &= \frac{2\pi \lambda_2}{\ln \frac{R_2}{R_1}} \\ \lambda_2 &= R_1 \alpha \ln \frac{R_2}{R_1} \end{aligned} \right\} \quad (9.22)$$

In this formula,  $R_2$  denotes the inside radius of the jacket A in figure 20, having a constant (room) temperature.

4281

CA-10 back

From equation (9.11) there follows

$$\left. \begin{aligned} q_1 q_2 &= - \frac{2\pi R_1 \alpha v^2}{\lambda_1 S} \\ \lambda_1 &= \frac{2\pi R_1 \alpha v^2}{S q_1 (-q_2)} \end{aligned} \right\} \quad (9.23)$$

$$\left. \begin{aligned} \frac{\rho c v^2}{\lambda_1} &= q_1 + q_2 \\ \rho c &= \frac{\lambda_1}{v^2} (q_1 + q_2) = \frac{2\pi \alpha}{S} \left[ \frac{1}{-q_2} - \frac{1}{q_1} \right] \end{aligned} \right\} \quad (9.24)$$

Equations (9.20), (9.23), and (9.24) give the complete solution of the problem of the experimental thermal parameters of the model.

Figure I<sup>7</sup> gives an example of an automatic record similar to those of figures 22 and 24. Its evaluation is similar to that of figure 23. The symbols  $\Delta$ ,  $\bullet$ ,  $\square$ , and  $\circ$  in figure 24 denote the points of the average curves of the photograph obtained in moving the heater upward in the model, and the crosses denote the points of the photograph obtained in letting the heater move downward. The motion occurred with constant velocities. All the curves are drawn in such a manner that the maximum ordinate corresponds to zero on the axis of abscissas.

As may be seen, the form of the curves on figures 23 and 24 is the same. Measurements on the graph of figure 24 gave the following values:

$$\left. \begin{aligned} \frac{1}{q_1} &= 470 \text{ sec} \\ \frac{1}{-q_2} &= 1150 \text{ sec} \end{aligned} \right\} \quad (9.25)$$

The measurements of the three curves on the same photograph (fig. I), gave the following value:

$$\int_{-\infty}^{+\infty} \theta \, dz = 0.242 \sum \theta = \frac{0.242 \times 773.5}{8.4} = 22.2 \text{ deg cm} \quad (9.26)$$

<sup>7</sup>The figures denoted by roman numerals refer to the photographic records.

In this record, 0.242 centimeter is the linear length corresponding to one work cycle of the switch (distance between the photo marks), and 8.4 millimeters per degrees is the sensitivity of the galvanometer determined by means of the graduated record; the upper horizontal series are the points corresponding to 0.300 millivolt, that is 7.15° C. The number of 773.5 millimeters is the sum of all the ordinates of the photo record.

The computation check by formula (9.21) gave

$$\int_{-\infty}^{+\infty} \theta dz = 22.4 \text{ deg cm} \quad (9.27)$$

The record was taken for the glass model of 11.28/13.28 millimeters in diameter for a heater power of 0.0532 watt = 0.0127 calorie per second. By formula (9.20) the following average value is then obtained:

$$\alpha = 1.46 \times 10^{-4} \text{ cal/deg sec cm}^2 \quad (9.28)$$

It should be remarked that of this number, the proportion falling to the signal copper ( $\lambda = 0.9$ ) wires of 0.41-millimeter diameter with cross-sectional area 0.00132 square centimeter, at a distance of 6 centimeters from each other along the model length (each of them 1.68 centimeters long to the jacket) is

$$\alpha_1 = \frac{0.90 \times 0.00132}{2\pi R_1 \times 6 \times 1.68} = 0.28 \times 10^{-4} \text{ cal/deg sec cm}^2 \quad (9.29)$$

By formula (9.22) the following is then obtained for the thermal conductivity of the magnesia:

$$\begin{aligned} \lambda_2 &= 0.62(1.46 - 0.28) \times 10^{-4} \times 1.27 \\ &= 1.00 \times 10^{-4} \text{ cal/deg cm} \end{aligned} \quad (9.30)$$

(The thermal conductivity of the air at 20° C is  $0.60 \times 10^{-4}$  cal/deg·cm). By formula (9.23) for the thermal conductivity of the model, there is obtained after substitution

$$\left. \begin{aligned} v &= 0.00311 \text{ cm/sec}; & S &= 0.38 \text{ cm}^2 \\ \lambda_1 &= \frac{\pi \times 2R_1 \alpha v^2}{Sq_1(-q_2)} \\ &= \frac{3.14 \times 133 \times 1.46 \times 10^{-4} (0.00311)^2 \times 470 \times 1150}{0.38} \\ &= 84 \times 10^{-4} \text{ cal/deg cm} \\ \lambda_1 S &= 31.8 \times 10^{-4} \text{ cal cm/deg} \end{aligned} \right\} \quad (9.31)$$

The molecular thermal conductivity of the water in the model channel is  $14 \times 10^{-4}$  calorie - centimeter per degree (i.e., less than half the thermal conductivity of the walls).

It should be noted that of this number, the proportion falling to the four constantan wires of diameter 0.21 millimeter is

$$\lambda'S' = 4 \times 0.054 \times 0.000345 = 0.75 \times 10^{-4} \text{ cal cm/deg} \quad (9.32)$$

The corrected value for the glass is, therefore, obtained as follows:

$$\begin{aligned} \lambda_1 S &= 31.0 \times 10^{-4} \text{ cal cm/deg} \\ \lambda_1 &= 82 \times 10^{-4} \text{ cal/deg cm} \end{aligned} \quad (9.33)$$

If formulas (5.27) are considered, then, for the models of 11.28/13.28 millimeters in diameter of the same kind of glass with which the majority of the tests were conducted, it is found that the thermal conductivity of the equivalent surrounding mass  $\lambda_e$  is obtained equal to 0.00141 calorie per degree - centimeter (i.e., of the same order as the thermal conductivity of the water). Thus, for these glass models, we have approximately  $\lambda = \lambda_e$ .

By formula (9.24) we obtain

$$\rho c = 1.64 \text{ cal/deg cm}^3 \quad (9.34)$$

Hydrostatic weighing gave  $\rho = 2.59$  grams per cubic centimeter. The thermal capacity of the model glass is then  $c = 0.63$  calorie per degree squared.

In the carrying out of this method, the following especially important difficulties require careful attention.

It is necessary that the heater actually be a "point" source (i.e., that the axial dimensions of the heater should not exceed the radial dimensions). With a heater three times the diameter length, good recordings were likewise obtained but their interpretation presents extreme difficulties.

Each of the upper set of thermocouples registers a rise in temperature when the heater passes by the lower thermocouples and registers a lowering temperature, even in comparison with the jacket, in the intermediate positions of the heater. The phenomenon is greatly weakened when the upper part of the glass tube of the heater (fig. 19) is wound with a wool filament over its entire length almost up to the inner diameter of the model. This difficulty is evidently caused by the convection of the air in the tube over the heater. Hence, to remove the air, it is expedient to arrange the model horizontally.

This method has a number of defects that lower its reliability. The thinner the model wall as compared with its diameter, the more heat conducting its material as compared with the heat insulation; the thinner the thermocouple wires, the more reliable is the method and the higher the quality of the investigated model.

## CHAPTER 10

EXPERIMENTAL INVESTIGATION OF FREE THERMAL CONVECTION IN VERTICAL  
MODELS OF ROUND CROSS SECTION FOR STEADY REGIME

4281

1. The Two Regimes of Thermal Convection and  
Their Dividing Critical Point

Numerous measurements, observations, and photorecordings carried out on different vertical models have led to the conclusion that for a moderate heating by a heater coil, situated in the lower part of the model, a convective motion of the fluid arises in the model. In its fundamental features, this motion is correctly described by the preceding theory.

The details of the observed phenomena are the following: After a moderate current is established in the heater circuit, the temperature distribution along the model undergoes more or less strong changes at first (see ch. 11). These changes gradually cease after the elapse of a certain time, and a definite steady temperature distribution is established. This distribution is characterized by an almost constant vertical temperature gradient along the model.<sup>8</sup>

The magnitude of this gradient within broad limits does not depend directly on the power input to the heater (table VIII) and only slightly changes with the temperature of that part of the model where the gradient is measured; on raising the temperature, the gradient decreases. The sense of the temperature gradient is always such that it is warmer below the gradient than above.

Thus, the phenomenon of convective heat transfer by a fluid in a vertical tube differs from the molecular heat transfer in solid bodies in the following properties: (1) by the practically constant gradient along the model, and (2) by its independence of the power input of the heater.

---

<sup>8</sup>If the fluid would solidify, the constant gradient along the model would change into a gradient decreasing by the exponential law (fig. V).

Figures V and VI compare examples of photorecordings of the temperature distribution along a model through convection, and in the case where the fluid is replaced by a brass rod tightly fitted into the model. The upper curve gives the temperature of the lower, warmest thermocouple (table VIII, pts. I and II).

Check tests established that this regime corresponds to the laminar motion of the fluid. Figure II shows a photograph of the path of the particles of aluminum powder suspended in water in the model, and illuminated from the side. The photograph shows how a flow with axial symmetry inside the heater is arbitrarily formed over the model length in the flow with diametral antisymmetry: on the right the warm fluid rises, on the left, the cold fluid descends (fig. III shows a photograph of the upper part of the same model).

For very small heating power inputs in the model filled with fluid, as in the case of a solid body, an exponential law of temperature distribution is observed. This law is valid only in those parts of the model where the temperature gradient has not reached the characteristic magnitude. It is necessary to assume that for these small powers there are no corresponding gradients of the convective motion, and the non-moving fluid behaves like a solid body. At each part of the model, the temperature gradient is proportional to the heating power.

Likewise, when a greater current flows into the heater circuit, a more or less violent nonsteady regime, changing rather rapidly to a new regime which only with reservation may be called steady, is observed at first. The temperature recording is now uneven and reveals erratic fluctuations. The vertical gradient of the temperature undergoes jumps (attaining 30 percent of its mean value). This mean gradient is practically proportional to the heating power at each part of the model.

By check tests using the suspended aluminum powder, it was found that the convective flow now has a turbulent structure; the scale of the turbulence being of the order of the channel diameter of the model.

Thus, for small vertical temperature gradients the fluid is apparently stationary, the heat transfer along the model probably was determined by the molecular thermal conductivity. On attaining the characteristic temperature gradient, a laminar convective fluid motion arises which is capable of transferring large thermal powers in a relatively wide range of these powers. To exceed the characteristic gradient

4281

CA-11

is possible only at the expense of disrupting the laminar motion of the fluid, that is, at the expense of rendering the flow turbulent.<sup>9</sup> The thermal properties of such turbulent convective flow resemble the properties of a solid body.

From the preceding considerations it is seen that the characteristic gradient has the following criterional value, namely, that the character of the fluid motion is determined by the magnitude of the gradient. Below this gradient, the fluid is calm, its flow being laminar, while above this gradient the flow becomes turbulent.

<sup>9</sup>For contrast we recall the conditions of laminar flow, namely, the equation of a streamline must not contain the time in explicit form. The equations of a streamline are as follows:

$$\frac{dx}{v_x} = \frac{dy}{v_y} = \frac{dz}{v_z}$$

or

$$\frac{dx}{dy} = \frac{v_x}{v_y}$$

$$\frac{dz}{dy} = \frac{v_z}{v_y}$$

For laminar motion it is necessary that

$$\frac{\partial}{\partial t} \left( \frac{v_x}{v_y} \right) = \frac{\partial}{\partial t} \left( \frac{v_z}{v_y} \right) = 0, \text{ i.e., } \frac{v_x \frac{\partial v_y}{\partial t} - v_y \frac{\partial v_x}{\partial t}}{v_y^2} = \frac{v_z \frac{\partial v_y}{\partial t} - v_y \frac{\partial v_z}{\partial t}}{v_y^2} = 0$$

then

$$\frac{\frac{\partial v_x}{\partial t}}{v_x} = \frac{\frac{\partial v_y}{\partial t}}{v_y} = \frac{\frac{\partial v_z}{\partial t}}{v_z}$$

or

$$\frac{\partial \ln v_x}{\partial t} = \frac{\partial \ln v_y}{\partial t} = \frac{\partial \ln v_z}{\partial t} = \Omega$$

For steady laminar flow,  $\Omega$  must be equal to zero.

The characteristic gradient determines the hydrodynamic critical point: a sharp qualitative change in the character of the fluid motion. The turbulent fluid motion may be characterized as above the critical.

## 2. Constancy of Value of Convection

### Parameter in Laminar Regime

Numerous measurements of photorecords and other measurements have shown that the convection parameter, equation (5.16)

$$\xi^4 = (kR)^4 = \frac{g\beta AR^4}{\nu\kappa} \quad (10.1)$$

actually possesses an almost constant value, as defined by formula (5.15), figure 4, and table II. For example, for glass models this value is approximately equal to 100. Considering the previous statement that for glass models the ratio  $\lambda_e/\lambda$  was found to be approximately 1, we arrive at the conclusion that formula (5.15) satisfactorily applies to glass models (table VIII).

Careful measurements, carried out by V. V. Slavnov on a brass model filled with water gave the value  $\xi^4 = 186 \pm 2$ . The corresponding value of the thermal conductivity of brass lies within the limits of the tabulated values. The preceding findings show that formula (5.15) is also sufficiently accurate for metal models. In particular, it is entirely evident that with an increase in the temperature, the parameter  $g\beta/\nu\kappa$  increases; the vertical temperature gradient  $A$  should decrease so that the convection parameter  $\xi^4$  maintains its critical value.

## 3. Quantitative Characteristic of Above-Critical

### Regime of Thermal Convection

As an orientating characteristic of the quantity of heat transferred by convection in the above-critical regime, we employ a provisional magnitude defined as follows:

$$Nu^* = \frac{Q}{\pi R^2 \lambda A} \quad (10.2)$$

where  $Q$  denotes the heating power;  $A$ , the time average of the temperature gradient for the above-critical regime and the remaining symbols have their previous meanings. If  $Q$  denotes the thermal power transferred by convection at a given section of the model (where the gradient

4281

CA-11 back

is equal to  $A$ ), the expression (10.2) could provisionally have been denoted as the Nusselt number  $Nu^{**}$  applied to heat transfer through convection from the low-lying parts to the high-lying parts of the model, from fluid to fluid (eq. (5.17)). The accurate meaning of the Nusselt criterion refers to the transfer of heat from a solid body to a fluid, or conversely. Thus, the parameter  $Nu^*$  in the preceding expression has, to a large degree, a provisional character. Nevertheless, from several series of tests with different glass models it was found that the values of  $Nu^*$  for the above-critical regime have a relatively small scatter about a mean value. Figure 25 shows the results obtained to a large scale, the different symbols corresponding to different models in different tests. As seen, the points arrange themselves about two intersecting straight lines where the vertical line corresponds to the laminar regime and the horizontal line to the above-critical regime. Figure 25 also shows, to a small scale, the relation between the previously mentioned intersecting straight lines, curve I, and two known functions of the true Nusselt criterion for the cases of transfer from a solid body to an unlimited fluid, curve II, and through a liquid layer, curve III (as a function of the convection parameter  $\xi^4$ ).

4281

From this graph the following conclusions may be drawn:

(a) Although  $Nu^*$  is of a provisional character, its approximate independence of the convection parameter  $\xi^4$  in the above-critical regime reflects an analogy of the thermal properties of the fluid in this regime with those of a solid body. (See initial part of curve III).

(b) The disposition of curve I is in striking contrast to that of the known curves II and III. This contrast corresponds entirely to the different meanings of the parameter  $Nu^*$  and the true Nusselt number  $Nu$ .

(c) The numerical value of  $Nu^*$  ( $1460 \pm 80$ ), determined from the data of table VIII, is undoubtedly much larger than the value of  $Nu^{**}$  having a better defined physical meaning. The value of  $Nu^*$  must be considered as an upper limit of the possible values of  $Nu^{**}$  (for the glass models investigated; see also formula (10.10)).

#### 4. Presence of Transverse Temperature Gradients

##### and Results of Their Measurements

One of the most important indications of the laminar convective thermal process described by the formulas of chapter 5, section 1, is the fact that in this process one side of the model is warmer than the other. The experimental verification of this is of great significance in establishing the reliability of these formulas.

For measuring the transverse gradient, it is necessary to provide the model with transversely situated thermocouples as described in chapter 9, section 1. The measurement of the transverse temperatures was carried out close to the critical powers. Under these conditions, the model represents a good heat conductor. Hence, the role of the heat insulation becomes small so that tests were conducted on glass models situated in air, without any special heat insulation.

It is convenient to compare the measured transverse temperature differences with the vertical characteristic gradient and to express them in terms of a number of model diameters over which the horizontal difference is equal to the vertical. Such "relative" transverse temperature differences expressed in model diameters have a definite physical sense for the laminar regime. From formula (5.5) and related formulas, it follows that the transverse temperature difference is equal to

$$\theta_{r=+R} - \theta_{r=-R} = \theta_+ - \theta_- = 2 \times 2 \times \frac{\nu k^2}{g\beta} v_1 \quad (10.3)$$

The "relative" transverse temperature difference will, by definition, be equal to

$$\frac{\theta_+ - \theta_-}{2AR} = \frac{2\nu k^2}{g\beta AR} v_1 \quad (10.4)$$

On the other hand, from formulas (5.10), (5.17), and (10.2), we obtain

$$Nu^{**} = \frac{Q}{\pi R^2 \lambda A} = \frac{\pi \rho c v \left\{ \right\}}{2g\beta \pi R^2 \lambda A} v_1^2 = \frac{v \left\{ \right\}}{2g\beta A \pi R^2} v_1^2 \quad (10.5)$$

where the braces denote the same expression that appears in the braces in formula (5.10). Eliminating the magnitude  $v_1$  from the equations (10.4) and (10.5), we obtain

$$\begin{aligned} Nu^{**} &= \frac{v \left\{ \right\}}{2g\beta A \pi R^2} \times \left( \frac{\theta_+ - \theta_-}{2AR} \right)^2 \times \frac{(g\beta AR)^2}{4\nu^2 k^4} \\ &= \frac{\left\{ \right\}}{8} \times \left( \frac{\theta_+ - \theta_-}{2AR} \right)^2 \end{aligned} \quad (10.6)$$

Thus, the thermal power transferred by the laminar convective flow is proportional to the square of the relative transverse temperature difference.

For glass models, when  $\lambda_e \approx \lambda$ ,  $\xi = kR \approx 3.2$  and  $\xi^4 \approx 100$ , the expression in braces in approximately equal to 30.3. Hence, approximately

$$\text{Nu}^{**} \approx 4 \left( \frac{\theta_+ - \theta_-}{2AR} \right)^2 \quad (10.7)$$

If formulas (5.22) and (5.23) are used, and the transverse temperature difference  $\theta_{e+} - \theta_{e-}$  is computed on the outer surface of the glass model, then for  $\lambda_2 \ll \lambda_1$ ,  $\theta_{e+} - \theta_{e-}$  is almost equal to or somewhat less than  $\theta_+ - \theta_-$ :

$$\theta_{e+} - \theta_{e-} \approx \theta_+ - \theta_- \quad (10.8)$$

Substituting the outer transverse temperature difference  $\theta_{e+} - \theta_{e-}$  for  $\theta_+ - \theta_-$  in formula (10.7), we shall obtain a somewhat lowered value for  $\text{Nu}^{**}$ .

The measurements revealed very considerable outer transverse temperature differences. For example, in a model of about 1.2/1.0 centimeters in diameter for a heating power of 0.169 calorie per second, a relative outer temperature difference of 10.4 tube diameters was found, corresponding to,

$$\text{Nu}^{**} \approx 430 \quad (10.9)$$

At the critical heating power on the boundary of the transition from the laminar to the above-critical regime a "maximal" transverse outer temperature difference of 15.5 diameters (1.3° C absolute) was obtained, which gives a value

$$\text{Nu}^{**} \approx 960 \quad (10.10)$$

This number is to be considered the lower limit for the  $\text{Nu}^*$  number previously computed from other considerations (sec. 3).

Further measurements showed that small deflections of the tube axis from the vertical increased the transverse temperature difference. Since these deflections simultaneously increase the critical power, they also increase the maximal value of the transverse difference. For example, for an inclination of the axis of the model of 5.75° from the vertical, the maximal (below-critical) transverse outer temperature difference was obtained equal to 2.0° C or 24 diameters. Hence, for an inclined model,  $\text{Nu}^{**} \approx 2300$  (ch. 17, sec. 4).

All these measurements are related to the magnitudes of the transverse temperature gradient.

#### 5. Fluctuation of Azimuth of Transverse Temperature Gradient

4281  
It was established that the azimuths of the transverse temperature difference (fig. 6) are more or less stable only for an inclined model. For example, at an inclination of  $5.75^\circ$  and a heating power of 0.169 calorie per second (laminar regime), the probable inclinations of the azimuth, as a result of numerous measurements, were approximately  $\pm 1.7^\circ$  of an arc. For the same inclination at the above-critical regime (heating power 0.68 cal/sec), a probable inclination of  $\pm 11^\circ$  of an arc was obtained. The sign of the transverse difference in the inclined model corresponds to the original assumption that the upper side is warmer than the lower side.

For a vertical model, the azimuth of the transverse temperature difference is very unstable even for the laminar regime. Random arrangements and arbitrary rotations of the plane of diametral symmetry are observed. For example, figure 26 shows the variation with time of the relative outer temperature difference, considering its azimuth. In figure 26 the simultaneous values of the relative transverse temperature difference (expressed in diameters and observed by means of both sets of thermocouples) are laid off on the coordinate axis. If these values are combined by the parallelogram rule, then with each pair of such values a definite direction of the vector of the relative transverse temperature difference may be associated. This direction coincides with the normal to the plane of antisymmetry whose length more accurately describes the transverse temperature difference than each of the separate components. These values were taken into consideration in the preceding discussion.

The preceding figure (fig. 26) shows in a half hour how the transverse temperature difference described almost the entire surroundings (the marks were made after each minute of time).

## CHAPTER 11

EXPERIMENTAL INVESTIGATION OF UNSTEADY REGIMES OF THERMAL  
CONVECTION IN MODELS OF ROUND CROSS SECTION

4281

## 1. Theoretical Considerations for Steady Process

Figure 27 shows a segment of a channel model. For imperfect heat insulation of this segment, the part of the heat  $q_1 = \rho c \theta v_z$  transported by convection downward from the source will be greater than the part of the heat  $q_2$  carried upward, so that a part of the heat  $q'$  will pass through the heat insulation over the length of the segment. Hence, the curves  $q$ ,  $v$ , and  $\theta$  at the upper boundary of the channel segment will be below the corresponding curves referred to the lower boundary of the same segment. For this reason, the part of the streamlines of the convective flow from the rising stream (on the right) will bend into the descending stream (on the left). At the central section the fluid velocities, though small, are not zero, and are directed horizontally. The theory of this phenomenon is discussed in chapter 15, section 5.

Experiment confirms this theoretical picture. Figure III shows a photograph of this convective flow which was made visible by adding to the water a certain amount of aluminum powder brightly illuminated from the side. A thin-walled glass tube with a diameter of 38 to 40 millimeters, without any heat insulation and heated at its lower part, was used for the model. The photograph shows the bending of the streamlines both near the cold top and along the model according to the scheme of figure 27 (fig. II).

Since in a laminar convective flow along the model a constant mean temperature gradient over the cross section is established, both this mean temperature and the heat losses through the imperfect heat insulation  $q'$  are a linear function of the vertical distances  $z$  along the model. The heat expenditure required to cover the losses from the top of the model to a given section  $z$  is a quadratic function of the distance  $z$ . The total heat supply  $Q$  covering these heat losses is also a quadratic function of  $z$ . Hence, the velocity  $v$  is again a linear function of the distance

$$v = v_m \cdot \frac{z}{z_m} \quad (11.1)$$

The origin from which the vertical distances  $z$  are computed is laid in the section where the convective motion ceases. Beyond this section the heat transfer continues, but this condition is probably only due to the molecular thermal conductivity of the fluid and of the model walls. This process corresponds to the transfer of heat through a solid rod, and the corresponding temperature is an exponential function of the distance  $z$ . The combining of both laws occurs for  $z = 0$  under the conditions of continuity of both the mean temperatures and the thermal flows (i.e., the temperature curve in this case has neither a jump nor a break).

Figure 28 shows the previously described distributions of temperatures and velocities to the correspondingly chosen scales. Above the point  $z = 0$ , the exponential law of temperature change combines with the absence of the convective velocity  $v$ .

Between the two sides of the model, where  $\cos \varphi = \pm 1$  and the velocities of the rising and descending flow are respectively maximal, the following transverse temperature difference is observed:

$$\theta_+ - \theta_- = 4 \frac{vk^2}{g\beta} v \quad (11.2)$$

Hence, on the same figure it is possible to represent  $\theta_+ - \theta_-$  by the same straight lines as  $v$  in a correspondingly chosen scale.

On the basis of equation (11.1) the effective path of the thermal flow for an infinitely small time interval  $dt$  may be computed, so that

$$dz = v dt = z \frac{v_m}{z_m} dt \quad (11.3)$$

By integrating this equation, the dependence of the path traversed by the flow as a function of the time can be determined:

$$\int \frac{dz}{z} = \ln z = \ln \left( v \frac{z_m}{v_m} \right) = \ln \left[ \frac{z_m g \beta}{v_m^4 v k^2} (\theta_+ - \theta_-) \right] = \frac{v_m}{z_m} (t - t_m) \quad (11.4)$$

From this formula it follows that the time  $t$  required for the convective flow to reach section  $z$  is a logarithmic function of  $z$ ,  $v$ , or  $(\theta_+ - \theta_-)$ .

4281

CA-12

## 2. Fundamental Differences in Unsteady Regimes in Presence and in Absence of Convection

In order to investigate nonsteady regimes, the electric heater of the model was connected to a storage battery through a program switch. This switch consisted of a separate telephone selector, successively disconnecting and connecting, thereby adding resistance in the heater circuit. The sections of this added resistance were chosen so that the power of the heater varied approximately in the ratios 0:1:2:3:4:3:2:1:0. The heating power corresponded to 0; 0.012; 0.025; 0.040; 0.054, and so forth, calories per second. Each stage was maintained for 3 hours. Figure IV shows an example of a record.

For comparison, figure V shows a similar record where a tightly fitting brass rod was introduced into the burette in the place of water. The power at each stage was maintained for 2 hours. Comparison of both photographs shows that the phenomena of convective heat transfer differ from the corresponding phenomena of the molecular heat transfer in a solid rod.

In the steady regime, the difference consists in the fact that the temperatures (distances of the horizontal segments of the curve from the zero line) of different thermocouples follow, for convective heat transfer, a linear law; and for a solid rod, an exponential law. The slight deviation of the former for the hottest thermocouples is due to their closeness to the heater, near which the horizontal components of the velocity are also sharply expressed (fig. II shows the lower part of the flow presented in fig. III).

In the unsteady regime, the difference consists in the fact that the change of temperatures with time according to the exponential law, markedly expressed for the solid rod, is only very approximately expressed in the convective case.

A particularly sharp difference is noted at the start of the record. Figures VI and VII show photo records taken for accelerated motion of the photographic plate and show how the thermal process reaches successively from thermocouple to thermocouple. Figure VIII shows a photograph, which was obtained by I. P. Merzlyakov on another model. The graph of figure 29 was constructed from the measurements of the initial parts of figures IV and VIII. On the axis of the abscissas is laid off, to arbitrary scale, the time corresponding to the first appreciable deviation of the temperature of the given thermocouple from the temperature of the jacket; on the axis of ordinates, the logarithm of the mean established temperature (relative to the jacket). The points adjust well to the straight lines.

Formula (11.4) thus obtains a first experimental verification.

### 3. Unsteady Processes Described by Transverse Thermocouples

The preceding type of photographic records describe the course of the mean temperature at a given section of the model. This mean temperature is established as a result of the heat losses transmitted by convection in heating a given segment of the model, and in covering the heat losses. Therefore, on the records the heat transfer appears only in the form of its result and not in itself. The intensity of the transfer may be followed more clearly from the observations of the transverse temperature difference  $\theta_+ - \theta_-$ .

For this purpose, a new burette model was provided as described in the preceding paragraphs (ref. 1, ch. 9, p. 991). This model has several transverse thermocouples, attached at distances 50 millimeters apart, and three averaging thermocouples which were attached alternately to the first thermocouples at a distance of 200 millimeters apart. The transverse thermocouples were constructed in the following manner. A copper wire of 0.41-millimeter in diameter was extended along the burette generator. Along the generators on the opposite side of the burette, eight rhombs of copper foil of 0.10-millimeter thickness, with a side one-third the burette diameter and an angle of  $60^\circ$ , were attached. A constantan wire of 0.21-millimeter diameter was soldered to the center of each rhomb and encompassed the burette as a belt. The ends of this wire were soldered to the longitudinal copper wire.

The copper wires soldered to the corners of the rhombs were connected to the change-over switch of a galvanometer. The longitudinal copper wire was connected directly to the galvanometer, and served as a common lead for all the thermocouples.

For stabilizing the azimuth of the laminar convective process the model was fixed at an angle of  $45^\circ$  to the vertical, without any heat insulation, so that the copper wire coincided with the upper generator and the rhombs coincided with the lower generator of the model. In this way, the transverse thermocouples measured the transverse outer temperature difference  $\theta_{e+} - \theta_{e-}$  to a certain scale (i.e., the velocity of convective flow  $v$ ).

By parallel tests with other models it was established that an inclination of the model up to  $45^\circ$  to the vertical does not strongly disturb the process of convective heat transfer in its most essential features (ch. 17).

4281

CA-12 back

Figure IX shows a sample of a record. The temperature of the lower averaging thermocouple is recorded above the zero line. The transverse temperatures of the bottom (first) and top (eighth) thermocouples are recorded below the zero line.

Figure X shows an example of a record when the velocity of motion of the photographic plate is increased, and the center (fourth) transverse thermocouple is connected to replace the averaging thermocouple. The photograph also shows the successive recording of the lower (upper curve), the middle and top thermocouples (lower curve), and the zero line. The arrow at the left of the record denotes the instant of connection of the heater, the arrow on the right denotes the instant of its disconnection. Figure 30 shows the time of reaching the convective process counting from the instant the heater is connected (abscissa), as a function of the logarithm of the established transverse temperature difference (ordinate). The points lie on a straight line.

In this way, formula (11.4) obtains a second experimental confirmation.

#### 4. Forced Thermal Fluctuations Produced by Modulation of Heater Power

Further tests, for a 6-minute period, were conducted with the second model described in section 3, and consisted in the periodic change (modulation, forced fluctuations) of the power of the heater. Figures XI and XII show an example of a record. The photographs show the retardation of the convective waves produced by switching the added power on and off (the instants of switching on and off are indicated by the arrows) as they move along the model. The corresponding shifts in phase on lag times of the convective signal may be computed by applying the methods of harmonic analysis. From a plot of the coordinates of the thermocouples and the corresponding deflections of the galvanometer the coordinate of the point where the convective flow ceases may be found by extrapolation. This point is considered to be the origin from which the longitudinal distances  $z$  are computed. Plotting the lag time as a function of the new coordinates of the thermocouples on another graph, we then obtain figure 31 (which gives the results of the evaluation of several tests). This graph shows that the points again lie on straight lines intersecting near the coordinates of the center of the heater and the thermal inertia of the heater, which retards the development of convective phenomena by approximately 80 seconds, may be determined.

In this way, formula (11.4) obtains a third experimental verification.

Figure XIII shows an example of a record of the temperature waves of Angstrom as applied to the convective transfer of heat. The interpretation of this record has not as yet been clarified.

## 5. Natural Thermal Damping Fluctuations in Convection for Models of Finite Length

In tests similar to those recorded in figures XI and XII, but corresponding to greater heating powers, the curves took the form of damped sinusoids (see also upper curves figs. VII(B) and VIII).

Figure 32 shows a typical curve on which the difference in temperatures, by means of the middle (fourth) transverse thermocouple, is recorded.

By tests of a preliminary character it was established that the smaller the "period" of the corresponding fluctuations, the greater the heating power, and the shorter the column of fluid that is in motion. The "damping" of the fluctuations increases with decrease in the heating power. These facts lead to the supposition that the fluctuations reflect the existence of a circular flow of fluid in the model. A definite portion of the fluid which has repeatedly received a higher temperature passes by a given thermocouple. In time this portion mixes and exchanges heat with the surrounding volumes of fluid, and the phenomenon decreases. Figure VIII shows how the period of these fluctuations is lengthened as the convective process extends to the more distant thermocouples (i.e., as the length of the fluid column put in convective motion increases).

## CHAPTER 12

END PHENOMENA OF THERMAL CONVECTION IN MODELS OF ROUND SECTION  
(INVESTIGATED BY TEMPERATURE RECORDING METHOD)

4281

1. General Distribution of the Temperatures Averaged over a  
Cross Section Along Entire Vertical Model

The hydrodynamic characteristic of the end phenomena is shown in figures II and III. From the physicomathematical investigation viewpoint, the very simple phenomena near the plane top (or bottom) of a model is of great interest.

For measuring the mean temperature over the periphery directly over the entire height of the fluid column (including the bottom and top) in which the thermal convection occurs, a special model was constructed (sketched in fig. 33). A brass rod (2) above and cylindrical glass reservoir (3) with plug bottom below were attached to the arms of the support (1). Through this bottom passes a small glass tube, closed by a plug, in which a brass piston (4) sits freely. The high-resistance enameled wire of the electric heater is wound on the tapered bottom part of this piston. A second cylindrical glass tube (5) with a diameter of about 1 centimeter is placed with slight friction over the rod (2), the tube, and the piston (4). One layer of thin copper enameled coil is wound about the middle of the glass tube (5), thus making up the measuring resistance thermocouple (6). The tube (5) is provided with a reservoir with running water (7) and supply funnel (8). The middle part of the tube (5) (with coil (6)) is surrounded by cotton heat insulation not shown on the sketch. In the reservoir (3), mercury is poured forming a tight mercury shutoff. Distilled water partially entering the reservoir (8) is poured above the mercury in the tube (5).

With the aid of a clock mechanism and a pile-driver arrangement, not shown on the sketch, the system of details 5, 6, 7, and 8 is brought into a very slow motion (11.8 mm/hr) in the vertical direction. The velocity of this motion coincides with the velocity of motion of the photographic plate in the recording apparatus. In this way the resistance thermometer (6) records at first the temperature of the piston (4) serving as the warm bottom of the water column at various heights, and finally the temperature of the end of the rod 2 serving as the cold top of the water column.

4281

The resistance (6) is connected to the scheme shown in figure 34 which represents a bridge, balanced for a certain mean test temperature. The resistances of the branch (9) are chosen in a manner such that they form simultaneously the critical resistance of the photographically recording galvanometer. The cutout switch (10) shunts 1.6 percent of the entire resistance of this branch of the bridge. Therefore, its closing unbalances the bridge in the same way the coil temperature raises by  $4^{\circ}$  C. The connecting in of the switch (10) is done by hand and serves to graduate the photorecord. Contact (11) disconnects automatically each hour for 10 seconds. The corresponding marks on the records serve as datum marks; they indicate the time and origin and the zero line. The parameters of all systems are chosen in such a manner to assure maximum sensitivity of the bridge for the minimum heating of the coil (6).

An example of a record is shown in figure 35 in which the coordinate axes are indicated, the vertical distance to full scale, and the temperature of the thermal resistance (6), and also the place occupied by the bottom and top of the model. In region 1 the curve corresponds to the end of the nonsteady regime after the heater and the water cooler are connected. Region 2 corresponds to the record of the temperature of the bottom, region 6 to the record of the temperature of the top, and region 7 to the record of the nonsteady regime after disconnecting the heater and the water cooler. The distance  $x$  represents the degree interval,  $4^{\circ}$  C, obtained by connecting the cutoff switch (10) for a short time.

Through the middle of the photograph a number of datum points pass that indicate the zero line giving the time marks. The temperature of the fluid column in the model, averaged over the periphery, changes strongly near the bottom and top, regions 3 and 5, and weakly in the center part of the model, region 4. The photorecords show indentations which reflect a certain instability of the convective process in region 4.

Figure 35 gives an instructive picture. It shows that with convection a small vertical temperature gradient corresponding to a lower temperature in the upper part is actually established along the center part of the model, and which at the bottom and top goes over into another law, the exponential law of temperature change.

The fact that the over-all temperature drop at the bottom in region 3 exceeds the over-all temperature drop at the top in region 5 is caused by the heat losses over the length of the column. The quantity of heat obtained from the bottom is expended not only in transferring the heat to the top but also in the heat losses over the extent of the model.

## 2. Variable-Length-Column

For the purpose of further study of the end phenomena, a second model was constructed and investigated and is presented in section in figure 36.

In the lower end of a glass tube (1), of diameter of about 1 centimeter, there is almost tightly inserted a copper plug (2), the clearance being closed by a piece of rubber tube (3). The enameled high-resistance wire of the heater 4 is wound on the plug (2), so that the entire plug serves as the hot flat bottom of the model. In the model there is inserted with slight friction a massive copper piston (5) with the piston rod ending in the lug (6). The upper part of the model is surrounded by the cooling reservoir (7) filled with water. The piston (5) thus forms a cold cover of the water column (8) in which is produced the convective motion under consideration. This column consists of distilled water poured into the tube (1) almost to the top. Two single-layer coils of the resistance thermometer (9) made of thin copper enameled wire connected to the two adjoining branches of the bridge are bound together 2 to 3 diameters apart on the glass of the tube. The bridge is balanced when both coils have the same temperature. In equilibrium, the switching on or off of the switch (11) is not accompanied by the deflections of the pointer of the photographically recording galvanometer. The switch (10), described in the preceding paragraphs, is used for controlling the sensitivity.

The piston (5) is linked at the lug (6) with a pile-driver apparatus and a time mechanism with which it can move up or down with the velocity of the photographic plate in the recording apparatus (11.8 mm/hr).

It is assumed that the coils (9) will have a temperature almost equal to the temperature of the bottom and top of the column (8). Thus, for a given power input of the heating coil (4), the readings of the galvanometer are approximately proportional to the "heat resistance" of the column (8). Moreover, by raising the lower edge of the piston above the upper coil of the resistance thermometer coil, it is possible to follow the temperature of the model, averaged over the periphery, below its cold top.

The preliminary tests with this model consisted of visual hydrodynamic observations of the motion between the bottom (2) and the top (5) of cork dust added to the water. The observations were made with the aid of a binocular microscope through the wall of the model. These observations showed that for a given heating power input the dust remained at rest for small distances between the bottom and top. As this distance was increased the Bénard cellular motion (ref. 1) arises. The greater the heating power, the smaller are the distances between top and bottom at which this motion occurs, and therefore the smaller are the particles and the more intense their motion. With further increase in distance, this cellular motion goes over into an antisymmetric motion, illustrated in the photographs, figures II and III.

At the conclusion of these preliminary hydrodynamic observations the model was enveloped in a cotton heat insulation and the investigation was continued by the temperature-recording method.

4281

Figure 37 shows an example of the records obtained. The scalar interval upward at the start of the record (on the left) corresponds to the indicated number of degrees centigrade. Part 1 of the curve describes the steady thermal regime when the piston (5) lies on the bottom (2). Part 2 of the curve corresponds to moderate distances of the piston from the bottom when convection has not yet set in. The greater this distance, the greater the difference of the temperatures between the bottom and top. This difference is almost proportional to the distance. Actually the curve represents the initial part of the exponential curve. The fluid here behaves like a solid body. The heat resistance is proportional to the length of the model column. Part 3 of the curve corresponds to the convective laminar regime. Over a considerable distance, the temperature difference is almost independent of the distance between the bottom and top: the heat resistance of the model is almost independent of its length; it is almost entirely determined by the end regions near the bottom and top.

CA-13

Of striking sharpness are the transitions from region 1 to region 2, the instant of breakaway of the piston from the hot bottom, the transition from region 2 to region 3, and the instant of occurrence of convective motion. Moreover, the latter transition occurs by several stages, which evidently corresponds to the successive changes of several cellular forms of the convective motion.

Region 3 ends when the lower face of the piston (5) passes by the upper measuring coil of the temperature measuring resistance. Then region 4 of the curve now begins; this region corresponds to the gradual decrease in the temperature difference between the measuring coils. This region (4) is determined by the condition that the upward moving piston carries away with it the adjoining region of large temperature gradients and low temperatures.

The drop in temperature near the top in region 5 is less than the drop at the bottom in region 2 (compare regions 5 and 3 in fig. 35). Region 5 corresponds to the cooling regime of the model after the heater is disconnected.

Figure 37 gives examples of photorecords corresponding to different heating powers indicated on each photograph. The records embrace a range of heating powers from 0.00165 to 1 calorie per second. At the beginning of some records the nonsteady regime, which accompanies the switching in of the heater coil, is observed.

From a comparison of these photographs, it is seen that the greater the heating power, the steeper and shorter the rise of the curves is in region 2 where the fluid behaves thermally almost like a solid body.

Of special interest is the record (5) in figure 37. The regions 1, 2, and 3 are developed in it almost in the same way as in the preceding curves. In region 3 indentations are observed which reflect the incomplete steady condition of the convective process for large heating powers to which large velocities of the convective motion correspond. These indentations on curve 5 are nearly four times as large as on curve 4, almost half as high as curve 5. This emphasizes the nonlinear character of the above mentioned incomplete steady condition of the process.

Furthermore, region 4 reveals a character that was not successfully interpreted.

The records, obtained with the piston lowered in the model, gave results agreeing entirely with those obtained in raising the piston and are shown in the previous curves.

As a whole the curves shown are very instructive, but we have not been successful in drawing any quantitative conclusions from them.

### 3. Moving-Plunger Method

An interesting and simple experiment may be carried out in the following manner. In the model, figure 38, a copper cylindrical plunger (1) which enters the model with slight friction is lowered on a thin thread. The height of the cylinder is approximately equal to its diameter, the inside diameter of the model cavity. If the mean temperature over the perimeter at any cross section of the model 2 is recorded and at the same time the cylinder is slowly drawn out from the interior of the model, a record is obtained similar to that shown in figure XIV. This record was produced with the aid of a temperature measuring resistance according to the scheme of figure 34. A short copper rod (3) fitting the model with slight friction was lowered into the model hollow before recording. Its upper face served as the hot bottom of the water column; the middle of the rod fitted within the heater.

As long as the cylinder lies on the bottom, a convective process is developed over it and the temperature of the measuring resistance (2) differs little from the temperature of the cold reservoir above the model. At the instant when the cylinder (1) breaks away from the bottom (3), the characteristic tooth appears on the curve, marked on the photograph, figure XIV, by the number 1. The number 2 denotes the instant when the upper face of the cylinder enters the plane of the measuring coil; the number 3 shows when its lower face issues from its plane. Over the distance 1 to 2, the measuring resistance records a gradual increase in temperature at the bottom of the model formed by the moving cylinder, that is, over it. It is noted that the closer the warm plunger approaches the measuring coil of the thermoresistance the more rapidly does its temperature rise.

On the segment 2 to 3 the plunger is situated inside the measuring coil. Its temperature rises, however, only slightly because of the finite heat conductivity of the material of the plunger. Point 4 corresponds to the instant of cutting off the current of the heater. Over the segment 3 to 4, the temperature under the plunger is recorded. There is noted at first the rapid rise of temperature connected with the removal of the piston, then its more gradual lowering, connected with the effect of heat, losses through the imperfect heat insulation are also noted.

Along the entire extent of the record, indentations are observed indicating the incomplete steady condition of the convective laminar process.

#### 4. Displacement Method

Particularly descriptive are the photorecords obtained in the same manner as in figure 38, but connected with the recording of the temperatures in many cross sections of the model and obtained by interchanging the short plunger with a long rod. Essentially, this method corresponds to the even displacement of a fluid by a solid rod (or conversely) in the process of convection.

The following photorecords were obtained with a glass model, as in figure 14, of diameter 10.76/12.77 millimeters on which the five lower thermocouples were arranged at distances of 10 millimeters from each other while the remaining ones were at distances of 30 millimeters from each other. In taking the different photographs the upper edge of the brass rod, moving inside the heater and forming the hot bottom of the model, occupied several different positions relative to the thermocouples. For example, on figure XV, two tests are recorded when this edge just passed in the center between the two lower averaging thermometers. The tests ended in the recording of the thermal process in the model during the motion in it of the brass rod that almost filled tightly the model cross section. The velocity of the motion was equal to the velocity of the photorecording (11.8 mm/hr). At one time the rod was drawn upward out of the model and at another time it was lowered into it. The photo films with the records obtained on them were placed together and printed on the paper by the contact method. Both records agree sufficiently well with each other down to the individual indentations, on the curves, indicating incomplete stability of the laminar convection.

In view of the importance of this question, such pairs of tests were repeated with different velocities of motion of the brass rod. Figure XVI gives examples of records obtained for a heating power of 0.090 calorie per second and velocity of motion of the photographic plate of 11.8 millimeters per hour. The upper record A corresponds to the same velocity of motion of the rod as the velocity of the plate, the second

4281

CA-13 back

to a velocity half as large, the third to a velocity an eighth as large. From a comparison of these records, it is seen that the differences of the "up" and "down" records are due to the time and not the coordinate of the rod. The slower the motion of the rod, the more accurately do the records coincide.

In the following figures several photographs are given which were obtained by the above method for different heating powers. The initial part of the record represents the distribution of the temperatures along the brass rod standing directly on the support inside the model. At the instant when the rod breaks away from the support its temperature begins to rise and the temperature of the rod to drop. The temperature difference increases at first proportionally to the thickness of the water layer. When the thickness of the layer reaches a definite value, which is smaller, the larger the heating power, a convective motion arises increasing the heat transfer and the cooling of the support; the temperature of the support ceases to rise. As the lower face of the rod in its rising motion passes by the level of one thermocouple after the other and carries away with it the lower temperatures, the temperature of each thermocouple rises corresponding to the temperature of the fluid at its level, averaged over the periphery.

The photographs given previously show in the first place that the characteristic law of change of the temperature, averaged over the periphery near the bottom or top of the water column in which the thermal convection occurs, is the exponential law. From measurements on the photographs, this functional relation is obtained:

$$\theta = \theta_0 \left( 1 - e^{-\frac{z}{SR}} \right) + Az \quad (12.1)$$

where  $\theta = 0$  when  $z = 0$ . The nondimensional number  $s$  is approximately equal to 1 or 2.

These photographs also show that the instability of the laminar convection regime is particularly intensified for considerable power inputs and for definite heights of the water column, namely, for multiples of about three to four times the inside model diameter (fig. XVI and XVII).

## 5. Conclusion

As a whole, however, all these records were unable to give a final quantitative picture of the end phenomena. The magnitude  $\theta_0$  in the last formula is one-fourth as large as may be expected from the comparison of the molecular heat conductivity of water with the heating power. In other words, the heat conductivity in the end phenomena appears to be four times larger than its tabulated (molecular) value. This important question requires further clarification.

## CHAPTER 13

OPTICAL METHODS OF INVESTIGATING CONVECTION IN  
MODELS OF SPECIAL FORM

## 1. Introductory Remarks

The distinctive feature of convective phenomena is that the velocities and temperatures change very remarkably within the fluid. These changes cannot be studied by observing the velocities and temperatures only at the boundaries of the apparatus in which the convection takes place. The investigation of the deep internal layers requires the application of some sounding device that penetrates into the body of the fluid.

The construction of even the most intricate thermometers that can be introduced into the stream of the convective flow complicates the problem because the convective flow, on encountering even the thinnest filament, becomes distorted relative to its initial direction and exchanges heat with the filament. For this reason those methods which permit a deep sounding of the convective phenomena, and at the same time are as far as possible without effect on the development and course of the process, are of great value.

The optical methods are methods of this type. A light ray in a transparent fluid exerts a negligible action on the fluid and at the same time may undergo changes in the fluid which permit studying the causes that produce them. The method of adding light-scattering particles to the fluid has long been employed in hydrodynamics. This method was used in preparing the photographs of figures II and III.

This chapter describes a group of methods that make use of the dependence of the index of refraction (the velocity of propagation of light) on the temperature. These methods are based on the fact, which is described with great accuracy by the known formula of Lorenz-Lorentz, and which may be formulated as follows: The changes in the index of refraction are almost exactly proportional to the changes in density of the given substance (depending in particular on the temperature). The experimental predecessors of these methods are the variants of the

penumbra (schlieren) method. One of these methods is coarse (secs. 2 and 3), being suitable only for demonstration purposes. Another, which is a development of the former, possesses great promise as a quantitative method (secs. 4 and 5).

## 2. Prismatic-Vessel Method

The convective phenomenon is produced in a vessel of special form - a high prism of triangular or trapezoidal cross section (A), presented in plane on figure 39. The vessel is filled with the fluid to be investigated and is placed directly in front of a large objective lens (C). A point source of light (S) is set up at twice the focal distance behind the objective. At twice the focal distance in front of the objective, a real image of this source is obtained, which is deflected toward the vessel as a prism with vertical refracting edge and expanded by it into a spectrum. A diaphragm (B) with small opening (a) is placed at this position. The light passing through the opening of the diaphragm falls on the objective of the camera. This objective may have a very small luminous power but must be achromatic to the light rays acting on the photographic plate. On the ground glass of the camera, a sharp image of the part of the prism A which is illuminated from behind through the large objective C is obtained.

This apparatus recalls the schlieren apparatus often applicable for the qualitative observation of convective-heat interchanges. The apparatus described differs in that the investigated object is given the form of a prism. This improvement gives a number of advantages (ref. 1).

If the vessel is filled with a homogeneous fluid, the deflection of the same color rays is the same in all parts of the prism. The diaphragm cuts out a definite region from the spectrum (e.g., the green region), and a green image is obtained on the ground glass. If, however, in the path of the light rays some place on the prism has a higher mean temperature (i.e., a smaller density), the mean index of refraction of this place will be less and the light will be slightly deflected. Only the more refracted blue rays may pass through the opening of the diaphragm. The heated part of the prism is imaged on the ground glass as a blue spot. The more strongly the mean temperature differs in two parts of the prism, the more strongly does the color of the images formed on the ground glass differ. The mean temperature may have such large changes that the corresponding spots will appear black; they will be formed by infrared or ultraviolet rays. In order that these parts may be seen, the diaphragm and its opening must be moved horizontally.

If several layers of fluid of different indices of refraction are arranged along the height of the prism, they will form bands of different colors on the ground glass. But, if along the height of the prism a

continuous change, characterized by the constant gradient of the index of refraction, is produced, the fluid in the prism will act as an auxiliary prism with horizontal refracting edge. For example, if it is warmer below than above, the prism deflects the rays not only toward the side but also upward. The rays of different color form a somewhat deflected and slightly diffused spectral band.

The plane of the diaphragm B is schematically presented in the upper left part of figure 39. The point O denotes the place where a white image of the light source would be obtained if the index of refraction of the fluid were equal to unity (the trace of the principal optical axis of the large objective C). The letters  $K\phi$  on the same level with the point O mark the spectrum formed by the warm part of the prism, and the letters  $K_1\phi_1$  mark the spectrum formed by the cool part. The line E represents the somewhat diffuse spectrum obtained when a moderate vertical gradient of the index of refraction is present in the prism. The line FB corresponds to a large vertical gradient.

If the opening of the diaphragm is placed at the point a, then the warm part of the prism of a blue color, and the cool part of a red color may be seen through it. But no rays pass through it from that part of the prism where a vertical gradient of the index of refraction has been established. This part will appear as black on the ground glass. In order to obtain an image of this part, the opening must be raised to point b or d. Through this opening the entire prism, except the part with the given vertical gradient, will appear as black.

Places with a horizontal gradient of the index of refraction will either strengthen or weaken the action of the prism A. Such places must not be confused with the heated or cooled parts, as is seen from the following considerations.

Figure 40 shows schematically the path of the rays in a prism, situated in a vacuum, in which there is a horizontal gradient of the index of refraction

$$n = n(x) \quad (13.1)$$

We put  $AE = BF = dx$ . In order that rays passing with minimum deflection (inside the prism perpendicular to the x-axis) be deflected in the direction BC, it is necessary that the optical length of the path ABC be equal to the optical length of the path EFG:

$$nAB + BC = \left( n + \frac{dn}{dx} dx \right) EG \quad (13.2)$$

where

$$\left. \begin{aligned}
 \angle BGC &= \frac{D + \epsilon}{2} \\
 \angle FBG &= \frac{\epsilon}{2} \\
 \frac{BC}{\sin \frac{D + \epsilon}{2}} &= BG = \frac{BF}{\cos \frac{\epsilon}{2}} = \frac{dx}{\cos \frac{\epsilon}{2}} \\
 AB &= x \operatorname{tg} \frac{\epsilon}{2} \\
 EG &= (x + dx) \operatorname{tg} \frac{\epsilon}{2}
 \end{aligned} \right\} \quad (13.3)$$

Substituting equation (13.3) into equation (13.2) gives

$$\begin{aligned}
 n x \operatorname{tg} \frac{\epsilon}{2} + \frac{dx}{\cos \frac{\epsilon}{2}} \times \sin \frac{D + \epsilon}{2} &= \left( n + \frac{dn}{dx} dx \right) (x + dx) \operatorname{tg} \frac{\epsilon}{2} \\
 \rightarrow n x \operatorname{tg} \frac{\epsilon}{2} + \left( n + x \frac{dn}{dx} \right) \operatorname{tg} \frac{\epsilon}{2} dx & \quad (13.4)
 \end{aligned}$$

whence

$$n + x \frac{dn}{dx} = \frac{d(nx)}{dx} = \frac{\sin \frac{D + \epsilon}{2}}{\sin \frac{\epsilon}{2}} \quad (13.5)$$

We set

$$\left. \begin{aligned}
 n &= n_0 + y; \quad \frac{dn_0}{dx} = 0; \quad y = y(x); & y \ll n_0 \\
 D &= D_0 + \delta; \quad n_0 = \frac{\sin \frac{D_0 + \epsilon}{2}}{\sin \frac{\epsilon}{2}}; & \delta \ll D_0
 \end{aligned} \right\} \quad (13.6)$$

The length  $\delta l$  ( $l$  is equal to the distance of the prism A from the opening a) denotes the horizontal displacement of the opening in the diaphragm B. This displacement is required in order to see the prism in light rays

for which the index of refraction is not equal to  $n_0$  but is equal to  $n = n_0 + y$ . Since, owing to the relations (13.5),

$$n_0 + y + x \frac{dy}{dx} \rightarrow \frac{\sin \frac{D_0 + \epsilon}{2} + \cos \frac{D_0 + \epsilon}{2} \times \frac{\delta}{2}}{\sin \frac{\epsilon}{2}} \quad (13.7)$$

we obtain

$$y + x \frac{dy}{dx} = \frac{d(xy)}{dx} = \frac{\cos \frac{D_0 + \epsilon}{2}}{2 \sin \frac{\epsilon}{2}} \times \delta = K \times (\delta l) \quad (13.8)$$

From the preceding formula the following conclusions can be drawn:

(1) In all cases where the gradients of the index of refraction  $dy/dx$  are known to be small, the color for a white source or the displacements  $\delta l$  for a monochromatic light source to a certain scale directly determine the index of refraction

$$y = K(\delta l) \quad (13.9)$$

The isolines of the same color (displacements) correspond to the topographic horizontal contour lines of the index of refraction (temperature).

(2) In those cases where the gradients are known to be large and occupy narrow parts of the prism so that the over-all changes of the index of refraction are not large, the color (or displacements) determines these gradients:

$$\frac{dy}{dx} = \frac{K \times (\delta l)}{x} \quad (13.10)$$

In the latter case it is convenient to represent the image of the prism as a "relief map" of the index of refraction (temperature) with a mirror surface illuminated under different angles. The bright lines on this relief map determine those places where its steepness corresponds to a given position of the light source (displacement).

Thus, in the image of the prism, the isolines of the same color represent either lines of equal temperature or lines of equal horizontal gradient.

For the photographic recording of the observed convective phenomena it is necessary somehow to distinguish the actinic colors of the spectrum from each other. In particular, this may be done by the following

method. A light source that would give a large number of lines (iron arc) must be chosen. From a preliminary spectrograph, a detailed determination is made on the given photographic plate of the relative intensity of all the successive spectral lines. If the process of heat convection in vessel A is photographed on the same material, isolines of the same color (i.e., of the same spectral line) will appear. By establishing the order and relative intensity of these spectral lines, conclusions as to the temperature distribution in the model may be drawn.

For purposes of rougher computations, a simplified device may be applied. A light source having a small number of bright lines (mercury arc) is used. One actinic line is chosen, and the model is photographed in the light of this line for several positions of the opening a of the diaphragm. Each photograph gives its isoline of the same color. The narrowness, sharpness, and the required length of exposure of this isoline are determined by the dimensions of the point source and the opening in the diaphragm (or their corresponding slits). It is useful to note that the objective C should be of a large luminous power, but its chromatic character is not important.

This method permits a demonstrational variant. For the light source S, according to figure 39, the crater of a Petrov electric arc is employed directly, and the camera is replaced by the arrangement shown in figure 41. The adjustment is begun by placing in the path of the rays deflected by the prism A a typical projection objective Q in such a manner that it will give a sharp image of the prism A on the screen z. A diaphragm D is then placed with its opening in the plane in which the image of the arc, expanded into a spectrum, is received. The opening in this diaphragm is placed in the green part of the spectrum so that the image of the prism is colored with an easily visible green color.

The difficulties of the further adjustment reflect the contradictory requirements of sufficiently illuminating the screen while maintaining the sensitivity. This adjustment reduces to the choice of the distances between the crater of the arc and the large objective C (the choice is accompanied by the shifting of the diaphragm D) and the choice of the diameter of the opening in diaphragm D. The adjustment must be coordinated with the optical arrangement employed. At the end of the adjustment of the apparatus and its testing it is recommended that a reversing prism P be placed immediately behind the diaphragm D so that the image on the screen will be upright.

The thermal convective phenomena are produced in the prismatic vessel A by spirals, balls, or lattices of high-resistance wire in which an electric current is allowed to flow. The prism A should be filled with nonvolatile heavy fluids that do not disturb the material of the vessel (in particular, the glue or paste that seals the prism edges). The most suitable fluids appear to be mixtures of glycerine and water.

In solving uncomplicated problems, the vessel filled with fluid may be in the form of a rectangular parallelepiped, with a glass prism placed before it. This arrangement is shown in figure 41 (A, the glass prism; B, the vessel with fluid).

The results of working with this optical method and checking by tests with light-scattering particles are as follows:

(1) In the absence of thermal phenomena in the mixtures of water and glycerine all the assumptions of the theory presented previously (including those of the stratified arrangements of solutions of different concentration) may be fully confirmed.

(2) It is possible to investigate the temperature distribution for the heating of a homogeneous fluid. For small heating powers, the temperature distribution differs in stability. On top of the heater a stationary column of rising warm fluid is observed pressing in its flow against the nearest wall. This distribution of the temperature gradients indicates the laminar fluid flow. In the center part of the model there is only the vertical component of the velocity; the phenomenon differs in the presence of considerable horizontal and in the absence of appreciable vertical temperature gradients. Near the heater and near the surface of the fluid vertical temperature gradients, together with horizontal velocity components of the fluid particles, are revealed.

The steady regimes, on connecting in the heater, proceed in the following manner. An instant after the heater is connected a cap of warm fluid is formed over it. This fluid rises quickly, leaving a track behind it; thus, it resembles a mushroom. On reaching the surface of the fluid, the cap wanders off to the side or breaks up and gradually vanishes. When the heater is disconnected, the observed phenomenon gradually fades, and in a few seconds the picture vanishes without a trace; the temperatures have balanced out.

For considerable heating power inputs the rising column of warm fluid does not remain stationary. Branches separate from the column and the phenomenon assumes a "ringlet" form (ref. 2, p. 75). The stronger the heating, the more violent is the motion observed in the fluid. Along with considerable horizontal gradients, considerable vertical temperature gradients occur at some places.

(3) It is possible to investigate convective phenomena when the model is divided into two segments by a thin metallic partition like a second bottom. The fluid of the lower segment is warmed by the heater and heats the partition, while the latter heats the fluid of the upper segment. Under these conditions, wide convective flows with small horizontal temperature gradients were observed in the upper segment. Near the partition considerable vertical temperature gradients were observed.

4281

CA-14 back

(4) When the lower half of the model was initially filled with a fluid of raised density (raised concentration of the glycerine in the water or lowered temperature) and a fluid of lower density (lowered concentration or raised temperature) was carefully poured on the upper half of the model, it was found that even a slight jump of density also blocks the convective flow like a solid interposed bottom (see ref. 2, p. 76, fig. 28, p. 83, and fig. 32). Near the boundary of the division considerable vertical temperature gradients are observed. A density jump is accompanied by a temperature jump.

As a whole, the image seen on the projection screen presents a fascinating picturesque spectacle.

### 3. Vertical-Deflection Method

For studying the phenomena of convective heat transfer at above-critical power inputs in round tubes, a special model suitable for observing large vertical temperature gradients is employed.

The model (fig. 42) consists of a vertical burette A with the enameled high-resistance wire of the heater B wound directly on the glass of the lower part. The center of the burette is surrounded by a prismatic vessel D in the form of a rectangular parallelepiped, with a cork bottom and two lateral glass walls. Placed on the upper part of the burette is a funnel E, serving as the cold reservoir. The burette, funnel, and prismatic vessel are filled with water. At times it is useful to place ice in the funnel.

The middle part of the model is set in front of a large objective C of a schlieren apparatus with horizontal knife edges F and G. These edges are adjusted in such manner that, in the absence of a thermal phenomenon, only the luminous divisions of the burette are clearly visible on the ground glass of the camera against the black background. When vertical temperature gradients arise (warmer below), the corresponding part of the burette acts as a prism, deflecting the rays upward. These rays pass over the second knife edge through an objective H and fall on the ground glass k of the camera, where a luminous image of this part of the burette is formed.

The tests show that, for small heating powers, no optically appreciable vertical temperature gradients arise. For heating powers larger than the critical, the entire fluid in the burette spontaneously breaks up along the vertical into a number of segments separated from each other by considerable temperature jumps. The boundaries of the segments shift spontaneously in a disorderly fashion. The most typical form of this displacement is in an advancing displacement. Along with it a second typical interchanging form is also often encountered: The luminous

boundary dividing two segments bends, stretches out, assumes the form of an integral sign, and breaks in half, each part very precipitately uniting with the opposite faces of the interchanging segments. These deformations of the parts of a large gradient reveal a "waltzing" interchange fluid motion of the two neighboring segments. The axis of this motion is some diameter of the tube.

4281 These tests show that the large gradients obtained at above-critical heating powers are nonuniformly distributed over the height of the tube. They are concentrated principally at the boundaries of definite regions; namely, the segment boundaries. Within the limits of each region an intensive laminar motion and heat transfer undoubtedly occur. In addition, however, a waltzing motion simultaneously intermingling the contents of two neighboring regions sometimes arises. In this way, when the heating power is increased, two processes occur together. First, the mean gradients increase; and secondly the frequency of the interchanging motion (and with it the heat transfer) increases. This is the explanation of the above-critical section on figure 25. This explanation contains an essential statistical element associated with the previously mentioned disorder of the phenomena.

#### 4. Lattice Method

In an experimental verification of the laws of heat propagation (and also of diffusion processes), it is, in the final analysis, usually necessary to check the correctness of the fundamental equation of heat conduction or the equation of diffusion that formally agrees with it. The essential term in these equations is the Laplacian of the temperatures or the concentrations. The direct computation of the Laplacian (i.e., the sum of the second derivatives with respect to the coordinates of the observed magnitudes of the temperatures or concentrations) by the method of finite differences is associated with large errors, since it is required to compute small differences of large magnitudes measured only approximately. Investigators must therefore have recourse to various indirect devices, for example, to approximate first the observed magnitudes by some conveniently chosen analytical functions of the coordinates, and then to compute the value of the Laplace operator of these functions by an analytical method.

Thus the direct experimental determination of the magnitude of the Laplacian, even for the conditions of the two-dimensional problem, is very desirable. An optical arrangement that permits solving this problem is described in the following paragraphs (fig. 43; see ref. 3).

The investigated model A, provided with positive lenses, is designed in such manner that it serves as the subject of the investigation and as the objective in the schlieren arrangement. The focal distance of this

objective should be large compared with the dimensions of the model (small luminous power of the model-objective). The model is illuminated by a point source of light S. In the absence of any thermal or diffusion process, the image of the light source is focused by the model-objective on lattice B representing a system of equidistant vertical and horizontal rods, at the intersections of these rods. Through the good objective Q, placed directly behind the lattice, the model-objective is focused on the ground glass D, on the photographic plate of the usual camera, or on the film of a moving-picture apparatus. This image will be dark, since it is obtained only from the rays scattered by the model, because the direct rays of the source are kept back by the intersections of the rods of the lattice B.

If a thermal or diffusion phenomenon now arises in the model, then at some regions a density gradient occurs and with it a gradient of the index of refraction. Such regions will act like prisms, deflecting the rays toward the greater densities. The light passing through these regions of the model does not fall at the intersection of the lattice but on a new part of the lattice, either on its rod or in the spaces between the rods. In the first case a dark image is obtained on the positive of the photograph, in the second case a luminous image is obtained. Thus, dark stripes that break up into two families appear on the photograph of the model. Each dark stripe corresponds to one rod of the lattice separated from the point of initial focusing by a definite distance. Hence, one family, corresponding to the horizontal rods of the lattice, forms on the photograph of the model isolines of equal vertical gradient of the index of refraction, and the second family forms isolines of equal horizontal gradient (equal density, temperature, and concentration). For the computation of the sensitivity see the following paragraphs.

The arrangement of the isolines permits the following interpretation. The number of isolines of equal vertical gradient corresponding to unit length of any vertical segment within the limits of the image of the model represents, to a known scale, the space rate of change of the vertical density gradient at this region of the model (i.e., the second derivative of the gradient with respect to the vertical coordinate). In the same way, the number of isolines of equal horizontal gradient corresponding to the horizontal unit of length represents the second derivative with respect to the horizontal coordinate. The sum of the two numbers (with account taken of their signs) will give the magnitude of the Laplacian of the density to the same scale (index of refraction, temperature, and concentration).

Therefore, the problem formulated is directly solved with a large degree of accuracy. In comparison with the method of section 2 (fig. 39) this method presents the following features:

(1) The most essential difference is that the diaphragm is replaced by a lattice.

(2) Such a narrow range of light waves is used (for photographing) that the incomplete achromatism of the model-objective does not constitute an obstacle.

(3) The large objective C is combined with the model A, which is the least important difference.

In the following photographs examples of the application of this method are given.<sup>10</sup> A cylindrical cavity in a surrounding metal mass with horizontal axis and of a diameter and length equal to 35 millimeters (see fig. 54) was used for the model. The cavity was bounded on both sides by spectacle glass and was filled with glycerine. The vertical distance is marked on the photographs by a straight plumb line.

Figure 44 corresponds to the case where a vertical temperature gradient (warmer below) is produced in the surrounding mass. As a result, a convective motion arose in the cavity; the warm liquid rises along the vertical diameter and drops along the sides. At those regions of the model where the fluid intensively warms or cools, at the bottom and top, the Laplacian has a large positive or negative value, the isolines of equal gradients then lying close together. This is particularly marked in relation to the vertical gradients. At the center part of the model, the heated fluid, on rising, carries away large amounts of heat, maintaining an almost unchanged temperature. In this part there are practically no isolines. More accurately, one isoline rolled into a fantastic ball is observed here. It can be deciphered by increasing the focal distance or by using a small meshed lattice.

Figure 45A corresponds to the case where a horizontal temperature gradient is produced in the surrounding mass. As a result, a convective motion is produced in the cavity; along the warm wall the fluid rises and along the cold wall the fluid descends. A considerable density of the isolines of both families is observed in those places of the model where the temperature of the fluid undergoes a large change. In the center of the model there are indications of only a feeble thermal process. The isoline forming a closed curve in the center of the photograph corresponds to an almost zero horizontal gradient. The isolines obliquely forming two pairs of mutually embracing figures belong to the family of equal vertical gradients.

It is useful to emphasize that in the phenomena of diffraction limit, the sensitivity of the described method is in the downward and not in the upward direction. The reason for this difference is that the lattice standing in front of the objective of large luminous power breaks it up into a multiplicity of objectives of small luminous power, and the

<sup>10</sup>G. N. Guk participated in the preparation of these photographs.

forming of the images of the stripes near one another is equivalent to the photographing of a small-meshed object. The image is produced by narrow pencils of light rays coming from the parts of the model that lie close together. In figure 46, P denotes the plane of the lattice,  $\phi$  the plane of the photographic plate,  $d$  the distance between the neighboring rods of the lattice, and  $x$  the distance between the corresponding stripes on the photograph. For simplicity, we assume that we are dealing with the nearest neighborhoods of the principal optical axis OO of the camera. From the rectangular triangles, we obtain, in an elementary manner

$$\left. \begin{aligned} l^2 + \left(\frac{x}{2} + \frac{d}{2}\right)^2 &= r_1^2 = l^2 + \frac{x^2}{4} + \frac{xd}{2} + \frac{d^2}{4} \\ l^2 + \left(\frac{x}{2} - \frac{d}{2}\right)^2 &= r_2^2 = l^2 + \frac{x^2}{4} - \frac{xd}{2} + \frac{d^2}{4} \end{aligned} \right\} \quad (13.11)$$

whence, after subtracting,

$$(r_1 - r_2)(r_1 + r_2) = xd \quad (13.12)$$

In correspondence with the results of the diffraction theory of optical instruments, the stripes obtained on the photograph are sharp if the difference  $r_1 - r_2$  is not greater than the half wavelength of the light  $\lambda/2$ . Setting approximately  $r_1 + r_2 = 2l$ , we obtain the following condition of the sharpness of the stripe:

$$xd \geq l\lambda \quad (13.13)$$

From this it is seen that for rough processes, when the gradient varies considerably even over small distances ( $x$  is small), the lattice should be coarse ( $d$  should be large). Conversely, for delicate thermal processes when a hardly appreciable thermal phenomenon gives wide stripes on the photographs ( $x$  is large), it is necessary and possible to use a small meshed lattice ( $d$  may be small).

The preceding method may be applied for quantitative measurements in all those cases where the qualitative schlieren method may be useful. The following paragraphs give some of the variants for this method.

(a) For increasing the luminous power and reducing the exposure time, in particular for moving pictures of steady processes, the point source of light may be replaced by a plane source. In this case it should represent a negative reproduction of the lattice (transparent vertical and horizontal convenient openings in a nontransparent layer) to a scale which assures a dark image in the absence of the phenomenon under investigation. However, it is necessary for the observable dimensions of the source to be small if they are observed from the model center ("small luminous power").

(b) The objective of the camera may be replaced by a concave mirror, on which the lattice is drawn. This variant considerably reduces the over-all dimensions of the apparatus.

(c) The objective of the model may also be replaced by a concave mirror. A light ray must then pass through the model twice, a circumstance which doubles the sensitivity of the method. This variant again considerably reduces the over-all dimensions of the apparatus.

For subjective observations the method further permits the following modification. The light source is replaced by an illuminated ground or milky surface on which a multicolored network of lines is drawn. The camera is replaced by an observer who views the model through a small opening, which is put in the place of the lattice. By observing from the color of the line its direction (vertical or horizontal) and its number (e.g., distinguishing the zero and fifth lines by special colors), we are rapidly able to gain an idea as to the character of the observed process from the configuration of the visible color pattern.

#### 5. Application of Lattice Method to Experimental

##### Investigation of Laminar Convection in Cavity of Convenient Shape<sup>11</sup>

As an example of the preliminary application of the lattice method, the investigation of the concrete problem mentioned in the heading of the section is described in the following paragraphs. A suitable cavity of 38 by 6 millimeters is bored in the center of a babbitt parallelepiped, shown in figure 47. The cavity is stopped with two spectacle glasses of 1.5 diopters each, and is filled with distilled water. For filling the cavity, a through channel of 3 millimeters is used. The volume of the cavity was 1/70 as large as that of the surrounding mass. It may thus be assumed that the conditions in the model are approximately the same as those of a slit in an infinitely large mass.

On both sides of the cavity parallel to its length through channels are bored, three on one side for inserting porcelain tubes with Nichrome heater inside, and two on the other side provided with connecting pieces for the supply of cold water. The model is pressed in a Textolite ring and is able, on the horizontal parallel rods of an optical bench, to assume any angle to the vertical.

The source of light is an opening of 0.2-millimeter diameter in the shade of a lamp. In these tests the vertical component of the temperature gradient was very small and was not of interest in this stage

<sup>11</sup>The present section was composed from data obtained by G. N. Guk.

of the investigations. For this reason, all the photographs were prepared with the lattice consisting of only the vertical rods. These rods of 1.3-millimeter diameter were arranged with a distance of 3 millimeters between their axes. The photo objective of 45-millimeter diameter, with a focal distance of 210 millimeters, was placed with the lattice about 560 millimeters from the middle plane of the model. The focal distance of the model filled with water was 480 millimeters.

Under these conditions the computation of the sensitivity may be made on the basis of the following considerations. Figure 48 shows two parallel rays traversing in the geometric paths, in the interior of the model. The distance between the rays is  $dy$ . The optical length of the path of one ray, passing through the fluid in a region with temperature  $\theta$  is  $sn$ , where  $n$  is the index of refraction of the fluid. The optical length of the neighboring ray is  $s\left(n + \frac{dn}{d\theta} d\theta\right)$ , since it passes inside the fluid having a different temperature. Thus, the two rays produce the optical difference of path of  $s \frac{dn}{d\theta} d\theta$  over the distance  $s$ . Hence, the wave front, and with it the light rays, is deflected by the small angle  $s \frac{dn}{d\theta} \frac{d\theta}{dy}$ . If this deflection of the rays corresponds to one cell of the lattice, then (see fig. 46)

$$s \frac{dn}{d\theta} \times \frac{d\theta}{dy} = \frac{x}{l} \quad (13.14)$$

whence

$$\frac{d\theta}{dy} = \frac{x}{ls} \frac{dn}{d\theta} \quad (13.15)$$

For water at 20° C,  $dn/d\theta$  constitutes approximately  $9 \times 10^{-5}$  degrees<sup>-1</sup>. Hence, for these dimensions of the model, we obtain

$$\left. \begin{aligned} x &= 0.3 \text{ cm} \\ l &= 56 \text{ cm} \\ s &= 4 \text{ cm} \\ \frac{d\theta}{dy} &= 15 \text{ deg/cm} \end{aligned} \right\} \quad (13.16)$$

The deflections (at a temperature above 4° C) are directed toward the cold regions of the model. On raising the temperature the magnitude  $dn/d\theta$  increases; hence,  $d\theta/dy$ , corresponding to one cell of the lattice,

decreases, so that the same absolute temperature gradients are now expressed by a higher number of the rod of the lattice. Hence, the stripes on the photographs that correspond to the warmer regions of the model lie closer together than in the antisymmetric cold regions.

The duration of the steady thermal regimes for this model was about 2 hours.

As illustrations, a number of photographs that were obtained with this model are here reproduced (magnified twice), figure XVIII, A, B, C, D, E, and F. On these photographs it is possible to follow the changes of the thermal picture for vertical slits at different heating powers. The center of each photograph shows the black image of the plumb line. In order that this line may always be seen, the apparatus was so adjusted that the image was bright in the absence of the thermal process: the bundle of rays does not fall on the rod but on the center of the cell of the lattice. As the heating power is increased the number of stripes increases, their form remaining almost unchanged. The S-shaped curvature of the central luminous stripe may be observed on all photographs. The stripe shows that the region of zero horizontal temperature gradient occupies the entire length of the central part of the model and is turned up toward the warm wall of the model and down toward the cold wall. This circumstance suggests that the vertical temperature difference in absolute value is close, if not equal, to the horizontal temperature difference. Because the vertical heating was not specially arranged, this difference has the natural sign of being warmer upward.

Figures XIX A and B show photographs obtained with an inclined slit. Figure XX shows photographs obtained with a horizontal slit.

4281

CA-15 back

## CHAPTER 14

## CONCLUDING SUMMARY OF EXPERIMENTAL INVESTIGATIONS

## OF LINEAR AND QUASI-LINEAR CASES

4281

As may be seen from the material presented in chapters 9 to 13, the theory described at the beginning of the book is essentially valid for laminar fluid motion.

1. The numerical value of the magnitudes entering the theoretical formula (5.15) is satisfactorily confirmed in experiments on models of different diameter and on models made of different materials (ch. 10, sec. 2).

2. The convection parameter is actually constant along the model height in those cases where convection takes place (table VIII). In the computations it is necessary to consider the trend of the standard convection curve (ch. 8, sec. 3).

3. The laminar motion in a closed model actually consists in the fact that the section of the model spontaneously divides into two parts: in one part the warm fluid rises upward, and in the other part the cold fluid descends downward (fig. III).

4. In laminar motion one side is actually warmer than the other (ch. 10, secs. 4 and 5).

5. Diametral antisymmetry, corresponding to the smallest root of the characteristic equation (5.15), is actually observed above the heater even with annular heating (fig. II).

6. In the center part of a vertical model the velocities of the laminar flow are, at least essentially, vertical and are accompanied by characteristic small vertical and considerable horizontal temperature gradients (ch. 13, sec. 2).

7. The conditions at the ends of the model do not play a deciding role in the steady regime except for the still doubtful case of short columns of liquid (ch. 12, sec. 5).

8. Near the plane boundaries of the model (warm bottom and cold top) the exponential law of the temperature averaged over the perimeter is approximately observed (formula (12.1)).

9. The unsteady phenomena of convection differ in striking features (ch. 11).

10. The laminar and above-critical convection regimes are separated from each other by a sharp critical point (ch. 10, sec. 1, fig. 25).

11. The above-critical regime is characterized by an approximate constancy of the provisional Nusselt number the value of which shows that in the above-critical regime, the thermal behavior of the model is equivalent to a solid body with a heat conductivity probably a thousand times as large as the molecular heat conductivity of the fluid (ch. 10, sec. 3).

## CHAPTER 15

CASES REQUIRING SOLUTION OF NONLINEAR EQUATIONS  
OF GRAVITATIONAL CONVECTION

4281

1. Practical Significance of Nonlinear Cases and  
Restriction of Scope of Problem

Chapter 5 shows that the analytical treatment in known functions is possible only for linear differential equations that describe only a specialized case; namely, the strict collinearity of the velocity vector of the flow, the tube axis, and the acceleration vector of the gravity, along with constant temperature gradient along the model. Chapter 11 shows that, as a result of the heat losses over the model, this requirement is not strictly observed even in a model of special construction. In nature and in industrial practice this requirement is still less strictly maintained even in more or less similar cases, for the following reasons:

- (1) The noncylindrical shape of the ducts (the ducts and tubes are of variable cross section)
- (2) The nonuniformity of the wall thickness or the coefficient of heat conductivity along the duct
- (3) The unexplained presence of heat sources or sinks that produce additional temperature gradients
- (4) The parametric nonlinearity of the process, the role of which is particularly marked in ducts of small dimensions (pores)
- (5) The end phenomena and the phenomena near the principal heat sources and sinks
- (6) The nonvertical position of the channel axis.

In every practical case some of these causes are very important, while in other cases they are decisive.

At the same time, however, the solution of a system of nonlinear partial differential equations does not lend itself to the application of the known functions introduced in practice and studied in connection with the solution of linear equations. Therefore, the mathematical methods may be of assistance in studying the processes of convection only in the form of certain complicated and laborious computational procedures (method of successive approximations).

The absence of any generalized mathematical guiding principle in regard to the theoretical cases of most interest makes it necessary to give considerable attention to the cases that will acquire the greatest practical significance in the future. In our present discussion, only the preliminary theoretical results are given for the following three investigations: the vertical circular tube with heat losses, the horizontal circular tube, and the spherical cavity.

## 2. Observations on General Method of Solution of Nonlinear Equations

No method of solving nonlinear differential equations in closed form is known. Considerable study has been made of functions that represent solutions of linear differential equations. These functions, only with rare exceptions, satisfy simple nonlinear differential equations. For example, the solution of an ordinary differential equation of the first order leads directly to series difficult to compute if this equation is nonlinear.

Therefore, the solution of the partial differential equations of gravitational convection, which are nonlinear and of high order, cannot be a simple problem. Other more or less investigated solutions of nonlinear equations may here serve as an analogy; for example, those which have important application to radio technology due to the brilliant work of the school of Soviet academicians L. I. Mandelshtam and N. D. Papaleksi. The different variants of the method of successive approximation have proven fruitful.

The essence of the method, as applied to the problems of gravitational convection, consists in the following three operations:

(1) The system of differential equations (2.1), (2.2), and (2.4), by elimination of all unknowns except one, reduces to a single differential equation of a raised order. An example of this operation is the transition from two harmonic equations of the second order to one bi-harmonic equation of the fourth order (ch. 3, sec. 3).

(2) By adapting to the special features of the case under consideration, special dependences of the required function on all the arguments except one are given for the indispensable condition of the separation of variables. In this way, we pass from the more general case of a partial differential equation to the narrowed case of an ordinary differential equation (in total derivatives). An example of this operation is the typical case of the introduction of an exponential function of time (ch. 6, sec. 3, eq. (6.11)). In eliminating the unknown dependence on the space coordinates by this method, use of the property of space symmetry is suggested.

(3) The ordinary nonlinear differential equation is solved by the method of successive approximations.

The essence of the method of successive approximations lies in first introducing or seeking, on the basis of physical considerations specialized for the case under consideration, a certain parameter that quantitatively characterizes the "measure of nonlinearity." The required function is then broken up into a sum of new functions of which each differs from the preceding by a multiplying factor; namely, the previously mentioned parameter of nonlinearity. Finally, the equation is expanded in powers of this parameter. Since this constant parameter is not zero, the entire equation can be satisfied only if the coefficients of the different powers of the parameter (the required functions of the remaining single argument) are zero. The single equation is thus converted into a system of simultaneous equations. Each of the equations is obtained as linear with respect to the successive required component entering the unknown function, but nonhomogeneous, containing on the right side the required components of the function and their derivatives in nonlinear combinations. In turn, the solution of these equations permits adding to the previously found solution a new accuracy-improving term - the successive approximation.

In this successive computation, a very large significance is possessed by the "zeroth" approximation, which starts the process of successive approximations and plays the decisive role. In choosing a new function as the zeroth approximation, we can describe qualitatively new processes (secs. 4 and 5). The linearized case (ch. 3) plays the role of the "fundamental" initial orientation for the investigation of certain special variants of these qualitatively different processes.

The order of the three operations previously mentioned may be chosen differently, depending on the special circumstances of each individual case, from considerations of facilitating the technique of the laborious computations. One of the operations may even be carried out only partially, then the second operation may be carried out, and finally the first operation may be completed (sec. 5). However, in whatever form the parts of these three operations are carried out in any computational procedure, in principle they represent only a single device.

In regard to the physical meaning of these operations, the second and third operation represent certain physical assumptions in mathematical form. In the choice of these assumptions a considerable part is played by the practical requirements, and by the possibility of realizing a physically verifiable experiment.

In this connection it should be emphasized that the "fundamental" equations discussed in chapter 3 do not represent the original general equations of gravitational convection, in which the nonlinear terms have been mechanically deleted. The nonlinear physical character of the equations is maintained and represented by the convective term  $Av$  in the equation (3.3) of heat conduction of Fourier-Kirchhoff. The structural mathematical linearization was found admissible only by virtue of the chosen special case where

$$\frac{\partial A}{\partial z} = \frac{\partial^2 \theta}{\partial z^2} = 0; \quad \frac{\partial A}{\partial x} = \frac{\partial A}{\partial y} = 0 \quad (2.10), (3.5)$$

and

$$v_x = v_y = 0; \quad \frac{\partial v_z}{\partial z} = 0 \quad (2.9)$$

Conversely, if the solution obtained in chapter 5, confirmed by the experiments described in chapter 10, is substituted in the initial equation (2.2) of chapter 2, crossing out the nonlinear term on the left side of the last equation, these equations, "linearized" in the same mechanical fashion, will not be satisfied. One may convince oneself of this by an elementary substitution.

For simplifying the laborious computations it is advisable to add a fourth operation to the three previously mentioned operations; namely, the reduction of the equations to nondimensional form.

### 3. Case of Heat Losses Through Imperfect Heat Insulation<sup>12</sup>

Chapter 11 discusses theoretical considerations and experiments connected with heat losses through the walls along the channel in which thermal convection is observed. These heat losses give rise to deviations from the strict assumptions from which we started in deriving the "fundamental" equations of chapter 3, and the reservations which were made in particular in section 5 of chapter 3.

<sup>12</sup>Sections 3 to 5 were compiled on the basis of data obtained by N. M. Pisarev.

We shall now take into account the structural nonlinearity of the equations of convection and solve the problem more strictly. We shall choose a cylindrical system of coordinates such that the Z-axis coincides with the channel axis and is in a direction opposite to that of the acceleration of gravity. The initial azimuth is chosen arbitrarily on the assumption of the absence of transverse temperature gradients far from the channel. The initial equations of gravitational convection in cylindrical coordinate form for the steady regime are the following (ref. 1 of ch. 2, p: 50):

The Navier-Stokes equations:

$$\left. \begin{aligned}
 v_r \times \frac{\partial v_r}{\partial r} + \frac{v_\phi}{r} \times \frac{\partial v_r}{\partial \phi} + v_z \times \frac{\partial v_r}{\partial z} - \frac{v_\phi^2}{r} &= -\frac{1}{\rho} \times \frac{\partial p}{\partial r} + \\
 v \left( \frac{\partial^2 v_r}{\partial r^2} + \frac{1}{r^2} \times \frac{\partial^2 v_r}{\partial \phi^2} + \frac{\partial^2 v_r}{\partial z^2} + \frac{1}{r} \times \frac{\partial v_r}{\partial r} - \right. \\
 \left. \frac{2}{r^2} \times \frac{\partial v_\phi}{\partial \phi} - \frac{v_r}{r^2} \right) \\
 v_r \times \frac{\partial v_\phi}{\partial r} + \frac{v_\phi}{r} \times \frac{\partial v_\phi}{\partial \phi} + v_z \times \frac{\partial v_\phi}{\partial z} + \frac{v_r \times v_\phi}{r} &= -\frac{1}{\rho r} \times \frac{\partial p}{\partial \phi} + \\
 v \left( \frac{\partial^2 v_\phi}{\partial r^2} + \frac{1}{r^2} \times \frac{\partial^2 v_\phi}{\partial \phi^2} + \frac{\partial^2 v_\phi}{\partial z^2} + \frac{1}{r} \times \frac{\partial v_\phi}{\partial r} + \right. \\
 \left. \frac{2}{r^2} \times \frac{\partial^2 v_r}{\partial \phi} - \frac{v_\phi}{r^2} \right) \\
 v_r \times \frac{\partial v_z}{\partial r} + \frac{v_\phi}{r} \times \frac{\partial v_z}{\partial \phi} + v_z \times \frac{\partial v_z}{\partial z} &= -\frac{1}{\rho} \times \frac{\partial p}{\partial z} + \\
 v \left( \frac{\partial^2 v_z}{\partial r^2} + \frac{1}{r^2} \times \frac{\partial^2 v_z}{\partial \phi^2} + \frac{\partial^2 v_z}{\partial z^2} + \frac{1}{r} \times \frac{\partial v_z}{\partial r} \right) - g\beta\theta
 \end{aligned} \right\} (15.1)$$

The Fourier-Kirchhoff equation:

$$v_r \times \frac{\partial \theta}{\partial r} + \frac{1}{r} \times v_\phi \times \frac{\partial \theta}{\partial \phi} + v_z \times \frac{\partial \theta}{\partial z} = v \left( \frac{\partial^2 \theta}{\partial r^2} + \frac{1}{r} \times \frac{\partial \theta}{\partial r} + \frac{1}{r^2} \times \frac{\partial^2 \theta}{\partial \phi^2} + \frac{\partial^2 \theta}{\partial z^2} \right) \quad (15.2)$$

The continuity equation:

$$\frac{\partial v_r}{\partial r} + \frac{1}{r} \times \frac{\partial v_\phi}{\partial \phi} + \frac{\partial v_z}{\partial z} + \frac{v_r}{r} = 0 \quad (15.3)$$

In correspondence with experimental results (ch. 11), to go over from the equations in partial derivatives to ordinary equations (in total derivatives), we assume the following dependence of the axial component of velocity on the vertical coordinate and on the azimuth:

$$v_z \equiv \frac{v}{R} \left( a + h \frac{z}{R} \right) \left( f_0 + f_1 \cos \phi + f_2 \cos 2\phi + \dots \right) \quad (15.4)$$

In this expression the first factor determines the dimension of the velocity. In the second factor the nondimensional component  $a$  determines the intensity of the convection phenomenon in the section  $z = 0$  (it has the sense of the Reynolds number). The second component determines the assumed linear dependence of this intensity on the coordinate  $z$  (ch. 11, sec. 1). At the same time this component contains the nondimensional "nonlinearity parameter"  $h$ . For  $h = 0$  we have the linearized problem, solved in the form of the "fundamental" equations of chapter 3. In the third factor the velocity is expanded in a Fourier series in multiples of the azimuth and contains the required nondimensional functions only of the radius  $r-f_0, f_1, f_2, \dots$

Making use of the considerations of symmetry and by analogy with the preceding, we write for the radial component

$$v_r = \frac{v}{R} h (F_0 + F_1 \cos \phi + F_2 \cos 2\phi + \dots) \quad (15.5)$$

Similarly, we write for the azimuthal component

$$v_\phi = \frac{v}{R} h (\Phi_1 \sin \phi + \Phi_2 \sin 2\phi + \dots) \quad (15.6)$$

From considerations of symmetry  $\Phi_0 = 0$ , the absence of uniform rotation of the channel fluid about its axis is assumed. In the linearized case the radial and azimuthal components were zero, since we had  $h = 0$  there.

The continuity equation gives

$$\begin{aligned} \frac{v h}{R} \left[ F'_0 + \frac{1}{r} F_0 + \left( F'_1 + \frac{1}{r} F_1 \right) \cos \phi + \left( F'_2 + \frac{1}{r} F_2 \right) \cos 2\phi + \dots \right] + \\ \frac{1}{r} \times \frac{v h}{R} (\Phi_1 \cos \phi + 2\Phi_2 \cos 2\phi + \dots) + \\ \frac{v h}{R} (f_0 + f_1 \cos \phi + f_2 \cos 2\phi + \dots) = 0 \end{aligned} \quad (15.7)$$

4481

CA-16 back

whence the following relations are obtained:

$$\left. \begin{aligned} F_0' + \frac{1}{r} F_0 + \frac{1}{R} f_0 &= 0 \\ F_1' + \frac{1}{r} F_1 + \frac{1}{r} \Phi_1 + \frac{1}{R} f_1 &= 0 \\ F_1(0) &= \Phi_1(0) \\ F_2' + \frac{1}{r} F_2 + \frac{2}{r} \Phi_2 + \frac{1}{R} f_2 &= 0 \\ \dots \dots \dots \end{aligned} \right\} \quad (15.8)$$

Owing to the presence of a boundary layer,

$$F_0(R) = F_1(R) = \Phi_1(R) = \Phi_2(R) = f_0(R) = f_1(R) = f_2(R) = \dots = 0 \quad (15.9)$$

Substituting the assumed expressions (15.4) to (15.6) into the Navier-Stokes equation (15.1), gives

$$\begin{aligned} & \left( \frac{v_h}{R} \right)^2 \left\{ (F_0 + F_1 \cos \varphi + F_2 \cos 2\varphi + \dots) \times \right. \\ & \quad (F_0' + F_1' \cos \varphi + F_2' \cos 2\varphi + \dots) + \\ & \quad \frac{1}{r} (\Phi_1 \sin \varphi + \Phi_2 \sin 2\varphi + \dots) \times \\ & \quad (-F_1 \sin \varphi - 2F_2 \sin 2\varphi - \dots) - \\ & \quad \left. - \frac{1}{r} (\Phi_1 \sin \varphi + \Phi_2 \sin 2\varphi + \dots)^2 \right\} = \\ & - \frac{1}{\rho} \times \frac{\partial p}{\partial r} + \frac{v_h^2}{R} \left\{ F_0'' + \frac{1}{r} F_0' - \frac{1}{r^2} F_0 + \right. \\ & \quad \left( F_1'' + \frac{1}{r} F_1' - \frac{2}{r^2} F_1 \right) \cos \varphi + \left( F_2'' + \frac{1}{r} F_2' - \frac{5}{r^2} F_2 \right) \cos 2\varphi - \\ & \quad \left. \frac{2}{r^2} \Phi_1 \cos \varphi - \frac{4}{r^2} \Phi_2 \cos 2\varphi - \dots \right\} \quad (15.10) \end{aligned}$$

$$\begin{aligned}
 & \left(\frac{vh}{R}\right)^2 \left\{ (F_0 + F_1 \cos \varphi + F_2 \cos 2\varphi + \dots) (\Phi_1' \sin \varphi + \Phi_2' \sin 2\varphi + \dots) + \right. \\
 & \quad \frac{1}{r} (\Phi_1 \sin \varphi + \Phi_2 \sin 2\varphi + \dots) (\Phi_1 \cos \varphi + 2\Phi_2 \cos 2\varphi + \dots) + \\
 & \quad (F_0 + F_1 \cos \varphi + F_2 \cos 2\varphi + \dots) (\Phi_1 \sin \varphi + \Phi_2 \sin 2\varphi + \dots) = \\
 & - \frac{1}{\rho r} \times \frac{\partial p}{\partial \varphi} + \frac{v^2 h}{R} \left( \Phi_1'' + \frac{1}{r} \Phi_1' - \frac{2}{r^2} \Phi_1 \right) \sin \varphi + \left( \Phi_2'' + \frac{1}{r} \Phi_2' - \frac{5}{r^2} \Phi_2 \right) \sin 2\varphi - \\
 & \quad \left. \frac{2}{r^2} F_1 \sin \varphi - \frac{8}{r^2} F_2 \sin 2\varphi + \dots \right\} \quad (15.11)
 \end{aligned}$$

$$\begin{aligned}
 & \left(\frac{v}{R}\right)^2 h \left(a + h \frac{z}{R}\right) \left\{ (F_0 + F_1 \cos \varphi + F_2 \cos 2\varphi + \dots) \times \right. \\
 & \quad (f_0' + f_1' \cos \varphi + f_2' \cos 2\varphi + \dots) - \\
 & \quad \frac{1}{r} (\Phi_1 \sin \varphi + \Phi_2 \sin 2\varphi + \dots) \times \\
 & \quad (f_1 \sin \varphi + 2f_2 \sin 2\varphi + \dots) + \\
 & \quad \left. \frac{1}{R} (f_0 + f_1 \cos \varphi + f_2 \cos 2\varphi + \dots)^2 \right\} = \\
 & - \frac{1}{\rho} \times \frac{\partial p}{\partial z} + \frac{v^2}{R} \left(a + h \frac{z}{R}\right) \left[ f_0'' + \frac{1}{r} f_0' + \right. \\
 & \quad \left( f_1'' + \frac{1}{r} f_1' - \frac{1}{r^2} f_1 \right) \cos \varphi + \\
 & \quad \left. f_2'' + \frac{1}{r} f_2' - \frac{4}{r^2} f_2 \cos 2\varphi + \dots \right] - g\beta\theta \quad (15.12)
 \end{aligned}$$

Equations (15.10) and (15.11) do not contain members depending on the vertical coordinate  $z$ ; therefore,

$$\left. \begin{aligned} \frac{\partial^2 p}{\partial r \partial z} &= 0 \\ \frac{\partial^2 p}{\partial \varphi \partial z} &= 0 \end{aligned} \right\} \quad (15.13)$$

It follows that the expression  $\partial p / \partial z$ , encountered in equation (15.12), does not depend either on the radius  $r$  or on the azimuth  $\phi$  but depends only on the vertical coordinate  $z$ . By analogy with the previously discussed case of the superposition of free and forced convection in correspondence with equation (5.33), we assume

$$\frac{\partial p}{\partial z} = -\rho g \beta A z \quad (15.14)$$

Differentiating equation (15.12) with respect to the radius  $r$ , we eliminate the pressure  $p$ . To facilitate the computation, we first transform this equation by carrying out the multiplication and grouping the terms with the same function of the azimuth, where we consider the following relations:

$$\left. \begin{aligned} 2 \sin^2 \phi &= 1 - \cos 2\phi \\ 2 \cos^2 \phi &= 1 + \cos 2\phi \\ 2 \cos \phi \times \cos 2\phi &= \cos \phi + \cos 3\phi \\ 2 \sin \phi \times \sin 2\phi &= \cos \phi - \cos 3\phi \end{aligned} \right\} \quad (15.15)$$

In this way we obtain

$$\begin{aligned} g\beta\theta &= \frac{v^2 \left( a + h \frac{z}{R} \right)}{R} \left\{ \left[ f_0'' + \frac{1}{r} f_0' - \frac{h}{R} \left( F_0 f_0' + \frac{1}{2} F_1 f_1' + \frac{1}{2} F_2 f_2' - \right. \right. \right. \\ &\quad \left. \left. \frac{1}{2r} \Phi_1 f_1 - \frac{1}{r} \Phi_2 f_2 + \frac{1}{R} f_0^2 + \frac{1}{2R} f_1^2 + \frac{1}{2R} f_2^2 \right) \right] + \\ &\quad \left[ f_1'' + \frac{1}{r} f_1' - \frac{1}{r^2} f_1 - \frac{h}{R} \left( F_0 f_1' + F_1 f_0' + \frac{1}{2} F_1 f_2' + \frac{1}{2} F_2 f_1' - \right. \right. \\ &\quad \left. \left. \frac{1}{r} \Phi_1 f_2 - \frac{1}{2r} \Phi_2 f_1 + \frac{2}{R} f_0 f_1 + \frac{1}{R} f_1 f_2 \right) \right] \cos \phi + \\ &\quad \left[ f_2'' + \frac{1}{r} f_2' - \frac{4}{r^2} f_2 - \frac{h}{R} \left( F_0 f_2' + F_2 f_0' + \frac{1}{2} F_1 f_1' + \right. \right. \\ &\quad \left. \left. \frac{1}{2r} \Phi_1 f_1 + \frac{2}{R} f_0 f_2 + \frac{1}{2R} f_1^2 \right) \right] \cos 2\phi + \dots \left. \right\} + g\beta A z = \\ &= \frac{v^2 \left( a + h \frac{z}{R} \right)}{R} \left\{ C_0 + C_1 \cos \phi + C_2 \cos 2\phi + \dots \right\} + g\beta A z \end{aligned} \quad (15.16)$$

Further,

$$\frac{\partial \theta}{\partial r} = \frac{v^2 \left( a + h \frac{z}{R} \right)}{g\beta R} \left\{ \right\}'_r \quad (15.17)$$

where the symbol  $\left\{ \right\}'_r$  denotes the derivative with respect to the radius  $r$  of the expression in braces in equation (15.16). Further the same symbol will be applied to the following derivatives of the same expression, with respect to the radius and the azimuth.

We now substitute the obtained expressions in the Fourier-Kirchhoff equation (15.2), so that

$$\begin{aligned} & \frac{vh}{R} (F_0 + F_1 \cos \varphi + F_2 \cos 2\varphi + \dots) \frac{v^2 \left( a + h \frac{z}{R} \right)}{g\beta R} \left\{ \right\}'_r + \\ & \frac{1}{r} \times \frac{vh}{R} (\Phi_1 \sin \varphi + \Phi_2 \sin 2\varphi + \dots) \frac{v^2 \left( a + h \frac{z}{R} \right)}{g\beta R} \left\{ \right\}'_\varphi + \\ & \frac{v}{R} \left( a + h \frac{z}{R} \right) (f_0 + f_1 \cos \varphi + f_2 \cos 2\varphi + \dots) \left[ A + \frac{v^2 h}{g\beta R} \left\{ \right\} \right] = \\ & \frac{v^2 \left( a + h \frac{z}{R} \right)}{g\beta R} \left[ \left\{ \right\}''_r + \frac{1}{r} \left\{ \right\}'_r + \frac{1}{r^2} \left\{ \right\}''_\varphi \right] \end{aligned} \quad (15.18)$$

After dividing, this equation is rewritten as

$$\begin{aligned} & \left\{ \right\}''_r + \frac{1}{r} \left\{ \right\}'_r + \frac{1}{r^2} \left\{ \right\}''_\varphi - \frac{g\beta A}{v\kappa} (f_0 + f_1 \cos \varphi + f_2 \cos 2\varphi + \dots) - \\ & \frac{v}{\kappa} \times \frac{h}{R} \left[ \frac{1}{R} (f_0 + f_1 \cos \varphi + f_2 \cos 2\varphi + \dots) \left\{ \right\} + \right. \\ & \left. \frac{1}{r} (\Phi_1 \sin \varphi + \Phi_2 \sin 2\varphi + \dots) \left\{ \right\}'_\varphi + \right. \\ & \left. (F_0 + F_1 \cos \varphi + F_2 \cos 2\varphi + \dots) \left\{ \right\}'_r \right] = 0 \end{aligned} \quad (15.19)$$

In view of the great complication of the equation obtained, it is hardly worth while to interpret the equation in its general form.

4281

## 4. Case of Axial Symmetry

We shall now dwell on a particular case which is distinguished by its evident simplicity. We assume that the entire phenomenon is symmetrical about the Z-axis. This case is experimentally observed within the heater that heats the model (e.g., fig. II). In this case

$$\left. \begin{aligned} f_1 = f_2 = \dots = F_1 = F_2 = \dots = \phi_1 - \phi_2 = \dots = 0 \\ \frac{\partial v_z}{\partial \phi} = 0 \\ \frac{\partial \theta}{\partial \phi} = 0 \end{aligned} \right\} (15.20)$$

4281

Only two nondimensional functions of the radius,  $f_0$  and  $F_0$ , are retained. Equation (15.19) is then rewritten as

$$\begin{aligned} & \frac{1}{r} \left[ f_0'''' + \frac{1}{r} f_0'''' - \frac{1}{r^2} f_0' - \frac{h}{R} (F_0' f_0' + F_0 f_0'' + \frac{2}{R} f_0 f_0') \right] + \\ & f_0^{IV} + \frac{1}{r} f_0'''' - \frac{2}{r^2} f_0'' + \frac{2}{r^3} f_0' - \frac{h}{R} (F_0'' f_0' + 2F_0' f_0'' + F_0 f_0'''' + \\ & \frac{2}{R} f_0 f_0'' + \frac{2}{R} f_0'^2) - k^4 f_0 - Pr \times \frac{h}{R} \left[ \frac{1}{R} f_0 (f_0'' + \frac{1}{r} f_0' - \right. \\ & \left. \frac{h}{R} F_0 f_0' - \frac{h}{R^2} f_0^2) + F_0 (f_0'''' + \frac{1}{r} f_0'' - \frac{1}{r^2} f_0' - \right. \\ & \left. \left. \frac{h}{R} [F_0' f_0' + F_0 f_0'' + \frac{2}{R} f_0 f_0'] \right) \right] = 0 \end{aligned} \quad (15.21)$$

It can otherwise be expressed in the following form:

$$\begin{aligned} \Delta \Delta f_0 - k^4 f_0 = & \frac{h}{R} Pr \left[ \frac{1}{R} f_0 (f_0'' + \frac{1}{r} f_0') + \right. \\ & F_0 (f_0'''' + \frac{1}{r} f_0'' - \frac{1}{r^2} f_0') \left. \right] + \frac{1}{r} (F_0' f_0' + F_0 f_0'' + \frac{2}{R} f_0 f_0') + \\ & (F_0'' f_0' + 2F_0' f_0'' + F_0 f_0'''' + \frac{2}{R} f_0 f_0'' + \frac{2}{R} f_0'^2) - \\ & \frac{h}{R} \left[ \frac{1}{R} f_0 (F_0 f_0' + \frac{1}{R} f_0^2) + F_0 (F_0' f_0' + F_0 f_0'' + \frac{2}{R} f_0 f_0') \right] \end{aligned} \quad (15.22)$$

where there was set

$$\left. \begin{aligned} f_0^{IV} + \frac{2}{r} f_0''' - \frac{1}{r^2} f_0'' + \frac{1}{r^3} f_0' &= \Delta\Delta f_0 \\ \frac{\nu}{\kappa} &= \text{Pr} \\ k^4 &= \frac{g\beta A}{\nu\kappa} \end{aligned} \right\} \quad (15.23)$$

From equation (15.22) it is seen that if  $h = 0$ , we have the previously discussed case of the "fundamental" linear equations (3.9). However, if  $h$  is different from zero, it is necessary to solve the nonlinear equation (15.22).

Applying the method of successive approximations for this purpose, we expand  $f_0$  and  $F_0$  into sums of unknown functions of the radius  $r$ , in powers of  $h$ :

$$\left. \begin{aligned} f_0 &= \psi_0 + h\psi_1 + h^2\psi_2 + \dots \\ F_0 &= \zeta_0 + h\zeta_1 + h^2\zeta_2 + \dots \end{aligned} \right\} \quad (15.24)$$

Substituting these expressions in equation (15.8) gives

$$\left. \begin{aligned} \zeta_0' + \frac{1}{r} \zeta_0 + \frac{1}{R} \psi_0 &= 0 \\ \zeta_1' + \frac{1}{r} \zeta_1 + \frac{1}{R} \psi_1 &= 0 \\ \dots \dots \dots \end{aligned} \right\} \quad (15.25)$$

Substituting equations (15.24) and (15.25) in equation (15.22) and equating the coefficients of like powers of  $h$ , we obtain the following set of equations:

$$\Delta\Delta\psi_0 - k^4\psi_0 = 0 \quad (15.26)$$

$$\begin{aligned} \Delta\Delta\psi_1 - k^4\psi_1 &= \frac{1}{R} \left\{ \text{Pr} \left[ \frac{1}{R} \psi_0 \left( \psi_0'' + \frac{1}{r} \psi_0' \right) + \right. \right. \\ &\zeta_0 \left( \psi_0''' + \frac{1}{r} \psi_0'' - \frac{1}{r^2} \psi_0' \right) \left. \right] + \frac{1}{r} \left( \zeta_0' \psi_0' + \zeta_0 \psi_0'' + \frac{2}{R} \psi_0 \psi_0' \right) + \\ &\left. \zeta_0'' \psi_0' + 2\zeta_0' \psi_0'' + \zeta_0 \psi_0''' + \frac{2}{R} \psi_0 \psi_0'' + \frac{2}{R} \psi_0'^2 \right\} \end{aligned} \quad (15.27)$$

4281

CA-17

$$\begin{aligned}
\Delta\Delta\psi_2 - k^4\psi_2 = & \frac{1}{R} \left\{ \text{Pr} \left[ \frac{1}{R} \psi_0 \left( \psi_1'' + \frac{1}{r} \psi_1' \right) + \frac{1}{r} \psi_1 \left( \psi_0'' + \frac{1}{r} \psi_0' \right) + \right. \right. \\
& \left. \left. \zeta_0 \left( \psi_1''' + \frac{1}{r} \psi_1'' - \frac{1}{r^2} \psi_1' \right) + \zeta_1 \left( \psi_0''' + \frac{1}{r} \psi_0'' - \frac{1}{r^2} \psi_0' \right) \right] + \right. \\
& \frac{1}{r} \left( \zeta_0' \psi_1' + \zeta_1' \psi_0' + \zeta_0 \psi_1'' + \zeta_1 \psi_0'' + \frac{2}{R} \psi_0 \psi_1' + \frac{2}{R} \psi_1 \psi_0' \right) + \\
& \zeta_0'' \psi_1' + \zeta_1'' \psi_0' + 2\zeta_0' \psi_1'' + 2\zeta_1' \psi_0'' + \zeta_0 \psi_1''' + \zeta_1 \psi_0''' + \\
& \frac{2}{R} \psi_0 \psi_1'' + \frac{2}{R} \psi_1 \psi_0'' + \frac{4}{R} \psi_0' \psi_1' - \frac{1}{r} \psi_0 \left( \zeta_0 \psi_0' + \frac{1}{R} \psi_0^2 \right) + \\
& \left. \left. \zeta_0 \left( \zeta_0' \psi_0' + \zeta_0 \psi_0'' + \frac{2}{R} \psi_0 \psi_0' \right) \right\} \quad (15.28)
\end{aligned}$$

4281

Equation (15.26) agrees with the previously discussed linearized case, equation (3.9). In the other equations we obtain a system of non-homogeneous linear biharmonic equations in the unknown functions  $\psi_1$ ,  $\psi_2$ , ... . On the right sides of each of these equations, functions previously defined from the preceding equations appear. All functions  $\psi$  and  $\zeta$  are even functions of the radius. The equations must be integrated under the general known boundary conditions: Each of the functions must be finite, continuous, and single-valued; it should give zero in the boundary layer at the channel walls and should satisfy the condition of "closedness." For example:

$$2\pi \int_0^R \psi_1 r dr = 0 \quad (15.29)$$

Equation (15.26) in regard to coinciding with the "fundamental" equation (3.9), should give the following solution for axial symmetry in the closed channel:

$$\left. \begin{aligned}
v_z = \frac{v_a}{R} \left[ \frac{J_0(ikr)}{J_0(ikR)} - \frac{J_0(kr)}{J_0(kR)} \right] \\
kR = 4.611 \\
(kR)^4 = 452.1
\end{aligned} \right\} \quad (15.30)$$

Whence by equation (15.8) for the radial component, we obtain to a first approximation

$$v_r = \frac{vh}{R} \times \frac{1}{kR} \left[ -\frac{-iJ_1(ikr)}{J_0(ikR)} + \frac{J_1(kr)}{J_0(kR)} \right] = \frac{vh}{R} \xi_0 \quad (15.31)$$

By substitution it can be confirmed that this radial component gives the value zero at the wall of the boundary layer (for  $r = R$ ).

In computing the functions  $\psi_1, \psi_2, \dots$  from equations (15.27), (15.28), and so forth, the following feature is revealed. The general solution of equation (15.27), for example, is the sum of the solutions of an equation of the form (15.26) (homogeneous) and of any particular solution of the nonhomogeneous equation (15.27). The first component of this sum satisfies the condition of closedness (15.29). The second component, however, may receive the following form. It is necessary to represent the required particular solution and the right side of equation (15.27) as a series of suitable orthogonal functions. By equating the coefficients, the coefficients of the required series are found.

In the given case, the suitable orthogonal functions are the Bessel functions of the first kind of zero order. They easily give zero at the boundary and therefore already satisfy the condition of the boundary layer. They likewise satisfy the conditions of finiteness, continuity, and single-valuedness. However, the obtained series will not always satisfy the condition of closedness (eq. (15.29)) but will satisfy only for a single value of the fluid parameter  $Pr$ . Because the right side of equations (15.27), (15.28), and so forth, are linear functions of this parameter, the required series and the condition of closedness will likewise be the same linear functions of the parameter.

Whether this single (real) value of the parameter  $Pr$  really exists (in particular, as a positive quantity) or whether it requires fantastic fluid properties is a question that is as yet not clear. However, the value of this parameter, obtained with the aid of equation (15.27), will certainly differ from the value of this parameter obtained with the aid of equations (15.28) and so forth. As a result, a contradiction is obtained.

In this way we arrive at the almost certain result that in the axisymmetrical case (eq. (15.4)) the proportionality of the vertical component of the velocity  $v_z$  to the binomial  $(1 + h z/R)$  is actually not realized. Similar cases and cases experimentally observed correspond to some other nonlinear dependence of this vertical component on the vertical coordinate  $z$  or to some other value of the parameter  $kR$ , differing from 4.611 (eq. (15.30)).

4281

CA-17 back

The hypothesis (eq. (15.4)) applied to the axisymmetrical case may be considered no more than a very rough initial approximation. Further on, several computations making use of this hypothesis will be given, but the significance of the conclusions from these computations should not as yet be exaggerated.

In view of the complicatedness of the process of the solution of the preceding equations, it is desirable to clarify important physical questions by which this solution is avoided. Perhaps the most important question is that of the thermal conditions on the boundaries at the channel walls, which are the cause of the nonlinear phenomenon previously described.

Let us multiply each term of equation (15.2) by an element of volume  $r dr d\phi dz$  and integrate between the limits of a layer of the height  $R$ . The last term on the left side will then give, considering equations (15.20) and (15.18),

$$\begin{aligned} \int_0^R \int_0^{2\pi} \int_0^R v_z \times \frac{\partial \theta}{\partial z} r dr d\phi dz &= 2\pi R \int_0^R v_z \left( A + \frac{v^2 h}{g\beta R^2} \right) r dr \\ &= 2\pi R \left[ A \int_0^R v_z r dr + \frac{v^2 h}{g\beta R^2} \times \frac{v \left( a + h \frac{z}{R} \right)}{R} \int_0^R f_0 \right] r dr \end{aligned} \quad (15.32)$$

where the first term in brackets is equal to zero, owing to the "closedness" of the channel. The first term on the left side of equation (15.2) will give

$$\begin{aligned} \int_0^R \int_0^{2\pi} \int_0^R v_r \frac{\partial \theta}{\partial r} r dr d\phi dz &= 2\pi R \int_0^R v_r \times \frac{v^2 \left( a + h \frac{z}{R} \right)}{g\beta R} \left\{ \right\}'_r r dr \\ &= 2\pi R \frac{v^2 h}{g\beta R} \times \frac{v \left( a + h \frac{z}{R} \right)}{R} \int_0^R F_0 \left\{ \right\}'_r r dr \end{aligned} \quad (15.33)$$

If the last integral is integrated by parts, we obtain

$$\int_0^R F_0 r \left\{ \right\}'_r dr = F_0 r \left\{ \right\}_0^R - \int_0^R \left\{ \right\} \left[ F_0' + \frac{1}{r} F_0 \right] r dr = \frac{1}{R} \int_0^R f_0 \left\{ \right\}'_r r dr \quad (15.34)$$

The substitution here vanishes because of the presence of the boundary layer. The transformations are made on the basis of the continuity equation, in particular equation (15.8).

Thus, both remaining terms on the left side of equations (15.2) to (15.18) are equal to each other. The physical sense of the expression (15.32) is defined as the heat transferred per second by convection upward from a layer of height  $R$ . The physical sense of the equal expression (15.33) is that it is the heat transported by the radial velocity component from the periphery to the inner parts of the fluid.

After integration, the right side of equations (15.2) to (15.18) gives

$$\int_0^R \int_0^{2\pi} \int_0^R \kappa \Delta \theta r \, dr \, d\phi \, dz = -\kappa 2\pi R^2 \left( \frac{\partial \theta}{\partial r} \right)_{r=R} \quad (15.35)$$

where the Ostrogradsky-Green theorem was applied. The entire equation (15.2), after integration and substitution, gives

$$4\kappa R \frac{v^3 h \left( a + h \frac{z}{R} \right)}{g\beta R^3} \int_0^R f_0 \left\{ r \right\} dr = -2\pi R^2 \kappa \frac{v^2 \left( a + h \frac{z}{R} \right)}{g\beta R} \left[ \left\{ r \right\} \right]_{r=R} \quad (15.36)$$

whence, the parameter of nonlinearity  $h$  is determined as

$$h = -\frac{\kappa}{v} \times \frac{R^3}{2} \times \frac{\left[ \left\{ r \right\} \right]_R}{\int_0^R f_0 \left\{ r \right\} dr} \quad (15.37)$$

On the other hand, the heat transferred by convection through the section  $z$  upward is equal, by virtue of relation (3.23), to

$$\begin{aligned} Q &= \rho c 2\pi \int_0^R v_z \theta r \, dr = \\ &= -2\pi \rho c \frac{v}{R} \left( a + h \frac{z}{R} \right) \int_0^R f_0 \left[ Az + \frac{v^2 \left( a + h \frac{z}{R} \right)}{g\beta R} \right] \left\{ r \right\} r \, dr = \\ &= \frac{2\pi \rho c v^3}{g\beta R^2} \left( a + h \frac{z}{R} \right)^2 \int_0^R f_0 \left\{ r \right\} r \, dr \end{aligned} \quad (15.38)$$

The term with  $A$  drops out because of the "closedness" of the channel. Over the distance of one centimeter of the channel height this heat increases by the amount

$$\frac{\partial Q}{\partial z} = 4\pi\rho c \frac{v^3 \left(a + h \frac{z}{R}\right)}{g\beta R^3} \int_0^R f_0 \left\{ \right\} r \, dr \quad (15.39)$$

Substituting this expression in relations (15.35), (15.36), and (15.37) gives

$$\frac{\partial Q}{\partial z} = -2\pi R \lambda \frac{v^2 \left(a + h \frac{z}{R}\right)}{g\beta R} \left[ \left\{ \right\}' \right]_{r=R} = -2\pi R \lambda \left( \frac{\partial \theta}{\partial r} \right)_{r=R} \quad (15.40)$$

and

$$\frac{\frac{\partial Q}{\partial z}}{Q} = \frac{2h}{R \left(a + h \frac{z}{R}\right)} \quad (15.41)$$

The last equation connects the parameter of nonlinearity  $h$  with the experimentally observed intensity of the heating (or the heat losses) through the channel walls.

The following further circumstance must be considered: The experimentally observable vertical gradient on the periphery of the channel cross section differs from the mean gradient  $A$  which plays an important part in this theory. In fact, limiting ourselves to the first term of the expansion (15.24) and making use of formula (15.16), we find

$$\left( \frac{\partial \theta}{\partial z} \right)_{r=R} = A + \frac{v^2 h}{g\beta R^2} \left( \psi_0'' + \frac{1}{r} \psi_0' \right)_{r=R} \quad (15.42)$$

Further, taking into account formula (5.38) and substituting in place of  $\psi_0$  its expression in terms of the Bessel functions (5.35) to (5.36), we obtain

$$\begin{aligned} \left( \frac{\partial \theta}{\partial z} \right)_{r=R} &= A - \frac{v^2 h}{g\beta R^2} (\Delta \psi_0)_{r=R} = \\ &= A - \frac{v^2 h k^2}{g\beta R^2} \left[ \frac{J_0(ikR)}{J_0(ikR)} + \frac{J_0(kR)}{J_0(kR)} \right] = A - 2 \frac{v^2 h (kR)^2}{g\beta R^4} \\ &= A \left[ 1 - 2Pr \times \frac{h}{(kR)^2} \right] = A \left[ 1 - \frac{2Pr \times h}{21.3} \right] \end{aligned} \quad (15.43)$$

For water at a temperature of about 20° C, Pr ≈ 7. Substituting, we obtain

$$\left(\frac{\partial\theta}{\partial z}\right)_{r=R} \approx A \left[ 1 - \frac{2}{3} h \right] \quad (15.44)$$

where the term in brackets represents the relative decrease of the experimentally observable peripheral vertical temperature gradient as compared with its gradient averaged over the section. Hence, for a certain value of  $h$  it may be found that this gradient is equal to the vertical gradient which corresponds to diametral antisymmetry. This is obtained when

$$\frac{(kR)_{\text{diam}}^4}{(kR)_{\text{axial}}^4} \approx 1 - \frac{2}{3} h$$

For glass models  $(kR)_{\text{diam}}^4 \approx 100$ ;  $(kR)_{\text{axial}}^4 = 452.1$ ; whence

$$h \approx \frac{3}{2} \left( 1 - \frac{100}{452.1} \right) \approx 1.17 \quad (15.45)$$

For this reason, in the case of an annular heater coil wound directly on the glass, the convective flow spontaneously changes from diametrically antisymmetrical over the heater into axially symmetrical inside the heater. The last equation (15.45) hardly reflects accurately the value of  $h$  (it may be expected that actually the corresponding value of  $h$  is less), but the phenomenon evidently has this character.

#### 5. Case of Diametral Antisymmetry

As a second example, let us consider the more complicated case of diametral antisymmetry of the fundamental flow, previously qualitatively described in chapter 11.

Because all three coordinates now play an essential part, it is necessary to make use of the earlier derived equation (15.19), in all its complicatedness. However, since on the basis of the experimental results of chapter 11 the antisymmetrical form must be considered as the basic form of the phenomenon, we now assume in equation (15.4) in place of equation (15.20),

$$f_0 \ll f_1 \gg f_2 \quad (15.46)$$

There is then immediately obtained from equation (15.8)

$$\begin{aligned} F_0 &\ll F_1 \gg F_2 \\ \Phi_1 &\gg \Phi_2 \end{aligned} \quad (15.47)$$

Since for  $h = 0$  all the enumerated functions vanish except  $f_1$ , we now apply a new notation, and in place of

$$f_0, f_2, F_0, F_2, \text{ and } \Phi_2$$

we shall write

$$hf_0, hf_2, hF_0, hF_2, \text{ and } h\Phi_2$$

Moreover, we set

$$\begin{aligned} f_1 &= \psi_0 + h\psi_1 + h^2\psi_2 + \dots \\ F_1 &= \zeta_0 + h\zeta_1 + h^2\zeta_2 + \dots \\ \Phi_1 &= \omega_0 + h\omega_1 + h^2\omega_2 + \dots \end{aligned} \quad (15.48)$$

The expression in braces in equation (15.16) then becomes

$$\begin{aligned} C_0 &= hf_0'' + \frac{h}{r} f_0' - \frac{h}{R} \left[ h^2 F_0 f_0' + \frac{1}{2} (\zeta_0 + h\zeta_1 + \dots) (\psi_0 + h\psi_1 + \dots) + \right. \\ &\quad \left. \frac{h^2}{2} F_2 f_2' - \frac{1}{2r} (\omega_0 + h\omega_1 + \dots) (\psi_0 + h\psi_1 + \dots) - \right. \\ &\quad \left. \frac{h^2}{r} \Phi_2 f_2 + \frac{h^2}{R} f_0^2 + \frac{1}{2R} (\omega_0^2 + 2h\omega_0\omega_1 + \dots) + \frac{h^2}{2R} f_2^2 \right] \\ &= h \left[ f_0'' + \frac{1}{r} f_0' - \frac{1}{2R} \zeta_0 \psi_0' + \frac{1}{2rR} \omega_0 \psi_0 - \frac{1}{2R^2} \omega_0^2 \right] + \\ &\quad h^2 \left[ -\frac{1}{2R} (\zeta_0 \psi_1' + \zeta_1 \psi_0') + \frac{1}{2rR} (\omega_0 \psi_1 + \omega_1 \psi_0) - \frac{2}{R} \omega_0 \omega_1 \right] + \dots \end{aligned} \quad (15.49)$$

$$\begin{aligned}
c_1 = & \psi_0'' + h\psi_1'' + h^2\psi_2'' + \frac{1}{r}\psi_0' + \frac{h}{r}\psi_1' + \frac{h^2}{r}\psi_2' - \frac{1}{r^3}\psi_0 - \\
& \frac{h}{r^3}\psi_1 - \frac{h^2}{r^3}\psi_2 - \frac{h}{R}\left[hF_0(\psi_0' + h\psi_1' + \dots) + \right. \\
& (\zeta_0 + h\zeta_1 + \dots)hf_0' + \frac{h}{2}(\zeta_0 + h\zeta_1 + \dots)f_2' + \\
& \frac{h}{2}F_2(\psi_0' + h\psi_1' + \dots) - \frac{h}{r}(\omega_0 + h\omega_1 + \dots)f_2 - \\
& \frac{h}{2r}\Phi_2(\psi_0 + h\psi_1 + \dots) + \frac{2h}{R}f_0(\psi_0 + h\psi_1 + \dots) + \\
& \left. \frac{h}{R}(\psi_0 + h\psi_1 + \dots)f_2\right] = \psi_0'' + \frac{1}{r}\psi_0' - \frac{1}{r^2}\psi_0 + \\
& h\left[\psi_1'' + \frac{1}{r}\psi_1' - \frac{1}{r^2}\psi_1\right] + h^2\left[\psi_2'' + \frac{1}{r}\psi_2' - \frac{1}{r^2}\psi_2 - \right. \\
& \left. \frac{1}{R}(F_0\psi_0' + \zeta_0f_0' + \frac{1}{2}\psi_0f_2' + \frac{1}{2}F_2\psi_0' - \frac{1}{r}\omega_0f_2 - \right. \\
& \left. \frac{1}{2r}\Phi_2\psi_0 + \frac{2}{R}f_0\psi_0 + \frac{1}{R}\psi_0f_2)\right] + \dots
\end{aligned}
\tag{15.50}$$

$$\begin{aligned}
c_2 = & hf_2'' + \frac{h}{r}f_2' - \frac{4h}{r^2}f_2 - \frac{h}{R}\left[h^2F_0f_2' + h^2F_2f_0' + \right. \\
& \left. \frac{1}{2}(\zeta_0 + h\zeta_1 + \dots)(\psi_0 + h\psi_1 + \dots) + \right. \\
& \left. \frac{1}{2r}(\omega_0 + h\omega_1 + \dots)(\psi_0 + h\psi_1 + \dots) + \frac{2h^2}{R}f_0f_2 + \right. \\
& \left. \frac{1}{2R}\psi_0^2 + \frac{h}{R}\psi_0\psi_1 + \dots\right] = h\left[f_2'' + \frac{1}{r}f_2' - \frac{4}{r^2}f_2 - \right. \\
& \left. \frac{1}{2R}\zeta_0\psi_0 - \frac{1}{2rR}\omega_0\psi_0 - \frac{1}{2R}\psi_0^2\right] + \\
& \frac{h^2}{R}\left[-\frac{1}{2}(\zeta_0\psi_1' + \zeta_1\psi_0') - \frac{1}{2r}(\omega_0\psi_1 + \omega_1\psi_0) + \frac{1}{2R}\psi_0\psi_1\right] + \dots
\end{aligned}
\tag{15.51}$$

428L

CA-18

Substituting these values in the Fourier-Kirchhoff equation (15.19), we obtain the successive coefficients for the different trigonometric functions of the azimuth in the following form:

For  $\cos 0$ :

$$\begin{aligned}
 & C_0'' + \frac{1}{r} C_0' - k^4 h f_0 - \text{Pr} \times \frac{h}{R} \left[ \frac{h}{R} f_0 C_0 + \right. \\
 & \quad \left. \frac{1}{2R} (\psi_0 + h\psi_1 + \dots) C_1 + \frac{1}{2R} h f_2 C_2 - \right. \\
 & \quad \left. \frac{1}{2r} (\omega_0 + h\omega_1 + \dots) C_1 - \frac{h}{2r} \Phi_2 C_2 + h F_0 C_0' + \right. \\
 & \quad \left. \frac{1}{2} (\xi_0 + h\xi_1 + \dots) C_1 + \frac{1}{2} h F_2 C_2' \right] + \dots = 0
 \end{aligned}
 \tag{15.52}$$

For  $\cos \varphi$ :

$$\begin{aligned}
 & C_1'' + \frac{1}{r} C_1' - \frac{1}{r^2} C_1 - k^4 (\psi_0 + h\psi_1 + \dots) - \text{Pr} \frac{h}{R} \left[ \frac{h}{R} f_0 C_1 + \right. \\
 & \quad \left. \frac{1}{R} (\psi_0 + h\psi_1 + \dots) C_0 + \frac{1}{2R} (\psi_0 + h\psi_1 + \dots) C_2 + \right. \\
 & \quad \left. \frac{h}{2R} f_2 C_1 + \frac{1}{2r} (\omega_0 + h\omega_1 + \dots) C_2 + \frac{h}{2r} \Phi_2 C_1 + \right. \\
 & \quad \left. (\xi_0 + h\xi_1 + \dots) C_0' + h F_0 C_1' + \frac{1}{2} h F_2 C_1' + \right. \\
 & \quad \left. \frac{1}{2} (\xi_0 + h\xi_1 + \dots) C_2' \right] + \dots = 0
 \end{aligned}
 \tag{15.53}$$

For  $\cos 2\varphi$ :

$$\begin{aligned}
 & C_2'' + \frac{1}{r} C_2' - \frac{4}{r^2} C_2 - k^4 h f_2 - \text{Pr} \frac{h}{R} \left[ \frac{h}{R} f_2 C_0 + \frac{h}{R} f_0 C_2 + \right. \\
 & \quad \left. \frac{1}{2R} (\psi_0 + h\psi_1 + \dots) C_1 + \frac{1}{2r} (\omega_0 + h\omega_1 + \dots) C_1 + h F_2 C_0' + \right. \\
 & \quad \left. h F_0 C_2' + \frac{1}{2} (\xi_0 + h\xi_1 + \dots) C_0' \right] + \dots = 0
 \end{aligned}
 \tag{15.54}$$

In these expressions the auxiliary functions  $C_0$ ,  $C_1$ , and  $C_2$  in the new notation have the following meaning:

$$\begin{aligned}
 C_0 = & h\Delta f_0 - \frac{1}{R} \left[ h^2 F_0 f_0' + \frac{1}{2} (\zeta_0 + h\zeta_1 + \dots) (\psi_0' + h\psi_1' + \dots) + \right. \\
 & \frac{h^2}{2} F_2 f_2' - \frac{1}{2r} (\omega_0 + h\omega_1 + \dots) (\psi_0 + h\psi_1 + \dots) - \\
 & \left. \frac{h^2}{r} \Phi_2 f_2 + \frac{h^2}{R} f_0^2 + \frac{1}{2R} (\psi_0 + h\psi_1 + \dots)^2 + \frac{h^2}{2R} f_2^2 \right] \\
 & = h \left[ \Delta f_0 - \frac{1}{R} \left( \frac{1}{2} \zeta_0 \psi_0' - \frac{1}{2r} \omega_0 \psi_0 + \frac{1}{2R} \psi_0^2 \right) \right] - \\
 & \frac{h^2}{R} \left[ \frac{1}{2} (\zeta_1 \psi_0' + \zeta_0 \psi_1') - \frac{1}{2r} (\omega_0 \psi_1 + \omega_1 \psi_0) + \frac{1}{R} \psi_0 \psi_1 \right] + \dots
 \end{aligned}
 \tag{15.55}$$

$$\begin{aligned}
 C_1 = & \Delta (\psi_0 + h\psi_1 + \dots) - \frac{h}{R} \left[ h F_0 (\psi_0' + h\psi_1' + \dots) + \right. \\
 & (\zeta_0 + h\zeta_1 + \dots) h f_0' + \frac{1}{2} (\zeta_0 + h\zeta_1 + \dots) h f_2' + \\
 & \frac{1}{2} h F_2 (\psi_0' + h\psi_1' + \dots) - \frac{1}{r} (\omega_0 + h\omega_1 + \dots) h f_2 - \\
 & \frac{1}{2r} h \Phi_2 (\psi_0 + h\psi_1 + \dots) + \frac{2}{R} h f_0 (\psi_0 + h\psi_1 + \dots) + \\
 & \left. \frac{h}{R} (\psi_0 + h\psi_1 + \dots) f_2 \right] = \Delta (\psi_0 + h\psi_1 + \dots) - \\
 & \frac{h^2}{R} \left( F_0 \psi_0' + \zeta_0 f_0' + \frac{1}{2} \zeta_0 f_2' + \frac{1}{2} F_2 \psi_0' - \frac{1}{2} \omega_0 f_2 - \right. \\
 & \left. \frac{1}{2r} \Phi_2 \psi_0 + \frac{2}{R} f_0 \psi_0 + \frac{1}{R} \psi_0 f_2 \right) + \dots
 \end{aligned}
 \tag{15.56}$$

4281

CA-18 back

$$\begin{aligned}
C_2 &= h\Delta f_2 - \frac{h}{R} \left[ h^2 F_0 f_2' + h^2 F_2 f_0' + \right. \\
&\quad \frac{1}{2} (\xi_0 + h\xi_1 + \dots) (\psi_0' + h\psi_1' + \dots) + \\
&\quad \left. \frac{1}{2r} (\omega_0 + h\omega_1 + \dots) (\psi_0 + h\psi_1 + \dots) + \right. \\
&\quad \left. \frac{2h^2}{R} f_0 f_2 + \frac{1}{2R} (\psi_0 + h\psi_1 + \dots)^2 \right] \\
&= h \left[ \Delta f_2 - \frac{1}{R} \left( \frac{1}{2} \xi_0 \psi_0' + \frac{1}{2r} \omega_0 \psi_0 + \frac{1}{2R} \psi_0^2 \right) \right] + \\
&\quad \frac{h^2}{R} \left[ \frac{1}{2} (\xi_0 \psi_1' + \xi_1 \psi_0') + \frac{1}{2r} (\omega_0 \psi_1 + \omega_1 \psi_0) + \frac{1}{R} \psi_0 \psi_1 \right] + \dots
\end{aligned}
\tag{15.57}$$

Now, grouping the terms of equations (15.52) to (15.54) with the same power of  $h$ , we obtain the following:

Terms not containing  $h$ :

$$\Delta\Delta\psi_0 - k^4\psi_0 = 0 \tag{15.58}$$

Terms containing  $h$  to the first power:

$$\begin{aligned}
\Delta\Delta f_0 - k^4 f_0 &= \frac{1}{2R} \Delta \left( \xi_0 \psi_0' - \frac{1}{r} \omega_0 \psi_0 + \frac{1}{R} \psi_0^2 \right) + \\
Pr \times \frac{h}{2R} &\left( \frac{1}{R} \psi_0 \Delta\psi_0 - \frac{1}{r} \omega_0 \Delta\psi_0 + \xi_0 \Delta\psi_0' \right)
\end{aligned}
\tag{15.59}$$

$$\Delta\Delta\psi_1 - k^4\psi_1 = 0 \tag{15.60}$$

$$\begin{aligned}
\Delta\Delta f_2 - k^4 f_2 &= \frac{1}{2R} \Delta \left( \xi_0 \psi_0' + \frac{1}{r} \omega_0 \psi_0 + \frac{1}{R} \psi_0^2 \right) + \\
Pr &\left( \frac{1}{R} \psi_0 \Delta\psi_0 + \frac{1}{r} \omega_0 \Delta\psi_0 + \xi_0 \Delta\psi_0' \right)
\end{aligned}
\tag{15.61}$$

The remaining equations have a more complicated form. In equation (15.58) we recognize the "fundamental" equation. The remaining equations enable the computation of the functions  $f_0$  and  $f_2$ . We note that the correction to  $\psi_0$  is found not to be below the second power of  $h$ , since the equation for  $\psi_1$  does not differ from the equation for  $\psi_0$  and therefore does not give "corrections" to the last function. That is, we may assume  $\psi_1 = 0$ .

The various functions encountered in these equations are connected with each other by the continuity equation which, in the new notation considering equations (15.8) and (15.48), is written in the developed form:

$$\left. \begin{aligned} F_0' + \frac{1}{r} F_0 + \frac{1}{R} f_0 &= 0 \\ F_2' + \frac{1}{r} F_2 + \frac{2}{r} \Phi_2 + \frac{1}{R} f_2 &= 0 \\ \zeta_0' + \frac{1}{r} \zeta_0 + \frac{1}{r} \omega_0 + \frac{1}{R} \psi_0 &= 0 \\ \zeta_1' + \frac{1}{r} \zeta_1 + \frac{1}{r} \omega_1 + \frac{1}{R} \psi_1 &= 0 \end{aligned} \right\} \quad (15.62)$$

In addition, it is also necessary to bear in mind the following relation. If equation (15.10) is differentiated with respect to the azimuth, and equation (15.11) is differentiated with respect to the radius, we obtain the following two expressions for  $\partial^2 p / \partial r \partial \varphi$ :

$$\left. \begin{aligned} \frac{1}{\rho r} \times \frac{\partial^2 p}{\partial r \partial \varphi} &= \frac{v^2 h}{rR} \left( -\Delta F_1 + \frac{2}{r^2} \Phi_1 \right) \sin \varphi + \dots \\ &= \frac{v^2 h}{R} \left( \Delta \Phi_1' - \frac{2}{r^2} F_1' + \frac{4}{r^3} F_1 \right) \sin \varphi + \dots \end{aligned} \right\} \quad (15.63)$$

where only the terms with the factor  $h \sin \varphi$  have been retained. Hence, in the new notation, the terms containing the first power of  $h$  have the coefficients:

$$\left. \begin{aligned} -\frac{1}{r} \Delta \zeta_0 + \frac{2}{r^3} \omega_0 &= \Delta \omega_0' - \frac{2}{r^2} \zeta_0' + \frac{4}{r^3} \zeta_0 \\ \frac{1}{r} \Delta \zeta_0 - \frac{2}{r^2} \zeta_0' + \frac{4}{r^3} \zeta_0 &= -\Delta \omega_0' + \frac{2}{r^3} \omega_0 \end{aligned} \right\} \quad (15.64)$$

4281

Substituting  $\omega_0$  from equation (15.62) in equation (15.64), we obtain

$$\left. \begin{aligned} \omega_0 &= -\frac{r}{R} \psi_0 - \zeta - r\zeta_0' \\ \zeta_0^{IV} + \frac{5}{r} \zeta_0''' + \frac{1}{r^2} \zeta_0'' - \frac{3}{r^3} \zeta_0' - \frac{6}{r^4} \zeta_0 \\ &= \frac{1}{R} \psi_0'''' + \frac{4}{rR} \psi_0''' + \frac{1}{Rr^2} \psi_0'' - \frac{3}{Rr^3} \psi_0' \end{aligned} \right\} \quad (15.65)$$

The solution of this system of equations must be used in the right sides of equations (15.59) to (15.61).

From this it is seen how laborious is the work on the solution of the nonlinear equations of gravitational convection even within the limits of the first approximation (i.e., the first few powers of the nonlinearity parameter  $h$ ). However, the method of solution that leads to the solution of a system of linear equations gives a clear perspective of how the result is to be attained.

In conclusion, it is useful to remark that the order of operations which is presented here evidently saves a maximum of computational work. It would perhaps have been more strictly logical to have made a substitution of the different powers of  $h$  directly in the initial hypotheses, equations (15.4) to (15.6), and not in equation (15.18) as was done in equations (15.18) and the following. What has been done here represents a double introduction of the same small parameter  $h$ . The results obtained by both methods are the same (sec. 2).

## 6. Convection in Horizontal Channel of Round Cross Section<sup>13</sup>

As a third example we consider the plane convective motion of a fluid arising in an infinite horizontal channel of round cross section bored in an infinite homogeneous solid surrounding block. In this block, by means of heat sources and sinks situated at an infinitely large distance, a temperature gradient constant in time is produced perpendicular to the channel axis. At a great (as compared with the channel diameter) distance this temperature field is homogeneous. In the neighborhood of the channel this homogeneous field will be distorted. For a stationary fluid the distortion will be in its molecular conductivity, and for a moving fluid the distortion will be in its convection as well as in its molecular conduction.

<sup>13</sup>This section was compiled from data obtained by E. M. Zhukhovitski.

We choose the axes of coordinates as shown in figure 49. By the conditions of symmetry,

$$\left. \begin{aligned} v_z &= 0 \\ \frac{\partial \theta}{\partial z} &= 0 \\ \frac{\partial v_y}{\partial z} &= \frac{\partial v_x}{\partial z} = 0 \end{aligned} \right\} \quad (15.66)$$

The equation of a streamline has the form, in Cartesian coordinates,

$$\left. \begin{aligned} \frac{dx}{v_x} &= \frac{dy}{v_y} \\ v_y dx - v_x dy &\equiv d\Psi = 0 \end{aligned} \right\} \quad (15.67)$$

and, in polar coordinates,

$$\left. \begin{aligned} \frac{dr_1}{v_r} &= \frac{r_1 d\phi}{v_\phi} \\ v_\phi dr_1 - r_1 v_r d\phi &\equiv d\Psi = 0 \end{aligned} \right\} \quad (15.68)$$

where the symbol  $\Psi$  denotes the stream function. It is evident that

$$\left. \begin{aligned} \frac{\partial \Psi}{\partial x} &= -v_y \\ \frac{\partial \Psi}{\partial y} &= v_x \\ \text{or} \\ \frac{\partial \Psi}{\partial r_1} &= -v_\phi \\ \frac{1}{r_1} \frac{\partial \Psi}{\partial \phi} &= v_r \end{aligned} \right\} \quad (15.69)$$

This transformation is possible if  $d\Psi$  in equations (15.67) or (15.68) is a total differential; that is, if

$$\left. \begin{aligned} \frac{\partial^2 \Psi}{\partial x \partial y} &= -\frac{\partial v_y}{\partial y} = \frac{\partial^2 \Psi}{\partial y \partial x} = \frac{\partial v_x}{\partial x} \\ \frac{\partial^2 \Psi}{\partial r_1 \partial \phi} &= -\frac{\partial v_\phi}{\partial \phi} = \frac{\partial^2 \Psi}{\partial \phi \partial r_1} = r_1 \frac{\partial v_r}{\partial r_1} + v_r \end{aligned} \right\} \quad (15.70)$$

The preceding equations coincide with the equations of continuity in Cartesian and polar coordinates, respectively:

$$\left. \begin{aligned} \frac{\partial v_y}{\partial y} + \frac{\partial v_x}{\partial x} &= 0 \\ \frac{\partial v_r}{\partial r} + \frac{v_r}{r_1} + \frac{1}{r_1} \frac{\partial v_\phi}{\partial \phi} &= 0 \end{aligned} \right\} \quad (15.71)$$

Thus, the introduction of the stream function is admissible.

The streamlines are characterized, according to equations (15.67) and (15.68) by the fact that along them  $d\Psi = 0$  (i.e.,  $\Psi = \text{constant}$ ). The greater the velocity, the more closely packed are the streamlines.

In order to use the Navier-Stokes equation and to eliminate the pressure gradient from the equation by applying the curl operator, we compute the curl of the velocity:

$$\left. \begin{aligned} [\nabla \underline{v}]_x &= \frac{\partial v_z}{\partial y} - \frac{\partial v_y}{\partial z} = 0 \\ [\nabla \underline{v}]_y &= \frac{\partial v_x}{\partial z} - \frac{\partial v_z}{\partial x} = 0 \\ [\nabla \underline{v}]_z &= \frac{\partial v_y}{\partial x} - \frac{\partial v_x}{\partial y} = -\frac{\partial^2 \Psi}{\partial x^2} - \frac{\partial^2 \Psi}{\partial y^2} = -\Delta \Psi \end{aligned} \right\} \quad (15.72)$$

Applying the curl operator to the Navier-Stokes equation we obtain

$$-\nabla[\underline{v}[\nabla \underline{v}]] = \nu \Delta[\nabla \underline{v}] + \beta[\nabla \theta g] \quad (15.73)$$

Substituting equations (15.69) and (15.72) in the preceding equation, we obtain the following scalar equation (the component on the z-axis of equation (15.73)):

$$\frac{\partial}{\partial x} \left( \frac{\partial \Psi}{\partial y} \Delta \Psi \right) - \frac{\partial}{\partial y} \left( \frac{\partial \Psi}{\partial x} \Delta \Psi \right) = \nu \Delta \Delta \Psi - g \beta \frac{\partial \theta}{\partial x} \quad (15.74)$$

or, carrying out the differentiation and multiplication on the left side,

$$\frac{\partial \Psi}{\partial y} \times \frac{\partial \Delta \Psi}{\partial x} - \frac{\partial \Psi}{\partial x} \times \frac{\partial \Delta \Psi}{\partial y} = \nu \Delta \Delta \Psi - g\beta \frac{\partial \theta}{\partial x} \quad (15.75)$$

The Fourier-Kirchhoff equation is now rewritten as

$$\frac{\partial \Psi}{\partial y} \times \frac{\partial \theta}{\partial x} - \frac{\partial \Psi}{\partial x} \times \frac{\partial \theta}{\partial y} = \kappa \Delta \theta \quad (15.76)$$

We pass to polar coordinates by means of the following well-known formulas:

$$\left. \begin{aligned} \frac{\partial}{\partial x} &= \cos \varphi \frac{\partial}{\partial r_1} - \frac{1}{r_1} \sin \varphi \frac{\partial}{\partial \varphi} \\ \frac{\partial}{\partial y} &= \sin \varphi \frac{\partial}{\partial r_1} + \frac{1}{r_1} \cos \varphi \frac{\partial}{\partial \varphi} \end{aligned} \right\} \quad (15.77)$$

The system (15.75) and (15.76), expressed in polar coordinates, then reads

$$\left. \begin{aligned} &\frac{1}{r_1} \left( \frac{\partial \Psi}{\partial \varphi} \times \frac{\partial \Delta \Psi}{\partial r_1} - \frac{\partial \Psi}{\partial r_1} \times \frac{\partial \Delta \Psi}{\partial \varphi} \right) \\ &= \nu \Delta \Delta \Psi - g\beta \left( \frac{\partial \theta}{\partial r_1} \cos \varphi - \frac{\partial \theta}{\partial \varphi} \times \frac{1}{r_1} \sin \varphi \right) \\ &\frac{1}{r_1} \left( \frac{\partial \Psi}{\partial \varphi} \times \frac{\partial \theta}{\partial r_1} - \frac{\partial \Psi}{\partial r_1} \times \frac{\partial \theta}{\partial \varphi} \right) = \kappa \Delta \theta \end{aligned} \right\} \quad (15.78)$$

The continuity equation has already been employed in forming the stream function  $\Psi$ . It is assumed that the equations have been parametrically linearized (ch. 2, sec. 2).

We have obtained a system of partial differential equations of a higher order (of the fourth order in  $\Psi$  and the second order in  $\theta$ ), nonlinear but homogeneous, and with constant coefficients (within the limits of parametrical linearization). It must be solved for those boundary conditions which were specially considered previously (ch. 4, secs. 1 and 2). With the introduction of the new function  $\Psi$  these boundary conditions are formulated as follows:

(1) Within the cross section of the channel ( $0 \leq r_1 \leq R$ ), the functions  $\Psi$  and  $\theta$  are finite, continuous, and single-valued, with the required number of derivatives.

(2) At the wall, for  $r_1 = R$ , there is an adhering boundary layer of the fluid (eq. (15.69)):

$$\left. \begin{aligned} \left(\frac{\partial \Psi}{\partial r_1}\right)_{r_1=R} &= 0 \\ \left(\frac{\partial \Psi}{\partial \phi}\right)_{r_1=R} &= 0 \end{aligned} \right\} \quad (15.79)$$

(3) Within the boundary layer there are no jumps of temperature and of heat flow:

$$\left. \begin{aligned} \theta_{r_1=R} &= \theta_{e r_1=R} \\ \lambda \left(\frac{\partial \theta}{\partial r_1}\right)_{r_1=R} &= \lambda_e \left(\frac{\partial \theta_e}{\partial r_1}\right)_{r_1=R} \end{aligned} \right\} \quad (15.80)$$

(4) In the neighborhood of the channel there are no heat sources and no sinks:

$$\Delta \theta_e = 0 \quad (15.81)$$

(5) At infinity, the temperature gradient is given as

$$\left. \begin{aligned} \left(\frac{\partial \theta_e}{\partial x}\right)_{r_1 \rightarrow \infty} &\rightarrow A \\ \left(\frac{\partial \theta_e}{\partial y}\right)_{r_1 \rightarrow \infty} &\rightarrow B \end{aligned} \right\} \quad (15.82)$$

For convenience of solution and without restricting its generality (since only derivatives are encountered in the equations), we assume that  $\Psi$  vanishes at the wall:

$$(\Psi)_{r_1=R} = 0 \quad (15.83)$$

To simplify our further discussion, equations (15.78) will be reduced to a nondimensional form. As a scale for the length we shall choose the channel radius  $R$ , and as a temperature scale we shall choose the product

$$A_0 R = R \sqrt{A^2 + B^2} \quad (15.84)$$

Moreover, we set

$$\left. \begin{aligned} r_1 &= Rr \\ \Psi(r_1, \varphi) &= \kappa F(r, \varphi) \\ \theta(r_1, \varphi) &= A_0 R \delta(r, \varphi) \\ \xi^4 &\equiv - \frac{g \beta A_0 R^4}{\nu \kappa} = Gr \times Pr \end{aligned} \right\} \quad (15.85)$$

The connection of the stream functions in terms of  $\kappa$  and not  $\nu$ , as would be expected from the form of the equation, is determined by the convenience of the further computations. Here  $r_1$  denotes the ordinary radius,  $r$  the nondimensional radius,  $\Psi$  the ordinary stream function,  $F$  the nondimensional stream function,  $\theta$  the ordinary temperature, and  $\delta$  the nondimensional temperature. After reduction it is found that the entire nondimensional system is now determined by the single nondimensional parameter  $\xi^4$ , having the criterional value

$$\left. \begin{aligned} \Delta \Delta F &= \frac{1}{Pr} \times \frac{1}{r} \left( \frac{\partial F}{\partial \varphi} \times \frac{\partial \Delta F}{\partial r} - \frac{\partial F}{\partial r} \times \frac{\partial \Delta F}{\partial \varphi} \right) - \\ &\quad \xi^4 \left( \frac{\partial \delta}{\partial r} \cos \varphi - \frac{1}{r} \frac{\partial \delta}{\partial \varphi} \sin \varphi \right) \\ \Delta \delta &= \frac{1}{r} \left( \frac{\partial F}{\partial \varphi} \times \frac{\partial \delta}{\partial r} - \frac{\partial F}{\partial r} \times \frac{\partial \delta}{\partial \varphi} \right) \end{aligned} \right\} \quad (15.86)$$

Because  $A_0$  denotes the arithmetical value of the square root in equation (15.84),  $\xi^4$  is essentially positive, since  $\beta$  is usually negative.

It is useful to observe that through the parameter  $\xi^4$  a relation is established between the mechanical and thermal aspects of the phenomenon: The absence of thermal phenomena ( $A_0 = 0$ ) or the absence of their effect on the mechanical side of the process (for  $\beta = 0$ ,  $\nu = \infty$  or  $\kappa = \infty$ ) leads to the value  $\xi^4 = 0$ . This value corresponds to the fact that both equations of the system of simultaneous equations (15.86) are converted into independent equations that do not constitute a system.

It is also necessary to remember that, in virtue of the assumption of parametric linearization of equations (15.86), they automatically become invalid for large values of  $\xi^4$ . For this reason, it is desirable

to seek a solution in the form of a series developed in powers of  $\xi^4$ . We set

$$\left. \begin{aligned} F &= \xi^4 F(1) + \xi^8 F(2) + \dots \\ \vartheta &= \vartheta(0) + \xi^4 \vartheta(1) + \xi^8 \vartheta(2) + \dots \\ \vartheta_e &= \vartheta_e(0) + \xi^4 \vartheta_e(1) + \xi^8 \vartheta_e(2) + \dots \\ F(0) &\equiv 0 \end{aligned} \right\} \quad (15.87)$$

The essential idea of the process of solution is that the solutions in the form of the series (15.87) are substituted in the equations of the system (15.86). By comparing the coefficients of equal powers of  $\xi^4$ , equations of the following form are obtained:

$$\left. \begin{aligned} \Delta\Delta F^{(n)} &= f(\vartheta(0); F(1), \vartheta(1); F(2), \vartheta(2); \dots \\ &\quad \dots; F^{(n-1)}, \vartheta^{(n-1)}) \\ \Delta\vartheta^{(n)} &= f_1(\vartheta(0); F(1), \vartheta(1); F(2), \vartheta(2); \dots \\ &\quad \dots; F^{(n-1)}, \vartheta^{(n-1)}) \end{aligned} \right\} \quad (15.88)$$

The functions  $f$  and  $f_1$  embrace the functions  $F$  and  $\vartheta$  of different indices, as well as their lower derivatives. The first equation of these equations represents a two-term biharmonic linear equation with constant coefficients, nonhomogeneous, containing the already previously defined known functions on the right side. The second equation represents the elementary harmonic equation of Poisson. In principle, there are no obstacles to the solution of these equations; a solution always exists. In regard to the solution of these equations, the following is useful (ref. 1).

Any function  $F_0$ , satisfying the homogeneous biharmonic equation

$$\Delta\Delta F_0 = 0 \quad (15.89)$$

can be represented in the form

$$F_0 = f_1 + r^2 f_2 \quad (15.90)$$

where  $f_1$  and  $f_2$  are harmonic functions. Any harmonic function  $f$ , finite inside a given circle of radius  $r = 1$ , can be presented in the form of the series.

$$f = \sum_{n=0}^{\infty} r^n (a_n \cos n\varphi + b_n \sin n\varphi) \quad (15.91)$$

Hence, the solution of the homogeneous biharmonic equation (15.89) can be presented (in finite functions) in the form

$$F = \sum_{n=0}^{\infty} \left[ r^n (a_n \cos n\phi + b_n \sin n\phi) + r^{n+2} (a_{1n} \cos n\phi + b_{1n} \sin n\phi) \right] \quad (15.92)$$

Further, we note that

$$\left. \begin{aligned} \Delta\Delta(r^a) &= a^2(a-2)^2 r^{a-4} \\ \Delta\Delta(r^a \cos n\phi) &= (a^2 - n^2) [(a-2)^2 - n^2] r^{a-4} \cos n\phi \\ \Delta\Delta(r^a \sin n\phi) &= (a^2 - n^2) [(a-2)^2 - n^2] r^{a-4} \sin n\phi \end{aligned} \right\} \quad (15.93)$$

The solution of the nonhomogeneous equation (15.88) is the sum of the solutions of the homogeneous equation (15.89) and a particular solution of the nonhomogeneous equation (15.88), where the sum must satisfy the boundary conditions. The requirement  $\Psi(R) = 0$  (eq. (15.83)) was introduced to simplify these boundary conditions.

Applying these considerations to the harmonic equation for the non-dimensional temperature  $\theta$ , we arrive at the same conclusions, except that in place of equation (15.93) the expressions obtained are more simple:

$$\left. \begin{aligned} \Delta(r^a) &= a^2 r^{a-2} \\ \Delta(r^a \cos n\phi) &= (a^2 - n^2) r^{a-2} \cos n\phi \\ \Delta(r^a \sin n\phi) &= (a^2 - n^2) r^{a-2} \sin n\phi \end{aligned} \right\} \quad (15.94)$$

In order to satisfy the boundary conditions of equations (15.81) and (15.82), we set

$$\left. \begin{aligned} \theta_e^{(0)} &= \frac{A}{A_0} r \cos \phi + \frac{B}{A_0} r \sin \phi \\ \theta_e^{(n)} &= \sum_{m=1}^{\infty} r^{-m} (c_m \cos m\phi + d_m \sin m\phi) \\ n &= 1, 2, 3, \dots \end{aligned} \right\} \quad (15.95)$$

We shall use these preliminary computations for the particular case where

$$\left. \begin{aligned} \left( \frac{\partial \theta_e}{\partial y} \right)_{r=0} &\equiv B = 0 \\ A &= A_0 \end{aligned} \right\} \quad (15.96)$$

that is, where the heating proceeds only laterally and the vertical component of the temperature gradient is zero at infinity. The substitutions and computations give the following results:

Zeroth approximation:

$$\left. \begin{aligned} F^{(0)} &= 0; \quad v_r^{(0)} = v_\phi^{(0)} = 0 \\ \theta^{(0)} &= AR\delta^{(0)} = 2 \frac{Ar_1 \cos \phi}{1 + \frac{\lambda}{\lambda_e}} \\ \theta_e^{(0)} &= AR\delta_e^{(0)} = \left( Ar_1 + \frac{AR^2}{r_1} \times \frac{1 - \frac{\lambda}{\lambda_e}}{1 + \frac{\lambda}{\lambda_e}} \right) \cos \phi \end{aligned} \right\} (15.97)$$

First approximation:

$$\left. \begin{aligned} F^{(1)} &= \frac{1}{16 \left( 1 + \frac{\lambda}{\lambda_e} \right)} \left( -\frac{1}{2} + r^2 - \frac{1}{2} r^4 \right) \\ v_r^{(1)} &= 0; \quad v_\phi^{(1)} = \frac{\kappa}{R} \times \frac{\xi^4}{8 \left( 1 + \frac{\lambda}{\lambda_e} \right)} r(r^2 - 1) \\ \theta^{(1)} &= AR \frac{\xi^4}{96 \left( 1 + \frac{\lambda}{\lambda_e} \right)^2} r \left( -2 \frac{(1 + 2\lambda/\lambda_e)}{1 + \lambda/\lambda_e} + 3r^2 - r^4 \right) \sin \phi \\ \theta_e^{(1)} &= -AR \frac{\lambda/\lambda_e}{48 \left( 1 + \frac{\lambda}{\lambda_e} \right)^3} \times \xi^4 \frac{1}{r} \sin \phi \end{aligned} \right\} (15.98)$$

Second approximation:

$$\begin{aligned}
 F^{(2)} &= Mr^2(-11 + 24r^2 - 15r^4 + 2r^6) \sin 2\varphi \\
 v_r^{(2)} &= \frac{x}{R} \xi^8 2Mr(-11 + 24r^2 - 15r^4 + 2r^6) \cos 2\varphi \\
 v_\varphi^{(2)} &= \frac{x}{R} \xi^8 2Mr(-11 + 48r^2 - 45r^4 + 8r^6) \sin 2\varphi \\
 \theta^{(2)} &= AR\xi^8 M \left\{ r \left[ (-a_1 + b_1 r^2 - c_1 r^4 + d_1 r^6 - e r^8) \times \right. \right. \\
 &\quad \left. \left. \cos \varphi + r^2(a_2 - b_2 r^2 + c_2 r^4 - d_2 r^6) \cos 3\varphi \right] \right\} \\
 \theta_e^{(2)} &= -AR\xi^8 M \frac{1}{r} \left( a_3 \cos \varphi - b_3 \frac{1}{r^2} \cos 3\varphi \right)
 \end{aligned}
 \tag{15.99}$$

In formulas (15.99) the following abbreviated notations are used:

$$\left. \begin{aligned}
 v_r &\equiv v_r^{(1)} + v_r^{(2)} + \dots \\
 v_\varphi &\equiv v_\varphi^{(1)} + v_\varphi^{(2)} + \dots
 \end{aligned} \right\} \tag{15.100}$$

$$\begin{aligned}
 \frac{1}{M} &= 184 \ 320 \left( 1 + \frac{\lambda}{\lambda_e} \right)^2 \\
 a_1 &= \frac{101 + 426 \frac{\lambda}{\lambda_e} + 153 \left( \frac{\lambda}{\lambda_e} \right)^2}{4 \left( 1 + \frac{\lambda}{\lambda_e} \right)^3}; \quad b_1 = \frac{109 + 229 \frac{\lambda}{\lambda_e}}{2 \left( 1 + \frac{\lambda}{\lambda_e} \right)^2}; \quad c_1 = 4 \times \frac{11 + 16 \frac{\lambda}{\lambda_e}}{\left( 1 + \frac{\lambda}{\lambda_e} \right)^2} \\
 d_1 &= \frac{35}{2 \left( 1 + \frac{\lambda}{\lambda_e} \right)}; \quad e = \frac{11}{4 \left( 1 + \frac{\lambda}{\lambda_e} \right)}; \quad a_2 = \frac{5 + 6 \frac{\lambda}{\lambda_e}}{3 \left( 1 + \frac{\lambda}{\lambda_e} \right)^2} \\
 b_2 &= \frac{3}{1 + \frac{\lambda}{\lambda_e}}; \quad c_2 = \frac{3}{2 \left( 1 + \frac{\lambda}{\lambda_e} \right)}; \quad d_2 = \frac{1}{6 \left( 1 + \frac{\lambda}{\lambda_e} \right)} \\
 a_3 &= \frac{\lambda}{\lambda_e} \times \frac{16 - 27 \frac{\lambda}{\lambda_e}}{\left( 1 + \frac{\lambda}{\lambda_e} \right)^3}; \quad b_3 = \frac{\lambda}{\lambda_e} \times \frac{1}{3 \left( 1 + \frac{\lambda}{\lambda_e} \right)^2}
 \end{aligned}
 \tag{15.101}$$

4281

Similarly, the third approximation, which will have a still more complicated form, may be computed.

Judging from the physical side of the convection process described by these equations, a value of the parameter  $\xi^4$  of the system (15.86), for which it would not have a finite solution, does not exist. Therefore, in analogy with the case of heat transfer through layers, it must be assumed that no restriction on  $\xi^4$  are imposed within the limits of the parametric linearization. The power series (15.87) converge certainly only for the values  $\xi^4 < 1$ . Hence, for  $\xi^4 \geq 1$ , these solutions may give divergent series. However, from the example computed previously up to the second approximation, the practical convergence of the series (15.87) is very strong. Apparently, the limits of applicability of the solutions in the form of the series (15.87) may thus be reliably decided only by experiment.

4281

The obtained solution permits the following physical interpretation. In the zeroth approximation no motion of the fluid is allowed (i.e., there is no convection). The fluid filling the channel behaves thermally as a solid body, with a different heat conductivity from that of the surrounding mass (typical problem of the theory of the potential).

As a result of the temperature distribution, which corresponds to the zeroth approximation, a very simple form of the convection currents arises in the first approximation; namely, the circular form (eq. (15.98)). The fluid rises along the hot wall and descends along the cold wall. The streamlines are closed circles. The radial component of the velocity is zero. In the central part of the channel the fluid rotates almost like a solid body. In connection with this motion a vertical temperature gradient arises in the channel and in the channel neighborhood (through  $\sin \phi$ ), the gravitational-thermal effect (ch. 16, sec. 1).

As a result of the additional change in temperature, which is described by the first approximation, a radial component of the velocity arises in the second approximation (eq. (15.99)), and the temperature field becomes more complicated. A dependence on three times the polar angle  $\phi$  occurs. Because  $M$  is very small, of the order of  $10^{-5}$ , the radial velocities attain the same order as the velocities of the circular motion of the first approximation for the values

$$\xi^4 = Gr \times Pr \approx 2 \times 10^5 \quad (15.102)$$

if the channel radius is taken as the determining dimension. However, if the diameter  $2R$  is taken as the determining dimension, as is done in engineering computations, the "engineering" value of the criterion will be

$$GrPr \approx 3.2 \times 10^6 \quad (15.103)$$

This number is close in value to that which corresponds to the break in the curves of the heat transfer through liquid films (fig. 25, curve III). This fact justifies the application on only two terms of the series, which thus evidently actually converge rapidly. Hence, it is necessary to assume that the accuracy assured by the second approximation within the range  $0 \leq \xi^4 \leq 10^3$  is very high.

For comparison with experiment, figure 50 shows the isolines of equal gradient computed by the preceding formulas. Qualitatively, these isolines correspond satisfactorily to the photographically obtained lines shown in figure 45A. However, fuller correspondence is obtained with figure 45B. This photograph shows the isolines which are observed in the same optical model if the heater and cooler are not placed to the right or to the left, as corresponds to figure 45A, but are placed at an angle of  $45^\circ$  to the vertical, as indicated on figure 45B. The reason for the better correspondence may be seen from the following considerations. Because of the limited linear dimensions of the model (which are only three times greater than the cavity dimension) under the conditions of figure 45A, the vertical temperature gradient (hotter upward) is not proportionally large by comparison with the theoretical case of infinite surrounding mass. Under the conditions of figure 45B this vertical gradient is somewhat concealed by the oblique displacement of the heater and of the cooler. Hence, the actual conditions approach those which correspond to the theory (horizontal gradient in an infinite surrounding mass).

The deviation of the theory from experiment must further be ascribed to the random value of the parameter  $\xi^4$  and to the random ratio of the heat conductivities assumed in the computation ( $\lambda/\lambda_e = 0.0083$ ).

The further working of this example also gives the hope of investigating the convection in an inclined channel, perpendicular to the horizontal component of the temperature gradient. The results of the computations must be compared with the results corresponding to the same effective direction of the gradient, the same ratio of heat conductivities, and the same value of the parameter  $\xi^4$  as those assumed in the computations.

## 7. Convection in Spherical Cavity<sup>14</sup>

In an infinite solid medium with coefficient of heat conductivity  $\lambda_e$ , let there be a spherical cavity of radius  $R$  filled with an incompressible (but thermally deformable) fluid with heat conductivity  $\lambda$ , heat capacity  $c$ , and coefficient of dynamic viscosity  $\mu$ , all independent

<sup>14</sup>The present section is compiled from data obtained by E. Drakhlin.

of the temperature. Let the temperature gradient  $A$  of the medium at infinity be given as constant in space and time. We shall find the temperature distribution in the fluid  $\theta(x,y,z)$  and in the solid medium  $\theta_e(x,y,z)$ , and the velocity distribution in the fluid  $v(x,y,z)$ . The origin of the Cartesian coordinates  $x,y,z$  will be taken at the center of the sphere.

We introduce the following notations. Let  $\theta_0$  be the volumetric mean value of the temperature;  $\rho_0 \equiv \rho_0(\theta_0)$  the fluid density in equilibrium,  $\rho \equiv \rho' - \rho_0$ ;  $p_0 \equiv p_0(\theta_0)$  the pressure in equilibrium,  $p' \equiv p - p_0$ ; let  $\rho' \ll \rho_0$ . We shall restrict ourselves to the first approximation for the temperature and the second approximation for the velocity:

$$\left. \begin{aligned} \theta' &\equiv \theta - \theta_0 \equiv \theta'(0) + \theta'(1) \\ \theta'_e &\equiv \theta_e - \theta_0 \equiv \theta'_e(0) + \theta'_e(1) \\ \underline{v} &= \underline{v}(1) + \underline{v}(2) \\ \underline{v}(0) &= 0 \end{aligned} \right\} \quad (15.104)$$

In the zeroth approximation the fluid is assumed to be stationary.

The boundary conditions have the following form:

$$\left. \begin{aligned} \underline{v}(R) &= 0 \\ \theta(R) &= \theta_e(R) \\ \lambda \left( \frac{\partial \theta}{\partial r} \right)_{r=R} &= \lambda_e \left( \frac{\partial \theta_e}{\partial r} \right)_{r=R} \end{aligned} \right\} \quad (15.105)$$

where  $r$  denotes the radius vector,  $r^2 = x^2 + y^2 + z^2$ . Considering the conditions of symmetry, we assume that the streamlines lie in planes parallel to the plane determined by the directions  $g$  and  $A$ . We choose this plane as the  $xy$ -plane and the direction of  $g$  as the direction of the  $y$ -axis.

We introduce the stream function  $\Psi$ :

$$\left. \begin{aligned} v_x &= - \frac{\partial \Psi}{\partial y} \\ v_y &= - \frac{\partial \Psi}{\partial x} \\ \Psi &= \Psi(1) + \Psi(2) \end{aligned} \right\} \quad (15.106)$$

Eliminating the pressure (eq. (15.75)), we obtain the following equations:

$$\Delta^* \Delta \Psi = - \frac{1}{v} \left[ \frac{\partial \Psi}{\partial x} \left( \frac{\partial^3 \Psi}{\partial x^2 \partial y} + \frac{\partial^3 \Psi}{\partial y^3} \right) - \frac{\partial \Psi}{\partial y} \left( \frac{\partial^3 \Psi}{\partial x \partial y^2} + \frac{\partial^3 \Psi}{\partial x^3} \right) \right] + \frac{g\beta}{v} \times \frac{\partial \theta'}{\partial x} \quad (15.107)$$

$$\kappa \Delta \theta' = v_x \frac{\partial \theta'}{\partial x} + v_y \times \frac{\partial \theta'}{\partial y} \quad (15.108)$$

where the symbol  $\Delta^*$  denotes the Laplacian in the coordinates  $x$  and  $y$ :

$$\Delta^* = \frac{\partial^2}{\partial x^2} + \frac{\partial^2}{\partial y^2}$$

In the zeroth approximation for the stationary fluid,

$$\Delta \theta'(0) = 0 \quad (15.109)$$

We solve this equation with the corresponding equation of the external problem

$$\Delta \theta'_e(0) = 0 \quad (15.110)$$

and with account taken of the boundary conditions (eq. (15.105)). We obtain the result from the theory of the potential (potential of a dielectric sphere in a homogeneous field):

$$\theta'(0) = \frac{3\lambda_e}{\lambda + 2\lambda_e} [A_x x + A_y y] \quad (15.111)$$

$$\theta'_e(0) = \left[ \frac{\lambda_e - \lambda}{\lambda + 2\lambda_e} \times \frac{R^3}{r^3} + 1 \right] \times [A_x x + A_y y] \quad (15.112)$$

where  $A_x$  and  $A_y$  denote the corresponding components of the temperature gradient vector at infinity  $A$ .

In the first approximation, equations (15.107) and (15.108) give

$$\Delta^* \Delta \Psi(1) = \frac{g\beta}{v} \times \frac{\partial \theta'(0)}{\partial x} \quad (15.113)$$

$$\kappa \Delta \theta'(1) = v_x(1) \times \frac{\partial \theta'(0)}{\partial x} + v_y(1) \times \frac{\partial \theta'(0)}{\partial y} \quad (15.114)$$

It is necessary here to make a small mathematical digression. Suppose we have the equation  $\Delta^* \Delta \Psi = Q$ , where  $\Psi(x, y, z)$  is an unknown

42511

CA-20 back

function and  $Q$  is a known polynomial of degree  $N$  relative to  $x, y, z$ , and let it be required to find  $\partial\psi/\partial x$  and  $\partial\psi/\partial y$  for the boundary conditions

$$\left(\frac{\partial\psi}{\partial x}\right)_{r=R} = \left(\frac{\partial\psi}{\partial y}\right)_{r=R} = 0 \quad (15.115)$$

We set

$$v_x = -\frac{\partial\psi}{\partial y} = \sum_{n=0}^s a_n x^{i_1^{(n)}} y^{j_1^{(n)}} z^{k_1^{(n)}} \left[ \left(\frac{r}{R}\right)^{2m} - 1 \right] \quad (15.116)$$

$$v_y = \frac{\partial\psi}{\partial x} = \sum_{n=0}^s b_n x^{i_2^{(n)}} y^{j_2^{(n)}} z^{k_2^{(n)}} \left[ \left(\frac{r}{R}\right)^{2m} - 1 \right] \quad (15.117)$$

where  $i_1^{(n)}$ ,  $i_2^{(n)}$ ,  $j_1^{(n)}$ ,  $j_2^{(n)}$ ,  $k_1^{(n)}$ ,  $k_2^{(n)}$ , and  $m$  are natural numbers, running independently of each other through the values  $0, 1, 2, \dots$ , and  $N+3$ . The number  $s$  is determined by the condition that on the right sides of equations (15.116) and (15.117) all the components of the preceding form, for which the sum of the powers of  $x, y, z$ , and  $r$  constitutes a series of natural numbers between the limits 2 and  $N+3$ , must be present. It may be shown that the expressions (15.116) and (15.117) solve the proposed problem, if the coefficients  $a_n$  and  $b_n$  are found. For this purpose it is first necessary to use the equation  $\Delta^*\Delta\psi = Q$  and, secondly, the mixed derivatives of  $\psi$  expressed in terms of  $a_n$  with the aid of equation (15.116) and in terms of  $b_n$  with the aid of equation (15.117) must agree.

Applying the previously described mathematical device, we solve equation (15.113), and find the components of the velocity (eq. (15.106)) to the first approximation. The computations give

$$v_x^{(1)} = \frac{3}{20} \times \frac{g\beta A_x R^4}{\nu^2} \times \frac{v_y}{R^4} \times \frac{\lambda_e}{\lambda + 2\lambda_e} (R^2 - x^2 - y^2 - z^2) \quad (15.118)$$

$$v_y^{(1)} = -\frac{3}{20} \times \frac{g\beta A_x R^4}{\nu^2} \times \frac{v_x}{R^4} \times \frac{\lambda_e}{\lambda + 2\lambda_e} (R^2 - x^2 - y^2 - z^2) \quad (15.119)$$

It may be verified that in this approximation the streamlines are circles, parallel to the  $xy$ -plane.

To find the temperature distribution in the first approximation, we solve equation (15.114) with the corresponding equation (15.110) of

the external problem for the boundary conditions of equation (15.105).  
As a result, we obtain

$$\begin{aligned} \theta'(1) = & a_1(z^4x + x^5 + y^4x + 2z^2x^3 + 2z^2xy^2 + 2x^3y^2) + \\ & a_2(z^2x + x^3 + xy^2) + a_3x + \\ & a_4(z^4y + x^4y + y^5 + 2z^2x^2y + 2z^2y^3 + 2x^2y^3) + \\ & a_5(z^2y + x^2y + y^3) + a_6y \end{aligned} \quad (15.120)$$

where

$$\left. \begin{aligned} a_1 & \equiv \frac{9}{560} \times \frac{g\beta}{\nu\kappa} \times \left( \frac{\lambda_e}{\lambda + 2\lambda_e} \right)^2 A_x A_y \\ a_2 & \equiv -\frac{9}{200} \times \frac{g\beta R^2}{\nu\kappa} \times \left( \frac{\lambda_e}{\lambda + 2\lambda_e} \right)^2 A_x A_y \\ a_3 & \equiv \frac{9}{2800} \times \frac{g\beta R^4}{\nu\kappa} \times \frac{(17\lambda + 18\lambda_e)\lambda_e^2}{(\lambda + 2\lambda_e)^3} A_x A_y \\ a_4 & \equiv -\frac{9}{560} \times \frac{g\beta}{\nu\kappa} \times \left( \frac{\lambda_e}{\lambda + 2\lambda_e} \right)^2 A_x^2 \\ a_5 & \equiv \frac{9}{200} \times \frac{g\beta R^2}{\nu\kappa} \times \left( \frac{\lambda_e}{\lambda + 2\lambda_e} \right)^2 A_x^2 \\ a_6 & \equiv -\frac{9}{2800} \times \frac{g\beta}{\nu\kappa} \times \frac{(17\lambda + 18\lambda_e)\lambda_e^2}{(\lambda + 2\lambda_e)^3} A_x^2 \end{aligned} \right\} \quad (15.121)$$

$$\theta_e'(1) = \frac{9}{350} \times \frac{g\beta A_x R^4}{\nu^2} \times \frac{\nu}{\kappa} \times \frac{\lambda\lambda_e^2}{(\lambda + 2\lambda_e)^3} \times \frac{A_y x - A_x y}{r^3} \quad (15.122)$$

The finding of the temperatures and velocities in the second approximation requires very laborious computations. The velocity components in the second approximation are polynomials of the seventh degree in the coordinates  $x, y, z$ . To obtain the coefficients in these polynomials it was necessary to solve a system of 44 linear algebraic equations.

The final expressions for the velocities in the second approximations have the following form:

$$\begin{aligned}
 v_x^{(2)} &= \frac{l_1}{k_1} (p_1 z^4 + p_2 x^4 + p_3 y^4 + p_4 z^2 x^2 + p_5 z^2 y^2 + \\
 &\quad p_6 x^2 y^2 + p_7 z^2 + p_8 x^2 + p_9 y^2 + p_{10}) \times \\
 &\quad (x^2 + y^2 + z^2 - 1)x + \frac{l_2}{k_2} (q_1 z^4 + q_2 x^4 + q_3 y^4 + \\
 &\quad q_4 z^2 x^2 + q_5 z^2 y^2 + q_6 x^2 y^2 + q_7 z^2 + q_8 x^2 + \\
 &\quad q_9 y^2 + q_{10}) (x^2 + y^2 + z^2 - 1)y \\
 v_y^{(2)} &= \frac{l_2}{k_2} (r_1 z^4 + r_2 x^4 + r_3 y^4 + r_4 z^2 x^2 + r_5 z^2 y^2 + \\
 &\quad r_6 x^2 y^2 + r_7 z^2 + r_8 x^2 + r_9 y^2 + r_{10}) \times \\
 &\quad (x^2 + y^2 + z^2 - 1)x + \frac{l_1}{k_1} (s_1 z^4 + s_2 x^4 + s_3 y^4 + \\
 &\quad s_4 z^2 x^2 + s_5 z^2 y^2 + s_6 x^2 y^2 + s_7 z^2 + s_8 x^2 + \\
 &\quad s_9 y^2 + s_{10}) (x^2 + y^2 + z^2 - 1)y
 \end{aligned} \tag{15.123}$$

where there has been set

$$\begin{aligned}
 R &= 1 \\
 k_1 &= 2^6 \times 3^3 \times 5 \times 7 \times 11 \times 13 = 8,648,640 \\
 k_2 &= 3 \times 4 \times 5 \times 7 \times 13 \times 4919 = 26,857,740 \\
 l_1 &= \frac{9}{20} \left( \frac{g\beta A_y R^4}{\nu^2} \right)^2 \times \frac{\nu^2}{R^8 \alpha} \times \left( \frac{\lambda_e}{\lambda + 2\lambda_e} \right)^2 \\
 l_2 &= \frac{9}{20} \left( \frac{g\beta A_y R^4}{\nu^2} \right)^2 \times \frac{\nu^2}{R^8 \alpha} \times \left( \frac{\lambda_e}{\lambda + 2\lambda_e} \right)^2 \frac{A_x}{A}
 \end{aligned} \tag{15.124}$$

and  $p_i$ ,  $q_i$ ,  $r_i$ , and  $s_i$  ( $i = 1, 2, \dots, 10$ ) represent constant numbers whose values are given in table IX. The values of  $q_{10}$  and  $r_{10}$  are given by

$$\left. \begin{aligned} q_{10} &= \frac{179,390}{3} - \frac{17\lambda + 18\lambda_e}{2800(\lambda + 2\lambda_e)} k_2 \\ r_{10} &= -\frac{237,439}{8} + \frac{17\lambda + 18\lambda_e}{2800(\lambda + 2\lambda_e)} k_2 \end{aligned} \right\} \quad (15.125)$$

As an illustration of these very complicated results let us consider as an example the case of heating from the side ( $A_y = 0$ ), where for simplicity of computation we put (see eq. (15.121))

$$\left. \begin{aligned} \text{GrPr} &= 560 \\ \lambda &= \lambda \end{aligned} \right\} \quad (15.126)$$

From equation (15.121) we obtain

$$\left. \begin{aligned} a_1 &= a_2 = 0 \\ a_3 &= -a_4 = A_x \\ a_5 &= \frac{14}{5} A_x \\ a_6 &= -\frac{7}{3} A_x \end{aligned} \right\} \quad (15.127)$$

The further computations show that in this case the distribution of the velocities (isolines of the velocities) in any plane passing through the  $z$ -axis (meridional plane) very strongly recalls the situation considered previously (fig. 6). The maximal value of the tangential velocity component is found to be at approximately 0.6 of the sphere radius, and is approximately equal to  $10.6 \kappa/R$  for a value of  $\text{GrPr}$  of 560. However, in the second approximation the streamlines are not obtained as circles but have an oval shape extended in the direction of the axis  $y = x$ , and are compressed in the direction of the axis  $y = -x$ . On the axes  $x$  and  $y$  the maximal value of the radial component is obtained for the assumed value  $\text{GrPr} = 560$  on half the sphere radius, and is equal to  $\pm 1.4 \kappa/R$ .

The convective process in the cavity produces, in the surrounding mass (within the limits of the first approximation), both the horizontal temperature gradient acting from without and the vertical gradient (eq. (15.122)):

$$\theta_e^{(1)} = -\frac{9}{350} \times \frac{q\beta R^4}{v\kappa} \times \frac{\lambda_e^2}{(\lambda + 2\lambda_e)^2} \times \frac{yR^3 A_x^2}{r^3} \quad (15.128)$$

A spherical cavity resembles a vertical thermal dipole whose intensity is proportional to the square of the external gradient  $A_x$  and to the seventh power of the radius of the sphere  $R$ . This expresses the gravitational-thermal effect of convection (formula (15.98)).

If followed in detail, it may be established that the entire course of the computations previously given represents a nonexplicitly carried out method of successive approximations based on the expansion of the solutions in powers of the Grashof number:

$$Gr = \frac{g\beta R^4}{\nu^2} \quad (15.129)$$

This fact appears in the structure of formulas (15.118) and (15.124).

The preceding example shows that the practical computation necessarily leads to such a series. Therefore, it is very convenient to give this series in explicit form at the very start of the computations, taking  $Gr$  as the small parameter of nonlinearity.

## CHAPTER 16

EXPERIMENTAL INVESTIGATION OF THERMAL CONVECTION  
IN CAVITIES OF SPECIAL FORM

## 1. Statement of Problem

A good discussion of the thermal convective phenomena in an infinite horizontal slit between two solid planes is found in the literature (the cells of Bénard, ref. 1, ch. 12). The main purpose of the present book is to investigate the opposite case, thermal convection in a vertical channel. It is natural to connect these extreme cases with the intermediate cases not only theoretically (ch. 15, secs. 6 and 7) but also experimentally, namely, the thermal convection in a hollow sphere and in a horizontal channel of circular section.

Both the previously discussed cases have great practical significance. First, such cavities are often contained in the composition of many heat insulating materials, either accidentally or by design. If convection arises in the liquid or in the gas filling these cavities, the effective heat conductivity of such insulating impregnation may be found to be much greater than that found from the magnitude of the molecular heat conductivity of the liquid or gas. Although the effective heat conductivity of the air inclusions is determined in structural practice the question must not be considered as exhaustively solved, and it is necessary to determine more accurately the part played by convection in this problem.

Secondly, the convective heat transfer in such cavities possesses a characteristic feature that requires detailed study; namely, that convection is characterized by the rising of the warm fluid particles while the cold particles descend. Hence, as a result of convection an additional vertical temperature gradient necessarily arises; that is, the fluid is warmer toward the top (formulas (15.98) and (15.128)). This additional convective gradient distorts the initial thermal field in the solid surrounding mass that contains the cavities. A specific gravitational-thermal effect arises (recalling the well-known galvano-magnetic Hall effect). The passage of the heat flow through the porous body in a horizontal direction is accompanied by additional heat of its upper part

and additional cooling of its lower part. The heat-flow vector ceases to be collinear with the temperature-gradient vector, a vertical deviation arising between them. Hence, the concept "effective thermal conductivity of a porous mass" loses its sense as a scalar and acquires that of a tensor whose components are connected with the gravity acceleration vector.

This circumstance is generally ignored in practice although its correct acknowledgment may result in the saving of many megacalories of heat for the country. In the following paragraphs only initial experimental studies, which have been conducted in this direction, are described.

4281

## 2. Convection in Spherical Cavity<sup>15</sup>

A divided model was constructed from a piece of Plexiglas of dimensions 47 by 47 by 62 millimeters, shown in section in figure 51. Both halves of the model were placed with their ground faces against each other and were hermetically compressed. Channels of about 1-millimeter diameter were drilled in the interior of the model. The double-insulated wires of thermocouples of copper-constantan of approximately 0.2-millimeter diameter were inserted in these channels in a manner such that the thermocouple junctions were located about 1 millimeter inside the spherical cavity. The channels with the thermocouple wires were closed with wax. The cavity was filled with distilled water through the channel K, of diameter of about 3 millimeters. The model was placed in the heater coil  $\pi$  and was covered with cooler X (a brass vessel containing ice and water).

In correspondence with the scheme of figure 52, 18 thermocouple junctions were arranged along the inside surface of the sphere. Their coordinates, expressed in geographical language, are given in table X. Further, thermocouples were located at the points A and B, immediately on the heater under the cooler.

The results of the measurements are presented in table XI and in the composite figure 53 corresponding to the eight different heating power inputs. On each individual graph of this chart the temperature is given as a function of the "longitude" of the corresponding thermocouple. The lines correspond to the same "latitude": line 1 corresponds to the upper pole, line 18 corresponds to the lower pole, the center line to the equator, and so forth. The lines A and B correspond to the temperatures of the upper and lower faces of the model, respectively. An analogous temperature distribution was also obtained by another method of measuring the temperature (an electrical method, see ch. 19, sec. 1).

<sup>15</sup>This section has been compiled from data obtained by N. A. Pleshkov.

The composite figure shows that the mean temperature of the equator is not equal to the mean of the temperatures of the poles. The temperature of the equator is above the mean when it is below 20° C, room temperature, and is below the mean when it is above the room temperature.

The temperature of the equator is higher than the average of the polar temperatures when the fluid in convective motion rises at the walls and descends along the vertical axis of the model. This phenomenon is favored by the low mean temperature of the entire model as compared with the room temperature; the model being heated not only by the heater but also through the side walls of the room. When the mean temperature of the model is higher than the room temperature the reverse phenomenon is obtained.

The composite figure also shows that on the mean temperature of each circle of latitude there are superposed waves, predominantly with a period of one rotation about the vertical diameter of the sphere (for large heating powers a half rotation). It is possible that these waves also arise as a result of the effect of the surrounding circumstances (windows, heating apparatus), since the tests were conducted in the winter and the model was not heat-insulated.

From these considerations the following preliminary conclusions may be drawn:

(a) Thermal convection in these tests took place and transferred further quantities of heat upward, in addition to the heat transferred by the molecular conductivity. Thus, the effective thermal conductivity of the fluid medium was greater than the molecular thermal conductivity of the fluid medium.

(b) The form of the convective flow was greatly subject to extraneous temperature effects, which must very carefully be eliminated in adjusting the more accurate measurements.

A noted example of thermal convection in a spherical cavity of large dimensions (aerostat heated by the sun) was investigated by E. V. Kudryavtsev (ref. 1).

### 3. Convection in Cylindrical Cavity with Horizontal Axis

Figures 44 and 45 show photographs of certain cases obtained on a model similar to that of figure 47. A sketch of the model is shown in figure 54. A rectangular block of a lead alloy of small heat conductivity (babbitt) was clamped through asbestos strips, between two Textolite disks. A cylindrical opening, stopped by two positive optical lenses, was drilled in the block. The obtained cavity made contact with the outer space by a through channel, by which the cavity was filled with

4281

CA-21 back

glycerine. The channel was then covered with stoppers on both sides. Tubular channels were drilled along the opposite sides of the block. The porcelain tubes of an electric heater coil and the connecting piece of the water cooling pipes, respectively, were inserted into the channels. The Nichrome spiral of the heater was inserted inside the opening of the porcelain tube. With the aid of the combination of the electric heater and the water cooler it was possible to produce the conditions of an approximately homogeneous thermal field perpendicular to the horizontal axis of the model in the block.

By mounting the model on the two horizontal bars of an optical bench it was possible to assign the temperature gradient in the block any orientation relative to the vertical (the heater was placed below, on the side, or above, at any angle). The angles were read by means of a small plumb line, sliding in front of the graduated circle attached to the Textolite disk.

The observations of the convective phenomena in this model both by means of suspended light-scattering particles, and by means of the optical lattice method, showed that two types of motion are typical; namely, circular and vertical-diametral.

The circular motion is obtained with the heater and cooler placed at the two sides of the model cavity. In this motion the fluid rises along the warm wall and descends along the cool wall. In this way the streamlines resemble almost true circles.

The vertical-diametral motion is obtained with the heater coil placed below and the cooler above. In this motion the fluid rises in the vertical-diametral plane and descends at the sides along the cylindrical walls. However, the reverse phenomenon is also possible. (See discussion of results in the preceding section.)

Both these types of motion are sufficiently stable and for the inclined positions of the model may evidently exist together. With any of these motions the presence of considerable vertical temperature gradients is clearly noted. It is thus clearly seen that the part played by the fluid in the cavity of the model is equivalent to the part played by a vertical thermal dipole, or more accurately, by a continuous chain of such dipoles placed along the horizontal axis of the model.

#### 4. Concluding Remarks

The previously described preliminary experiments and their results do not as yet give a complete answer to the question discussed at the beginning of the chapter. Their main significance lies in the fact that they outline the whole experimental difficulty of the problems. In

particular, combined methods must be employed. For example, the optical method of observation must be combined with the method of temperature recording, and so forth. It is likewise necessary to very carefully exclude external influences that are unaccounted for, to take noneliminable effects into account, and so forth. A development of suitable appliances and equipment for the tests is thus required.

## CHAPTER 17

THERMAL CONVECTION IN INCLINED MODEL OF  
CIRCULAR CROSS SECTION<sup>16</sup>

4281

## 1. Description of Experimental Setup

For the experimental investigation of thermal convection in a closed circular model heated at one end and inclined at various angles to the vertical, models of the same type as those described in chapter 9 (sec. 1) were used.

At its center the model was attached to the horizontal axis of a special stand; and, with the aid of a clock mechanism, it rotated approximately once each day. In this manner the axis of the channel very smoothly assumed various angles with the vertical, starting from zero (heater on bottom) through  $\pi$  (heater on top) up to  $2\pi$  (heater again on bottom). The temperatures were read by means of automatic devices as described in chapter 9, section 3. The usual apparatus was used as a photographic recording device, the recordings of which have been presented previously in various sections (Cartesian recording).

## 2. Laminar Regime

An extract from the photographic record (fig. XXI) may serve as an example. The recording was conducted for five days, with no essential differences observed in the recording of some days from that of others. The temperature of the aluminum jacket of the model was taken as the zero temperature. The five averaging thermocouples nearest to the heater coil were arranged 1 centimeter from each other, and the remaining ones 3 centimeters from each other.

When the heater was located at the top, the temperature along the model varied according to the exponential law, the temperatures of the parts nearer the heater (upper curves) being considerably higher than the others. The temperatures of the parts some distance from the heater were almost equal to the temperature of the jacket. The instant when the model occupied a strictly vertical position with the heater on top

<sup>16</sup>This chapter was compiled from data obtained by V. A. Tetuyev.

was distinguished by a natural sign; the air enclosed in the part of the cold reservoir at the end of the model opposite to the heater entered the channel of the model in a floating bubble and partially displaced the water there. When this occurred the temperature of all the thermocouples rose with a sharp jump. The greater the temperature gradient at the location of the given thermocouple, the greater was the magnitude of the jump. The reverse floating of the air bubble from the interior of the model occurred at the instant when the channel of the model occupied a horizontal position. The corresponding instant was marked on the photo record by a small reverse jump, the cooler fluid moving toward the heater.

When the heater is placed below, laminar convection takes place in the model. The column of fluid has a greater effective thermal conductivity; the curves are situated at almost equal distances from each other, the temperature gradient along the column being the same. This gradient depends on the angle between the axis of the channel and the vertical; in general, the smaller this angle the smaller the gradient. However, at the instant of strictly vertical position of the tube the temperature gradient in the region near the heater possesses a singular, sharp maximum. This maximum becomes inappreciable only at a distance from the heater approximately equal to 17 channel diameters.

The photo recording apparatus was later perfected. An aluminum disk was attached on the same horizontal axis about which the model rotated. Pieces of two-sided (nonwarping) photo films were attached to this disk by simple clips. The galvanometer was arranged in such manner that its point moved along the horizontal radius of the disk. In this manner the photo records were obtained in the form of polar diagrams on which the angles were equal to the angles between the axis of the channel and the vertical.

The following figures show examples of the photo records obtained with this apparatus. Figure XXII corresponds to a somewhat larger heating power than figure XXIII. These polar records permit the same interpretation as the Cartesian records of figure XXI.

The small air bubble of these records was carefully removed and the heat expansion of the water was absorbed by an elastic compensator (a piece of rubber tube with a Mohr pinch cock). The zero point on the photo records was taken as the temperature of the hottest thermocouple. The peripheral curve refers to the temperature of the aluminum jacket of the model. Figure XXIII notes the end of the nonstationary process marked by the starting of the model in motion from the position of "heater above." Figure XXIV shows a double print of the two last photographs. Both photographs coincide with each other in the convective part.

### 3. Generalization of Experimental Results

The attempts to evaluate the obtained curves led to the following conclusion. In general, in each position of the model the temperature distribution along the model corresponds to figure 28; the linear law of temperature distribution coincides (without jump or break) with the exponential law. The first is characteristic for convective regimes and for the parts of the model nearest to the heater. The second is characteristic for the molecular heat conduction and is observed in the vertical model far from the heater. The observed small deviations of the records from symmetry and from the coincidence mentioned are readily explained by the unsteady regimes. The velocity of rotation may be reduced, and the records will then be more symmetrical and the coincidence with the previously mentioned schematic figures will increase.

However, in this general coincidence there are also essential deviations. In the first place, the characteristic convective gradient depends on the angle as an even function (increases with increasing angle). Secondly, the exponent likewise depends on the angle as though the thermal conductivity of the fluid changed with increase of the angle and assumed an extreme (molecular) value for an angle equal to  $\pi$  (heater on top).

The preliminary interpretation of the first of these facts leads to the following considerations. If in the "fundamental" equations of chapter 3 it is assumed that the force of gravity acts along the vertical of the model, then it is natural to assume that for the inclined model only the axial component of the gravitational force will act upon the model. Hence in formula (3.7) it is necessary only to replace the magnitude  $g$  by  $g \cos \alpha$ ; that is, to retain  $\cos \alpha$  in formula (3.1). The comparison of this hypothesis with the results of the measurements on the photographs showed that this hypothesis is satisfactorily justified within the interval of almost from zero to angle of  $45^\circ$  with the vertical. Near zero the agreement is disturbed by the previously mentioned small sharp maximum. For angles greater than  $45^\circ$  it appears that the gravitational acceleration is to be multiplied not by  $\cos \alpha$  but by a larger magnitude that is nearer unity than  $\cos \alpha$ . The comparison of this fact with the material presented in chapter 11 leads to the preliminary conclusion that the higher the heat insulation of the model the wider the applicability of the "cosine law."

In fact, the heat losses of the convective flow in the thermal conductivity of the walls require the disruption of the antisymmetry of the flow and in the former plane of antisymmetry also require the origination of an additional ascending flow along the axis, and of a descending flow at the wall (see ch. 16, sec. 2). It must be assumed that in an inclined model the projections of the streamlines and the provisional "surface of antisymmetry" take the form represented in figure 55. In this way the velocity component normal to the axis of the model gives so considerable

a value that the linear treatment does not lead to a satisfactory description of the actual state of affairs.

A preliminary interpretation of the second of the abovementioned facts (i.e., the change of the apparent molecular thermal conductivity in an inclined model) is as yet difficult to give. Particularly strange is the fact that the apparent conductivity of the almost horizontal model, when it must be assumed that there is convection in it, is less than in the vertical model with "heater above," when convection can hardly occur in it. This fact is reflected in the last figures, in that they have a greater extension in width than in height, the temperature of the hottest thermocouple relative to the jacket being higher for the almost horizontal than for the vertical model for the same heating power input.

#### 4. Above-Critical Regime

At an increased heating power for the almost vertical model (near zero angle of inclination, heater below) the above-critical regime of the heat convection occurs. In figure XXVA and B are shown the polar photographs corresponding to a considerable heating power of  $\approx 0.80$  calorie per second and to a large sensitivity of the galvanometer ( $1^\circ\text{C}$  corresponding to 6.25 mm). The zero point is taken as the temperature of the upper averaging thermocouple, the farthest removed from the heater, represented on the photographs by a true arc of a circle. The relative temperature of the jacket is recorded below this arc. The photographs show how the regime of the convection, maintained laminar by the inclination of the model at large angles of inclination, is sharply changed into the above-critical regime for small angles. The smooth equidistant curves are sharply replaced by diffuse bands that reflect both the lowering of the effective thermal conductivity of the fluid and the instability of the process.

On figure XXVIA and B are shown the polar photo records corresponding to a large heating power and to so small a galvanometer sensitivity ( $1^\circ\text{C}$  corresponding to 0.66 mm) that the four curves of the preceding record in the laminar regime almost indistinguishably coalesce into one. This coalescence is aided by the increase in the convection parameter of water  $g\beta/v\kappa$  due to the increased mean temperature of the fluid in the model for this raised power (see ch. 8). On the last photograph below the zero line (the arc of the circle) the temperature of the aluminum jacket of the model is again recorded; and still further below, the temperature of the Dewar flask, the datum mark of the temperature. The increased heating power led to increased difficulty of laminarization in a wider angle than before ( $34^\circ$  to  $35^\circ$  of arc on fig. XXVIA and B as compared with  $13^\circ$  to  $14^\circ$  on fig. XXVA and B). On figure XXVII, because of the increased sensitivity, it is possible to distinguish the detailed character of the instability at the above-critical regime.

4281

'CA-22

From a comparison of the last photographs the following question may be asked: Is not the small sharp maximum near the zero angle on figure XXI an indication of the incipient above-critical regime that clearly develops at large powers; is a laminar regime in general possible with a strictly vertical model and complete absence of external cross temperature gradients? In this connection it is useful to emphasize that the tests described in this chapter were conducted in a room with temperature under good thermostatic control.

## CHAPTER 18

## CONCLUSION

The material presented in this report must in no sense be considered as exhausting the problem of gravitational convection under the conditions of the internal problem. On the contrary, the inexhaustibility of any branch of science is again emphasized. However, this material may serve as a guide for further research in the fields which immediately relate to industrial problems as well as to problems of physico-mathematical investigation.

An orientating list of those preliminary questions which are directly suggested by the material presented in this report and the further study of which should develop into well-founded technico-scientific investigations is as follows:

1. Investigate from the material in the literature how the ideas of Lomonosov on convection have been worked out by Russian and Soviet scientists.
2. Consider and theoretically rework the foundations for the setting up of the equations of gravitational convection with a view toward rendering them more accurate and extending the range of their applicability.
3. Extend the results of this work to convection of a nongravitational (electrostatic, magnetic, or other) nature.
4. Investigate the "external problem" of gravitational convection as a particular case of the "internal problem."
5. Extend the investigation to different fluids and work out a measuring procedure of the convection parameter  $g\beta/v\kappa$  as a chemico-analytic index for fluids.
6. Investigate convection in gases for the same analytical purposes.
7. Investigate the convective phenomena of the preceding type in multiple phase systems with stratification near the temperature of mutual solution, and make use of the turbidity of the fluid connected with the formation of an autonomous phase as a "thermoscopic" factor.

8. Clarify the question as to the setting in of the critical regime of gases as sharply as of liquids, and investigate its characteristic properties.

9. Investigate the phenomena in models of noncircular section.

10. Investigate the phenomena in models of variable section.

11. Carefully investigate water and other important industrial fluids, considering the values of the convection parameter, and issue tabulated results.

12. Compile and publish tables of various cylindrical functions of the argument ( $-\sqrt{ix}$ ) for use in engineering computations of those cases of convection where the temperature above is higher than the temperature below (ch. 5, sec. 5).

13. Investigate the work of exhaust apparatus and flues with natural and forced circulation, considering the super-position of free and forced convection (ch. 5, sec. 4).

14. Extend table 1 to the case where the temperature above is higher.

15. Clarify the question of the heat conductivity of a fluid in end phenomena.

16. Give a greater quantitative clarification of the semiempirical relation (ch. 11) regarding the velocity of approach flow.

17. Investigate the "natural" thermal fluctuations in unsteady regimes applying to industrial needs.

18. Investigate the diffusion (concentration) and thermodiffusive convection analogous to the thermal convection investigated in this report.

19. Investigate on models the convection process in the cooling of castings (both its hydrodynamic and thermal aspects).

20. Experimentally render more accurate the value of the Nusselt number and explain how, and on what parameters, it depends.

21. Analytically investigate the nonlinear above-critical case.

22. Experimentally investigate convection in a spherical cavity for a horizontal temperature gradient.

23. Supplement the theory of convection in a horizontal tube with the case of heating from below.

24. Experimentally investigate, in an exhaustive manner, the problem of convection in a circular horizontal channel (from the theory of ch. 15, sec. 6).

25. Investigate the problem of convection in an inclined channel for any orientation of the temperature gradient.

26. Investigate the process of the transition or the coexistence of convection with axial symmetry and diametral antisymmetry, for heat losses at the wall.

27. Investigate convection in a cylindrical cavity in regard to the parametrical nonlinearity (for narrow capillaries, as, e.g., the pores of boiler scale).

28. Investigate the effect of the fluid-column length on the degree of stability of the convective motion in the column (figs. XVII and XVIII).

29. Investigate the problem of the gravitational-thermal effect, and construct the tensor of the effective thermal conductivity of porous materials on the basis of the considerations of chapters 5 (table 1), 15, and 16.

30. Investigate the gravitational-thermal and gravitational-concentration detector effect; that is, the occurrence of vertical gradients of temperature or concentration in zones containing liquids or gases for periodic changes of temperature or concentration.

## CHAPTER 19

## SUPPLEMENTARY TOPICS

1. Electrolytical Method of Measuring Temperatures<sup>17</sup>

Reference 1 shows that the difference of potentials  $E$ , observed between two like metallic electrodes immersed in a solution of a salt of the same metal, is expressed by the formula

$$E = \frac{R}{ZF} (T_1 \ln K_{O1} - T_2 \ln K_{O2}) \quad (19.1)$$

where  $K_{O1}$ , and  $K_{O2}$  denote, respectively, the constant of equilibrium at the absolute temperatures  $T_1$  and  $T_2$ ,  $Z$  the valence of the metal ions, and  $R$  the gas constant. The expression  $R/F$  constitutes 198.4 microvolts per  $1^\circ \text{C}$ .

It may be expected that the expression in parentheses will, in a small temperature interval  $T_1$  to  $T_2$ , be proportional to this interval

$$E = A(T_1 - T_2) \quad (19.2)$$

The value of the factor  $A$  was determined experimentally for copper electrodes and for solutions of copper sulphate in water.

The electromotive force was measured between two pieces of enameled electrotechnical copper wire of 0.41-millimeter diameter by means of a Raps compensator. The bared ends of the wire were wound on the bulbs of two thermometers which were placed in the copper sulphate solution.

A saturated solution was used for the first test. The chemically pure solution of copper sulphate in distilled water was placed in two small beakers which were connected by a siphon capillary. The copper sulphate crystals were in small excess in both beakers. One of the beakers was heated by a heater coil of high-resistance enamel wire that was wound on the glass of the lower part of the beaker. The other beaker

<sup>17</sup>This section was compiled from data obtained by N. A. Pleshkov.

was at room temperature. The bulbs of the thermometers were immersed in the beakers, and served simultaneously as agitators. The electrodes were held short-circuited throughout and were connected in the compensator only for the short intervals of measurement. In the temperature interval of  $10^{\circ}\text{C}$  (eight readings), the coefficient A in equation (19.2) was constant and was equal to 100 microvolts per degree.

In the other test, which included 34 readings in the interval of  $30^{\circ}\text{C}$ , the electrodes were either short-circuited or were disconnected for considerable intervals. With open electrodes the coefficient A was obtained equal to 62 microvolts per degree; for closed electrodes the coefficient maintained its previous value of 100 microvolts per degree. Since the closing and opening of the electrodes was effected in the course of the measurement process, the coefficient A was now defined as

$$A_1 = \frac{\partial E}{\partial T_1}; \quad T_2 = \text{constant} \quad (19.3)$$

The same experiment for open electrodes, repeated for a 20-percent solution of chemically pure copper sulphate gave the value  $A_1 = 65.7$  microvolts per degree in the interval of  $21.5^{\circ}\text{C}$  for 25 readings. The test, which was conducted very slowly, showed that the figures obtained on raising the temperature agreed well with the figures obtained on lowering the temperature. At the same time it was revealed that an appreciable electromotive forces (110 microvolts), arising from the nonidentical chemical composition of the electrodes, also existed for  $T_1 = T_2$ .

In a 15-percent solution of industrial copper sulphate in distilled water, with open electrodes in an interval of  $45^{\circ}\text{C}$  with 13 readings upward and 6 reading downward and with exposure at a higher temperature, it was found that  $A_1 = 61$  microvolts per degree. This test also showed that the values of  $A_1$  agreed well with each other in the upward and downward reading. However, while the temperature was held at the higher value a change of the initial electromotive force occurred, from 120 to 240 microvolts.

The tests conducted with the saturated solution of the industrial strongly contaminated copper sulphate, dissolved in piped water in the interval of  $26^{\circ}\text{C}$  (16 points upward and 18 downward), gave the value  $A_1 = 74$  microvolts per degree and also revealed a displacement of the initial electromotive force when held at the maximum temperature.

The internal resistance of the investigated compounds was rather large (of the order of 30,000 ohms). Hence, to replace the compensated measurements of the electromotive force of such a "thermo-electrolytic element" by measurements of the current was not advisable. In fact, for the usual (small resistance) galvanometers, these will be measurements of the "short-circuit current." The strength of the current is determined

not only by the electromotive force of the element but also by its internal resistance (including here the polarization effects). The test confirmed that the dependence of the galvanometer readings connected directly to the element on the temperature difference is nonlinear: On increasing the temperature of one of the electrodes the resistance of the compound decreases, and the galvanometer readings increase nonproportionally.

To verify the suitability of this device for measurements under conditions of industrial practice, the following test was conducted. A glass tube of 2.5-centimeter diameter and of 45-centimeter length was filled with sand contaminated with earth dust and was treated at room temperature with a saturated solution of industrial copper sulphate in piped water. At both ends the tube was stopped with corks, in which thermometers were inserted. The thermometer bulbs were wound with the bared ends of enameled electrotechnical wire of 0.41-millimeter diameter, forming the electrodes. At one end the tube was wound with the high-resistance enameled wire of an electrical heater. In the interval of the temperature differences up to 18° C (nine readings) the measurements with the open circuit electrodes gave the value  $A_1 = 62$  microvolts per degree, and in the interval 22° to 40° (six readings) the measurements with the closed circuit electrodes gave the value  $A_1 = 80$  microvolts per degree. A considerable change in the initial electromotive force was noted during the assemblage and while the apparatus was held at high temperatures.

These data show that, by taking a number of precautions, the electrolytic method may be suitable for technical measurements of temperature difference. The main defect of this method is the change in the initial electromotive force in prolonged tests. This change is connected with diffusion processes. For water solutions, the diffusion coefficient is 100 times less than the temperature-conductivity coefficient. Hence, the balancing of the concentrations at the electrodes will proceed 100 times more slowly than the balancing of the temperatures, because the diffusion can only pass through the fluid while the heat can also pass through the wall. The consideration of this fact aids in perfecting the measurement procedure.

## 2. Problem of Geothermal Gradient

Geologists frequently insert thermometers in drilled wells in order to measure the temperature of the layers of the earth's core. In doing so they assume that, in the absence of liquids that enter from without, the liquid in the well is at rest and at each depth has the temperature of the surrounding stratigraphical layers. However, the temperature is higher in the depth of the well than at the ground surface, and conditions for convective heat transfer may arise.

Most geologists are sceptical as to the possibility of thermal convection in drilled wells (ref. 2). However, the liquid in the well can be at rest only at small temperature gradients. On attaining a characteristic gradient, the liquid is set in motion and will transfer a very large quantity of heat upward. For a well of 12-inch diameter (30 cm) filled with fresh water, the characteristic gradient will be  $30^4 \approx 10^6$  less than in our first model (of about 1-cm diam.). It is approximately  $A = 10^{-7}$  degree per centimeter, which corresponds to a geothermal gradient of the order of  $10^7$  centimeters per degree =  $10^5$  meters per degree = 100 kilometers per degree.

In order to obtain the mean world geothermal gradient of 30 meters per degree (i.e., the characteristic gradient  $A = 3.3 \times 10^{-4}$  deg/cm), it is necessary to examine a well of about 4.2-centimeter diameter, filled with fresh water.

The geothermal gradient for the characteristic gradient must be determined by the formula

$$\frac{1}{A} = \frac{g\beta}{\nu\kappa} \times \frac{R^4}{(kR)^4} \quad (19.4)$$

Chapter 8 gives the parameter  $g\beta/\nu\kappa$  for fresh water and certain other liquids (eq. (19.4)). The tube radius  $R$  must be expressed in centimeters; the characteristic number  $(kR)^4$  has a value of about 100 (for a more accurate value see fig. 4).

If the heat source below is of sufficient power (i.e., if the thermal conductivity of the hot layers at the bottom of the cavity is sufficiently large), an above-critical regime of heat transfer arises. In this regime the effective thermal fluid conductivity is much higher than the molecular (tabulated) fluid conductivity and may be evaluated approximately by the formula (see ch. 10, secs. 3 and 4)

$$1500 > \frac{\lambda_{\text{eff}}}{\lambda} \equiv \text{Nu}^{**} > 960 \quad (19.5)$$

The value of  $\lambda$  that enters here for the tabulated thermal conductivity of fresh water is, in technical dimensions, approximately equal to 0.5 kilocalorie/(deg)(m)(hr).

Geologists are familiar (ref. 3) with the disturbances of the field of the earth's core that are connected with the dissemination within the true stratification of rocks of bodies of some other (mining) varieties of different form and composition. A drilled well is a body of this kind. The effective thermal conductivity of this body may be determined by the preceding formulas. It is then possible to consider the distortion that

it introduces in the temperature of the surrounding layers, and the errors that these measurements give.

### 3. Problems of Natural Ventilation

Suppose we have a chamber, separated from the surrounding air by a thick horizontal wall, containing a cylindrical channel. The channel length is large compared with the diameter; the edges are rounded. If the temperature below the channel is higher than above, the arrangement will be favorable for convection. We restrict ourselves for the present to a single opening so that the quantity of outside air that enters the chamber is equal to the quantity of air flowing out from the same channel (conditions of diametral antisymmetry).

4281

Favorable conditions of ventilation obtain only for the laminar regime, when the horizontal components of the velocity of the air in the channel are not large. At the above-critical regime the mixing of the air in the channel sharply impairs the conditions for ventilation. The laminar regime arises only for a characteristic gradient and is observed when the channel length  $l$ , the channel radius  $R$ , and the difference in temperature between the external air and that in the chamber  $\theta' - \theta''$  satisfy the condition

$$\frac{g\beta(\theta' - \theta'')R^4}{\nu\kappa l} \approx 200 \quad (19.6)$$

which follows from formula (5.15). This value of 200 corresponds to the small thermal conductivity of the air as compared with that of solid bodies (fig. 4). For example, brick masonry has a conductivity 40 times as large as air. Substituting the parameters of air for a temperature of 20° C, we obtain approximately

$$\frac{\theta' - \theta''}{l} \times R^4 \approx 2 \quad (19.7)$$

For example, for a wall thickness of 1/2 meter and an opening of 2R = 10-centimeter diameter, the conditions of laminar convection arise for a temperature difference

$$\theta' - \theta'' \approx \frac{2 \times 50}{5^4} = 0^\circ, 16 \text{ C} \quad (19.8)$$

The maximum possible quantity of heat transferred by the laminar regime corresponds to the critical point, where it is equal to the above-critical quantity. For the critical point, we thus obtain approximately

$$Q_{kp} = Q_{\lambda} Nu_{kp}^{**} \approx \lambda \kappa R^2 \frac{\theta' - \theta''}{l} Nu^{**} \quad (19.9)$$

For example, for air

$$Q_{kp} \approx 6 \times 10^{-5} \pi \frac{2}{R} \text{Nu}^{**} \approx 4 \times 10^{-4} \frac{\text{Nu}^{**}}{R} \quad (19.10)$$

Setting  $\text{Nu}^{**} \approx 10^3$ , we obtain

$$Q_{kp} \approx \frac{0.4}{R} \text{ cal/sec} \quad (19.11)$$

The narrower the channel, the larger the critical quantity of heat transferred. For example, for a channel opening of  $2R = 10$ -centimeter diameter, the quantity of heat transferred is negligible (about 0.02 cal/sec).

For shorter channels, most of this quantity of heat passes directly with the air. The air passing upward does not have sufficient time to lose much heat in the downward counterflow of air through the secondary molecular thermal conductivity. Therefore, we can approximately set

$$Q_{kp} = \rho c (\theta' - \theta'') V \quad (19.12)$$

whence the volume velocity is determined as

$$V = \frac{Q_{kp}}{\rho c (\theta' - \theta'')} \quad (19.13)$$

For example, for air

$$V = \frac{0.4}{3 \times 10^{-4} R^2 (\theta' - \theta'')} \approx \frac{2 \times 10^3}{R^2 (\theta' - \theta'')} \quad (19.14)$$

If we replace the temperature difference by the characteristic gradient, we have

$$V \approx \frac{2 \times 10^3}{2l} R^2 \approx 3 \times 10^2 \frac{S}{l} \text{ cm}^3/\text{sec} \quad (19.15)$$

Thus, for the conditions of the existence of the characteristic gradient, the volume of air exchanged is proportional to the area of the channel cross section  $S$ , and is inversely proportional to the channel length  $l$  ("Ohm's law").

For the preceding example this gives

$$V \approx 300 \text{ cm}^3/\text{sec} \quad (19.16)$$

If the channel is short or if its edges are sharp, the action of the end effects may disturb the assumed laminar regime and impair the conditions of ventilation.

4281

CA-23 back

If the critical gradient is exceeded, the conditions favorable for ventilation are so sharply impaired that it is more convenient to divide the channel into a number of channels by constructing longitudinal vertical partitions. In this way it is possible to adjust the opening of the channel to the characteristic dimensions for each gradient. At the same time the conditions of ventilation may become more favorable because an independent flow of air is established in each small channel lobe. Ventilation may then be realized without counterflow in a single channel.

#### 4. Problem of Velocity of Evaporation<sup>18</sup>

Assume that in a dense homogeneous mass, filling the lower half-space, a vertical cylindrical well filled with water is drilled (fig. 56). The weak turbulence of the air over this channel maintains a constant absolute humidity of  $C_1$  grams per cubic centimeter at the channel mouth. Strictly isothermal conditions are assured in the entire setup.

Since water vapor and air have molecular weights of 18 and 29, respectively, the drier the air above the well, the lighter the more humid air inside the upper part of the well. For definite conditions in the upper part of the well, the following gravitational diffusion convection may arise: The lighter vapors entering the well from above may rise in the drier air. We shall clarify these conditions and establish the velocity of the process of the drying out of the channel water.

The diagram in figure 56 shows the dependence of the mean humidity over a cross section in the well, on the level of the section:

$$C = C(z) \quad (19.17)$$

Directly above the water level in the well the constant ("100 percent") humidity  $C_0(\theta)$  prevails, determined by the temperature of the experiment. For example, for the temperature  $20^\circ\text{C}$ ,  $C_0 = 1.73 \times 10^{-5}$  grams per cubic centimeter. If the relative humidity above the mouth of the well is 60 percent at  $20^\circ\text{C}$ , then  $C_1 = 1.04 \times 10^{-5}$  gram per cubic centimeter.

For a barometric pressure of 760 millimeters of mercury and some humidity  $C$ , the partial pressures of the vapor  $p$  and of the air  $p_b$  are equal, respectively, by Clapeyron's equation

$$p = \frac{R_0 T}{\mu} C; \quad p_b = \frac{R_0 T}{\mu_b} C_b \quad (19.18)$$

<sup>18</sup>This section was compiled from data obtained by V. B. Shein.

$$p + p_b = 760 = R_0 T \left( \frac{C}{\mu} + \frac{C_b}{\mu_b} \right) \quad (19.19)$$

whence

$$\frac{dC_b}{dC} = - \frac{\mu_b}{\mu} \quad (19.20)$$

where  $R_0$  is the gas constant,  $T$  the absolute temperature, and  $\mu$  and  $\mu_b$  the molecular weight of water and air, respectively. The density of the mixture of air and vapor is equal to

$$\rho = C + C_b \quad (19.21)$$

Therefore, the concentration density coefficient (formula (2.7)) is

$$\begin{aligned} \beta_1 &= \frac{1}{\rho} \times \frac{d\rho}{dC} = \frac{1}{\rho} \times \left( \frac{\partial \rho}{\partial C} + \frac{\partial \rho}{\partial C_b} \times \frac{dC_b}{dC} \right) \\ &= \frac{1}{\rho} \left( 1 - \frac{\mu_b}{\mu} \right) = - \frac{0.61}{\rho} \text{ cm}^3/\text{g} \end{aligned} \quad (19.22)$$

By analogy with equation (5.15) and from figure 4 we find for the dense walls of the well, impenetrable both for air and water, the value of the convection parameter (Z-axis directed downward)

$$\xi^4 = \frac{g\beta_1 R^4}{\kappa D} \times \frac{dC}{dz} = 67.4 \quad (19.23)$$

Therefore, the critical value of the cross-sectional mean of the vertical concentration gradient is

$$\frac{dC}{dz} = 67.4 \times \frac{\nu D}{g(-\beta_1)R^4} = 67.4 \times \frac{18 \times 10^{-5} \times 0.25 \times 1.3 \times 10^{-3}}{1.3 \times 10^{-3} \times 981 \times 0.61 \times R^4} = \frac{5.07 \times 10^{-6}}{R^4} \quad (19.24)$$

where there has been set for air:  $D = 0.25$ -square centimeter per second,  $C_b = 0.0013$  gram per cubic centimeter, and  $\eta = 18 \times 10^{-5}$  gram per centimeter per second.

The critical depth  $z_0$ , from the mouth to the water surface in the well at which the critical gradient of the concentration is just barely attained, will therefore be

$$R^4 = \frac{C_0 - C_1}{z_0} = 5.07 \times 10^{-6} \quad (19.25)$$

$$z_0 = R^4 \frac{C_0 - C_1}{5.07} \times 10^6$$

For our assumption we obtain

$$z_0 = R^4 \frac{(1.73 - 1.04) \times 10^{-5}}{5.07 \times 10^{-6}} = R^4 \frac{0.69}{5.07} \times 10 = 1.36 R^4 \text{ cm} \quad (19.26)$$

The considerations that were adduced here by analogy with thermal convection are suitable for those vertical distances that exceed the well diameter:

$$\begin{aligned} z_0 &\geq 2R \\ 2R &\leq 1.36 R^4 \end{aligned} \quad (19.27)$$

Hence, for the well radius

$$\begin{aligned} R^3 &\geq \frac{2}{1.36} = 1.47 \text{ cm}^3 \\ R &\geq 1.14 \text{ cm} \end{aligned} \quad (19.28)$$

The critical distribution of the concentration is represented in figure 56 by the straight line AB. If in the process of drying only the level  $z_1$ , but not the level  $z_0$ , is attained, then by analogy with figure 35, we are justified in expecting the mean cross-sectional concentration distribution, shown by the curved line AEF. The curved line represents, on the average, the critical gradient joining at the edges with the concentrations  $C_1$  and  $C_0$  by the exponential transitions.

Both transitions are the same because there are no losses of substance through the well walls, in contrast to the heat losses shown in figure 35. Mentally replacing these two transitions by the double transition, we obtain the curve AGF.

The velocity of transfer of the vaporized fluid is practically determined in its convective part by the diffusion resistance of the exponential transitions. This resistance may be evaluated by considering the formula of the end phenomena (12.1) as the resistance of a part of the well of length  $2R$ . The effect of convection on the process of evaporation is restricted only by a certain lowering of the fluid of the active moisture deficit on the surface. This deficit assumes the value represented by the segment

$$HF = \frac{C_0 - C_1}{z_0} (z_0 - z) \quad (19.29)$$

Hence, the velocity of evaporation is equal to

$$\frac{\pi R^2 \rho_0 dz}{dt} = \pi R^2 D (C_0 - C_1) \left( \frac{z_0 - z}{2Rz_0} + \frac{1}{z_0} \right) \quad (19.30)$$

On the left of this expression the total flow of the vapor mass of the vaporizing water appears, having the constant fluid density  $\rho_0$ . On the right the same flow is divided into two diffusion components. The first of these components represents the "overcoming of the diffusive resistance" of the exponential transition (with further transfer of this flow by convection); the second component represents the molecular diffusion flow accompanying the convection and corresponds to the critical concentration gradient

$$\frac{C_0 - C_1}{z_0} \quad (19.31)$$

Dividing the equation (19.31) by the area of cross section of the well  $\pi R^2$  and separating the variables, we obtain, after integration,

$$\left. \begin{aligned} \frac{dz}{z_0 + 2R - z} &= \frac{D(C_0 - C_1)}{\rho_0 2Rz_0} dt \\ \ln \frac{z_0 + 2R - z}{z_0} &= - \frac{D(C_0 - C_1)}{2Rz_0 \rho_0} t \\ \frac{z_0 + 2R - z}{z_0} &= e^{- \frac{D(C_0 - C_1)}{2Rz_0 \rho_0} t} \end{aligned} \right\} \quad (19.32)$$

$$z = 2R + z_0 \left( 1 - e^{- \frac{D(C_0 - C_1)}{2Rz_0 \rho_0} t} \right) \quad (19.33)$$

where as initial conditions there was set

$$z = 2R \quad \text{when} \quad t = 0 \quad (19.34)$$

The initial velocity of drying (for  $t = 0$ )

$$\left(\frac{dz}{dt}\right)_0 = \frac{D(C_0 - C_1)}{2R\rho_0} \quad (19.35)$$

is found to be inversely proportional to the well radius.

The exponential dependence of  $z$  on  $t$  is approximately shown in figure 57. At the instant  $t = t_1$ , when  $z$  reaches the value  $z_0$ , the convection ceases and there remains only molecular diffusion described by the simplified equation

$$\frac{\pi R^2 \rho_0 dz}{dt} = \pi R^2 D \frac{C_0 - C_1}{z} \quad (19.36)$$

Dividing by the area  $\pi R^2$ , separating the variables, and integrating give successively

$$\left. \begin{aligned} z \, dz &= \frac{D(C_0 - C_1)}{\rho_0} \, dt \\ z^2 &= \frac{2D(C_0 - C_1)}{\rho_0} (t + t_2) \end{aligned} \right\} \quad (19.37)$$

The constant of integration  $t_2$  is chosen so that  $z$  is equal to  $z_0$  for that value  $t_1$  which corresponds to this instant, according to the equations

$$\ln \frac{2R}{z_0} = - \frac{D(C_0 - C_1)}{2Rz_0\rho_0} t_1 \quad (19.38)$$

$$z_0^2 = \frac{2D(C_0 - C_1)}{\rho_0} (t_1 + t_2)$$

Eliminating  $t_1$ , we obtain

$$\frac{\rho_0 z_0^2}{2D(C_0 - C_1)} - t_2 = t_1 = \frac{2Rz_0\rho_0}{D(C_0 - C_1)} \ln \frac{z_0}{2R} \quad (19.39)$$

Thus

$$t_2 = \frac{2Rz_0\rho_0}{D(C_0 - C_1)} \left[ \frac{1}{2} \times \frac{z_0}{2R} - \ln \frac{z_0}{2R} \right] \quad (19.40)$$

where the expression in brackets is positive under the assumed conditions.

The transition of the exponential law of drying to the parabolical law proceeds at that level of water in the well which is determined by the coordinate  $z = z_0$ . Substitution shows that the drying curve  $z = z(t)$  does not suffer either a jump or a break here.

Thus the actual process of drying water out of wells represents two interchanging processes (fig. 57); namely, an exponential  $aa$  and a parabolical  $bb$ . In the parabolical process the humidity distribution (now constant in cross section) as a function of the depth of the water level is expressed by the straight line  $AK$  (fig. 56).

It is possible that for the conditions

$$2R < z < z_0 \quad (19.41)$$

in reality, the regime of convection will not be laminar but will be the above-critical turbulent regime. This possibility is particularly large for small values of  $z$  that are very much less than  $z_0$ . Before obtaining experimental data on the above-critical phenomena in gases, it is difficult to say anything positive on this regime. In these computations it is assumed that the magnitude  $s$  in formula (12.1) is equal to 2.

4281

CA-24

## REFERENCES

## Chapter 1

1. Arabadzhi, V. I.: On the Electrical Wind from a Sharp Point. ZhTF (Jour. Tech. Phys.), XX, no. 8, fig. 1, 1950, p. 967. (See also Smoluchowski, Phys. Zs., 6, 1905, p. 529.)
2. Koltashev, N. G., Stroganova, A. M., and Taskina, N. E.: The Effect of a Magnetic Field on the Deposit of Coagulates, pp. 47-59; Mogendovich, M. R., and Tishankin, V. F.: On the Mechanism of the Effect of the Magnetic Field on the Reaction of the Settling of Erythrocytes, pp. 79-86. Collection of articles: The Biological and Therapeutic Action of the Magnetic Field and of Strictly Periodic Vibrations. Molotovgiz, 1948.
3. Ageikin, D. I.: Determination of Heat Transfer Through Thermomagnetic Convection. DAN (reps. of Acad. Sci.), 74, no. 2, 1950, pp. 229-232.
4. Lomonosov, M. V.: Works, AN SSSR, vol. 7, 1934, pp. 1-11; 158-167.
5. Mikheyev, M. A.: Fundamentals of Heat Transfer. Second ed., Gosenergoizdat, 1949.
6. Rayleigh: On Convection Currents in a Horizontal Layer of Fluid, When the Higher Temperature is on the Under Side. Phil. Mag. and Jour. Sci., ser. 6, vol. 32, no. 192, Dec. 1916, pp. 529-547.
7. Shishkin, A. S.: UFN, XXXI, no. 4, 1947, p. 463.
8. Gutman, L. N.: On the Laminar Thermal Convection over a Stationary Source of Heat. Jour. Appl. Math. and Mech., vol. 13, no. 4, 1949, p. 435. (Russian).

## Chapter 2

1. Landau, L., and Lifshits, E.: The Mechanics of Dense Media. Gostekhizdat, 1944, p. 204. (See also A. Oberbeck, Ann. d. Phys. und Chem., Band VII, 1879, pp. 271-292.)
2. Rapoport, S. A.: On the Character of the Heat Exchange in High Viscosity Fluids. ZhTF, XX, no. 9, 1950, pp. 1120-1130.
3. Boussinesq, J.: Théorie analytique de la chaleur, II, sec. 261, 1903, p. 172.

## Chapter 3

1. Smirnov, V. I.: Higher Course in Mathematics. GITI, M.-L. (Moscow-Leningrad), vol. III, 1933, p. 388.
2. Koyalovich, B. I.: On a Partial Differential Equation of the Fourth Order. Spb., 1902.
3. Kuzmin, R. O.: Bessel Functions. ONTI, M.-L., 1935.
4. Shpilrein, Y. N.: Tables of Special Functions. GITI, M.-L., I, 1933.
5. Jahnke, E., and Emde, F.: Tables of Functions. ONTI, NKGP, Khardov-Kiev, 1934; OGIZ, M.-L., 1948.
6. Lyusternik, L. A., Akushski, P. Y., and Ditkin, V. A.: Tables of Bessel Functions. GITI, M.-L., 1949.

## Chapter 4

1. Mikheyev, M. A.: Fundamentals of Heat Transfer. Fig. 123, 1949, p. 229.
2. Kantorovich, L. V., and Krylov, V. I.: Methods of Approximate Solution of Partial Differential Equations. Ch. 1, sec. 2, M.-L., 1936, pp. 26-52.

## Chapter 5

1. Mikheyev, M. A.: Fundamentals of Heat Transfer. Fig. 30, p. 78, or fig. 33, p. 86, M.-L., 1949.
2. Shpilrein, Y. N.: Tables of Special Functions. I, GITI, M.-L., 1933, pp. 101; 151.

## Chapter 6

1. Frank, F., and Mises, R.: Differential and Integral Equations of Mathematical Physics. II, ONTI, M.-L., 1937 (Russian), p. 633 and following.
2. Carslaw, H. S.: Theory of Heat Conduction. OGIZ, M.-L., 1947 (Russian), p. 169 and following.

4281

CA-24 back

3. Lykov, A. V.: Heat Conduction of Nonsteady Processes. G.E.I., M.-L., 1948, p. 119.
4. Ostroumov, G. A.: On the Problem of the Steady Regimes of Free Laminar Heat Convection in Ducts of Round Cross Section. Pt. II - Theoretical. ZhTF, XX, no. 11, 1950, pp. 918-1000.
5. Sokolskaya, L. N.: Convection in Molten Metals. Izv. AN SSSR, sec. of Tech. Sci., no. 9, 1949, p. 1365.

## Chapter 9

1. Ostroumov, G. A.: ZhTF, XXX, no. 8, 1950, pp. 918-1000.
2. Mikheyev, M. A.: Fundamentals of Heat Transfer. M.-L., 1949, p. 27.

## Chapter 12

1. Bénard, H.: Les tourbillions cellulaires dans une nappe liquide. Revue gen. des Sci., XI, no. 23, pp. 1261-1271, 15. XXI 1900; pp. 1309-1328, 30. XII 1900. Les tourbillions cellulaires dans une nappe liquide transportante de la chaleur par convection en régime permanente. Ann. de Chem. et de Phys., 7-me série, t. XXIII, 1901, pp. 62-144.

## Chapter 13

1. Afanasyev, P. V.: New Method of Measuring Free Diffusion in Solutions. DAN LVIII, No. 7, 1947, p. 1383. (See also G. A. Ostroumov, Izvestia ENI pri Molotovskom Gosuniversitete, vol. 12, no. 4, 1947, pp. 113-126.)
2. Mikheyev, M. A.: Fundamentals of Heat Transfer. GEI, M.-L., 1949.
3. Kolesnikov, A. G.: Isv, AN SSSR, seria geograf. i geofiz., no. 5, 1940, p. 639.

## Chapter 15

1. Frank, F., and Mises, R.: Differential and Integral Equations of Mathematical Physics. ONTI, M.-L., II, formula 32, 1937, p. 283.

## Chapter 16

1. Kudryavtsev, E. V.: Model for Natural Convection at Large Defining Dimensions. Izv. AN SSSR, Div. Tech. Sci., no. 1, 1949, pp. 53-66.

## Chapter 19

1. Brodski, A. I.: Phys. Chem., vol. II, sec. 447 (417), GKhI, 1948, p. 700.
2. Kraskovski, S. A.: Work of Commission on Geothermics, no. 1, Geothermal Measurements in USSR (1928-1938), Izd. AN SSSR, 1941.
3. Korytnikova, N. N.: On the Relation Between Plutonic Temperatures and the Thermal Coefficients of Intrusive Rock and the Form of Plutonic Structures. Izv. AN SSSR, seria geofiz., no. 3, 1943, pp. 115-143.

Translated by S. Reiss  
National Advisory Committee  
for Aeronautics

TABLE I

4281

$\xi$	$\xi^4$	I( $\xi$ )		G( $\xi$ )		H( $\xi$ )		F <sub>2</sub> ( $\xi$ )
		$\frac{\lambda}{\lambda_e} = 0$	$\frac{\lambda}{\lambda_e} = 0.1$	$\frac{\lambda}{\lambda_e} = 0.3$	$\frac{\lambda}{\lambda_e} = \frac{\lambda_e}{\lambda} = 1$	$\frac{\lambda_e}{\lambda} = 0.3$	$\frac{\lambda_e}{\lambda} = 0.1$	$\frac{\lambda_e}{\lambda} = 0$
0	0	6.9282	7.6210	9.0067	13.890	9.0067	7.6210	6.9282
2.0	16.0	6.56	7.10	8.17	11.94	7.35	6.04	5.38
2.2	23.43	6.28	6.74	7.65	10.86	6.47	5.21	4.58
2.4	33.48	5.94	6.30	7.03	9.50	5.34	4.15	3.56
2.6	45.70	5.67	5.90	6.37	7.99	4.02	2.89	2.32
2.8	61.47	5.16	5.23	5.36	5.83	2.22	1.19	.67
3.0	81.0	4.49	4.36	4.10	3.08	.04	-.86	-1.31
3.2	104.8	3.70	3.32	2.57	-.8	-.67	-3.41	-3.78
3.4	133.7	2.76	2.09	.76	-3.92	-5.85	-6.40	-6.68
3.6	167.9	1.62	.60	-1.42	-8.53	-9.66	-9.99	-10.15
3.8	208.6	.23	-1.17	-3.98	-13.80	-13.96	-14.01	-14.03
4.0	256.0	1.37	-3.20	-6.86	-19.66	-18.70	-18.43	-18.29
4.2	311.2	-3.22	-5.50	-10.07	-26.04	-23.79	-23.14	-22.82
4.4	347.8	-5.25	-8.01	-13.53	-32.85	-29.18	-28.12	-27.60
4.6	447.8	-7.23	-10.30	-16.45	-37.98	-32.92	-31.47	-30.75
4.8	530.9	-9.16	-12.48	-19.10	-42.31	-35.90	-34.07	-33.15
5.0	625.0	-10.61	-13.97	-20.69	-44.2	-36.8	-34.7	-33.6
5.2	731.2	-11.71	-14.91	-21.3	-43.7	-35.5	-33.2	-32.0
5.4	850.3	-12.17	-14.99	-20.6	-40.4	-31.8	-29.4	-28.2
5.6	983.5	-12.10	-14.36	-18.9	-34.7	-26.2	-23.8	-22.6
5.8	1132.0	-11.47	-13.00	-16.1	-26.8	-18.7	-16.4	-15.3
6.0	1296.0	-10.46	-11.15	-12.5	-17.4	-10.0	-7.96	-6.91

1921

TABLE II

$\xi = kR$	$\frac{\lambda_e}{\lambda}$	$\xi^4$
2.865	0	67.4
2.9	.07	70.7
3.0	.31	81.0
3.1	.62	92.4
3.2	1.02	104.9
3.3	1.59	118.6
3.4	2.43	133.6
3.5	3.78	150.0
3.6	6.27	168.0
3.7	12.5	187.4
3.8	58.4	208.5
3.8317	$\infty$	215.8

TABLE III

Number of points (fig. 8)	kR	-(kR) <sup>4</sup>	v <sub>m</sub>	Regime of			
				Convection		Temperatures	
				Free	Forced		
1	4.611	452.1	0	None	None	Warmer upward	
2	5.00	625.0	5	} Present			
3	4.00	256.0	5		} Upward	} Warmer upward and at walls	
4	3.00	81.0	5				
5	0	0	5	} None			} Constant along length and over pipe cross section
6	3.00	81.0	5				
7	4.00	-256.0	2		} Present	} Colder upward and at walls	
8	4.611	-452.1	0				
9	5.00	-625.0	-1				

TABLE IV

[ $|kR| = 4.611$ ;  $(kR)^4 = -452.1$ ;  $a = 0.179$ ;  
 $v_0$  - Arbitrary scale.]

$\frac{r}{R}$	$\frac{v}{a}$	$\frac{gBR^2\theta}{v_a}$	$\frac{r}{R}$	$\frac{v}{a}$	$\frac{gBR^2\theta}{v_a}$
0	19.79	408	0.520	0.943	-18
.043	19.51	404	.564	-.84	-62
.087	18.98	392	.607	-2.38	-103
.130	18.03	380	.651	-3.63	-138
.173	16.82	344	.694	-4.56	-169
.217	15.27	310	.737	-5.11	-194
.260	13.46	277	.781	-5.27	-212
.304	11.48	225	.824	-5.05	-227
.347	9.39	178	.867	-4.42	-236
.384	7.70	129	.910	-3.40	-240
.434	5.02	78	.954	-1.97	-242
.477	2.92	29	.9976	-1.17	-242
			1.00	0	-242

4281

TABLE V

$\frac{r}{R}$	$\frac{v}{v_m}$	$\frac{gBR^2\theta}{vv_m}$	$\frac{v}{v_m}$	$\frac{gBR^2\theta}{vv_m}$
		$(kR)^4 = -625$	$(kR)^4 = +625$	
0	-14.8	-336	0.0124	-166
.2	-11.4	-280	.177	-162
.4	-3.52	-78	.66	-122
.6	3.36	108	1.28	42
.8	4.80	174	1.48	435
1.0	0	132	0	1040
		$(kR)^4 = -256$	$(kR)^4 = +256$	
0	7.50	112	0.68	-12.1
.25	5.75	84.0	.86	-9.1
.50	2.20	21.8	1.25	14.2
.75	-.64	-50.0	1.32	23.7
.95	-.485	-85.0	-----	-----
1.00	0	-92.0	0	55.8
		$(kR)^4 = -81$	$(kR)^4 = +81$	
0	2.89	23.2	1.42	-1.45
.33	2.28	17.2	1.45	-1.71
.67	.945	2.5	1.37	11.35
.933	.100	-10.0	-----	-----
1.00	0	-12.8	0	25.1

TABLE VI

Substance	$\theta$ , °C	$-\beta \frac{1}{\rho}$	$\nu$ , cm <sup>2</sup> /sec	$\lambda$ , cal ° sec/cm	$Pr = \frac{\nu}{\kappa}$	$\rho c$ , cal ° cm <sup>3</sup>	$\frac{g\beta}{\nu\kappa}$ , 1/° cm <sup>3</sup>
Water	0	$-5 \times 10^{-5}$	$18 \times 10^{-3}$	0.00132	13.3	1.005	-2,050
	10	6.5	13	.00136	9.49	1.000	3,600
	20	18	10	.00140	7.06	.997	12,500
	30	30	8.05	.00144	5.51	.994	25,200
	40	38	6.59	.00148	4.37	.990	37,500
	50	45	5.56	.00152	3.59	.987	51,100
	60	51	4.79	.00156	3.00	.982	65,800
	70	57	4.15	.00160	2.54	.979	82,300
	80	62	3.66	.00164	2.20	.974	100,000
	90	68	3.26	.00168	1.92	.970	121,000
	100	74	2.95	.00172	1.72	.965	144,000
Mercury	20	$18 \times 10^{-5}$	$1.15 \times 10^{-3}$	0.020	0.026	0.45	3,400
Ethyl alcohol	18	$110 \times 10^{-5}$	$15 \times 10^{-3}$	0.00043	16	0.46	770,000
Glycerin	18	$50 \times 10^{-5}$	8.5	0.0007	8,900	0.73	60
Air	20	$\frac{1}{293}$	$157 \times 10^{-3}$	0.0000603	0.722	0.000282	100

TABLE VII. - STANDARD CONVECTIVE

CURVE FOR WATER

Temperature, $\theta$ , °C	Vertical distance, $\left(\frac{g}{R}\right)^4 z$ cm <sup>-3</sup>
0	0
4	-4,150
10	6,150
20	83,100
30	270,000
40	591,000

4281

CA-25

TABLE VIII

## Part I

	Temperature, $\theta$ , °C	Power, $Q$ , cal./sec	Gradient, $A$ , deg/cm	$(kR)^4$	Nu*	Remarks
1	21.9	0.012	0.103	90	116	Model I, preliminary diam., 0.98
2	28.6	.08	.97	108	260	Upper set
3	31.1	.08	.83	105	295	Center
4	33.5	.08	.77	107	333	Lower
5	27.5	.12	.95	99	432	Upper
6	30.5	.12	.85	104	455	Center
7	32.5	.12	.82	110	480	Lower
8	31.5	.27	.82	105	1030	Upper
9	33.8	.27	.66	94	1300	Center
Mean $104 \pm 2$						
10	26.4	.061	.087	103	495	Model I, ser. III
11	22.0	.122	-----	---	1420	Model IV, diam., 3.8

4281

## Part II

	Temperature, $\theta$ , °C	Power, $Q$ , cal./sec	Gradient, $A$ , deg/cm	$(kR)^4$	Nu*	Remarks
12	36.0	0.27	0.80	121	1100	Lower set
13	42.5	.49	1.11	214	1440	Upper
14	45.4	.49	1.02	217	1500	Center
15	49.1	.49	1.30	308	1220	Lower
16	48.1	.746	1.90	377	1300	Upper
17	48.7	.746	1.80	423	1300	Center
18	54.8	.746	2.26	620	1040	Lower
19	21.1	0.38	0.15	181	2410	} Model I, ser. II, diam., 0.98
20	30.5	.65	.39	560	1550	
21	39.8	1.05	1.02	2170	930	
22	34.5	3.80	1.31	2260	2660	
23	42.9	1.73	1.19	2640	1300	
24	37.7	3.80	1.62	3160	2130	
25	47.0	1.53	1.21	3200	1120	
26	56.5	2.07	1.58	5400	1130	
27	50.1	2.50	1.83	5500	1200	
28	47.5	3.80	2.32	6300	1450	
29	64.4	2.70	1.74	8700	1310	
30	29.2	0.170	0.097	133	1620	} Model I, ser. III, diam., 0.98
31	29.8	.245	.152	217	1490	
32	29.9	.435	.229	327	1760	
33	29.7	.331	.231	328	1320	
34	32.9	.550	.345	568	1470	
35	36.1	.680	.509	956	1220	
36	96.3	4.94	2.50	19,500	1540	
Mean Nu*						
1460 $\pm$ 80						

TABLE IX

i	$P_i$	$q_i$	$r_i$	$s_i$
1	1,065	$-\frac{472,915}{88}$	$\frac{1,103,985}{88}$	-1,065
2	570	$-\frac{1,068,531}{88}$	$\frac{1,412,039}{88}$	-3,990
3	3,990	$-\frac{310,279}{88}$	$\frac{517,651}{88}$	-570
4	1,635	$-\frac{897,487}{44}$	$\frac{1,384,776}{44}$	-7,035
5	7,035	$-\frac{162,731}{44}$	$\frac{5,727,136}{44}$	-1,635
6	4,560	$-\frac{621,337}{44}$	$\frac{896,777}{44}$	-4,560
7	-3,874	$\frac{10,206,561}{264}$	$-\frac{13,737,022}{264}$	3,874
8	-3,379	$\frac{15,592,945}{264}$	$-\frac{18,260,720}{264}$	15,755
9	-15,755	$\frac{5,382,745}{264}$	$-\frac{7,642,112}{264}$	3,379
10	2,809	$q_{10}$	$r_{10}$	-2,809

TABLE X. - LOCATION OF THERMOCOUPLES

Number of thermocouples	1	2	3	4	5	6	7	8	9
Latitude, deg	90	45	45	45	45	0	0	0	0
Longitude, deg	--	0	90	180	270	0	45	90	135
Number of thermocouples	10	11	12	13	14	15	16	17	18
Latitude, deg	0	0	0	0	-45	-45	-45	-45	-90
Longitude, deg	180	225	270	315	0	90	180	270	---

4281

CA-25 back

TABLE XI. - INVESTIGATION OF CONVECTION IN SPHERICAL CAVITY

Number of thermocouples	Latitude	Power rates								
		0.196	0.37	0.595	1.09	1.92	3.00	4.14	6.5	3.00 angle 20°
A	Cooler +90°	9.5	3	3.5	3.5	6.25	9.5	8.5	8.25	6.85
1		15.75	14.25	14.25	14.75	17.1	21	18.75	25.75	18.35
2	+45°	17.5	16.5	16.5	17.5	19.5	23	20	27	20.85
3		17	15.75	15.75	16.88	19.25	22.5	19.5	26.88	21.3
4		17.25	16	16	17	19.38	23.05	20.5	26.25	21.3
5		17.75	16.63	16.6	17.5	19.6	22.65	20.75	26	20.85
6	Equator	18.5	17.5	17.5	18.75	21.37	25	22.75	30.5	22.35
7		18	17	17.17	18.38	21.5	25.45	23	31	23.85
8		17.9	16.9	16.87	18	20.5	24.5	21.75	30.75	23.97
9		18	16.83	16.75	18	20.5	24.25	21.65	29.1	23.72
10		18.3	17	16.87	18.13	21	24.75	22.88	29.75	23.6
11		18.75	17.38	17.25	18.7	21.25	25.1	23.5	29.75	22.85
12		18.88	17.5	17.75	18.9	21.25	24.25	23.5	29.25	22.47
13		18.75	17.6	17.75	18.9	21	24.5	23.12	29.5	22.6
14	-45°	19	18	18.25	19.75	23.25	27.5	26.5	34.75	26.1
15		18.5	17.82	18	19.62	23.25	27.5	27	35.6	27.72
16		18.8	17.85	18.25	19.75	23.75	28	27.75	36.26	27.47
17		19.25	18.25	18.5	19.9	23.62	27.9	28	36	26.35
18	-90° Heater	19.25	18.63	19.25	21.0	26.12	32	32.5	44.25	31.1
B		23.25	25.25	27.75	34.75	56.25	64.5	78	124.75	69.35

4281

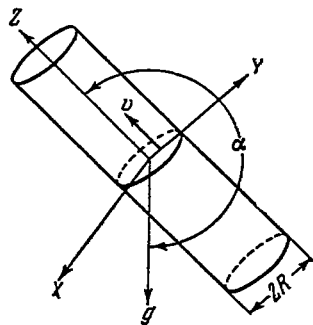


Figure 1. - Orientation of axes of coordinates.

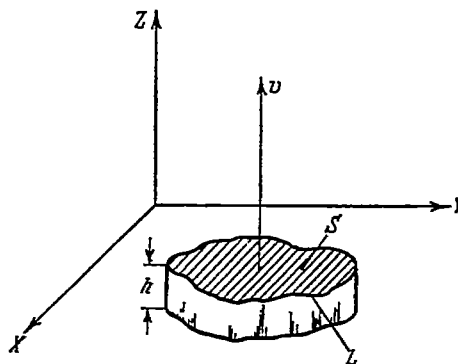


Figure 2. - Computation of volumetric velocity of convection.

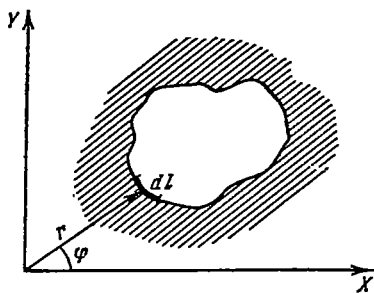


Figure 3. - Scheme of solution of problem of gravitational thermal convection.

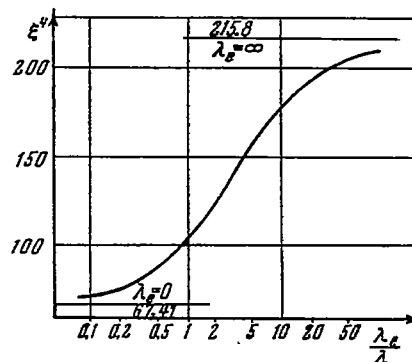


Figure 4. - Dependence of convection criterion on relative thermal conductivity of surrounding mass.

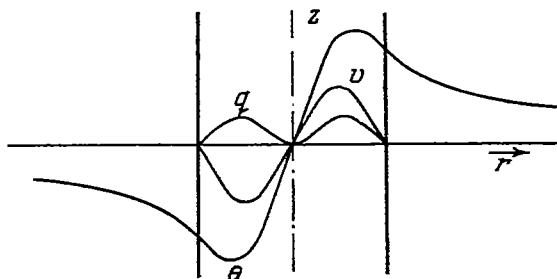


Figure 5. - Distribution of convection velocities  $v$ , temperatures  $\theta$ , and heat flows over diameter of vertical channel of round cross section. Heat conductivity of surrounding mass is equal to that of the fluid.

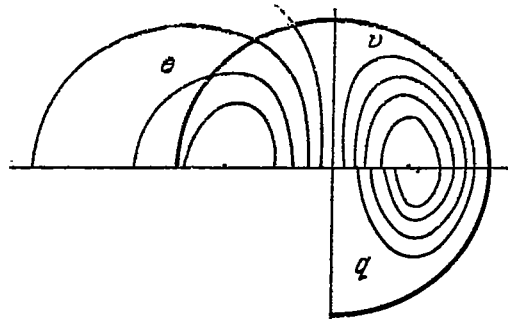


Figure 6. - Isolines of equal velocities, temperatures, and heat flows over section of vertical channel. Heat conductivity of surrounding mass is equal to that of the fluid.

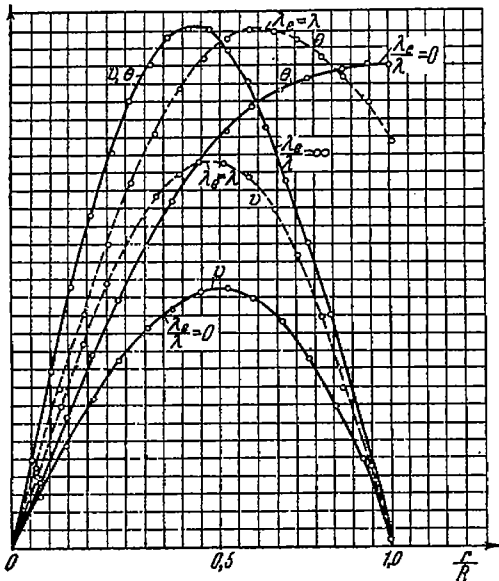


Figure 7. - Distribution of velocities and temperatures over radius of vertical channel of round cross section. Heat conductivity of surrounding mass is small, equal, or infinitely large in comparison with heat conductivity of fluid.

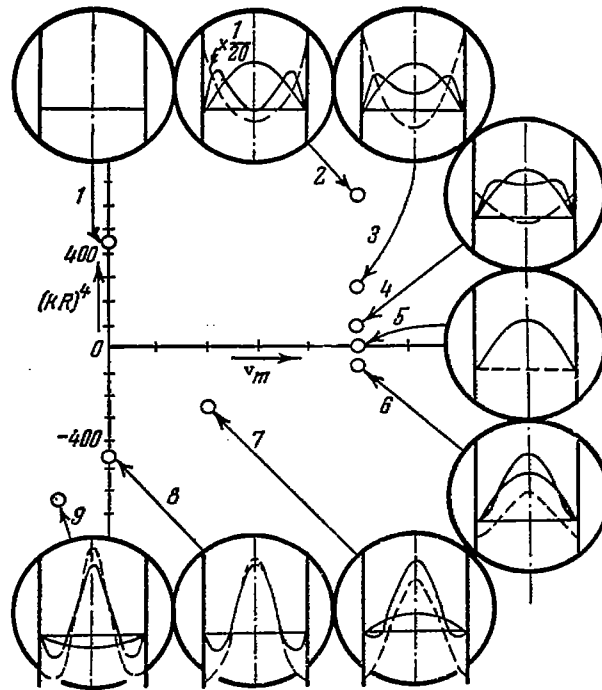


Figure 8. - Superposition of forced and free thermal convection in vertical channel of round cross section. Distribution of velocities and temperatures over channel diameter for different combinations of magnitude of vertical temperature gradient and magnitude of volumetric velocity of forced motion of fluid. Axial symmetry.

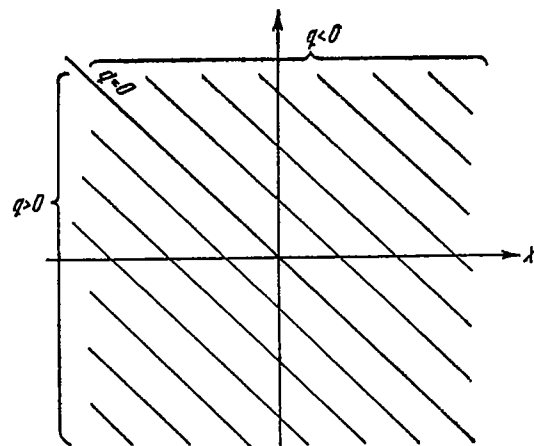


Figure 9. - Isolines of equal damping exponents in the plane of auxiliary coordinates - equidistant straight lines.

4281

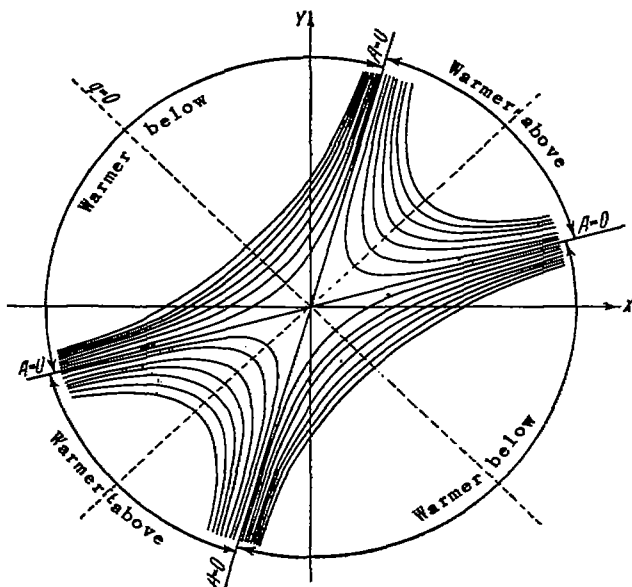


Figure 10. - Isolines of equal vertical temperature gradients in the plane of auxiliary coordinates; two families of hyperbolas, referred to their asymptotes.

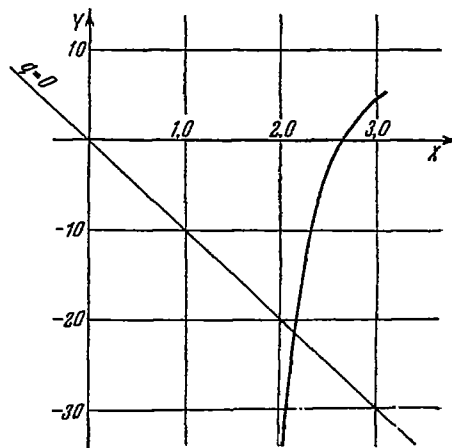


Figure 11. - Isolines of closedness of a channel in the plane of auxiliary coordinates; transcendental curve.

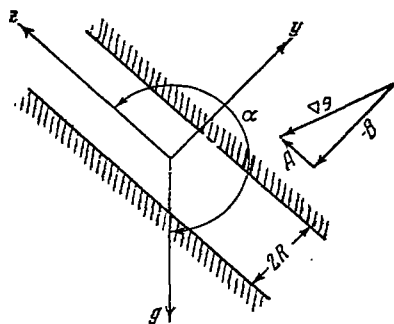


Figure 12. - Position of axes of coordinates and components of the temperature gradient for an inclined slit. Total width of slit,  $2R$ .

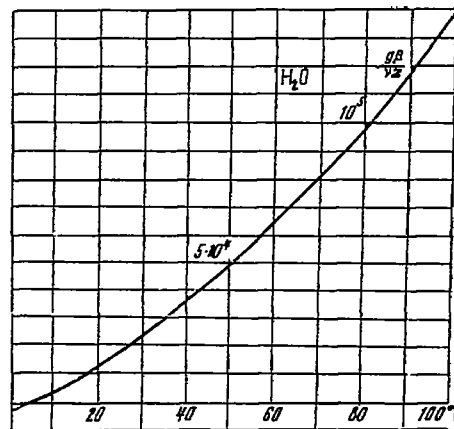


Figure 13. - Temperature dependence of the convection parameter of water.

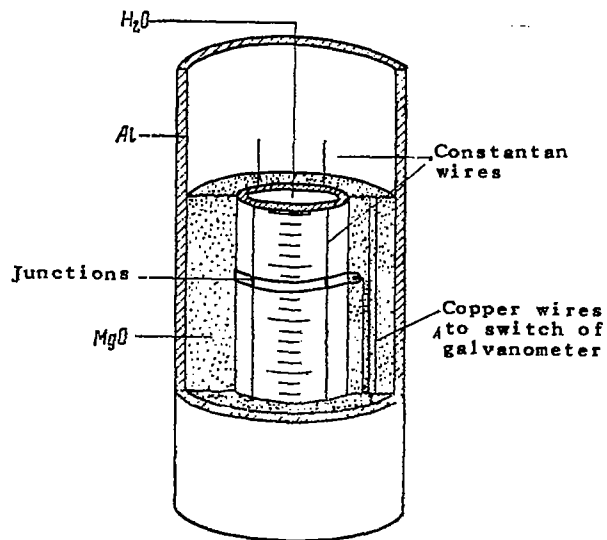


Figure 14. - Section of glass model for investigation of thermal convection. Cross section of the burette, the charge of magnesia, the aluminum jacket, the arrangement of the thermocouple junctions and the lead wires.

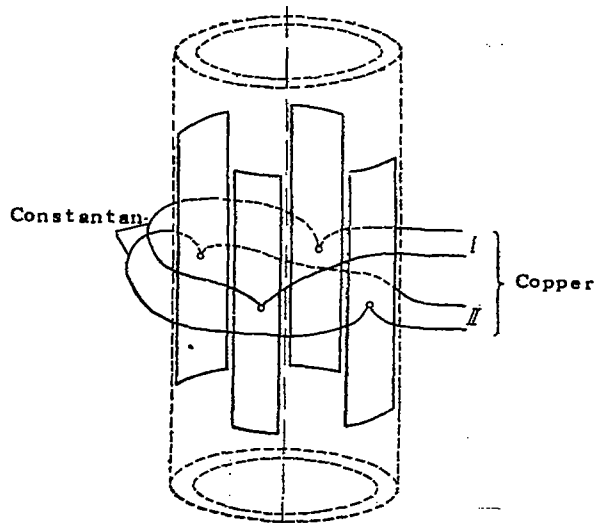


Figure 15. - Arrangement scheme of two pairs of "transverse" thermocouples for determination of azimuth of diametral antisymmetry.

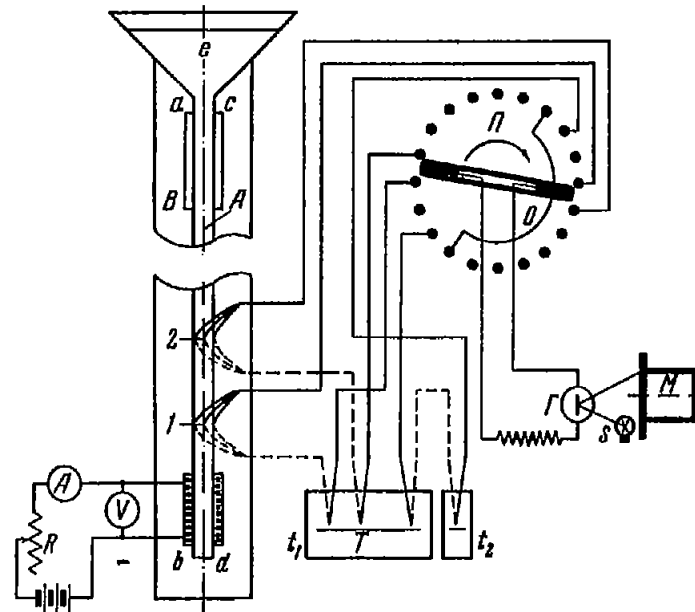


Figure 16. - Structural and electrical scheme of metal model for investigation of thermal convection: abcd, Dimensions of the brass tube of the model A; e, funnel; B, charge; 1 and 2, two stages of averaging thermocouples;  $t_1$ , working thermometer in Dewar flask;  $t_2$ , control thermometer in other Dewar; II, automatic switch of galvanometer G; O, neutral lead; S, light source; M, photorecording apparatus.

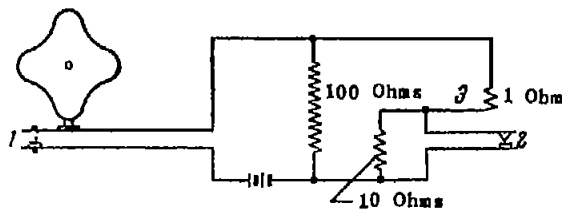


Figure 17. - Scheme of connecting in automatic switch for low-voltage current source: 3, Electromagnet of automatic switch; 1, working contact, connected in from cam disk of small synchronous motor; 2, block contact opened by armature of electromagnet at the moment of operation.

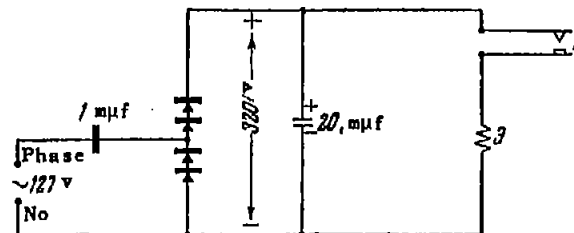


Figure 18. - Scheme of connecting in automatic switch for high-voltage current source (hard rectifier): F, Electromagnet of switch; 1, working contact, connected in from cam disk.

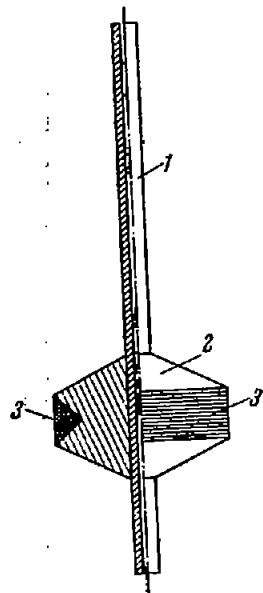


Figure 19. - Construction of movable heater coil for thermal investigation of prepared model: 1, Glass tube; 2, copper pulley; 3, high resistance coil of heater.

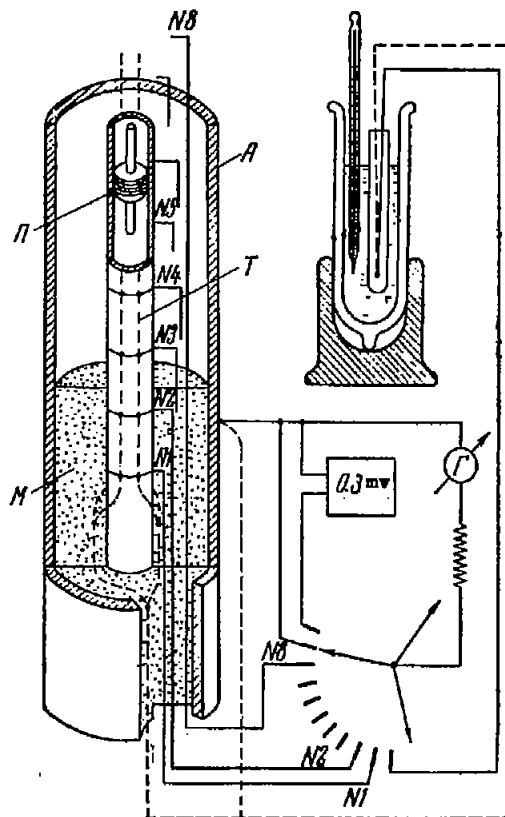


Figure 20. - Constructional scheme of model and electrical scheme of thermal investigation of model: A, Jacket of model; M, charge of magnesia; II, movable heater coil; numbers 1 and 8, stages of averaging thermometers connected to bars of automatic switch. Graduated voltage corresponding to  $7.15^{\circ}\text{C}$ , 0.3 millivolts;  $\Gamma$ , self recording galvanometer.

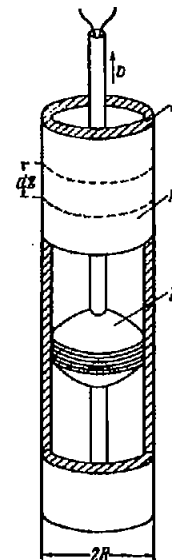


Figure 21. - Derivation of heat balance in connection with thermal investigation of prepared models: 1, Tube of model; 2, movable heater coil moving with velocity  $v$ ;  $S$ , cross-sectional area of model tube;  $dx$ , element of model length.

4281

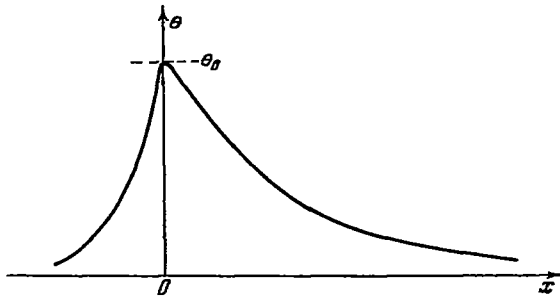


Figure 22. - Variation of temperature in a given section of model in thermal investigation as a function of time (or coordinate).

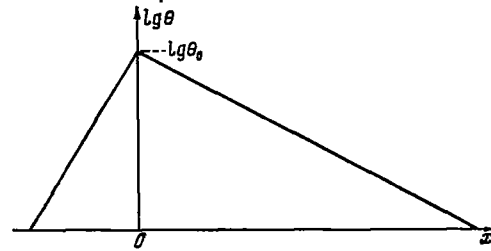


Figure 23. - Variation of logarithm of temperature in a given section as a function of time (or coordinate).

CA-26 back

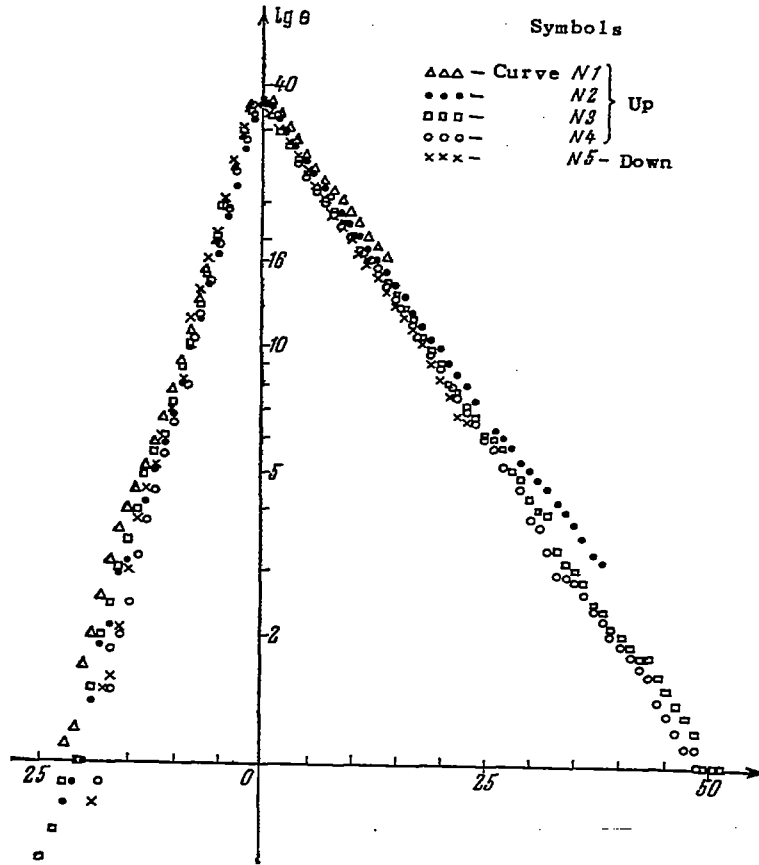


Figure 24. - Result of evaluating center photograph of figure I. For motion of heater upward and motion of heater downward, the points satisfactorily reproduce the form of figure 23. Temperature scale: 38 divisions correspond to 4.5°C. Numbers of time marks on axis are laid off of abscissas. Zero is taken as instant of maximum temperature.



4281

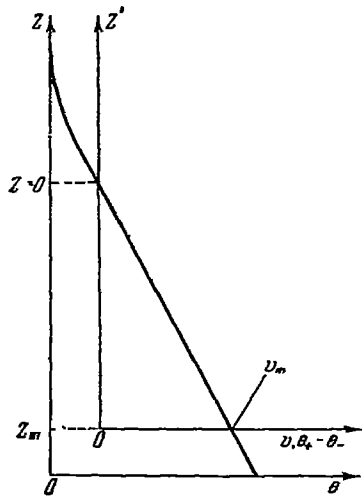


Figure 28. - Assumed distribution of velocities  $v$ , temperatures  $\theta$ , and transverse temperature differences  $\theta_+ - \theta_-$  for model heated from below for case of presence of heat losses through walls in laminar regime of thermal convection. Convection ceases at height  $z = 0$ . Above this section heat transfer occurs only through molecular conduction according to exponential law. Temperature of surrounding medium is taken as zero temperature. In section  $z_m$  velocity has value  $v_m$ .

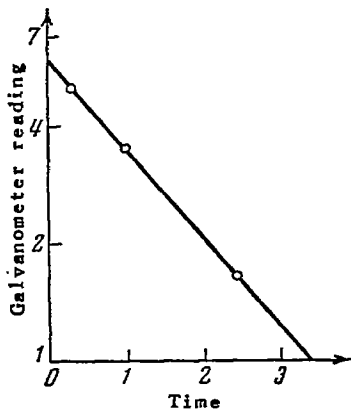


Figure 30. - Linear dependence of logarithm of transverse steady temperature difference on time for attaining convective process.

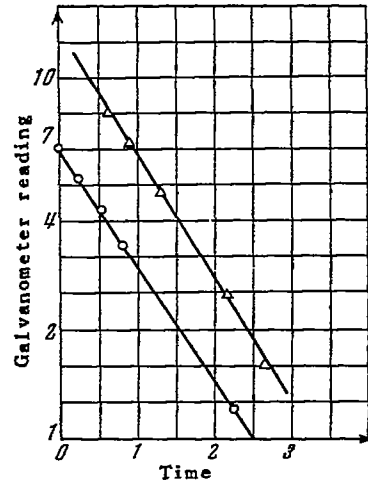


Figure 29. - Linear dependence of logarithm of steady temperature on time convective process takes to reach corresponding thermocouple.

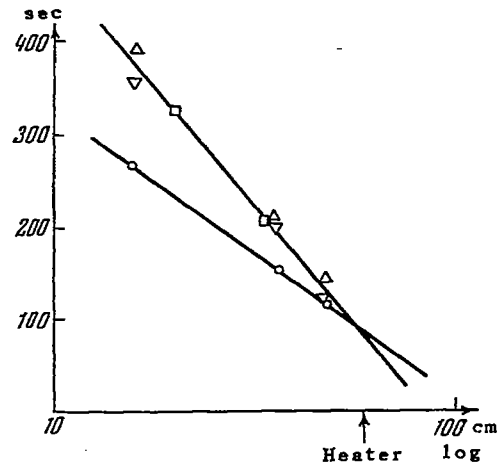


Figure 31. - Result of harmonic analysis of photographs of figure XI. The linear dependence of (mean) phase angle of a heat wave on logarithm of coordinate of transverse thermocouple.

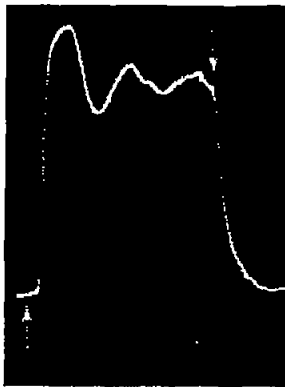


Figure 32. "Natural" thermal vibrations in a model inclined at an angle of  $45^\circ$  to vertical, described by center transverse thermometer. Arrows indicate instants of connecting and disconnecting of heater coil. Power, 3.0 calories per second.

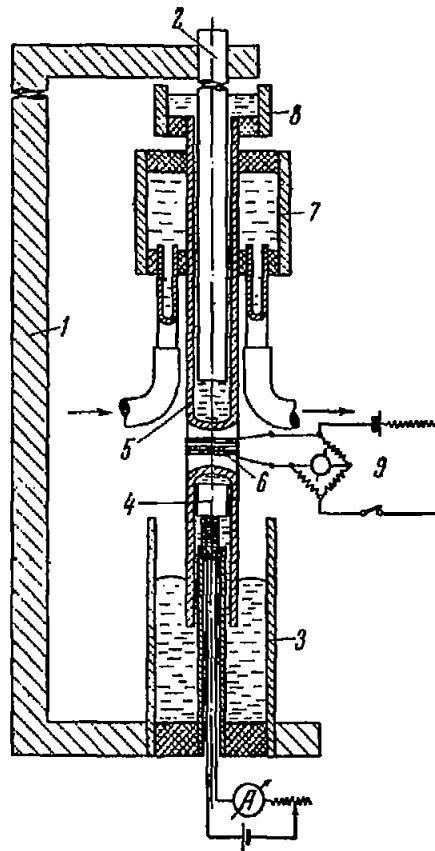


Figure 33. - Apparatus for investigation of mean peripheral temperature over entire length of vertical model: 1, Stand; 2, piston; 3, reservoir with mercury; 4, hot bottom of liquid column; 5, movable tube of model; 6, temperature measuring resistance coil; 7, water cooling; 8, supply reservoir; 9, bridge circuit for measuring temperatures.

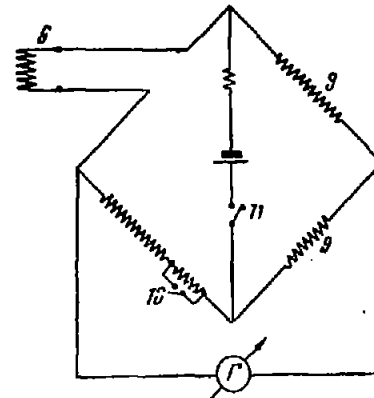


Figure 34. - Bridge circuit for measuring temperatures: 6, Measuring resistance coil; 9, branches of bridge; 10, knife switch for indicating temperature scale on photographs; 11, automatic device for indicating zero line and time marks on photographs.

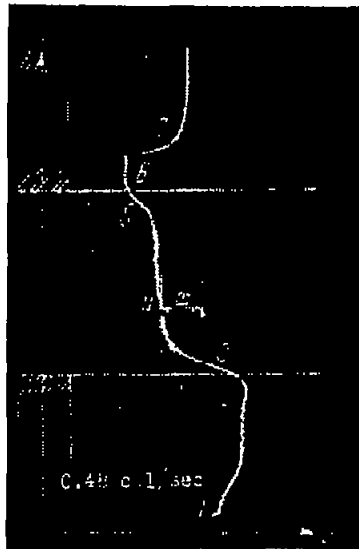


Figure 35. - Distribution of mean peripheral temperature over height of vertical model. Left - sketch of displacement along vertical of hot bottom and cold top of water column. Right - automatic photorecord of temperature;  $x$  - scale deflection  $4^{\circ}\text{C}$ ; 1 - end of non-steady regime after connecting in heater; 2 - temperature of hot bottom; 3 - exponential law of distribution of mean peripheral temperature in fluid near hot bottom; 4 - characteristic temperature gradient in center part of column; 5 - exponential law of temperature distribution near cold top; 6 - temperature of cold top; 7 - exponential law of change with time of temperature of top after simultaneous connecting of heater and water cooler. Zero line is marked by hourly time marks.

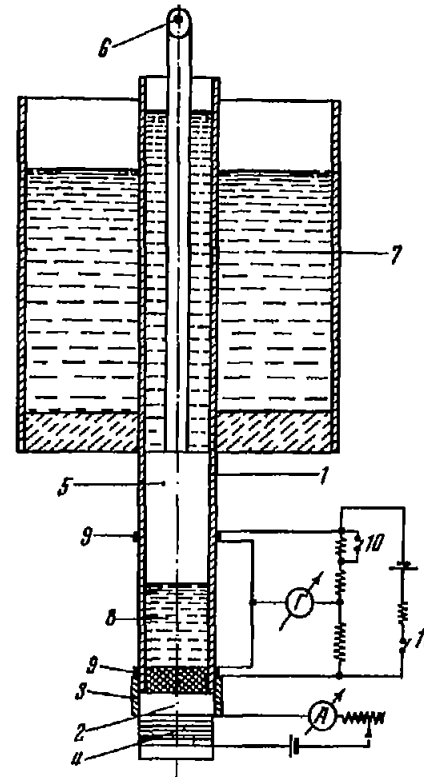


Figure 36. - Sketch of apparatus for investigation of temperature distribution by method of variable-length column: 1 - Vertical model tube; 2 - hot bottom; 3 - rubber packing; 4 - heater coil; 5 - movable piston - cold top of fluid column; 6 - lug for pile driver cable; 7 - cold reservoir; 8 - fluid column where convective motion takes place; 9 - two temperature measuring resistances forming two arms of measuring bridge; 10 - knife switch of scale deflection; 11 - automatic device for marking time and zero line.

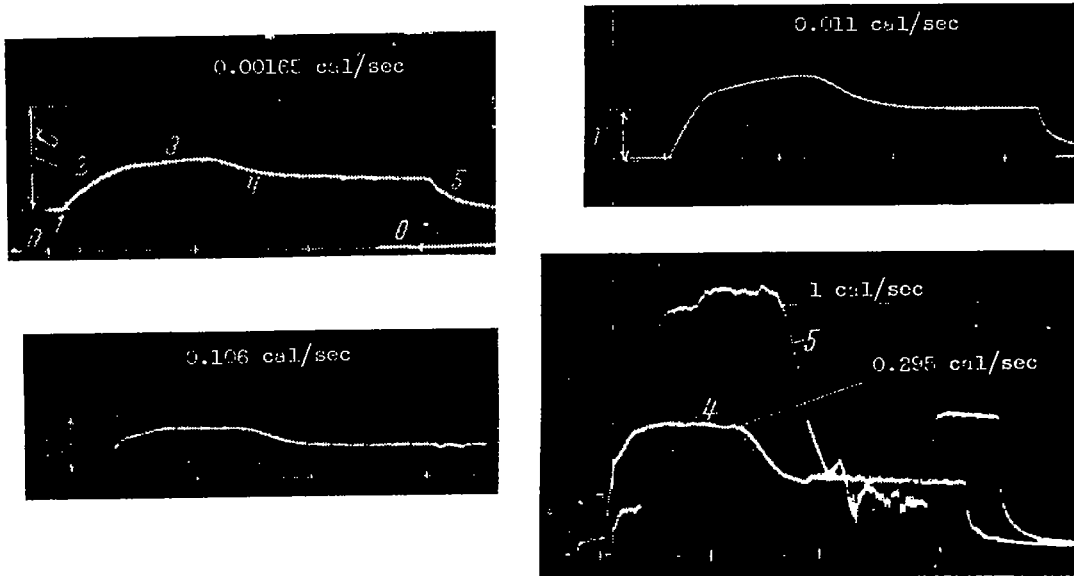


Figure 37. - Records of temperature differences by method of variable-length column.

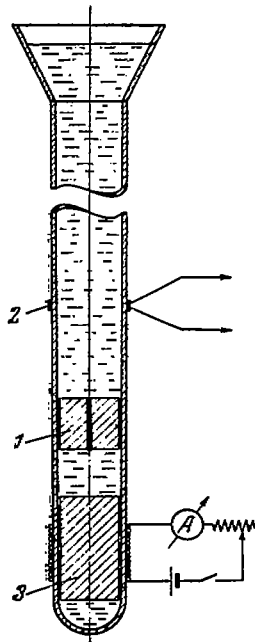


Figure 38. - Method of movable plunger: Movable plunger on filament; 2, resistance thermometer coil; 3, hot bottom of model.

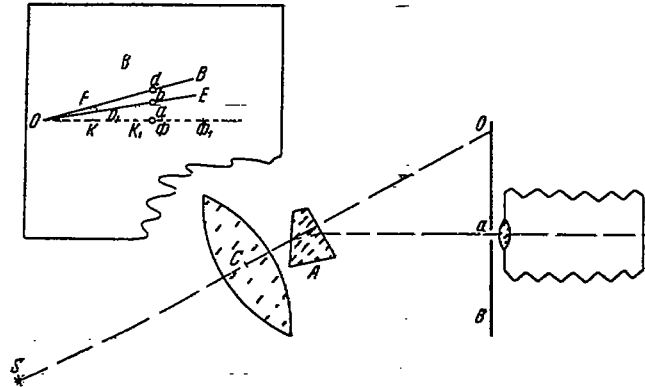


Figure 39. - Optical method of prismatic vessel: S, Point source of light; C, large objective; A, prismatic vessel in which thermal phenomenon is produced; B, diaphragm with aperture a; O, trace of undeflected image of light source;  $K\phi$ ,  $K_1$ ,  $\phi_1$ , DE, and FB, arrangement of bands of spectrum on diaphragm B for various processes in prismatic vessel; a, b, and d, various locations of aperture a with respect to spectrum bands.





Figure 44. - Convection in cylindrical horizontal channel observed by lattice method. Vertical straight line is plumb line. Two isoline systems: Crosswise systems of mutually embracing curves and oval systems in center are isolines of equal horizontal gradient; other lines are isolines of equal vertical gradient.

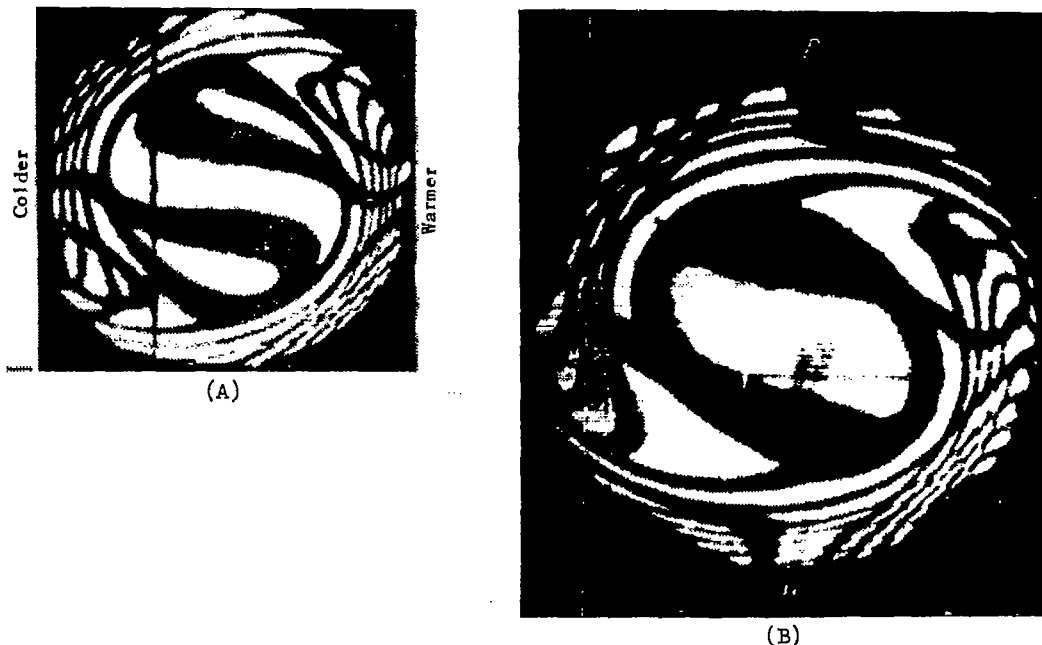


Figure 45. - Convection in cylindrical horizontal channel observed by lattice method: A, Heating from right, cooling from left; vertical line is plumb line. B, heating from right down, cooling from left up. Two pairs of mutually embracing isolines along with isolines of equal vertical gradients. Isolines forming closed ovals in center belong with isolines of equal horizontal gradients.

4281

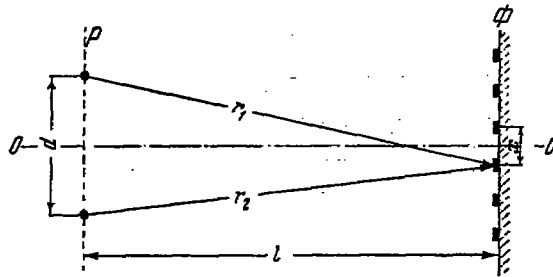


Figure 46. - Computation of diffraction phenomena:  
 OO, Optical axis of photographic apparatus; P, rods in plane of lattice;  $\phi$ , photographic plate;  $l$ , approximate focal distance;  $d$ , distance between rods of lattice;  $x$ , distance between bands on photograph.

CA-27 back

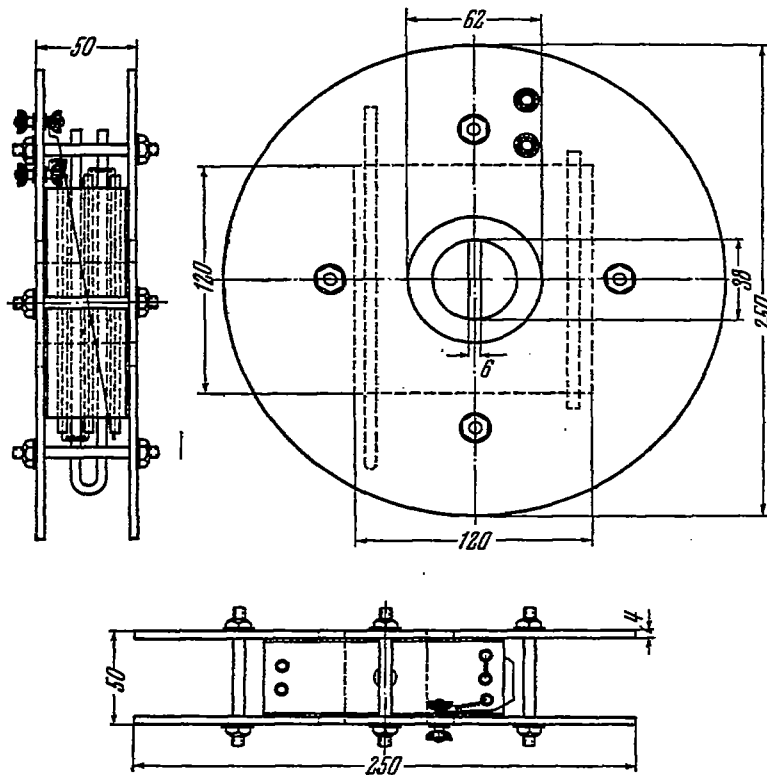


Figure 47. - Model for investigation of convection in an inclined slit by optical lattice method.

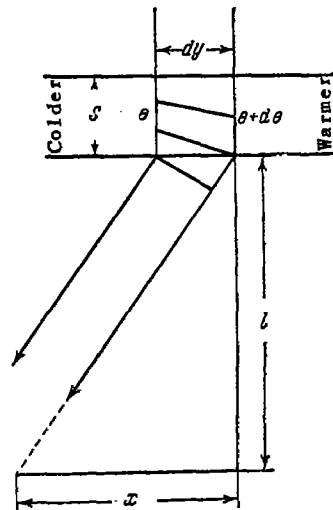


Figure 48. - Computation of sensitivity of optical lattice method:  $s$ , Thickness of model;  $l$ , distance from model to lattice;  $x$ , distance between lattice rods. Position of wave front of light wave.

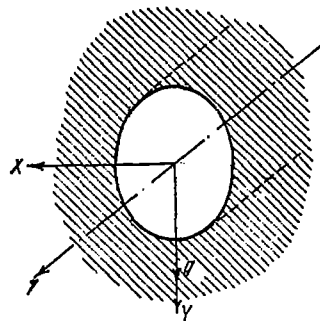


Figure 49. - Position of axes of coordinates for horizontal channel.

4281

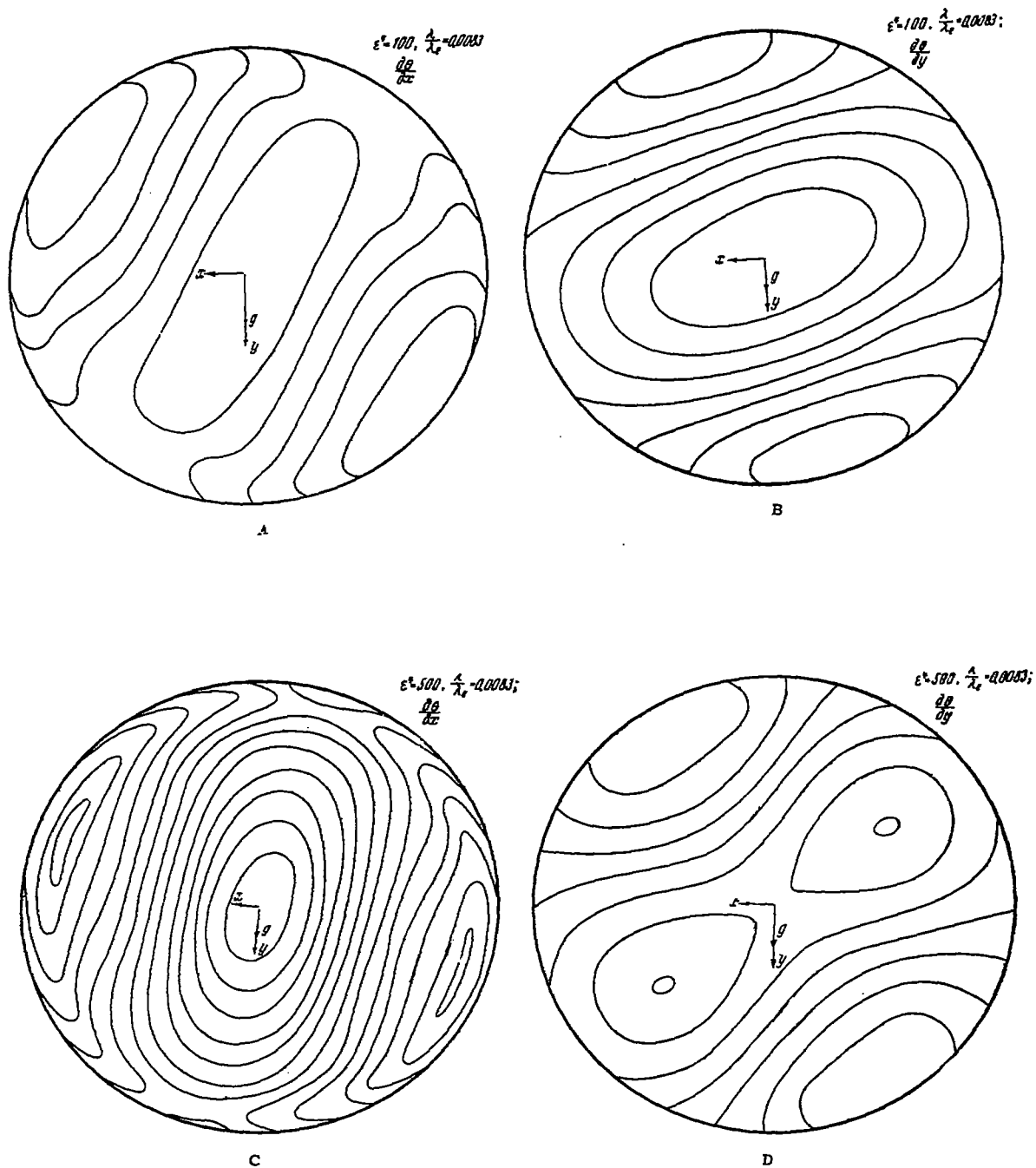


Figure 50. - A, B, C, and D, isolines of equal components of temperature gradient in horizontal channel, theoretically computed, including second approximation. Heating is from right.

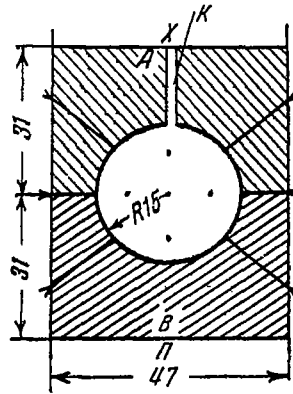


Figure 51. - Model for investigation of thermal convection in a spherical cavity: H, Heater; X, cooler; K, channel for filling model with water; A and B, location of external thermocouples; dots indicate location of 18 interior thermocouples.

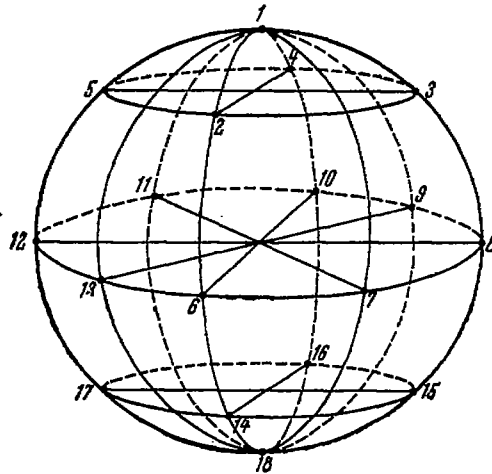


Figure 52. - Location and numbering of interior thermocouples in model for investigating thermal convection in spherical cavity.

4281

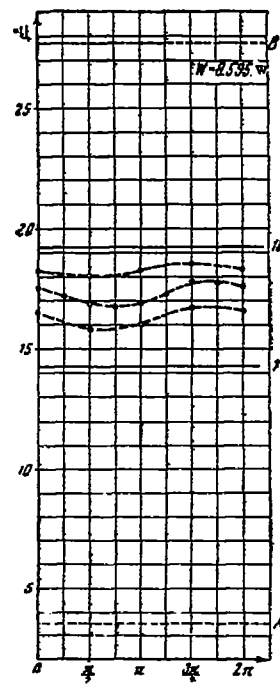
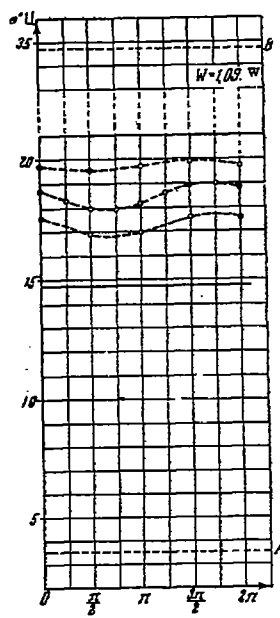
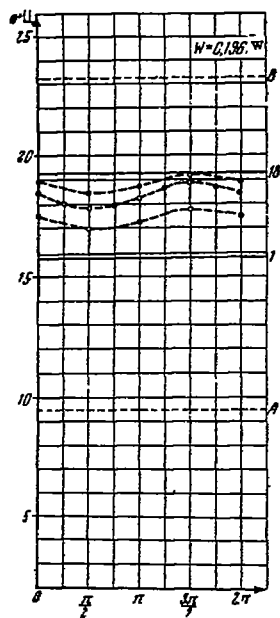


Figure 53. - 1 to 3 - Results of investigation of thermal convection in spherical cavity.

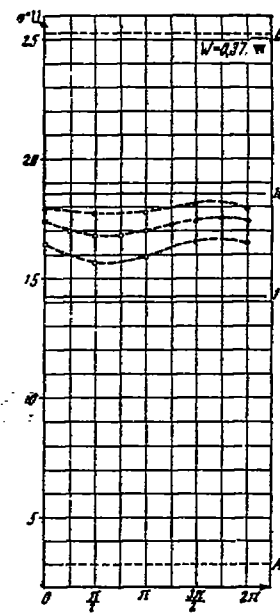
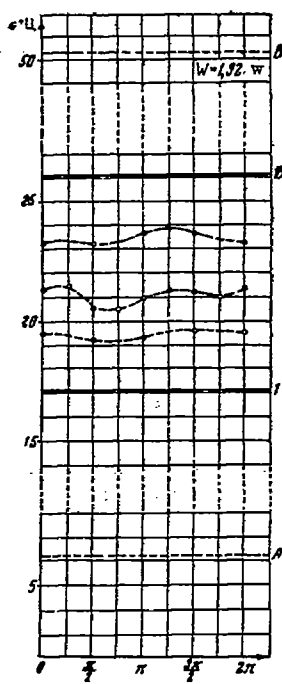
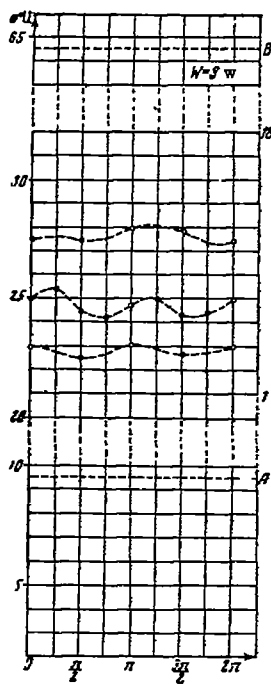


Figure 53. - 4 to 6 - Results of investigation of thermal convection in spherical cavity.

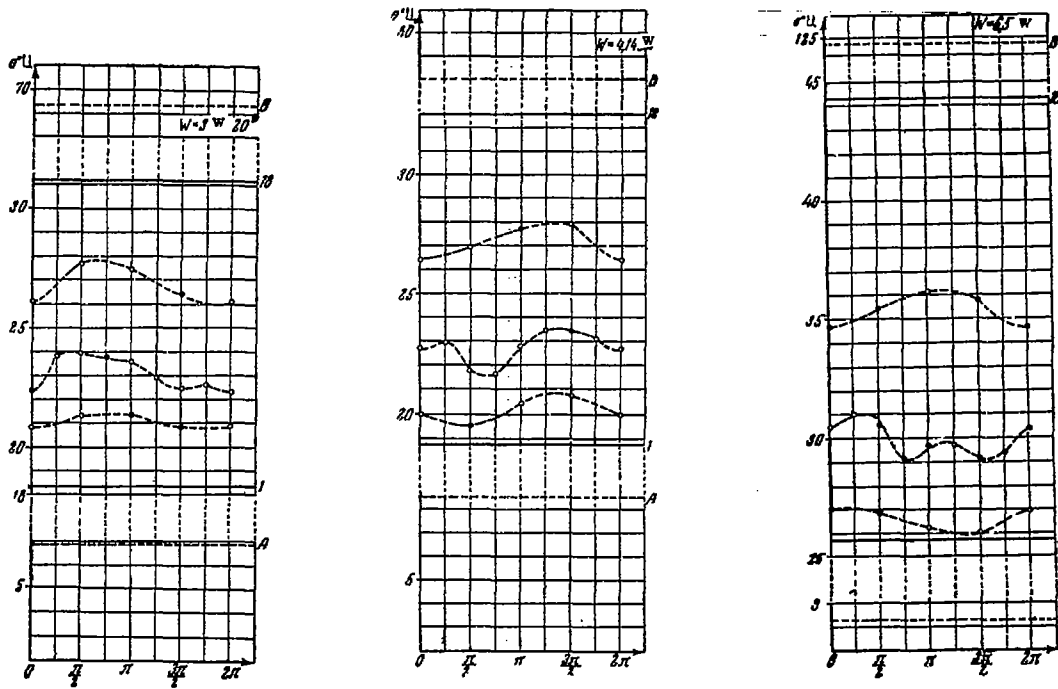


Figure 53. - 7 to 9 - Results of investigation of thermal convection in a spherical cavity. Last graph refers to case of axis of symmetry of model inclined to vertical by  $20^\circ$  angle.

4281

CA-28

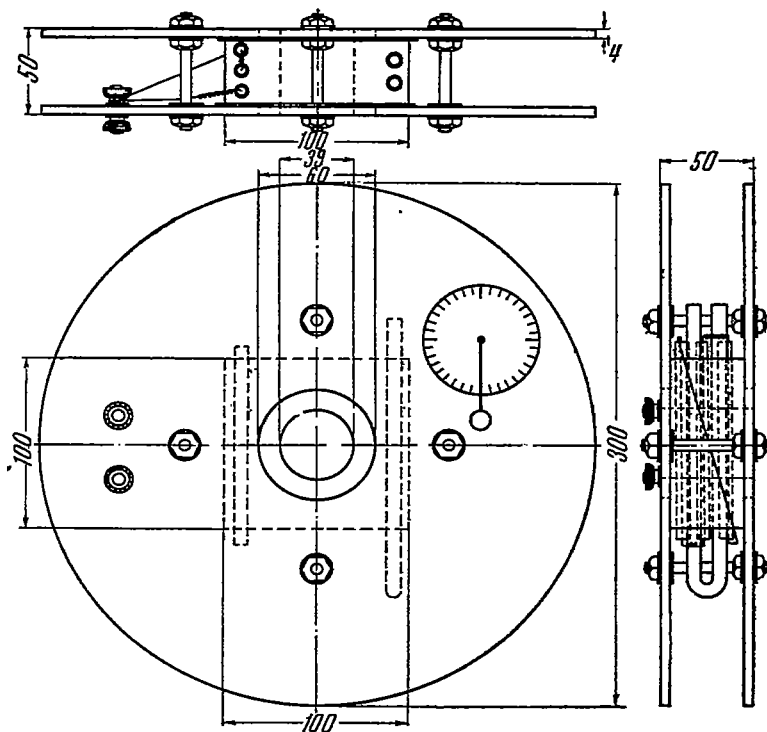


Figure 54. - Model for investigating convection in horizontal channel of round cross section by optical lattice method.

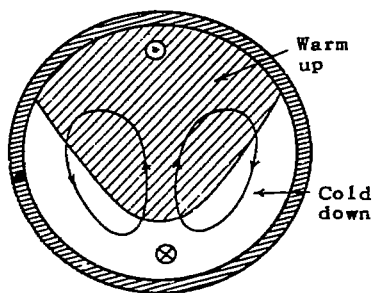


Figure 55. - Assumed distribution of convective flows over section of inclined round pipe.

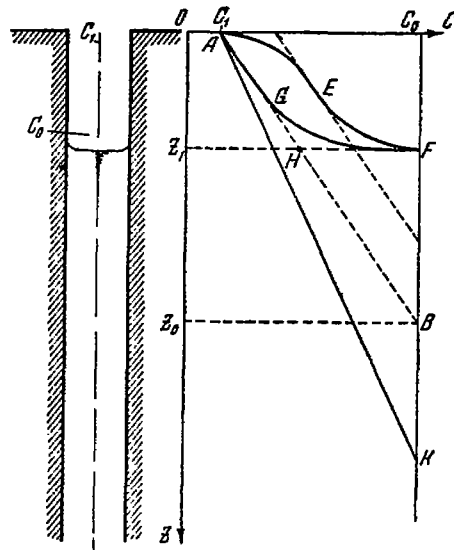


Figure 56. - Vertical well filled with evaporating water and distribution of cross-sectional mean humidity. Line AEF corresponds to convective process. Line AB corresponds to critical gradient of humidity;  $z_0$ , critical depth. Line AK corresponds to purely molecular diffusion of water vapor.

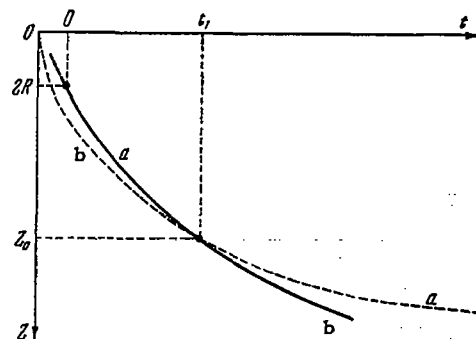
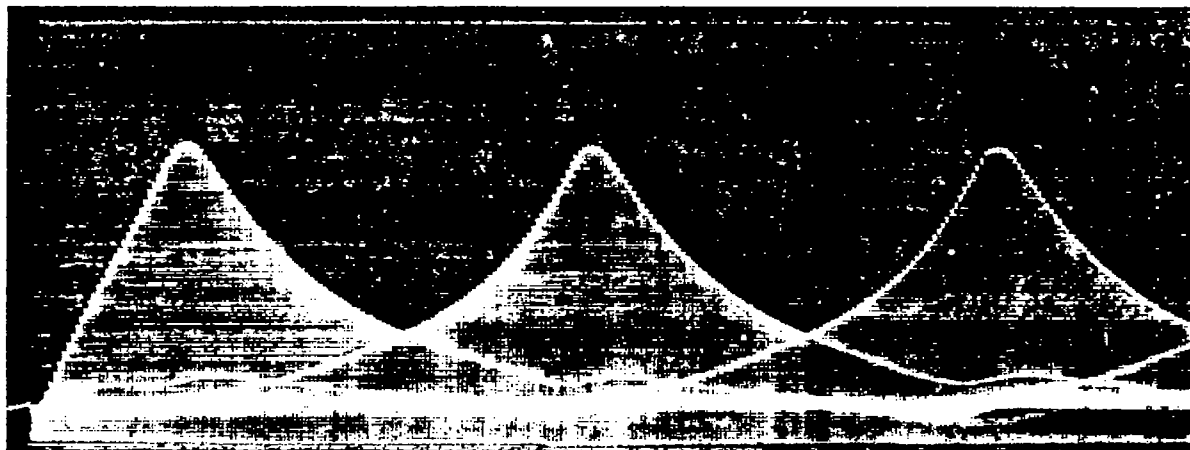


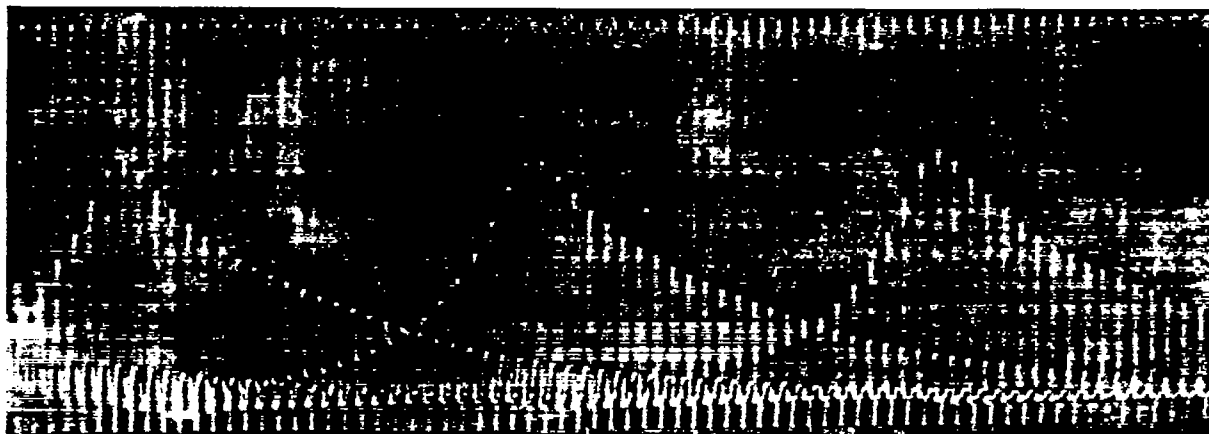
Figure 57. - Theoretical curve of water evaporation in vertical well. The exponential curve  $aa$  corresponds to convection regime. Parabola  $bb$  corresponds only to the molecular diffusion. On attaining critical depth, the exponential drying law goes over into the parabolic.

4281

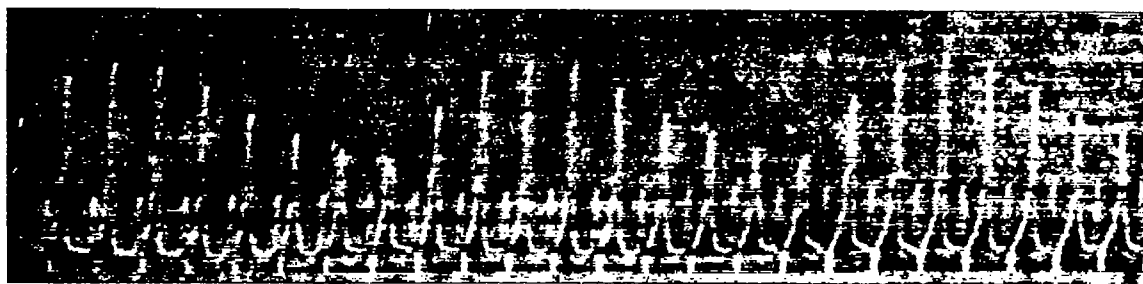


(A)

CA-28 back



(B)



(C)

Figure I. - Examples of automatic photo recordings in thermally investigated models. Upper record - 0.3 millivolt graduation curve (corresponds to  $7.15^{\circ}\text{C}$ ). Lower record - datum temperature of Dewar flask. The switching galvanometer cycle (time marks) 82.5 seconds. Upper photograph A - velocity of heater motion is too small, the curves are almost symmetrical. Center photograph B - velocity of heater motion is the most advantageous, photograph is suitable for measurements. Lower photograph C - velocity of motion is large, increase in temperature is almost independent of velocity of heater motion. Graduation record is not marked on lower photograph. On all photographs only initial or middle parts of entire length of record are given.



Figure II. - Thermal convection in pipe of round cross section observed with aid of light-scattering particles. Below - enameled wire of high-resistance heater. Axial-symmetrical phenomenon developing inside heater (along periphery fluid rises, along the axis fluid descends) spontaneously changes into diametrically antisymmetrical phenomenon developing over heater (on right fluid rises, on left fluid descends). Diameter of tube, 3.8/4.0 centimeters (model IV, table 8).



Figure III. - Form of streamlines photographed by means of light-scattering particles (upper part, figure II). Tube without heat insulation. Above - face of cold top. Right - fluid rises. Left - fluid descends.

4281

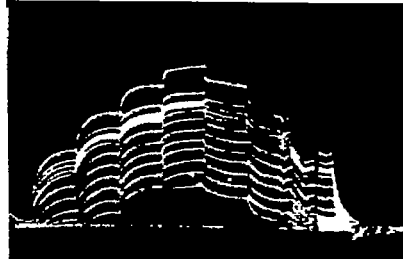


Figure IV. - Nonstationary regime of laminar thermal convection, determined by method of temperature recording with aid of program switch in vertical model. Maximum power, 0.54 calorie per second. Duration for each power stage, 3 hours. Upper line-- record of lower set of thermocouples.

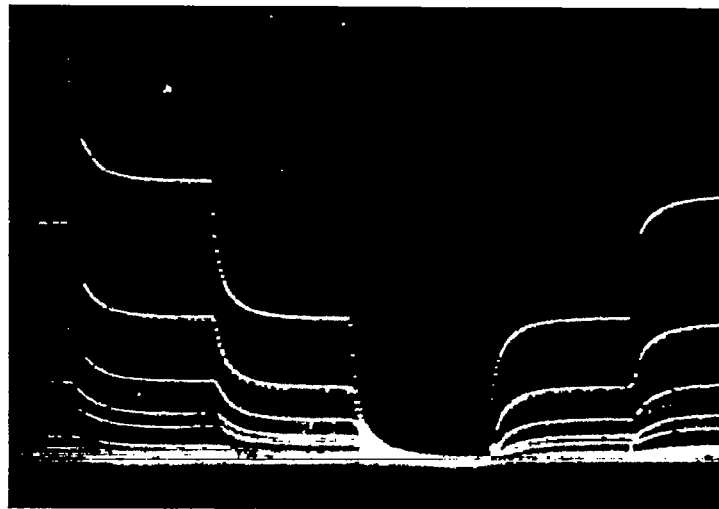
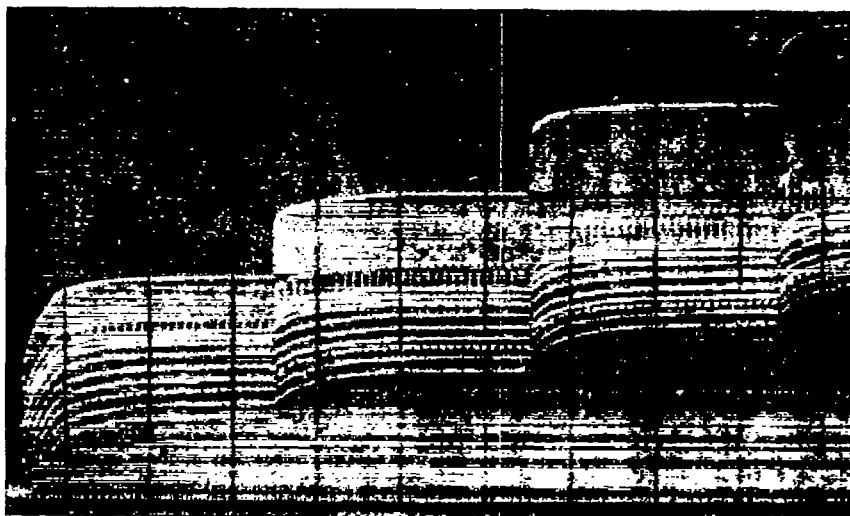
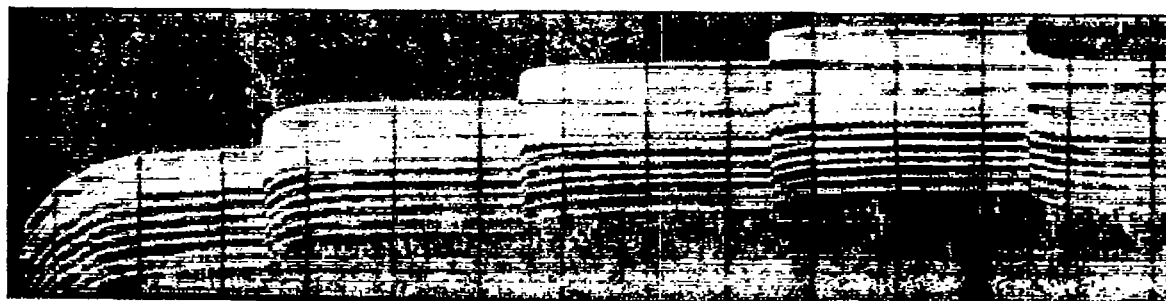


Figure V. - Nonstationary regime of brass rod introduced into model in place of fluid. Sharp difference in thermal phenomena in solid rod as compared with phenomena in fluid (fig. IV) is noted.



(A)



(B)

Figure VI. - Evaluation of figure V by means of accelerated record. Vertical gaps are hour marks of time. A - corresponds to powers: 0.092, 0.186, 0.304, and 0.42 calorie per second. B - corresponds to powers: 0.028, 0.056, 0.09, and 0.13 calorie per second.

4281

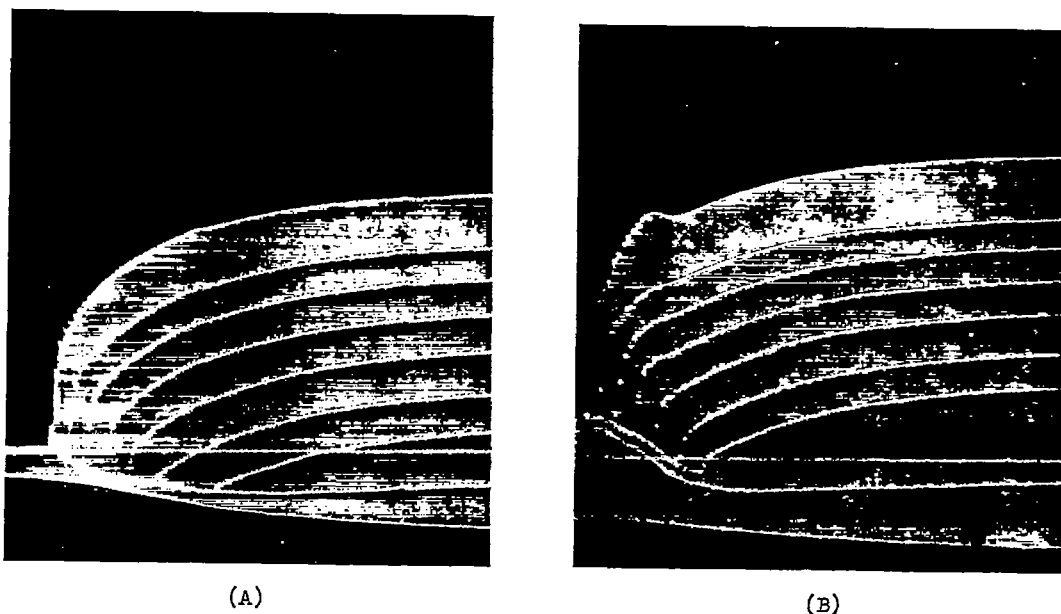


Figure VII. - Record of starting period in vertical model. Temperature of Dewar  $13.2^{\circ}\text{C}$ . Duration of cycle of switching, 82.5 seconds. Record A - 0.48 watt; B - 0.50 watt. First occurrence of "natural" vibrations is noted.

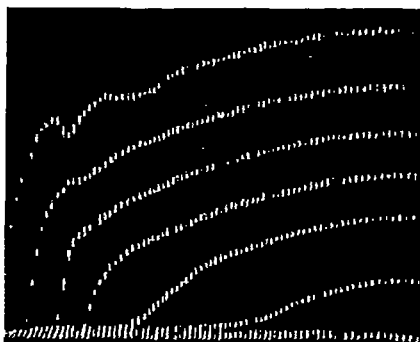


Figure VIII. - Nonstationary regime of thermal convection in vertical model: Reaching of convective thermal process in turn to succeeding stages of averaging thermocouples.

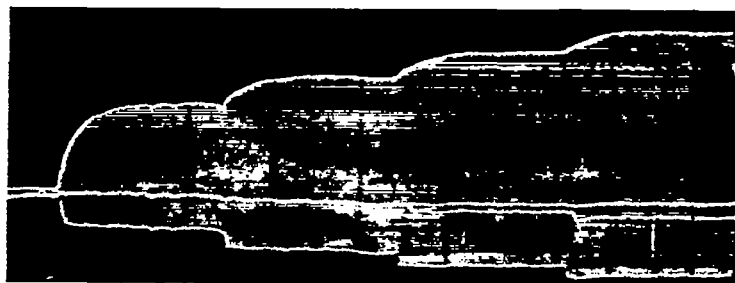


Figure IX. - Photorecord of temperature of lower averaging thermocouple-upper curve, and two transverse thermocouples; lower and upper curves below zero line. Note almost instantaneous reaction of transverse thermocouples, characterizing intensity of process of heat transfer, in comparison with smooth reaction of averaging thermocouples, characterizing result of process of heat transfer by convection. The model axis inclined  $45^{\circ}$  to vertical.

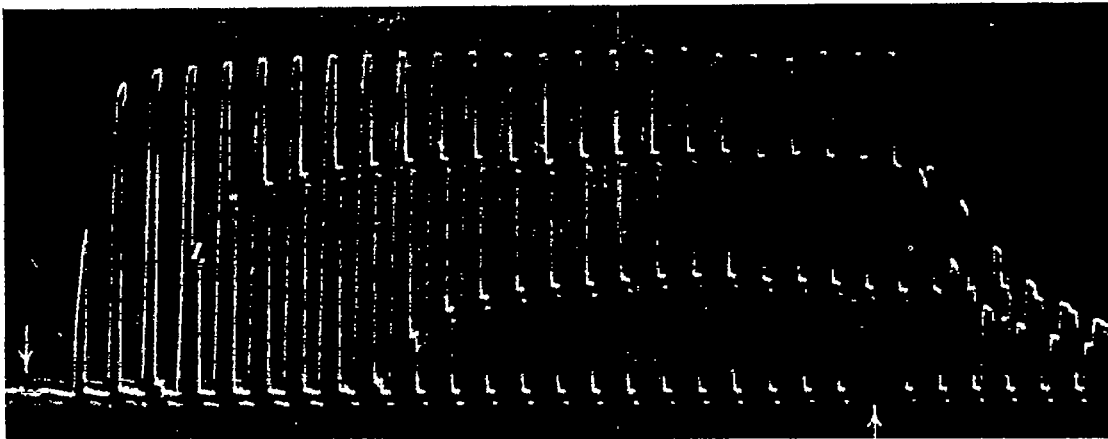


Figure X. - Photorecord of three transverse thermocouples in nonstationary regime. Arrows indicate instants of switching heater on and off. Duration of cycle of switching of galvanometer (distance between time marks) is equal to  $7.5 \times 4 = 30$  seconds. Model axis is inclined  $45^\circ$  to vertical.

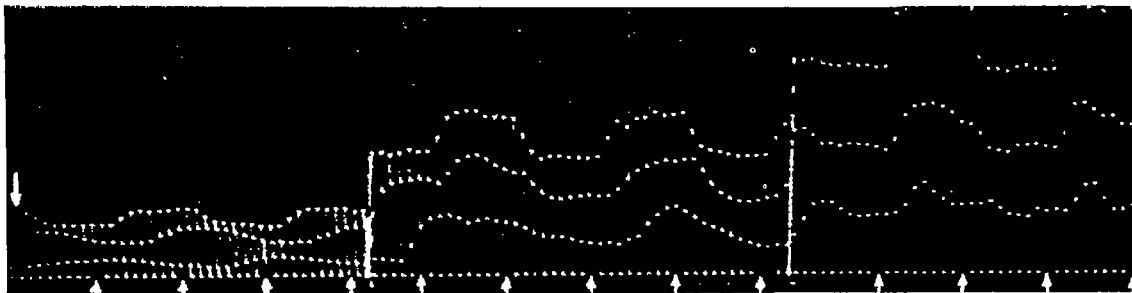


Figure XI. - Part of record by transverse thermocouples of forced thermal vibrations in model inclined  $45^\circ$  to vertical. Period of forced vibrations, 6 minutes. Switching cycle of galvanometer equal to  $5 \times 4 = 20$  seconds; power from left to right, 0.174, 0.71, and 1.58 calorie per second; depth of modulation in lowering of 20 percent in power. Shown are disturbances caused by natural vibrations (at large powers).

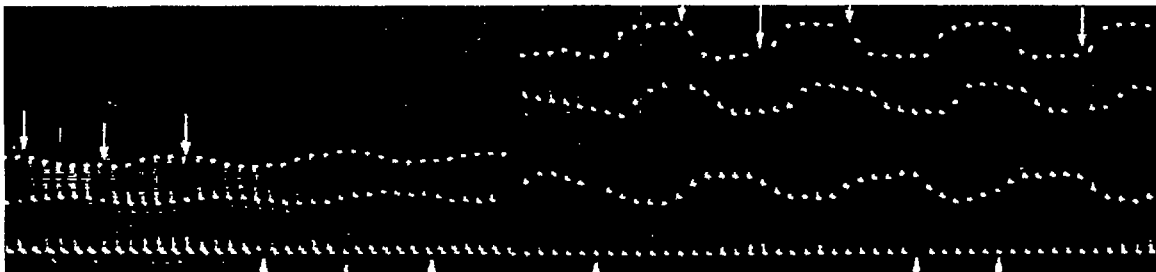


Figure XII. - Forced thermal vibrations in model inclined at  $45^\circ$  angle. Cycle of galvanometer switching,  $7.4 \times 4 = 30$  seconds; powers from left to right, 0.71 and 1.58 calorie per second; depth of modulation in lowering of 10 percent in power.

4281

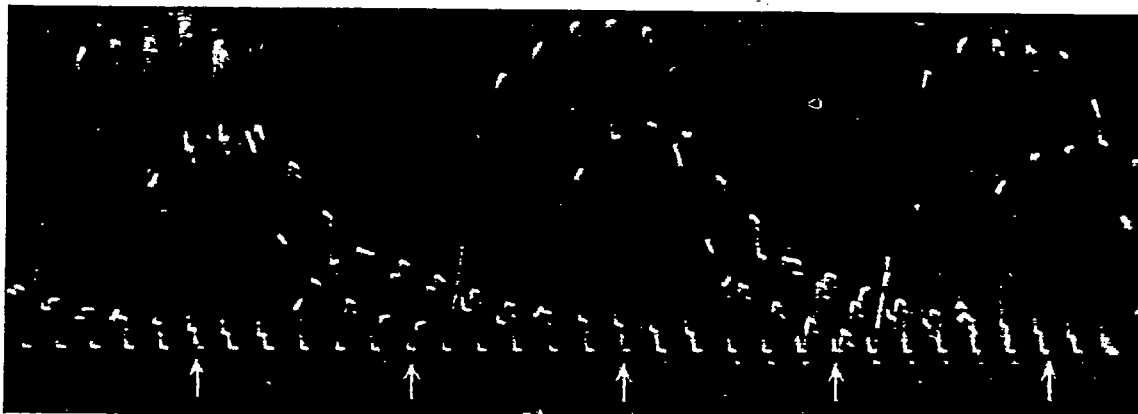


Figure XIII. - Thermal waves of convection along model inclined  $45^\circ$  to vertical, recorded by three transverse thermocouples. Center of record. Duration of cycle of galvanometer switching,  $7.5 \times 4 = 30$  seconds. Period 6 minutes. Arrows mark instants of switching heater on and off.

CA-29

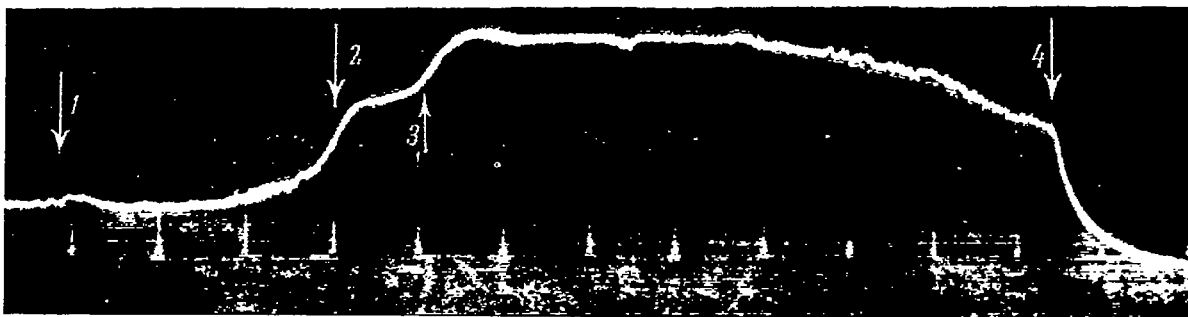


Figure XIV. - Record of temperature by method of movable plunger: 1 - Instant of start of plunger from hot bottom; 2 - upper face of plunger enters measuring coil; 3 - lower face of plunger issues from measuring coil; 4 - disconnecting of heater. Zero line is marked with hour marks of time. Model vertical.



Figure XV. - Record by many thermocouples of temperature change in displacement method. Double photo reproduction of motion of displaced rod upward and downward. Note good agreement for both kinds of motion. Model is vertical.

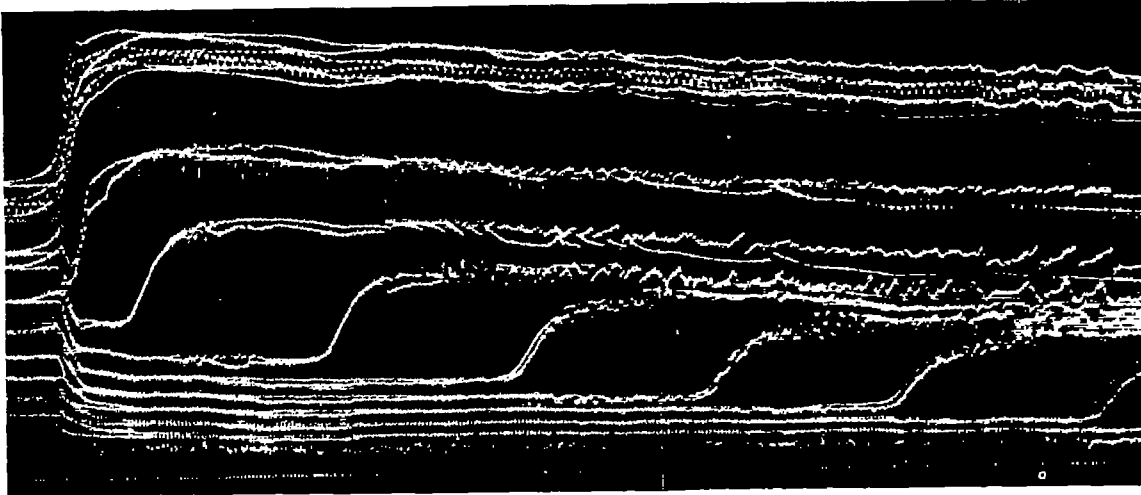


Figure XVIA. - Record by many thermocouples of changes in temperature by displacement method, double photo reproductions. Heating power, 0.09 calorie per second. Model vertical. Velocity of photographic plate, 11.8 millimeters per hour. Velocity of rod, 11.8 millimeters per hour.

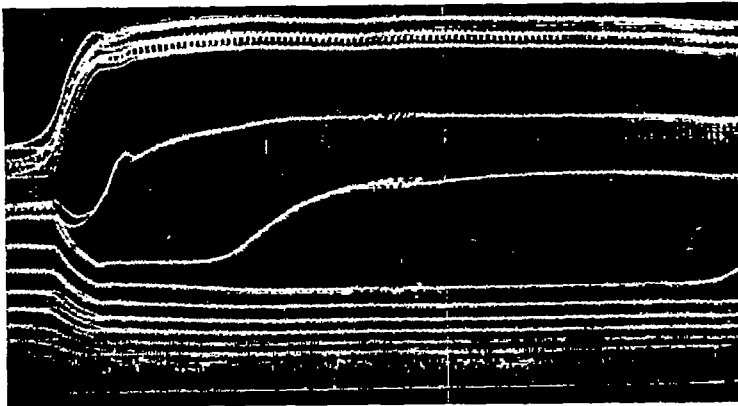
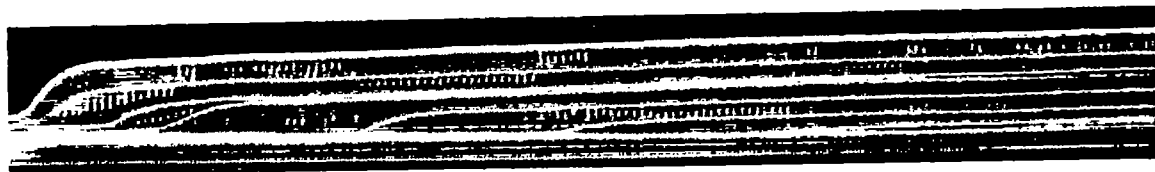


Figure XVIB. - Same conditions as figure XVIA. Velocity of rod one-third as large.



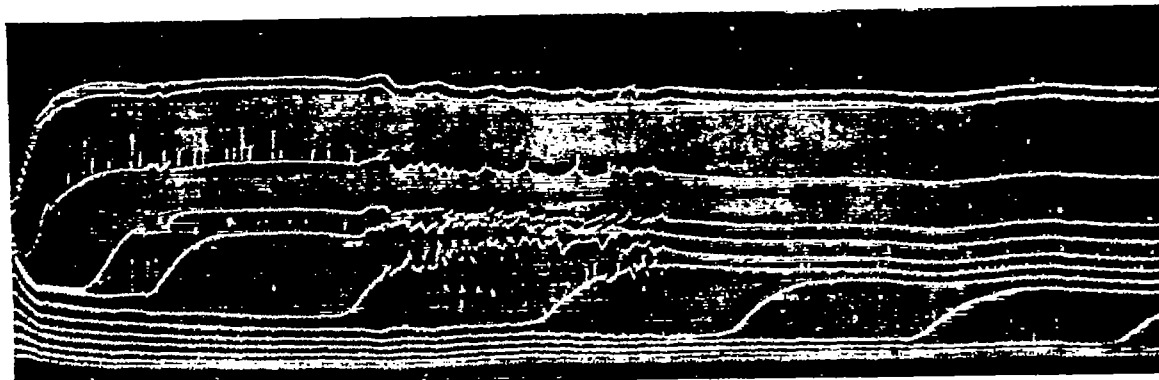
Figure XVIC. - Same conditions as figure XVIA. Velocity of rod one-eighth as large. Agreement of curves in motion of rod upward and downward is better the slower the motion.

4281

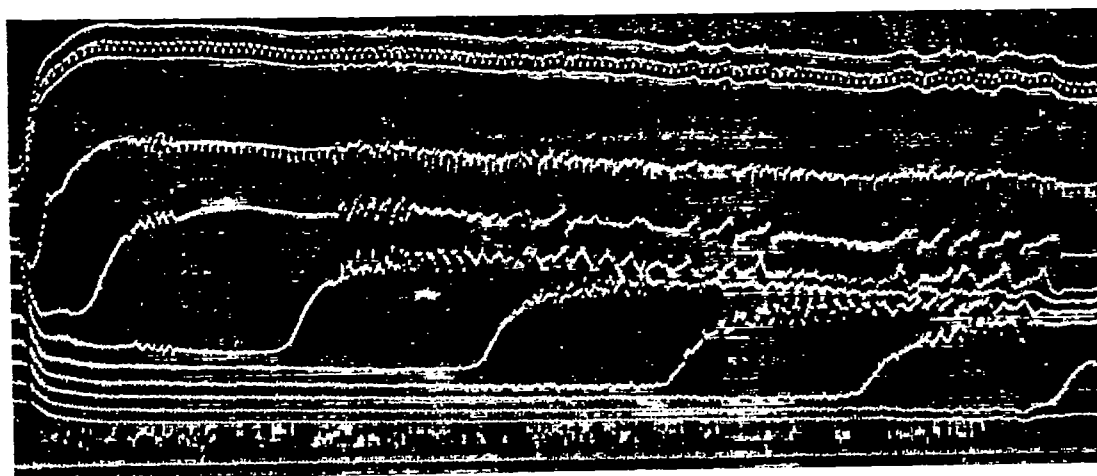


(A)

CA-29 back



(B)



(C)

Figure XVII. - Displacement method. Record for different heating powers. A - 0.014 calorie per second; B - 0.056 calorie per second; C - 0.090 calorie per second. Note exponential variation of temperature near face of displaced rod and increase in instability for certain lengths of fluid column. Model is vertical.

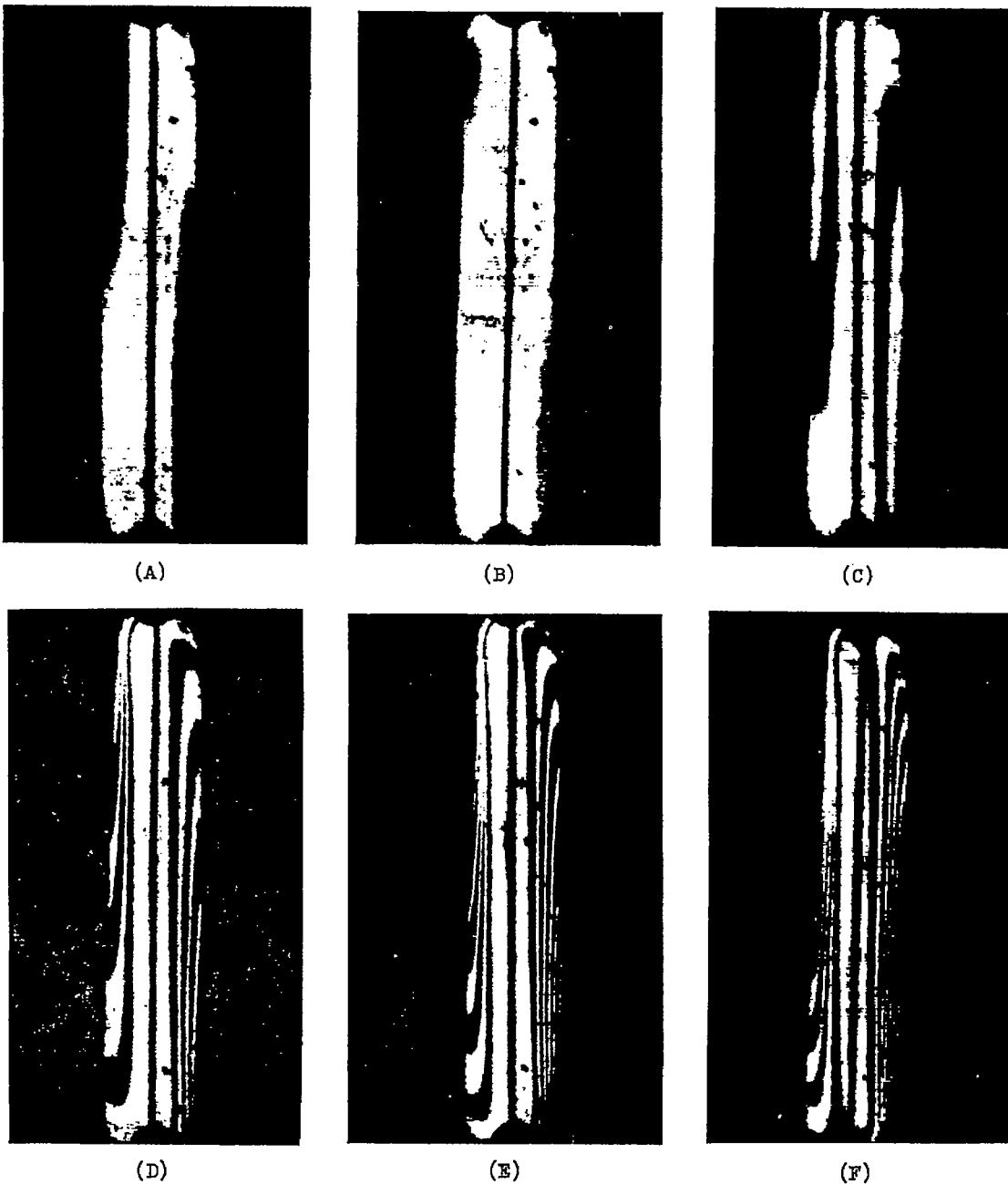


Figure XVIII. - Convection in vertical slit investigated by optical lattice method. Lattice: Rods of diameter, 1.3 millimeters; distance, 1.7 millimeters; gap, 3 millimeters between axes. Center of photograph is vertical plumb line. A - heating power, 18 watts; B - 24 watts; C - 35 watts; D - 58 watts; E - 72 watts; and F - 87 watts. Effect of diffraction observed on photographs D, E, and F from the left upward: bands are blurred; on photograph E same is observed on right downward.

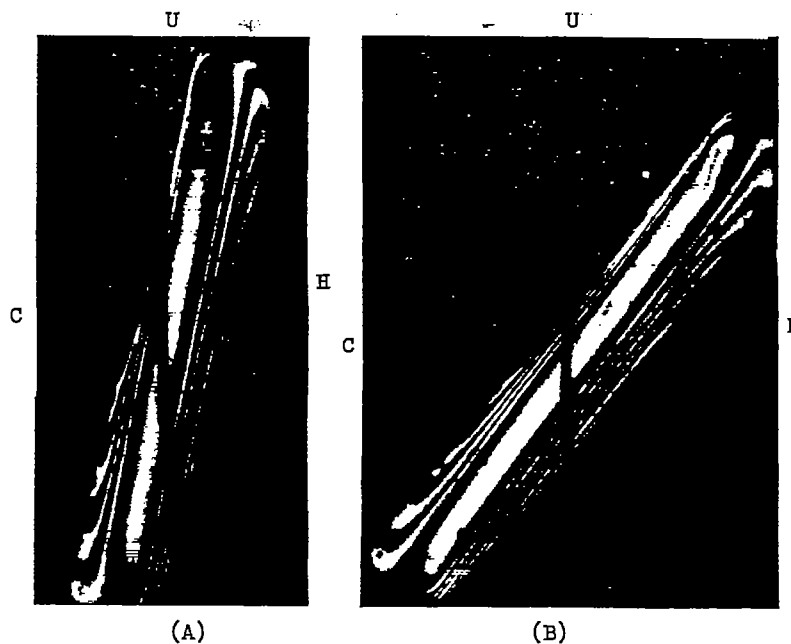


Figure XIX. - Convection in inclined slit investigated by lattice method. Letters C, H, and U denote cold, hot, and upper part of model. Power, 87 watts. Photograph A - inclination  $15^\circ$  to vertical, B -  $35^\circ$  to vertical. Note apparent curving of plumb line because photo objective was focused on central plane of model; the plumb line, being closer to objective. Objective in strongly deflected rays forming image of lateral parts of model "saw" plumb line to right of central plane of model; in non-deflected central rays, to left of central plane of model.

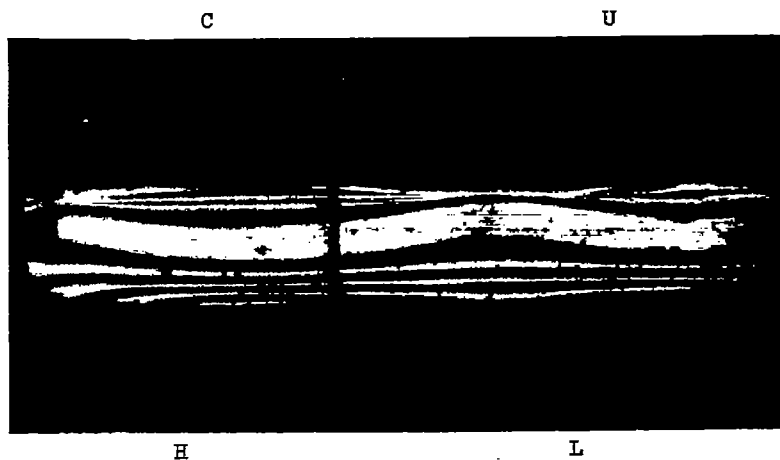


Figure XX. - Convection in horizontal slit investigated by lattice method. Letters C, H, U, and L mark cold, hot, upper, and lower parts of model. Heating power, 64 watts. Lattice rods horizontal. Vertical plumb line is seen. Bands indicate presence of convection (Laplacian of temperatures not zero). Wave-like form of bands indicates cellular structure of convective flow; lowering of bands corresponding to downward flow, raising to upward flow.

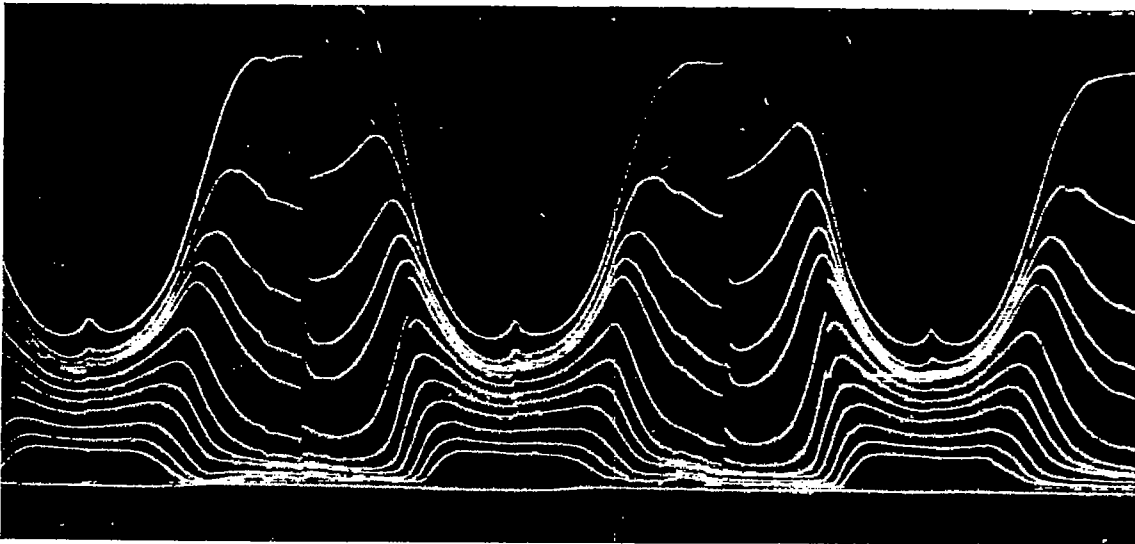


Figure XXI. - Part of five day photorecording of temperature distribution along model rotating about horizontal axis. Rotation cycle, 24 hours. Time increases from right to left. Lowerings of record correspond to positions "heater below," convective motion taking place. Risings of record correspond to "heater on top," heat transfer by molecular conduction. Temperature of aluminum jacket is the zero temperature.

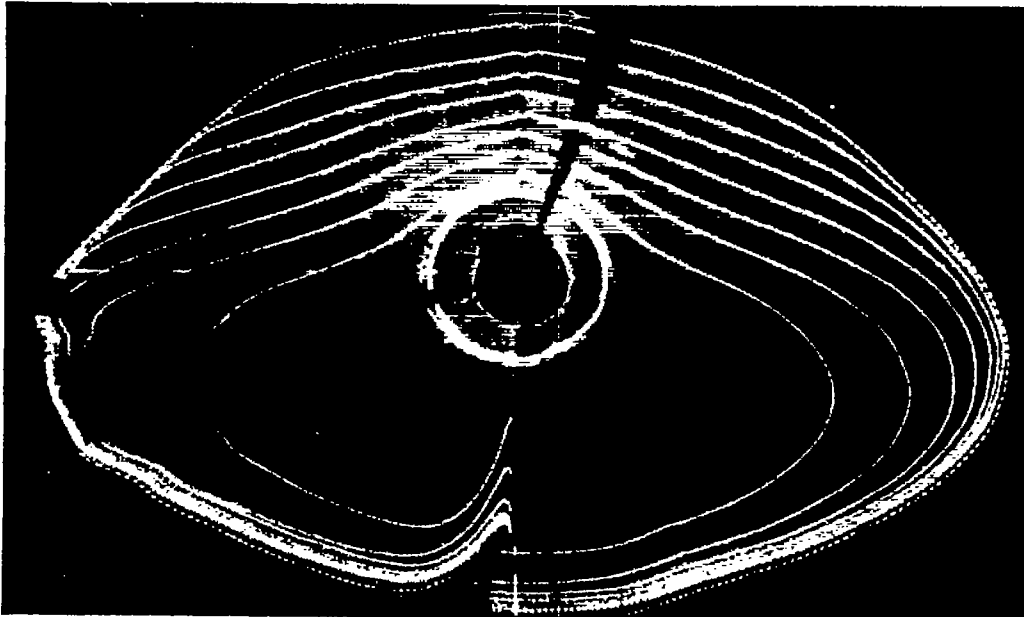


Figure XXII. - Photorecord of temperature distribution along rotating model (one rotation per 24 hr). Arrow indicates direction of rotation in arrangement where heater is below. Convection produces equidistant photorecords of temperatures of equidistant thermocouples. Temperature of hot thermocouple is taken as zero curve (circular record). Dotted peripheral record corresponds to temperature of aluminum jacket. Note unsteady initial period at start of recording. Heating power is approximately one-half to one-third as large as in preceding record.

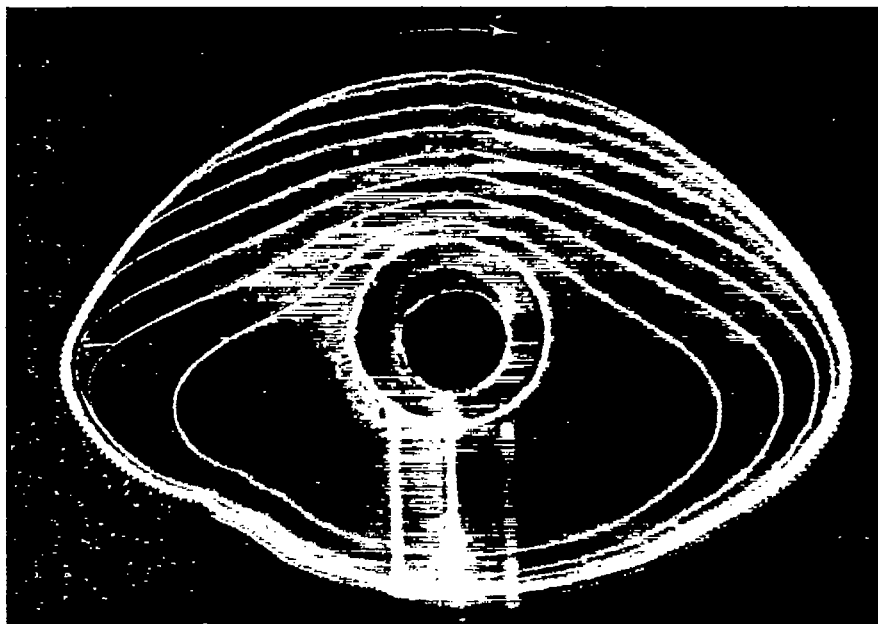


Figure XXIII. - Photorecord similar to preceding record. Heating power  $1\frac{1}{2}$  times smaller than on last record.

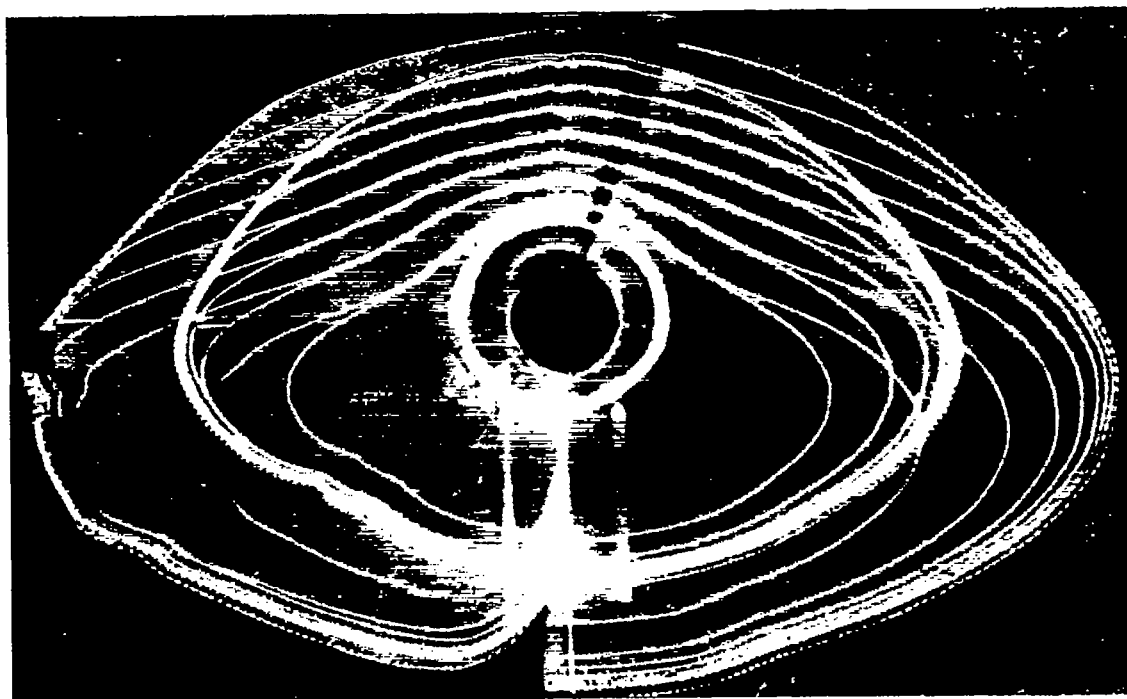
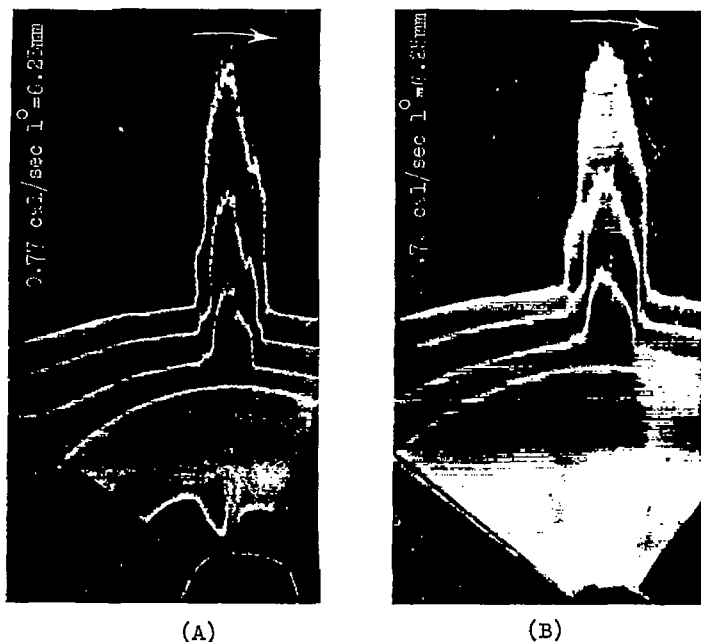


Figure XXIV. - Double reproduction of photographs XXII and XXIII. Both photorecords coincide in convective part.



4281

Figure XXV. - Photorecord of temperature distribution along a rotating model. Velocity of rotation once per 24 hours. Direction of rotation indicated by arrow. Temperature of coldest thermocouple is zero (arc of circle). Temperature of equidistant even averaging thermocouples is recorded upward. Temperature of jacket is recorded below. Above - critical regime of thermal convection arises for almost vertical arrangement of model. Note remains of unsteady starting regime at start of record. Heating power is moderate.

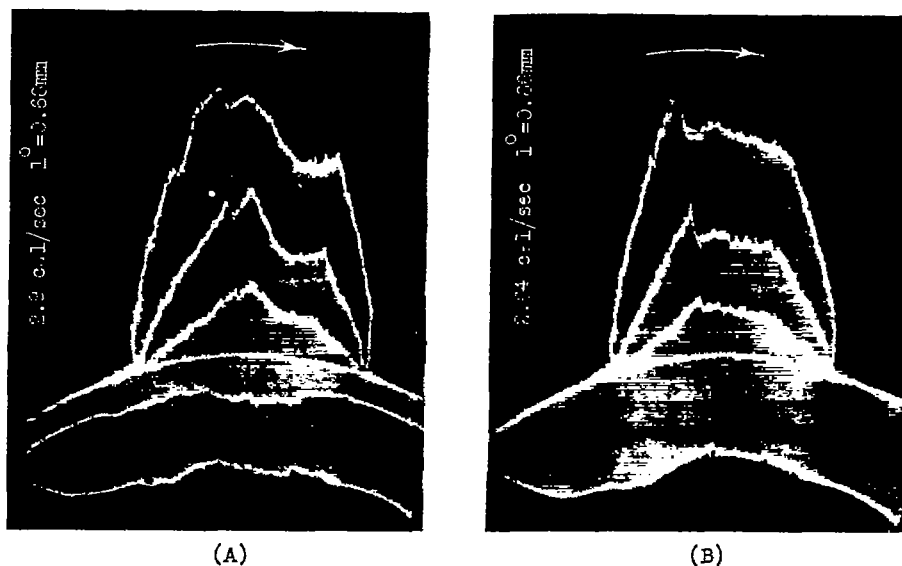


Figure XXVI. - Same as on preceding figure, considerable heating power. Sensitivity of galvanometer reduced. Jacket temperature is recorded below (this record does not appear on photo b). Temperature of datum (Dewar) recorded lower.

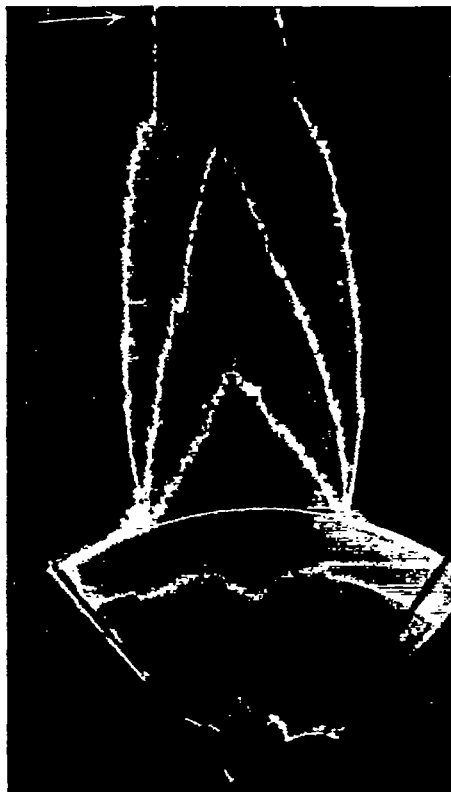


Figure XXVII. - Same as on preceding figure. Sensitivity increased. Photograph shows clearly character of unsteadiness in above-critical regime.